Tracing the sources, transport and dispersal of suspended sediment from the Burdekin River catchment into the Great Barrier Reef lagoon

PhD thesis submitted by

Zoe T. Bainbridge B.App.Sc (Hons)

in May 2015

for the degree of Doctor of Philosophy

in the College of Marine and Environmental Sciences

James Cook University

Statement on the Contribution of Others

Research funding

James Cook University/CSIRO Tropical Landscapes Joint Venture and School of Earth and Environmental Sciences co-funded scholarship

JCU Graduate Research School

JCU TropWATER

North Queensland Dry Tropics

Australian Government's Marine and Tropical Sciences Research Facility

CSIRO (Petra Kuhnert/Rebecca Bartley)

Thesis committee

Associate Professor Scott Smithers, College of Marine and Environmental Sciences, James Cook University

Dr Stephen Lewis, TropWATER, James Cook University

Jon Brodie, TropWATER, James Cook University

Dr Scott Wilkinson, Land and Water Flagship, CSIRO

Dr Petra Kuhnert, Computational Informatics, CSIRO

Editorial support

Scott Smithers

Stephen Lewis

Scott Wilkinson

Jon Brodie

Petra Kuhnert

Eric Wolanski

Jorge Álvarez-Romero

Rebecca Bartley

Grant Douglas

Stephen Hillier

Jim Wallace

Brent Henderson

Peter Hairsine

Anonymous reviewer of published chapter 2, the Associate Editor, Basil Gomez, Murray Hicks and two anonymous reviewers of published chapter 3 and the Submission Editor and two anonymous reviewers of accepted chapter 4.

Co-authorship in chapters for peer-reviewed publication

This thesis includes some collaborative work. Whilst undertaking this collaboration I was responsible for project conceptualisation, field study design and data collection, laboratory and data analysis and synthesis of results into a publishable format. Stephen Lewis, Scott Smithers, Jon Brodie, Scott Wilkinson, Petra Kuhnert, Grant Douglas (Chapter 4), Stephen Hillier (Chapter 4), Eric Wolanski (Chapter 2), Jorge Álvarez-Romero (Chapter 2) and Brent Henderson (Chapter 3) all provided a range of editorial advice, technical instruction and contributed to publications associated with this thesis.

Specifically, in Chapter 2 I undertook field sampling with assistance from SL and SS, I prepared the samples for and took the microphotograph images, analysed the samples for particle size, interpreted the data, conceptualised and constructed the figures and tables and wrote the chapter. EW, JB and SL contributed to study design, provided technical instruction and editorial comments. JA-R provided editorial comments, ran the ocean colour algorithm and created Fig 2.3 (Eduardo Teixeira da Silva is acknowledged for processing the raw satellite imagery for this figure). Pia Harkness assisted with map production (Fig 2.1).

In chapter 3 I designed the field study and undertook the sampling with assistance from SL (and others mentioned in acknowledgements), I co-ordinated and trained the grazier volunteer network, analysed selected samples for particle size, processed the raw data, constructed the annual sediment budget and other figures, interpreted and wrote the chapter. PK and BH developed the LRE model (Kuhnert et al. 2012), with Burdekin catchment-specific process understanding provided by myself and SL. SL, SS and JB contributed to study design and provided editorial assistance. Adella Edwards assisted with the final production quality versions of Figures 3.1 and 3.3.

Chapter 4 utilises field data collected in Chapter 3. In this chapter I recovered the <10 µm sediment fraction of stored water samples, prepared them for X-ray diffraction, interpreted the raw diffraction data with technical assistance from SH and Raphael Wust, further analysed the particle-size specific catchment budget of Chapter 3, interpreted the data, designed and constructed the figures and tables, and wrote the chapter. All co-authors contributed to various aspects of study design or final data interpretation, and provided editorial comments.

Every reasonable effort has been made to gain permission from and acknowledge the owners of copyright material. I would be pleased to hear from any copyright owner who has been omitted or incorrectly acknowledged.

Acknowledgements

I am indebted to my supervisory team, for your invaluable wisdom and guidance along this journey. A very special thank you to my principal and co-supervisors Scott Smithers and Stephen Lewis – for your endless support, patience, friendship and editing, and your invaluable instruction in undertaking and publishing clear science. Jon Brodie, my mentor, thank you for all you have taught me since I volunteered to work for ACTFR on a tiny Burdekin project all those years ago, and for encouraging me to undertake this PhD. I am immensely grateful for the additional support received by my CSIRO supervisors Scott Wilkinson and Petra Kuhnert part-way through the thesis – I have learnt so much from you both, and you have helped to shape and strengthen this thesis in many ways. I am also grateful to Rebecca Bartley, Grant Douglas, Eric Wolanski and Steve Hillier, from whom I have been fortunate to receive additional guidance and scientific inspiration during the course of this PhD.

A huge thank you to Damien Burrows and Susan Lesley, and TropWater more generally, for administrative, financial and emotional support throughout my PhD. I am also appreciative of the academic and administrative support provided by the School of Earth and Environmental Sciences (now CMES), especially Adella Edwards, Clive Grant, Paul Givney, Glenn Connolly, Bec Steele, Melissa Crawford and Beth Moore, as well as Jodie Wilson and the Graduate Research School team. I am grateful to the CSIRO's Ian Watson, Di Popham, Keith Bristow and Jim Wallace for their support and guidance through this endeavour. Finally I am extremely grateful to Scott Crawford, Di O'Donnell, Ian Dight and Paul Duncanson of NQDT for believing in the community volunteer project and finding ways for me to continue the network between funding cycles.

I am grateful to a number of people for their contributions to this thesis including Raphael Wust for generous assistance with initial clay mineral interpretation discussions; Michelle Tink, Pat Cunningham and Brett Baker and the TropWATER laboratory for all their assistance and for making long days in the lab much more enjoyable; Brendan Jones for XRD analytical support; the Queensland Government's DSITIA Loads Monitoring Program (Ryan Turner) for providing additional water samples and Reef Policy Project (RP65G) for providing the Old Reef sediment sample;

Morgain Sinclair, Geoff Pocock and Phil Kerr of the DNRM for providing streamflow gauging station data, and collection of water samples at Inkerman in 2011; Brett Baker and Peter Lawn for plume sampling assistance; and a number of TropWATER and Qld Government staff for field support including Alan Mitchell, David Reid, Michelle Cooper, Peter Verwey, Shane Ross, Sarah Thornton, Tom Coughlin, and to Katrina Cullen for starting the grazier network. Finally I am forever indebted to the network of graziers across the Burdekin who embraced this project and whose collection efforts were invaluable in capturing real time suspended sediment in transport across this large, episodic catchment: John & Lindy, Nevil & Stacey, Chris & Kathy, Bill & Milly, Keith & Alma, Pat & Colleen, Jim & Kim, John, Trevor & Selina, Cath, David & Di, Robyn & Richard, Mick & Amanda, Tim & Alison, Shane & Trish, Elsie & Jack, Chris & Jenny, Kath & Dan, John & Janet, Jamie & Gail, Glen & Kellie, Tony & Dominie. To the additional volunteers in the Haughton and Don River catchments (data reported in outputs associated with this thesis) my gratitude is also extended to Steve and Kristine, Owen & Marjorie, Jenny & Graham, and Russell Todd from Bowen State High School. Tony Bailey and Gary Caddies of Sunwater are also acknowledged for their dedicated daily wet season sampling of the Burdekin Falls Dam spillway.

Thank you to my GBR water quality colleagues for support throughout this PhD, especially Jane Waterhouse, Joanne Burton, Bronwyn Masters, Louise Hateley, Amelia Wenger, Michelle Devlin, Caroline Petus, Britta Schaffelke, Colette Thomas, Dom O'Brien, John Bennett and Nyssa Henry, many of whom were involved in a MTSRF conference dance floor discussion that kicked-off my PhD enrolment! I am forever indebted to my regular field companions, Steve Lewis and Aaron Davis, for all those long days travelling and sampling across the Burdekin, and your encouragement in completing this thesis. To my friends outside the science world, thank you for your continued support and comic relief as needed.

Finally, and most importantly, I wish to thank my family for all the support, patience and encouragement you have shown throughout this journey. A special mention to Will's wonderful Grandmas who travelled the distance of this country multiple times over the past year to support me in this endeavour, and of course to my husband Mitch, for being there through all the highs and lows of this project! I am forever grateful.

Abstract

Increased turbidity and sedimentation associated with the delivery of greater quantities of fine sediments to the coast due to anthropogenic modification of catchments have seriously degraded many near-shore marine ecosystems around the world. Within the Great Barrier Reef (GBR), Australia, there is growing evidence that increased turbidity and sedimentation associated with agricultural development of the coastal catchments have negatively impacted valuable ecosystems, including coral reefs and seagrass meadows. Further, research over the past decade has determined fine (<63 µm) organic and nutrient-rich terrigenous sediments have the greatest negative effects on tropical marine ecosystems because they: a) efficiently adsorb and transport other contaminants; b) aggregate and form organic-rich flocs; and c) can remain in suspension within the water column where they impede light penetration and reduce photic depth. However, limited field studies have examined the composition and transformation of suspended sediment in flood plumes over space and time (e.g. into organic-rich sediment flocs) within the GBR, or determined the source and nature of the sediment delivered by flood plumes that is most widely dispersed across the GBR lagoon.

The Burdekin River catchment (130,400 km^2) is the largest discrete source of suspended sediment to the GBR, with an average annual export of 3.93 million tonnes. This accounts for ~30% of the total average annual load from the entire GBR catchment area (426,000 km^2). Identifying major catchment source areas of this sediment and an improved understanding of how it is transported through the Burdekin catchment and dispersed within GBR coastal waters are required to better manage this threat. The overall aim of this research is to characterise and source suspended sediments discharged by Burdekin River flood plumes into the central GBR lagoon, that are most likely to negatively affect coral reef and seagrass ecosystems. Novel sediment budget and clay mineral-based tracing techniques were applied to this large, seasonally-dry tropical catchment to examine and quantify suspended sediment sources and transport across the catchment to marine continuum. These techniques have historically been applied only to smaller (i.e <10,000 km^2) temperate river catchments. The transformation and dispersal of suspended sediments and associated nutrients carried by Burdekin coastal flood plumes within the GBR lagoon were also investigated. This study specifically focused on the sources, transport and dispersal of particular fine

sediment size fractions that are not normally separated for attention, recognising the increased ecological risk of clay (<3.9 µm) and fine silts (3.9–15.6 µm) to downstream marine ecosystems.

The research reported in chapter 2 examined the hydrodynamic, biological and chemical processes controlling the transformation and dispersal of suspended sediments and particulate nutrients carried in flood plumes discharged from the Burdekin River into the GBR lagoon. An examination of flood plume sediment dynamics from 2007/08 to 2010/11 found all sand (>63 µm) and the majority (>80%) of clay and silt (<63 µm) sized-sediment rapidly settle once floodwaters mix with seawater, where salinity can be as low as 0.1 psu, usually within 10 km of the coastline. Microphotographs of sub-surface plume water within this zone revealed flocs of sediment particles were settling bound by organic matter, with floc sizes >100 µm in diameter. This is the first evidence of biologically-mediated flocculation processes occurring in the flood plumes of the large, sediment-laden dry tropical rivers discharging into the GBR. It is likely that particulate nutrients play a key role in driving this biologically-mediated flocculation and accelerated settling of river suspended sediment through heterotrophic bacteria production in this turbid zone, where low light and salinity conditions usually prevent marine phytoplankton blooms.

The analyses in chapter 2 also identified clay and fine silt (<16 µm) sized-sediments to be preferentially transported in Burdekin flood plume waters during peak flood conditions, and were observed as discrete mineral particles or, once suspended sediment had reduced to <10 mg L^{-1}, as small flocs in plume waters adjacent to the coast. As light conditions improved within plume waters over following weeks and marine biological activity increased, these clay and fine silt particles were observed in microphotographs encased in biological matter, forming large, low-density floc aggregates (100–200 µm), with sampling indicating that they maintain this state after seaward propagation at least 100 km from the river. Hence, this study identified clay and fine silts to have the greater dispersal potential within the GBR lagoon, and these fine mineral particles are often dispersed within large, buoyant organic-rich flocs. These flocs pose a risk to benthic organisms (e.g. coral reefs and seagrass meadows) because they: a) increase turbidity; b) worsen smothering impacts due to their ‘sticky’ nature; and c) are more easily remobilised during dry season wind-driven resuspension events.

Research reported in chapter 3 identified the major sources and spatial and temporal variability of suspended sediment yielded from Burdekin sub-catchments from a series of annual catchment-wide sediment source and transport budgets. These budgets incorporate suspended sediment loads (calculated from suspended sediment concentration and streamflow data) collected at seven strategic sub-catchment, reservoir outlet and end-of-river gauging station locations over five consecutive water years (Oct 1 to Sept 30: 2005/06 to 2009/10). The study confirmed that this budget approach of source identification in large, tropical catchments can reliably discriminate consistent, dominant sub-catchment sources of end-of-river suspended sediment export. Two major sub-catchments (Upper Burdekin and Bowen Rivers) distinguished by key geomorphic features including steep topography, erosive soils and wetter coastal climates generated sediment yields (147–530 t km^2 yr^{-1}) an order of magnitude higher than their inland, low relief and drier counterparts (<23 t km^2 yr^{-1}).

Research examining the transport of specific sediment-size fractions within tropical catchments has been limited to date, and this study also quantified sub-catchment contributions of the clay (<4 µm), fine silt (4–16 µm) and coarse (i.e. >16 µm) sediment fractions. Sediment trapping within a reservoir (capturing 88% of the catchment) and the preferential transport of clays and fine silts downstream of this structure were also examined. The data reveal that the highest clay and fine silt loads, of most interest to environmental managers of the GBR, are not always sourced from areas that yield the largest total suspended sediment load (i.e. all size fractions). For example, the 'bulk' sediment loads to the end-of-river were dominated by the Bowen River source (3.76 million tonnes) compared to BFD overflow source (2.52 million tonnes), but the BFD overflow source contributed a higher clay-specific load than the Bowen sub-catchment (1.32 million tonnes and 1.03 million tonnes, respectively). However, the clay-specific yield from the smaller Bowen River source (145 t km^{-2} y^{-1}) is 10-fold higher than the BFD overflow source (11 t km^{-2} y^{-1}). The results demonstrate the importance of incorporating particle size into catchment sediment budget studies undertaken to inform management decisions to reduce downstream turbidity and sedimentation.

Chapter 4 examined the potential of clay mineralogy as a sediment tracing technique for catchment studies with a specific focus on tracing terrigenous sediment in flood plumes back to a catchment origin. A comprehensive clay mineral dataset (231 samples) representing 31 river and upstream tributary sites over multiple streamflow events and water years found consistency in clay mineral relative abundances, with a ratio of common clay minerals (illite/illite+expandable clays) clearly distinguishing basaltic (ratio of 0–7), granitic (28) and sedimentary (42–52) geological sources. These ratios also clearly distinguished the Upper Burdekin-BFD reservoir source (34–35) from the expandable clays-rich Bowen River source (11), and were used in conjunction with the sediment budget approach to provide multiple lines of evidence to guide the remediation of fine sediment sources. Further, the I/I+E ratio provided evidence of relative enrichment of the expandable (smectite-rich) clays within remaining flood plume sediment after this bulk deposition near the river mouth, with increasing salinity. The distinctive geological source-related "fingerprints" found in this study validate the relative proportions of clay minerals as a valuable tracing tool in large and geologically complex catchments, and across freshwater-marine continuums. This study also found 1-2 samples from any given source area is sufficient to generate a reproducible signature, highlighting the efficacy of this technique and its potential application for similar sediment tracing and climatic studies in other catchments.

This thesis has utilised complementary, multiple lines of evidence to trace the source and fate of fine sediments across a large, seasonally-dry tropical catchment and adjacent coastal waters, and has demonstrated the applicability of sediment budget and clay mineral-based tracing techniques rarely utilised at such scales. This approach to sediment source identification is suitable for broader application across the GBR catchment area and lagoon, and similar coastal settings. The importance of incorporating sediment particle size into sediment source investigations has been highlighted by this study, and should also guide further research examining the ecological effects of terrigenous sediment (and associated nutrients and other contaminants) on coral reefs, seagrass meadows and other marine ecosystems.

Contents

List of Tables

List of Figures

Outputs associated with this thesis

Peer-reviewed publications

Bainbridge, Z., Lewis, S., Smithers, S., Wilkinson, S., Douglas, G., Hillier, S., Brodie, J. Accepted. Clay mineral source tracing and characterisation of Burdekin River (NE Australia) and flood plume fine sediment. Journal of Soils and Sediments, doi: 10.1007/s11368-015-1282-4.

Bainbridge, Z., Lewis, S., Smithers, S., Kuhnert, P., Henderson, B., Brodie, J. 2014. Fine-suspended sediment and water budgets for a large, seasonally-dry tropical catchment: Burdekin River catchment, Queensland, Australia. Water Resources Research 50, 9067-9087.

Bainbridge, Z., Wolanski, E., Alvarez-Romero, J., Lewis, S., Brodie, J. 2012. Fine sediment and nutrient dynamics related to particle size and floc formation in a Burdekin River flood plume, Australia. Marine Pollution Bulletin 65, 236-248.

Supporting publications

Bartley, R., **Bainbridge, Z.**, Lewis, S., Kroon, F., Wilkinson, S., Brodie, J., Silburn, M. 2014. Relating sediment impacts on coral reefs to watershed sources, processes and management: A review. Science of the Total Environment 468-469, 1138-1153.

Lewis, S., **Bainbridge, Z.**, Kuhnert, P., Sherman, B., Henderson, B., Dougall, C., Cooper, M., Brodie, J. 2013. Calculating sediment trapping efficiencies for reservoirs in tropical settings: A case study from the Burdekin Falls Dam, NE Australia. Water Resources Research 49, 1017-1029.

Brodie, J., Wolanski, E., Lewis, S., **Bainbridge, Z.** 2012. An assessment of residence times of land-sourced contaminants in the Great Barrier Reef lagoon and the implications for management and reef recovery. Marine Pollution Bulletin 65, 267-279.

Kuhnert, P., Henderson, B., Lewis, S., **Bainbridge, Z**., Wilkinson, S., Brodie, J. 2012. Quantifying total suspended sediment export from the Burdekin River catchment using the loads regression estimator tool. Water Resources Research 48, W04533.

Additional publications produced during candidature

Davis, A.M., Lewis S.E., O'Brien, D.S., **Bainbridge Z.T.**, Bentley C., Mueller, J.F., Brodie, J.E. 2014. Water resource development and high value coastal wetlands on the lower Burdekin floodplain, Australia. In: 'Estuaries of Australia in 2050 and

beyond', Estuaries of the World. Wolanski, Eric (Ed.), pp. 223-245. Springer, Dordrecht, 292pp.

Davis, A., Thorburn, P., Lewis, S., **Bainbridge, Z.,** Attard, S., Milla, R., Brodie, J. 2013. Environmental impacts of irrigated sugarcane production: Herbicide run-off dynamics from farms and associated drainage systems. Agriculture, Ecosystems & Environment 180, 123-135.

Brodie, J., Kroon, F., Schaffelke, B., Wolanski, E., Lewis, S., Devlin, M., Bohnet, I., **Bainbridge, Z**., Waterhouse, J., Davis, A. 2012. Terrestrial pollutant runoff to the Great Barrier Reef: An update of issues, priorities and management responses. Marine Pollution Bulletin 65, 81-100.

Davis, A., Lewis, S., **Bainbridge, Z.,** Glendenning, L., Turner, R., Brodie, J. 2012. Dynamics of herbicide transport and partitioning under event flow conditions in the lower Burdekin region, Australia. Marine Pollution Bulletin 65, 182-193.

Lewis, S., Schaffelke, B., Shaw, M., **Bainbridge, Z**., Rohde, K., Kennedy, K., Davis, A., Masters B., Devlin, M., Mueller, J., Brodie, J. 2012. Assessing the additive risks of PSII herbicide exposure to the Great Barrier Reef. Marine Pollution Bulletin 65, 280-291.

Bainbridge, Z., Dight, I., Yorkston, H., Lewis, S., Brodie, J. 2011. Catchment management in a dry tropical river near the Great Barrier Reef. In C. Wilkinson and J.E. Brodie (Eds) Catchment Management and Coral Reef Conservation. Global Coral Reef Monitoring Network and Reef and Rainforest Research Centre, Townsville, Australia, 96-97.

Lewis, S.E., Smith, R., Brodie, J.E., **Bainbridge, Z.T.,** Davis, A.M., Turner, R. 2011. Using monitoring data to model herbicides exported to the Great Barrier Reef, Australia. In Chan, F., Marinova, D. and Anderssen, R.S. (eds) MODSIM2011, 19th International Congress on Modelling and Simulation. MSSANZ, Dec 2011, pp. 2051-2056. ISBN: 978-0-9872143-1-7.

1. Introduction

1.1. Impacts of sediment on coastal coral reef and seagrass ecosystems

The negative impacts of elevated terrigenous sediment loads and associated contaminants on tropical coastal and inshore marine ecosystems such as coral reefs and seagrass meadows are well documented (Coles et al., 2011; Erftermeijer et al., 2012; Fabricius, 2005; Risk, 2014; Waycott et al., 2009). As sediment is dispersed via river flood plumes into near-shore marine waters, or is later resuspended, the turbidity of the water column increases which, in turn, reduces photic depth (i.e. the availability of light for photosynthesis down through the water column; Fabricius et al., 2014). Reduced photic depth can seriously compromise coral reef and seagrass communities that require illumination to photosynthesise and survive, and may eventually lead to loss of ecosystem function through reduced biodiversity (Erftermeiger and Lewis, 2006, Erftermeiger et al., 2012; Fabricius, 2005). As suspended terrestrial sediment and associated particulate matter settles, coral colonies and seagrass plants can be smothered by increased sedimentation (Erftermeiger and Lewis, 2006; Flores et al., 2012; Philipp & Fabricius, 2003; Rogers, 1990). Survival depends on the rate at which sediments accumulate, the rate of sediment removal associated with wind and current regimes, the type of sediments and associated contaminants deposited, the thickness of accumulated deposits, and the mechanisms organisms have for coping (e.g. seagrass can modify shoot length, some coral species use tentacles and mucus to remove sediment) (Erftermeiger and Lewis, 2006; Rogers, 1990). Recent surveys of the health of coral reefs off north-western Australia found that elevated turbidity and sedimentation rates as a result of localised dredging were strongly associated with an increase in coral disease outbreaks (Pollock et al., 2014). Elevated turbidity and sedimentation also affect other reef habitat communities, including reef fish (Wenger and McCormick, 2013; Wenger et al., 2012) and sponges (Bannister et al., 2012). Such studies highlight how water quality degradation (i.e. elevated sediments, nutrients and other contaminants such as pesticides) can produce a range of additional negative effects on marine communities (see section 3.5.6).

Long-term monitoring of seagrass meadows and coral reefs in the Great Barrier Reef (GBR), north-eastern Australia, reveals a decline in the health, species diversity and spatial extent of these ecosystems (Coles et al., 2015; Collier et al., 2012; De’ath et al., 2012; DeVantier et al., 2006; Fabricius and De’ath, 2001; Fabricius et al., 2005; Thompson et al., 2013). Declining water quality is one of a number of stressors, including rising sea surface temperatures, more frequent outbreaks of crown of thorns starfish and cyclones, all of which currently affect the condition and longer-term resilience and survival of the GBR (Brodie et al., 2012a; De’ath et al. 2012). Water quality improves with distance offshore across the GBR, with water clarity and coral biodiversity also increasing offshore with distance from the coast (Cooper et al., 2007; De’ath and Fabricius, 2010; Thompson et al., 2014). In shallow water (i.e. <20 m depth) continental shelf reef settings such as the inner GBR, turbidity and reduced light associated with the resuspension of fine terrigenous sediment is the most significant impact affecting benthic communities in the months following discrete discharge and flood plume events (Fabricius et al., 2013; 2014; Storlazzi et al., 2009; Thompson et al., 2014; Wolanski et al., 2005). Recently, Fabricius et al. (2014) demonstrated a significant statistical relationship between reduced photic depth in the inshore and mid-shelf areas of the central GBR and higher terrestrial inputs from adjacent river catchments. While there is evidence for a general decline in GBR reef health, there are also many inshore coral reef communities that thrive in naturally turbid conditions (Browne et al., 2013; Perry et al., 2008). Coastal seagrass communities have not fared as well, with both localised (Petus et al., 2014; Preen et al., 1995) and regional scale (Coles et al., 2015) declines associated with cyclonic and flood discharge events over recent decades.

Experimental research of Weber et al. (2006; 2012) identified that fine (<63 µm) organic and nutrient-rich terrigenous sediments induced higher photophysiological stress in corals than nutrient-poor sandy sediments. Finer sediment particles have larger surface areas than coarse-grained sediment, and can adsorb more nutrients, pesticides and other contaminants to their surface (e.g. Laceby et al., 2014). These finer sediment particles readily form organic-rich aggregates, or flocs in marine waters (Dagg et al., 2004; Gibbs and Konwar, 1986) and corals smothered by these flocs, even over relatively brief periods, experience rapid degradation of coral tissue (Fabricius and Wolanski, 2000; Weber et al., 2012). Exposure of corals to fine terrestrial sediments (<63 µm) combined with elevated dissolved nutrient levels (i.e. nitrate, phosphate) has also been shown to reduce fertilization rates of corals (Humphrey et al., 2008). Another study showed that the settlement of new coral recruits was significantly limited once substrates were covered by only thin deposits (i.e. 0.047 mm thick) of fine (<63 µm) terrestrial sediment (Perez et al., 2014). Finer clays (<3.9 µm) and silts (3.9−63 µm) are more easily resuspended than coarser sediments, and have a greater impact on light attenuation within the water column (Davies-Colley and Smith, 2001; Fabricius, 2005; Wolanski et al., 2008). Hence, it is these finer sediments (<63 µm) of terrigenous origin that are most damaging to tropical marine ecosystems due to their increased ability to adsorb and transport other contaminants, to aggregate and form organic-rich flocs and to considerably reduce photic depth.

Whilst research over the past decade has established that finer clay and silt-sized terrigenous sediments have the potential to cause most damage to GBR ecosystems, few studies have examined their catchment sources, marine dispersal processes and final distribution (see only Bannister et al., 2012; Douglas et al., 2006a; Kroon et al., 2012; Orpin et al., 2004; Smith et al., 2008; Wolanski et al., 2008). Significant knowledge gaps thus exist in these areas (see also reviews in supporting publications Bartley et al., 2014 (Appendix B) and Brodie et al., 2012b (Appendix C)). Specifically, little research has been conducted examining the composition and transformation of suspended sediment in plumes over space and time (e.g. into organic-rich sediment flocs), and determining the source and nature of this sediment that travels long distances within flood plumes. Limited understanding of these issues constrains our ability to identify and manage the sediment of greatest risk in the catchment area, and our understanding of how suspended sediment from rivers imparts its ecosystem impact.

1.2. Tracing sediment across the catchment to marine continuum

Internationally, studies that trace flood plume or reef flat terrigenous sediment to upstream catchment and land use sources are rare (e.g. Godiva et al., 2010 (Brazil) and Takesue et al., 2009 (Hawaii) and review by Risk, 2014). This is a clear knowledge gap if we are to manage and reduce the impact of terrestrial sediment on valuable marine ecosystems. Within the GBR, research across the catchment to marine continuum has been undertaken for the Johnstone (McCulloch et al., 2003b) and Fitzroy (Douglas et al., 2006a; Smith et al., 2008) Rivers. Significantly, these studies found basaltic-derived sediments to be preferentially transported the furthest distance offshore (i.e. 10–20 km).

Brooks et al. (2013) recently undertook a comprehensive field study of the Normanby catchment, Cape York, including geochemical tracing of sediments into adjacent Princess Charlotte Bay (PCB). This study identified the coastal floodplain as the dominant source (82%) of terrestrial fine sediment to PCB (a source area not considered in earlier desktop modelling efforts). Despite the importance of these innovative studies, further examination of the flood plume chemical, biological and hydrodynamic processes that control the transformation of terrigenous sediment into harmful, organic-rich sediment flocs is still required. Given the strong relationship between sediment particle size and organic matter content (Koiter et al., 2013), further quantification of the catchment sources of the clay and fine silt fractions (<15.6 µm) is needed, with many previous sediment tracing studies focusing more broadly on the fine ('mud') sediment (<63 µm) fraction (e.g. Storlazzi et al., 2009).

Traditionally, sediment erosion and sourcing studies have primarily sought to address the detrimental effects of sediment and associated contaminants on aquatic and riparian ecosystems, focusing within the catchment boundary (Walling et al., 2011). Hence sediment tracing studies across the catchment and extending into the marine continuum are rare. These studies have also tended to be largely restricted to smaller, temperate river catchments (i.e. <10,000 km^2), with limited application for the larger, tropical river systems that discharge to marine ecosystems (Nagle et al., 1999; Tooth, 2000; Wilkinson et al., 2013). Sampling limitations associated with the spatial and temporal variability of these tropical river catchments have typically restricted research in these settings. Thus there is a growing array of sediment budget and source tracing tools (Koiter et al., 2013; Walling et al., 2011) that have seen limited application in tropical environments, particularly addressing the transport and deposition of sediment across both catchment (i.e. reservoir trapping) and marine (i.e. flood plume dynamics) scales.

1.3. Burdekin River catchment, north-eastern Australia

The Burdekin River catchment (~130,400 km^2) is the largest discrete source of suspended sediment to the GBR (Fig. 1.1), accounting for approximately 30% of the total annual average load from the entire GBR catchment area (~426,000 km^2; Kroon et al., 2012). The Burdekin River has an average annual discharge of 9.18 million ML, and a range of 0.25–54 million ML over a 91-year gauge record (1921–2012; DERM, 2012), reflecting the considerable inter-annual variability associated with this dry-tropical environment. The annual delivery of suspended sediment to the GBR from the Burdekin River is equally variable with an average of 3.93 (80% CI=3.4–4.5) million tonnes and a range of 0.004 to 15.7 million tonnes established for the 24-year period between 1986 and 2010 (Kuhnert et al., 2012). Geochemical records from inshore coral cores influenced by Burdekin River discharge, changes in accumulation rates in sediment cores, and recent catchment modelling all suggest annual sediment export is five to ten times higher than pre-European suspended sediment loads (Bartley et al., 2014; Kroon et al., 2012; Lewis et al., 2014; McCulloch et al., 2003a). Although these sediment loads would be considered low compared to tropical rivers globally (see section 3.5.2), this marked increase in sediment export since European settlement (~1850) threatens GBR ecosystem health. Indeed, Fabricius et al. (2014) have correlated a wetter period (2007–2012) of increased Burdekin River discharge with reduced photic depth within the inshore and mid-shelf regions of the central GBR, and with outbreaks of the crown of thorns starfish (Brinkman et al., 2014; Fabricius et al., 2010). The Burdekin catchment is currently the target of considerable Australian Government 'Reef Programme' expenditure to reduce soil erosion across this catchment.

Figure 1.1 MODIS satellite image (natural colour) of the Queensland coastline and the sediment laden Burdekin River flood plume draining into the Great Barrier Reef near Cape Bowling Green, during the 2011 flood event (Source: NASA Earth Observatory).

Historically research on the Burdekin River has focused on the quantification of end-of-river suspended sediment export (Amos et al., 2004; Belperio, 1979) and transport and fate within the GBR lagoon (Devlin and Brodie, 2005; Lewis et al., 2014; Orpin et al., 2004; Wolanski and Jones, 1981). Sediment source erosion modelling has been used to infer spatial patterns of erosion within the catchment (McKergow et al., 2005; Prosser et al., 2001), however few catchment-specific field data have been available to verify these predictions. In recent decades Government investment within the catchment has seen an increase in sediment sourcing and erosional process studies to inform on-ground investment (reviewed in Bartley et al., 2014). Using instrumented (e.g. series of hillslope runoff flumes) focal drainage areas <14 km^2 (Bartley et al., 2010) and sub-catchment scale (7,000 km^2) geochemical source tracing (Wilkinson et al., 2013), recent research within the Burdekin catchment has identified sub-surface (i.e. >10 cm depth) erosion processes (e.g. gullies, channels, rills) to be the dominant source of sediment loads. Hence the prioritization of sub-surface erosion types for sediment source management is of particular importance for the Burdekin, and other seasonally-dry tropical catchments of northern Australia with similar soils (see review in Bartley et al., 2014; see also Caitcheon et al., 2012; Olley et al., 2013; Thorburn et al., 2013). The new data conflict with earlier catchment modelling efforts which suggested hillslope erosion was the dominant sediment contributor in the Burdekin catchment (McKergow et al., 2005).

Despite this advance in our understanding of Burdekin sediment erosion processes, the systematic identification of source areas across the river basin, and linking sediments entrained in flood plumes to upstream catchment sources have not been successfully achieved to date. The first Burdekin study to trace estuarine and inner shelf sediments to upstream river sources applied the magnetic tracing technique on the medium sand-sized fraction (250–355 µm) (Maher et al., 2009). However, this pilot study had a restricted source area coverage that did not capture the entire Burdekin catchment, and did not consider the finer sediment fractions (i.e. <63 µm), established to be of greater ecological risk to downstream marine ecosystems (Davies-Colley and Smith, 2001; Fabricius, 2005; Weber et al., 2006). Hence there are a number of knowledge gaps relating to sediment sourcing, transport and fractionation/transformation across the entire Burdekin catchment and adjacent coastal flood plumes that require further investigation. Using the Burdekin catchment as a case study, this research will contribute more broadly to understanding of suspended sediment transport processes in seasonally-dry tropical environments, with a focus on the sources and depositional processes (e.g. influence of reservoirs) of specific sediment size fractions. The study will also use the Burdekin catchment to examine the applicability of sediment tracing methods across a catchment to marine plume continuum within a large dry tropical river system, with relevance to how they may be applied to similar systems globally.

1.4. Geography of the study catchment

The Burdekin River catchment is located within the seasonally-dry tropics of north-eastern Australia (Fig. 1.2). It is the second largest catchment draining into the GBR lagoon. The Burdekin catchment includes five major sub-catchments: the Upper Burdekin River; the Cape River; the Belyando River; the Suttor River and; the Lower Burdekin (Fig. 1.2). All but the Lower Burdekin sub-catchment drain into Lake Dalrymple - an artificial lake impounded behind the Burdekin Falls Dam (BFD). Although Lake Dalrymple has a capacity of 1.86 million ML, the dam has overflowed (See Fig. 1.3) every wet season but one since its construction was completed in 1987 (Faithful and Griffiths, 2000), indicating the enormous run-off from this large catchment (capacity to annual inflow ratio =0.24). The Bowen River is the only major sub-catchment that discharges directly into the Burdekin River downstream of the BFD, comprising ~50% of the Lower Burdekin sub-catchment area.

The majority of the catchment is classified as a ‘hot semi-arid’ climate (BSh) under the Köppen-Gieger classification scheme (Peel et al., 2007), although the inter- and intra-annual rainfall and river flood variability of northern Australia is more pronounced than for other semi-arid climates across the globe (see Petheram et al., 2008). Annual rainfall variability is ‘moderate’ to ‘moderate-high’ across the Burdekin according to the Australian Bureau of Meteorology’s ‘index of variability’, representing the 10th and 90th percentiles over average rainfall (www.bom.gov.au/climate/averages/maps.shtml). Rainfall is strongly seasonal, with >80% of annual rainfall and river discharge occurring during the wet season months December to April (Lewis et al., 2006; Lough, 2007). Mean annual rainfall also varies greatly across the catchment, ranging from >1500 mm yr^{-1} in the ‘tropical wet and dry’ Upper Burdekin coastal ranges and Broken River headwaters (north-eastern and eastern corners) to 500 mm yr^{-1} in the driest south-west

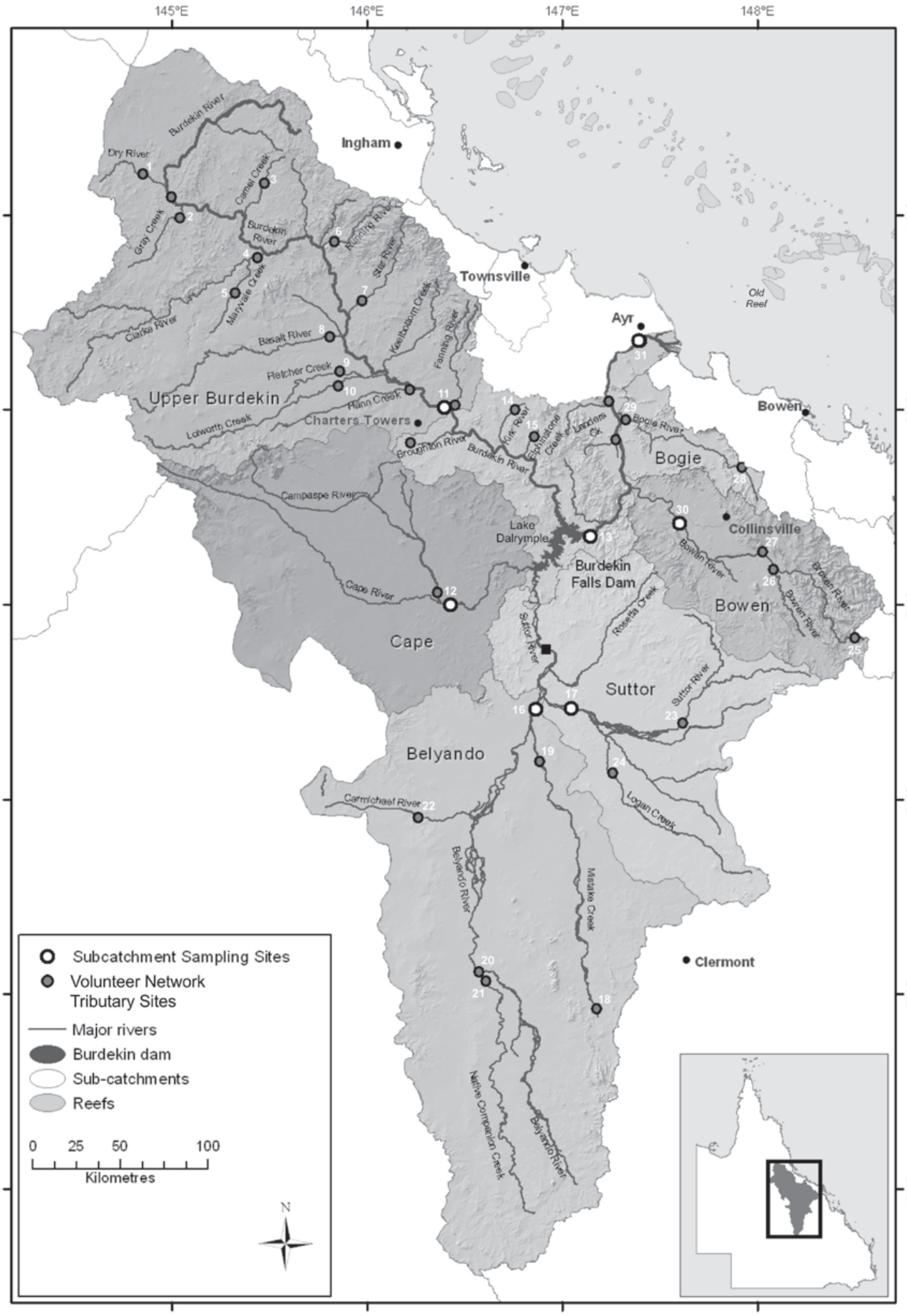

Figure 1.2 Map of the Burdekin River catchment indicating the five major sub-catchment areas, Burdekin Falls Dam and end-of-river sample site locations (white circles) and ungauged tributary network sample sites (grey circles).

corner of the Belyando sub-catchment (Fig. 1.4). This range is the largest for any watershed along the Australian east coast (Rustomji et al., 2009). Locally this region is defined as ‘seasonally-dry tropical’, a definition that is also adopted in this study. Because of the seasonally-dry tropical climate most streams within the Burdekin catchment are ephemeral, and streamflow predominately occurs as ‘flood events’ where streams rapidly rise when fed by wet season rainfall runoff. Negligible streamflow typically occurs during the dry season (May−November). Wetter years often result from monsoonal and cyclonic events, which are strongly modulated by the La Niña wetter phase of the El Niño–Southern Oscillation (ENSO) cycle (Lough et al., in press; Rustomji et al., 2009). This climatic variability significantly influences sediment runoff generation and transport each wet season; for example, drought-breaking floods carry considerably higher suspended sediment loads (Amos et al., 2004; Kuhnert et al., 2012; Mitchell and Furnas, 1996).

Figure 1.3 Burdekin Falls Dam spillway at flood peak in 2009 (5th February).

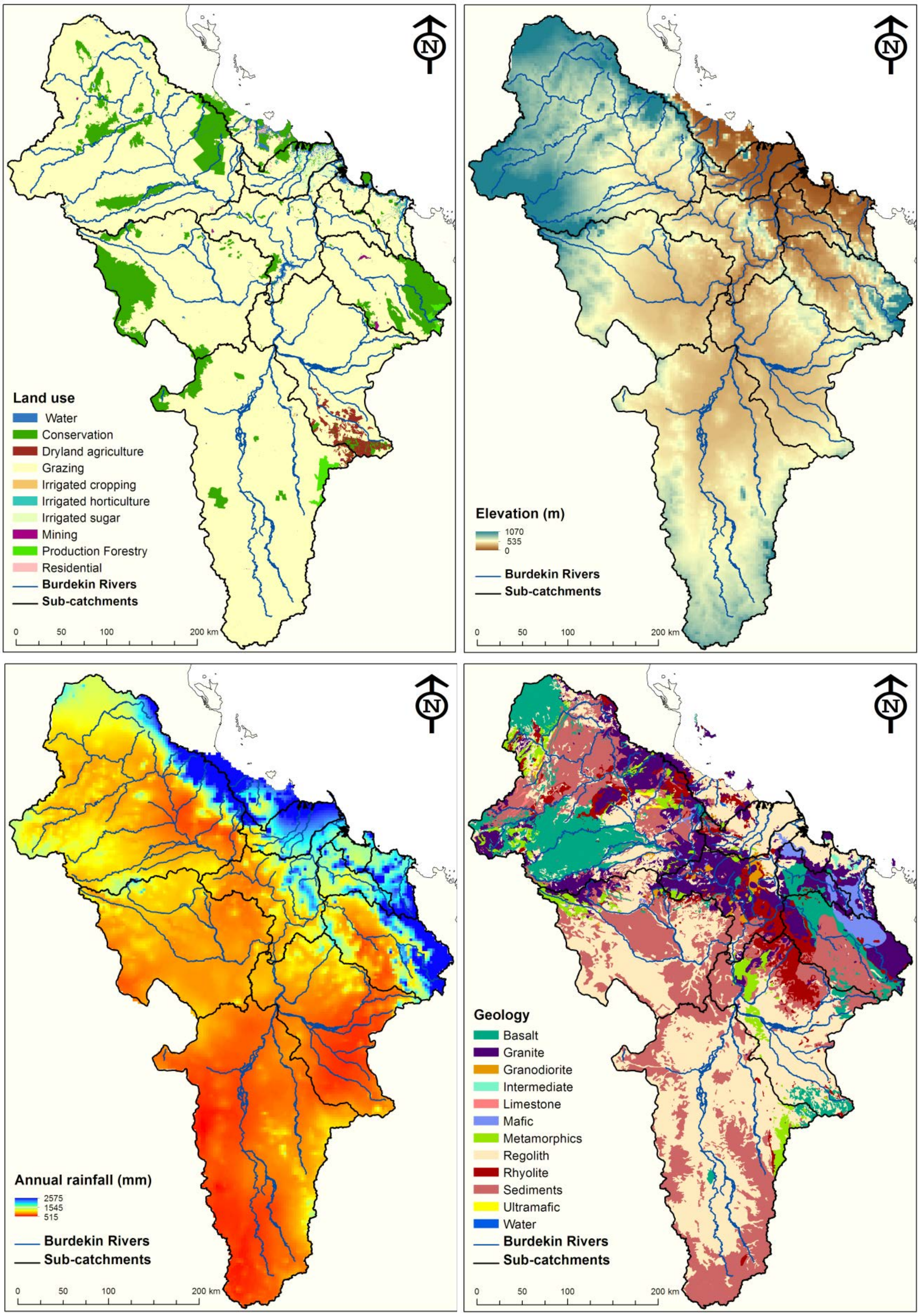

Figure 1.4 Burdekin River land use, elevation, annual average rainfall and geology (Source: Geoscience Australia).

The coastal mountain ranges that enclose the eastern margins of the Bowen and Upper Burdekin Rivers have peaks rising up to 1,070 m and are steeply sloped, vegetated with rainforest, and receive the highest mean annual rainfall (up to 2,370 mm yr^{-1}) across the Burdekin (Fig. 1.4). Steep mountain ranges reaching 900 m in height also form the western boundary of the Upper Burdekin. Large areas within this sub-catchment are strongly undulating, draining into an incised river channel lined with inactive terraces and high upper banks (Fig. 1.5). Eucalypt savannah woodlands dominate the Upper Burdekin sub-catchment. The Bowen sub-catchment is also characterised by low undulating hills and steeper ridges in the upper catchment, and an incised valley system through remnant volcanic hills (Roth et al., 2002). Volcanic and sedimentary rock types dominate these two sub-catchments (Fig. 1.4). Extensive areas of erodible red duplex soils, black and red basaltic soils, and sodic duplex soils occur in the Upper Burdekin. Red-brown earths, yellow soils, granite/sandstone derived gravely/sandy soils and black earths cover large areas of the Bowen River catchment (Roth et al., 2002). In comparison the inland western sub-catchments (the Cape, Belyando and Suttor Rivers) drain gently undulating lowlands and alluvial plains, with wide multi-thread rivers, and with lower maximum elevations (300–450 m) located along the western boundary of the Cape and Belyando Rivers. Eucalypts, acacias (Brigalow Belt) and grasslands dominate these drier sub-catchments, with average annual rainfall below 700 mm yr^{-1} (Fig. 1.4). Remnant sedimentary basins and cracking clay soils form the dominant rock and soil types within these sub-catchments, with grey/brown clays and red/yellow earths also widespread in the Belyando and Suttor sub-catchments (Roth et al., 2002).

Figure 1.5 Upper Burdekin River at Sellheim streamflow gauge during the 2009 flood peak.

Cattle grazing across eucalypt savannah woodlands is the dominant (>90%) land use in the Burdekin catchment. Vegetation clearing across the Burdekin is variable and most widespread in the Brigalow country of the Belyando, Suttor and Cape Rivers for improved pastures and cropping (Roth et al., 2002). More details about this region can be found in Roth et al. (2002) and the regional Natural Resource Management (NRM) body, North Queensland Dry Tropics website (www.nqdrytropics.com.au).

1.5. Thesis aims and objectives

The primary aim of this thesis is *to characterise and source Burdekin River flood plume suspended sediment, which is most likely to directly affect coral reef and seagrass ecosystems of the central GBR, north-eastern Australia*. Novel sediment budget and tracing techniques are applied to this large, seasonally-dry tropical catchment to examine and quantify suspended sediment sources and transport across the catchment to marine continuum, and to test their validity at this scale. The transformation and dispersal of suspended sediments and associated nutrients exported from the Burdekin catchment within the GBR lagoon through coastal flood plumes are also investigated. This study specifically focuses on the sources, transport and dispersal of different sediment size fractions, recognising the increased risk of finer sediment fractions (<15.6 µm) pose to downstream marine ecosystems (section 1.1). The specific research objectives of this study include:

Objective 1: Identify and describe the hydrodynamic, biological and chemical processes controlling the transformation and dispersal of suspended sediments and particulate nutrients in flood plumes delivered to the GBR lagoon from the Burdekin River.

Objective 2: Identify and characterise the sediment types that are likely to affect the greatest area of the GBR and have the most severe direct impacts on GBR ecosystems.

Objective 3: Identify major sources of suspended sediment in the Burdekin catchment, including the spatial and temporal variability of suspended sediment sub-catchment contributions, by constructing a catchment-wide budget and partition the budget into defined (Objective 2) suspended sediment particle size fractions.

Objective 4: Examine the potential of clay mineralogy-based tracing to discriminate discrete sediment sources and trace flood plume suspended sediment within a large, geologically complex catchment.

1.6. Overview of research methods

River water surface (top 0.5 m) ‘grab’ samples were collected from 31 sites across the Burdekin River catchment in an extensive sampling campaign conducted over seven consecutive water years (2004/05–2010/11). Water years (1st October to 30th September) are used to describe annual discharge throughout this study, as the summer wet season and associated river discharge falls across calendar years. Each site was frequently sampled to capture all stages of the hydrograph over multiple streamflow events that occurred each wet season. Sampling sites included seven streamflow gauge locations draining the five major sub-catchments of the Burdekin River, a major reservoir outlet and the end-of-river freshwater discharge point. In addition, a network of 24 landholders was established and formally trained to collect water samples at ungauged minor tributary locations across the Burdekin. These sites were established to increase the spatial density of the dataset collected across this sparsely populated (~25,000 people) and large (130,400 km^2) river catchment, and included locations inaccessible to external visitors during floods. Sampling of the gauged sites and retrieval of the landholder collected samples included frequent field trips (often covering 800+ km/trip) repeated each wet season, with over 1,600 water samples collected in total during the study.

River water samples were used to measure total suspended solids (TSS) concentrations and to calculate suspended sediment loads for each gauged site over consecutive sampled wet seasons. These loads were used to construct a series of catchment-wide suspended sediment budgets for five of the studied water years. A subset of collected water samples from across the sites (504 samples) were analysed for sediment particle size using laser diffraction (Malvern Mastersizer 2000) to examine particle size-specific sub-catchment load contributions. A comprehensive clay mineral dataset of 231 samples was also produced using X-ray diffraction on the <10 µm sediment fraction to further characterise and quantify Burdekin sediments and their sources.

Complementing the catchment sampling campaign, samples were collected from the Burdekin River flood plumes adjacent to the mouth over the later wet seasons of the study from 2007/08 to 2010/11. These samples were collected from the surface waters of the turbid inner plume (i.e. ‘Primary’ water type; see Petus et al., 2014, Appendix A) immediately following peak discharge at the end-of-river site, and along a suspended sediment-salinity gradient within 10 km from the river mouth. Samples were analysed for TSS, sediment particle size, clay mineralogy and salinity. An enhanced sampling effort of the 2010/11 flood plume included additional sub-surface sample collection and analysis of nitrogen and phosphorus species concentrations as well as extending the spatial monitoring coverage to include sites containing coral reefs and seagrass meadows. Microphotographs of collected plume water samples were also captured in the laboratory immediately following sample collection to further examine the physical properties of the suspended particulate matter.

1.7. Significance of research

A novel approach to the study of suspended sediment sources, transport and dispersal across the catchment to marine continuum is presented for a large, seasonally-dry tropical river located in the GBR, Australia. Characteristics of terrigenous sediments ‘of most risk’ to tropical marine ecosystems are firstly defined through the examination of adjacent coastal flood plumes, and are then utilised to examine and quantify the catchment sources of this sediment. Based on a spatially and temporally intensive sampling campaign conducted over seven water years, this study provides a rare suspended sediment dataset collected during a series of unusually large rainfall and river discharge years (Fig. 5.1) capturing the entire catchment area of this dry tropical river. This research contributes to our understanding of suspended sediment sources, transport and depositional (i.e. reservoirs) processes for large, seasonally-dry (or semi-arid) tropical river systems, and specifically, the quantification of the finer clay and silt particle size fractions of most harm to tropical marine ecosystems. Catchment-wide sediment budgets using sub-catchment suspended sediment loads, and sediment tracing using clay mineralogy across the catchment and adjacent coastal flood plume are applied to test the validity of these techniques in a poorly studied environment, and to provide multiple lines of evidence for the identification of suspended sediment sources.

1.8. Thesis structure

This thesis is presented as a series of research chapters formatted for journal publication. The interactions between each of the study objectives and data chapters are illustrated in Figure 1.6. This figure also illustrates the linkages across the catchment and marine components of this thesis. Supplementary figures and tables relevant for each data chapter as well as supporting publications are provided as appendices.

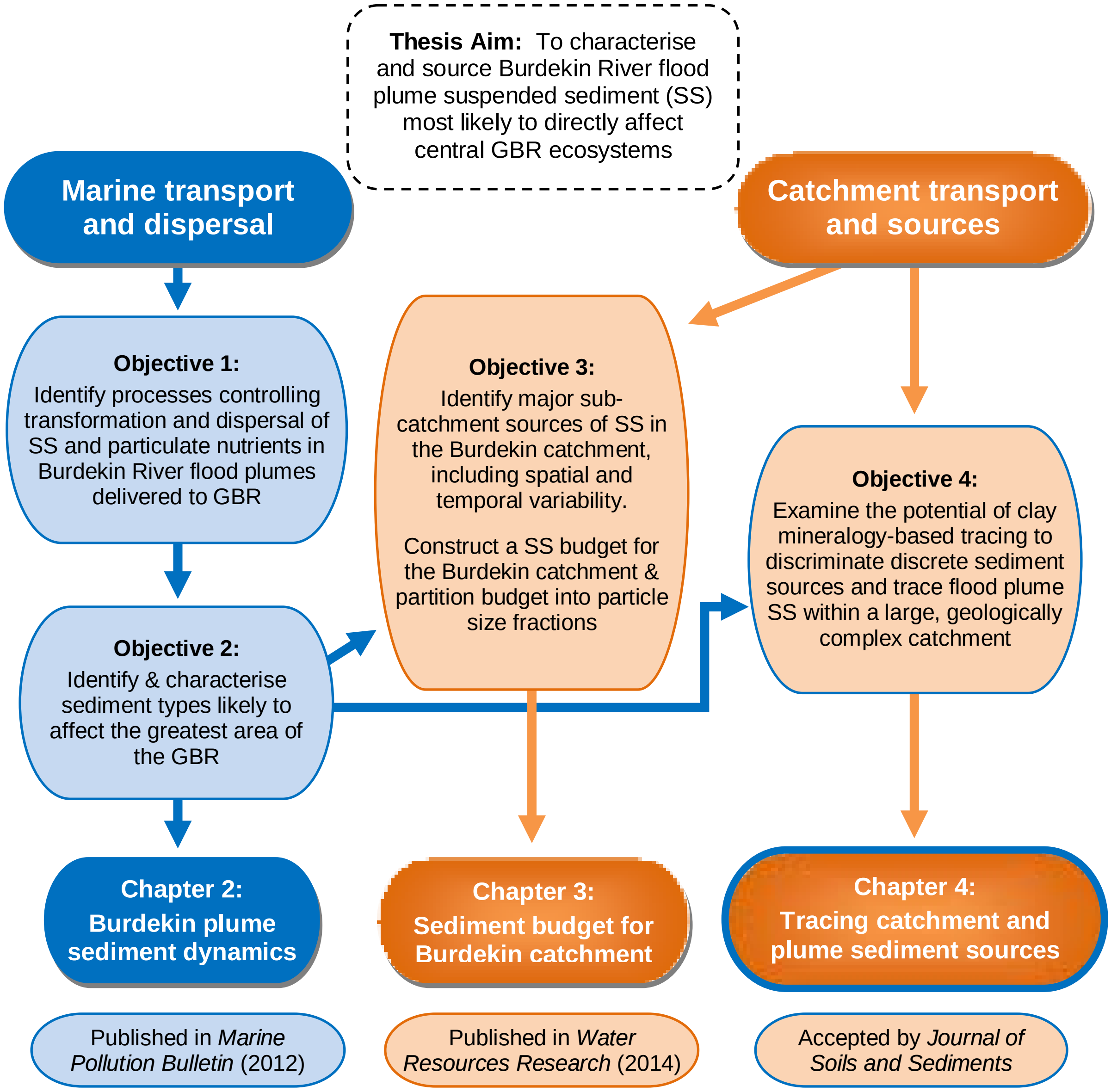

Figure 1.6 Research framework and thesis structure.

Chapter 2 examines suspended sediment and particulate nutrient interactions within a Burdekin River flood plume, including the influence of particle size and flocculation processes on the dispersion of terrestrial sediment within the GBR lagoon. Following a large wet season Burdekin River discharge event (2010/11) adjacent flood plumes were sampled along a suspended sediment-salinity gradient from the river mouth to examine sediment and nutrient transformations within plume waters. Microphotographs of suspended particulate matter captured from collected water samples were used to further examine how terrestrial sediment was dispersed within the GBR. The dispersal of particulate nutrients in flood plumes has received little attention in the GBR and this chapter also seeks to address this research gap. This chapter quantifies the sediment size fraction most likely to affect the largest area of the GBR to refine catchment sediment source identification undertaken in Chapters 3 and 4. Chapter 2 is presented in the format of a scientific research paper and has been published in the journal *Marine Pollution Bulletin* (Bainbridge et al., 2012).

Chapter 3 uses annual streamflow discharge and sub-catchment suspended sediment loads calculated for each of the seven gauged study sites to construct a series of catchment-wide budgets for five consecutive water years (2005/06 – 2009/10). These annual water and sediment budgets represent the five major sub-catchments of the Burdekin, a major reservoir outlet (BFD) and the end-of-river site, and include annual sediment trapping estimates for this reservoir as reported in supporting publication Lewis et al. (2013; Appendix D). Annual suspended sediment loads for each site are calculated using the Loads Regression Estimator tool developed in supporting publication Kuhnert et al. (2012; Appendix E) and includes a measure of uncertainty for each load. The sediment budgets are used to examine inter-annual variability in sub-catchment source contributions to end-of-river sediment export, as well as the influence of the BFD reservoir and seasonally-dry tropical climate on annual sediment export. Tributary 'hot-spot' sediment sources are also examined using TSS concentration data collected by the landholder volunteer network.

The previous chapter identified the preferential transport of clay and fine silt sediment fractions (i.e. <15.6 μm) within the GBR, highlighting the importance of incorporating sediment particle size into catchment sediment budgets. Global studies investigating the transport of specific sediment size fractions within tropical catchments have been limited to date. Chapter 3 addresses this knowledge gap and incorporates the research findings of Chapter 2 by constructing a revised sediment budget quantifying the contribution of clay (<3.9 µm), fine silt (3.9–15.6 µm) and coarse (>15.6 µm) sediment fraction loads across the Burdekin catchment. The trapping of each of these specific size fractions within the BFD reservoir is also considered. This chapter is presented in the format of a scientific research paper and has been published in the journal *Water Resources Research* (Bainbridge et al., 2014).

Chapter 4 tests the applicability of a clay mineral sediment source tracing technique on this large, seasonally-dry tropical catchment. Most commonly sediment source tracing studies have been conducted on small river catchments (<10,000 km^2 area), and utilise the isotopic or geochemical properties of sediment as tracers. Sediment tracing using clay minerals has the capacity to discriminate sub-catchment and geologically distinctive source-related 'fingerprints' and may be more robust than traditional tracers which can be compromised by transformation processes (e.g. particle selectivity, mineralization, adsorportion/desorption). This chapter builds on the sub-catchment source identification in Chapter 3 to further discriminate geological source areas of end-of-river and flood plume sediments, encompassing the catchment and marine continuum. In particular, this study confirmed the reliability of a clay mineral ratio to isolate distinct geological sources, proving its applicability more broadly across the GBR catchment area and other geologically diverse catchments. This chapter also provides an additional line of evidence to support the sediment budgets, and focuses only on the <10 µm sediment fraction. The clay mineral dataset includes over 200 sediment samples collected over six consecutive wet seasons and covers a large spatial area from upstream tributary sources to the adjacent flood plume. This chapter is also presented in the format of a scientific paper and has been accepted by the *Journal of Soils and Sediments*.

Chapter 5 discusses and summarises the key findings of each research chapter in the context of the four identified research objectives. The research gaps addressed by this study are outlined, including contributions to the following fields of research: a) sediment sourcing and tracing; b) sediment transport and catchment budgets, specifically in seasonally-dry tropical (semi-arid) environments and for large river catchments; c) reservoir influence on sediment particle size and clay mineral transport;

and d) flood plume sediment fractionation and dispersal. Limitations of this study and further research opportunities are also discussed and the main conclusions of this research project are outlined.

2. Fine sediment and nutrient dynamics related to particle size and floc formation in a Burdekin River flood plume

Bainbridge Z.T., Wolanski E., Alvarez-Romero J.G., Lewis S.E. and Brodie J.E. 2012. Fine sediment and nutrient dynamics related to particle size and floc formation in a Burdekin River flood plume, Australia. Marine Pollution Bulletin 65, 236-248. DOI: 10.1016/j.marpolbul.2012.01.043

Abstract

The extreme 2010/11 wet season resulted in highly elevated Burdekin River discharge into the Great Barrier Reef lagoon for a period of 200 days, resulting in a large flood plume extending >50 km offshore and >100 km north of the river mouth. Exported suspended sediment was dominated by clay (<4 µm) and fine silt (4–16 µm) fractions and most sediment initially settled within ~10 km of the river mouth, and before salinity rose to 0.1 psu. Biologically-mediated flocculation of these particles enhanced deposition in the initial low salinity zone. This is the first study in the GBR to investigate particle size partitioning within river flood plumes and confirms the importance of flocculation processes in the dispersion and deposition of terrestrial particulate matter in the GBR lagoon. Fine silt and clay particles and nutrients remaining in suspension were carried as far as 100 km northward from the mouth, binding with planktonic and transparent exopolymer particulate matter to form large floc aggregates (muddy marine snow). These aggregates, due to their sticky nature, likely pose a risk to benthic organisms (e.g. coral and seagrass) through smothering, and also by contributing to increased turbidity during wind-induced resuspension events.

Keywords: Great Barrier Reef; muddy marine snow; grain size; catchment runoff; sediment export; nitrogen; flocculation.

2.1. Introduction

The mechanisms that control the dispersal and fate of land-derived suspended sediment and nutrients discharged to coastal waters must be understood if the risks to marine ecosystems (i.e. sedimentation, turbidity and eutrophication) are to be identified and managed. The physical and biological processes that govern the initial dispersal of sediments and nutrients exported from coastal catchments are poorly understood for tropical rivers that drain into the GBR lagoon, yet these processes influence the physical characteristics and hydrodynamic behaviour of these contaminants and the subsequent effects on receiving estuarine and marine ecosystems (Brodie et al., 2012a). A general decline in the overall ecosystem health of the GBR has partially been linked to an increase in suspended sediment, nitrogen and phosphorus terrestrial loads exported to the lagoon, resulting from agricultural development of the adjacent catchment area (Brodie et al., 2011, 2012a; Bruno and Selig, 2007; De'ath and Fabricius, 2010; Hughes et al., 2011 but see also Sweatman et al., 2011; Sweatman and Syms, 2011). Determining the key mechanisms that disperse and partition these contaminants in the lagoon is critical to identify those that pose the greatest threat to marine ecosystems.

Most terrestrial sediment and nutrients are exported to the GBR lagoon by wet season discharge from coastal rivers (Devlin and Brodie, 2005; Devlin et al., 2012). Previous studies demonstrate that much of the suspended load settles out within 5 km of the coastline (Belperio, 1983; Devlin and Brodie, 2005; Wolanski and Jones, 1981; Wolanski et al., 2008), where it may be later resuspended by wind-generated waves and currents and transported to north-facing embayments or transported offshore as near-bottom nepheloid layers (Brinkman et al., 2004; Lambeck and Woolfe, 2000; Lambrechts et al., 2010; Larcombe et al., 1995; Orpin et al., 2004; Webster and Ford, 2010). Dissolved nutrients carried in flood plumes initially disperse conservatively along the salinity gradient from the river mouth (Brodie et al., 2010; Devlin and Brodie, 2005). After the bulk of fine sediment has settled out of the plume, the biologically available nutrient component (e.g. dissolved inorganic nitrogen) is rapidly taken up by phytoplankton as the reduced turbidity increases light availability for primary production (Dagg et al., 2004; Davies et al., 2004; Rabalais et al., 1996; Robertson et al., 1993; Turner et al., 1990). Particulate nutrients in fine terrestrial sediments are also an important component in biogeochemical cycles within the GBR (Brodie et al., 2011;

Furnas et al. 2005) and account for 60–80% of the total terrestrial nutrient load to the lagoon (Furnas, 2003; Kroon et al., 2012). However, the dispersal of particulate nutrients in flood plumes has received little attention in the GBR.

Fine sediment and associated nutrients carried by river plumes flocculate upon mixing with seawater to form larger aggregates due to changes in physico–chemical conditions (e.g. pH and ionic strength) and biological activity (Dagg et al., 2004). Bacteria as well as selected phytoplankton (e.g. diatoms) and metazoans produce mucopolysaccharides which through coagulation and inclusion of detritus, faecal matter and microorganisms form large, sticky transparent exopolymer particles (TEP: see Dagg et al., 2004; Passow et al., 2001). These TEP form muddy marine snow as they aggregate with mineral particles in coastal waters (Ayukai and Wolanski, 1997; Fabricius et al., 2003; Passow et al., 2001). Bacteria form TEP in highly turbid, low salinity plume waters (i.e. typically TSS concentrations >50 mg L^{-1} and salinities <26 psu) with low photosynthetically active radiation (PAR: Bianchi et al., 1992, 1994; Ducklow and Kirchman, 1983), while TEP are commonly produced by phytoplankton (e.g. diatoms) in less turbid plume waters with increased levels of PAR (Ayukai and Wolanski, 1997; Passow et al., 2001). The fine sediment and nutrients that drive this biological activity are closely linked and must be studied together.

Using the Burdekin River as a case study, this investigation builds on existing research and examines the influence of sediment particle size and flocculation processes on the transport and deposition of exported terrigenous sediment and associated nutrients in river flood plumes discharged to the GBR lagoon. The data are derived from sampling of a Burdekin River flood plume produced by a major discharge event (10.69 million ML) in the 2010/11 wet season.

2.2. Materials and methods

2.2.1. Freshwater and plume sample collection

The Burdekin River had a total discharge of 34.83 million ML in the 2010/11 water year (Oct–Sept), which is the 3rd largest discharge measured since 1922 at the end-of-river gauging station at Inkerman/Clare (Fig. 2.1; DERM, 2012). The sampling focused on flood event No. 1 that occurred between the 24th December 2010 and 18th January

2011, with a total discharge of 10.69 million ML which represents 31% of the total flow (Fig. 2.2a). A peak discharge of 888,775 ML day^{-1} occurred on the 27th December (DERM, 2012). River water (zero salinity) samples were collected at Inkerman Bridge throughout this discharge event, as well as two subsequent flood events from the 31st January to 22nd February (No. 2) and 4th March to 18th April (No. 3), to capture further changes in sediment dynamics (see Fig. 2.2a for frequency). The Inkerman sampling site is ~26 km downstream of the Clare gauging station (GS120006B).

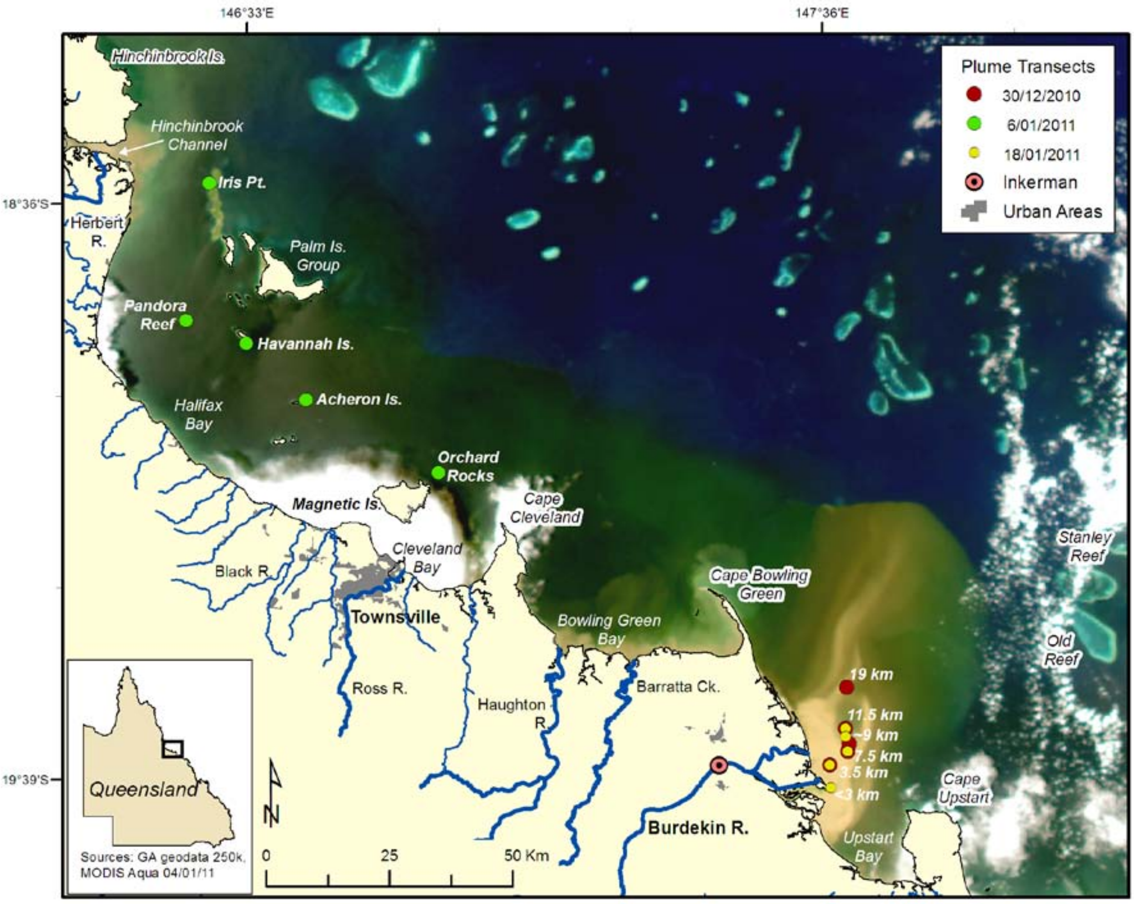

Figure 2.1 Location map superimposed on a MODIS satellite image of the Burdekin River flood plume captured on the 4th January, 2011. The turbid inner plume is clearly visible along the coast adjacent to the river mouth, with the plume extending ~50 km out from the coast. The three plume sampling transects are displayed, as well as the freshwater sampling site at Inkerman. White patches along the coastline near Townsville and Cape Upstart are clouds.

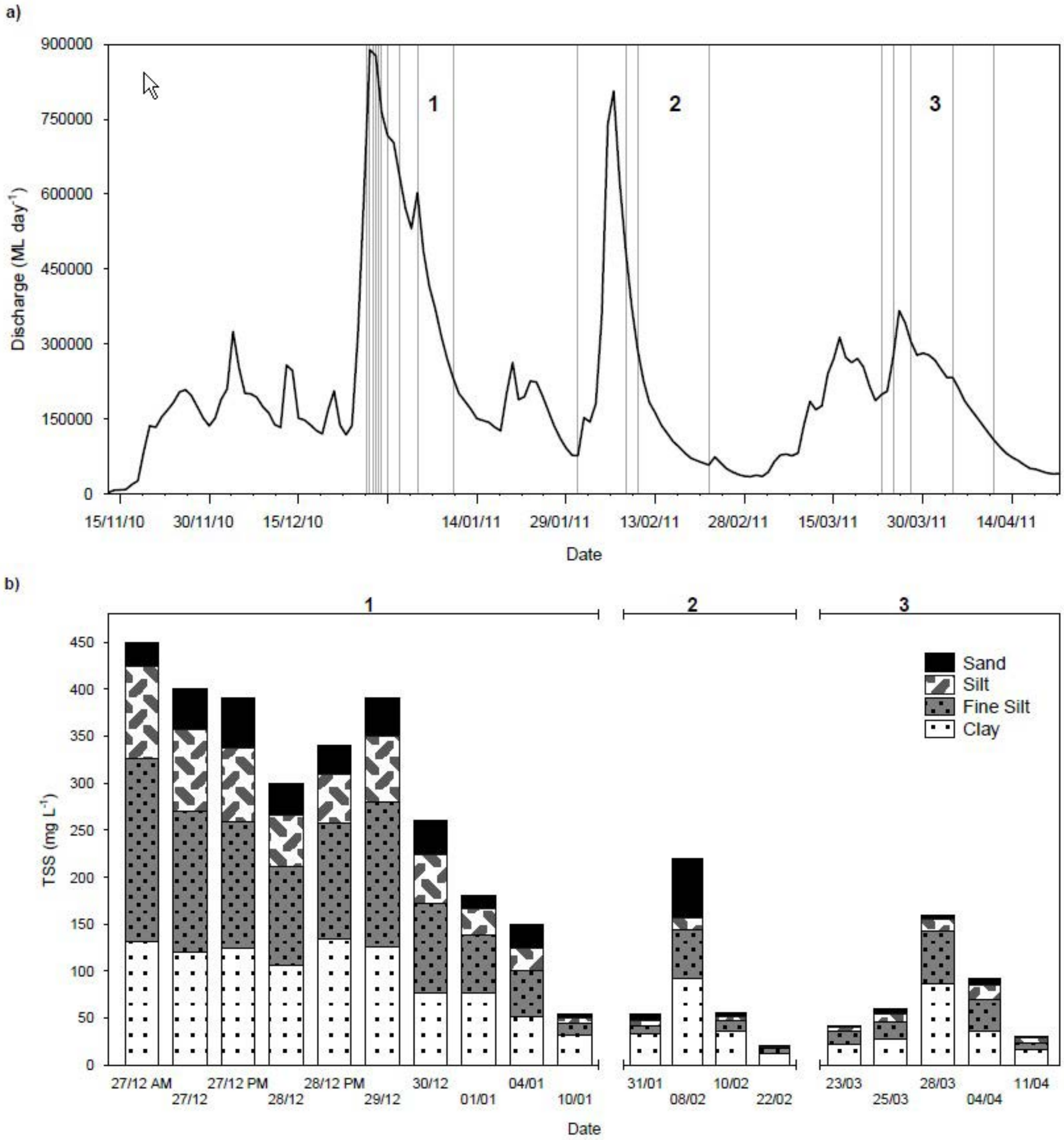

Figure 2.2 (a) Time-series of Burdekin River discharge at Clare (120006B) during the 2010/11 wet season. River water sample collection dates at Inkerman are overlayed as grey vertical lines grouped into three flood events. (b) Graph of TSS concentrations for the Burdekin River (Inkerman) surface water samples grouped into the three separate flood events as displayed in (a). The sediment particle size composition of each sample is also represented using four particle size classes: clay (<4 µm), fine silt (4–16 µm), coarse silt (16–63 µm) and sand (>63 µm).

The inshore turbid ‘inner’ plume, directly adjacent to the river mouth was sampled three days after the flood peak (30th December; Plume Transect 1). Samples were collected along the central plume axis following the salinity gradient from the river mouth to 19 km offshore (Fig. 2.1). This transect was repeated 3 weeks later (18th January; Plume Transect 3) to examine the evolution of the plume, however due to tidal and safe navigation constraints Transect 3 only extended 11.5 km offshore. A northern transect was also conducted from Magnetic Island to the Palm Island Group (6th January; Plume Transect 2) to sample the northerly migration of the Burdekin River plume previously observed by Devlin and Brodie (2005), Wolanski and Jones (1981) and Wolanski and van Senden (1983). This northern plume extent was confirmed during this study using near real-time MODIS Rapid Response (true colour) satellite imagery (see Fig. 2.1; http://rapidfire.sci.gsfc.nasa.gov).

River water samples were collected from the surface (top 0.5 m) in pre-rinsed 1L polypropylene bottles and transported on ice to the TropWATER Laboratory, James Cook University (JCU), Townsville for analysis of total suspended solids (TSS), volatile suspended solids (VSS), and the School of Earth and Environmental Sciences (JCU) for particle size analysis. One litre plume water samples were collected from the surface and sub-surface (2 and 5 m depth) for TSS, VSS and particle size analyses. Unfiltered nutrient samples (surface waters only) were sub-sampled into 60 mL Sarstedt sterile polypropylene vials, with filterable nutrients filtered on-site through pre-rinsed filter modules (Sartorius MiniSart 0.45 µm cellulose acetate) into six 10 mL Sarstedt polypropylene vials. Nutrient samples were immediately placed on ice and frozen within 6-h of sampling. Vertical salinity profiles (i.e. surface to seafloor at varying depths) were conducted at each site using a SBE 19plus (V2) CTD profiler (Sea-Bird Electronics, USA). Salinity is expressed in practical salinity units (psu). Data from these vertical profiles were used to create salinity contour maps of the inner plume using the Surfer software program (v.7.0, Golden Software, USA), including five salinity profiles along each inner plume contour map transect.

2.2.2. Laboratory analysis

Water samples were analysed for TSS, VSS, total nitrogen (TN), total phosphorus (TP), as well as the dissolved nutrient fractions (i.e. <0.45 µm) including total filterable nitrogen (TFN), total filterable phosphorus (TFP), ammonia, nitrate, nitrite and filterable reactive phosphorus (FRP).

Dissolved and particulate nutrients

Samples for TN, TP, TFN and TFP were digested in an autoclave using an alkaline persulfate technique (modified from Hosomi and Sudo, 1986) and the resulting solution simultaneously analysed for nitrate-N and orthophosphate-P by segmented flow auto-analysis using an O.I. Analytical (Texas, USA) Flow Solution IV chemistry analyser. The analyses of nitrate, nitrite, ammonia and FRP were conducted using segmented flow auto-analysis techniques following standard methods (APHA, 2005). Particulate nutrient concentrations were calculated by subtracting the total filterable nutrient concentrations from the total nutrient concentrations. Similarly, dissolved (filterable) organic nitrogen (DON) and phosphorus (DOP) were calculated by subtracting nitrate, nitrite and ammonia (for nitrogen) and FRP (for dissolved inorganic phosphorus) from the TFN and TFP concentrations, respectively.

Total and volatile suspended solids

TSS (in mg L^{-1}) was measured gravimetrically by weighing the fraction remaining on a pre-weighed Whatman GF/C filter (nominally 1.2 μm pore size), dried at 103–105°C for 24 h, after vacuum filtration of a measured volume of sample (Method 2540D; APHA, 2005). The residual filter paper was ignited to 550°C, with the weight loss on ignition indicating the volatile solid (i.e. organic) component (Method 2540E; APHA, 2005).

The Water quality Analyser tool (eWater CRC and the Queensland Department of Environment and Resource Management; website: ewater.com.au) was used to calculate a TSS load for flood No. 1 at Inkerman using the linear interpolation technique (Lewis et al., 2007). Although only surface data (i.e. top 0.5 m) were used in the calculation of this load, previous research by Amos et al. (2004) has shown that TSS concentrations are relatively constant with depth through the channel cross-section for the Burdekin River at Inkerman. Due to the limited TSS concentration data available for flood events No. 2 and No. 3, loads were not calculated for these events.

Particle size and floc analysis

Particle size analysis was restricted only to samples with higher TSS concentrations (generally >10 mg L^{-1}), which included all river samples and the plume surface samples collected along inner Plume Transect 1 (30/12/10) shortly after peak discharge conditions. Particle size distributions for the water samples were determined using the Malvern Mastersizer 2000, a laser diffraction particle-size analyser with a lens range of 0.02–2000 μm. The parametisation methodology of Sperazza et al. (2004) was applied, and all data presented are the mean of three measurement runs. Flood plume samples were first treated with a 1% solution of sodium hexametaphosphate (Calgon®) and sonicated for 20 minutes immediately prior to analysis to disperse flocculated particles and ensure the measurement of absolute particle size only (Jonkers et al., 2009; Malvern, 1997; Sperazza et al., 2004). On the basis of particle size distributions derived using this method sediments were classified as one of four size classes based on the Udden-Wentworth sediment grain size scale (Leeder, 1982): (1) clay (<3.9 µm); (2) very fine and fine silt (3.9–15.6 µm; hereafter referred to as fine silt); (3) medium and coarse silt (15.6–63 µm; hereafter referred to as coarse silt); and (4) sand (>63 µm). The clay and fine silt fractions are defined as <4 µm and <16 µm, respectively hereafter in the thesis for simplicity. Microphotographs of flood plume suspended particulate matter (i.e. mineral particles, algal cells, biological remains, muddy marine snow) were collected using Ayukai and Wolanski's (1997) method.

Satellite image processing

Ocean colour algorithms applied to satellite imagery have been used to study the movement and composition of flood plumes (e.g. Andréfouët et al., 2002; Brodie et al., 2010; Devlin et al., 2012). Complementary to the use of algorithms, true-colour classification techniques can provide information on surface water characteristics (e.g. suspended sediment, see Duane Nellis et al., 1998) and offer a valuable alternative to traditional plume mapping. MODIS Aqua and Terra true colour satellite images (1 km resolution - available from NASA OceanColor website: http://oceancolor.gsfc.nasa.gov/cgi/browse.pl) were used to identify and map the Burdekin River flood plumes following the Devlin et al. (2012) method. In addition a combination of spectral enhancement and unsupervised classification (ISO method) of the images using ERDAS Image Analyst extension for ArcGIS 10 were used to depict turbidity changes in plume surface waters (Fig. 2.3). Observed variation in turbidity was validated against MODIS Level 2 products (see Appendix Fig. A2.4) and is depicted by a transition in colours on the classified imagery in Fig. 2.3 from red (turbid zone), yellow (transitional) to green (plume boundary). Wind direction was added to the images using a three-day average (i.e. date of image capture and 2 days prior) from the Australian Institute of Marine Science's (AIMS) Data Centre 'Cape Bowling Green' weather station (http://data.aims.gov.au) to provide a context for plume movement between images taken at different times. Image selection in Fig. 2.3 was based on the best available sub-set given atmospheric and cloud coverage interferences.

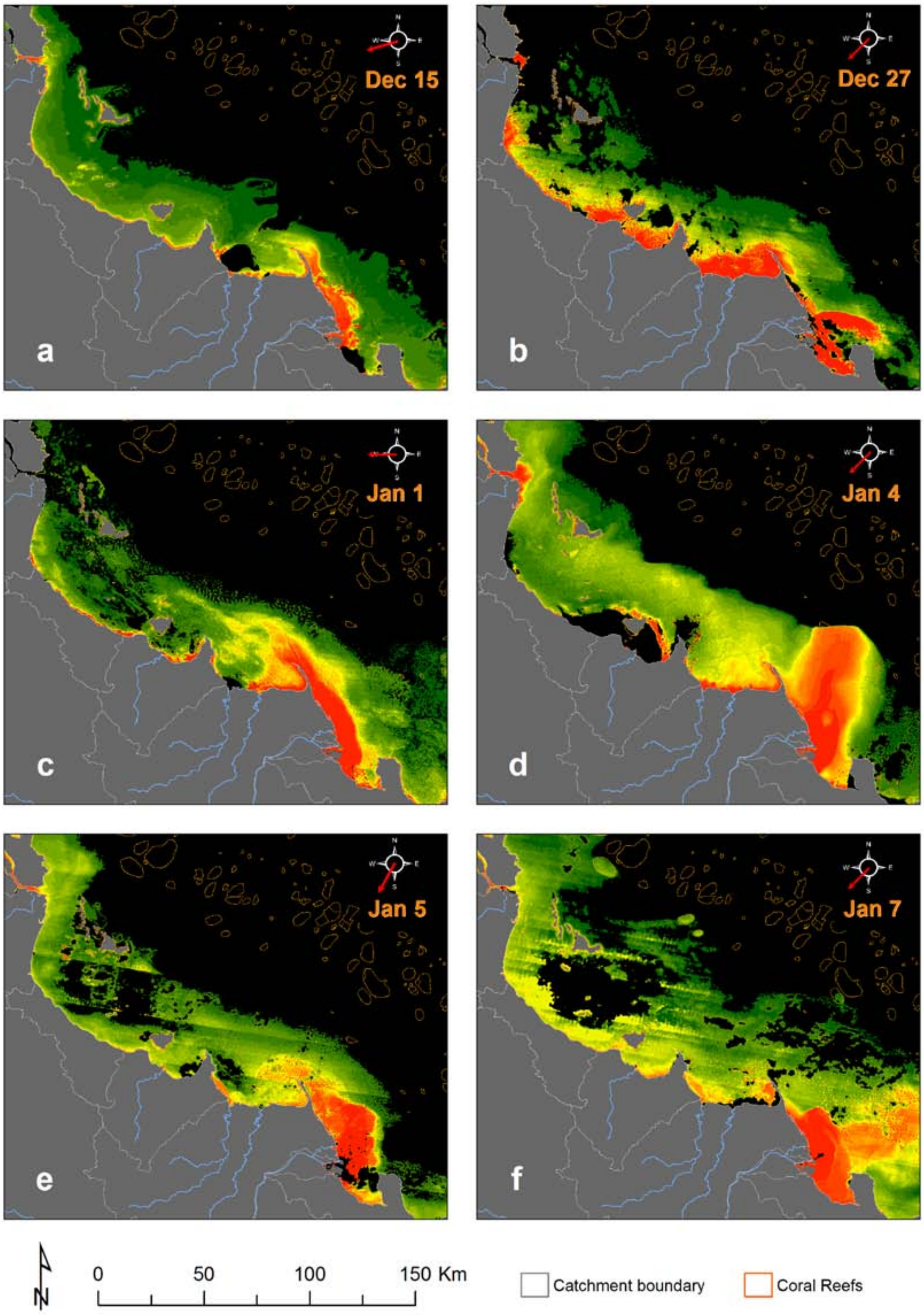

Figure 2.3 Classified true-colour MODIS satellite images show the evolution of the Burdekin River flood plume from the 15/12/10 to 07/01/11. The images show the changes in the flood plume from the inner turbid plume (red) through the transition (yellow) to the less turbid plume boundary, delineated by the darker green colour, which is still observable as green water in true-colour images (see Fig. 2.1). Three-day average wind direction is displayed on each image, and corresponding wind speed was <4 m s^{-1} (a), >7 m s^{-1} (b), <7 m s^{-1} (c), <4 m s^{-1} (d) and <3.5 m s^{-1} (e and f). Black areas marked over the plume depict areas where no data were retrieved due to cloud cover. Supp. Video 1 (in Bainbridge et al., 2012) provides additional imagery dates and an expanded scene capture.

2.3. Results

2.3.1. Burdekin River discharge and suspended sediment export

TSS concentrations in the Burdekin River (Inkerman) during flood No. 1 ranged from 450 mg L^{-1} during the flood peak to 55 mg L^{-1} at the tail of the event (Fig. 2.2b) and the total suspended sediment export was calculated at 2.8 million tonnes. Clay and fine silt fractions dominated the suspended sediment load throughout the event (36% and 35%, respectively), with smaller proportions of coarse silt and sand (18% and 12%, respectively). During the two subsequent floods (No. 2 and 3) concentrations rose again during the flood peaks, however there was a general decline in TSS concentrations during the wet season from an average of 290 mg L^{-1} in flood event No. 1 to 75 mg L^{-1} in event No. 3 (Fig. 2.2b). The proportion that the coarse silt and sand fractions represented of total suspended sediment concentrations also declined from 30% in flood event No. 1 to 20% in event No. 3 (Fig. 2.2b).

2.3.2. Plume dynamics

Although flood event No. 1 was the first major flood of the season, ~6 million ML had been discharged by earlier subordinate flows (see Fig. 2.2a). As a result, a flood plume was already established prior to this major flood event and was clearly visible on satellite images along the coastline by 15th December 2010 (Fig. 2.3a). This earlier established plume was constrained near the river mouth to the tip of Cape Bowling Green (see Fig. 2.1 for location details). Wind speed increased during late December (>7 m s^{-1} from the NE over 3 days to 27th December) and as the flood hydrograph at Inkerman peaked the turbid plume pushed out east of Cape Upstart (Fig. 2.3b). Significant flood discharge was held within Upstart Bay where it remained visible as a turbid plume from the 27th December to the 8th January (see Fig. 2.3 and Supp. Video 1 in Bainbridge et al., 2012). Flood discharge from the Black, Ross and Haughton Rivers developed smaller turbid plumes over the same period. By January 1, the Burdekin River turbid plume extended NW well past the tip of Cape Bowling Green (Fig. 2.3c). The maximum northward and offshore extent of this plume occurred between the 1st and 4th January 2011, when plume waters extended at least 50 km offshore and at least as far north as the eastern side of the Palm Island Group (Fig. 2.3c and d). As winds abated (<3.5 m s^{-1}) on January 5 the boundaries of the turbid plume contracted shoreward (Fig. 2.3e), before again extending E-NE to cover Old and Stanley Reefs by January 7 (see

Fig. 2.3f and Supp. Video 1. extended image from January 7 in Bainbridge et al., 2012). The plume size contracted once again a day later (Supp. Video 1 in Bainbridge et al., 2012). A comparatively smaller plume from the Herbert River developed from the 15th December–4th January (Fig. 2.3a–d; see also Supp. Video 1 for extended images). The maximum extent of the Herbert River turbid plume was <10 km from the Hinchinbrook Channel that occurred on January 4, after which turbid water was confined to the channel (Fig. 2.3d–f).

The Burdekin River plume lifted off the bottom in the shallow coastal waters 3–4 kilometres offshore, where it remained a buoyant freshwater layer ~2 m thick over the sampling transect (Appendix Fig. A2.1a). Vertical salinity profiles showed surface salinities (psu) ranged from 0.1–10 with distance from the river mouth along the initial sampling transect that coincided with peak discharge at Inkerman, and increased to 3.7–24 across the same transect when repeated three weeks later (Fig. 2.4a and b; Appendix Fig. A2.1). Surface salinities along the northern plume transect (6th January 2011) ranged from 26 psu at Orchard Rocks (Magnetic Island) to 31 psu at Iris Point (Orpheus Island), the most northerly site tested (Fig. 2.4c).

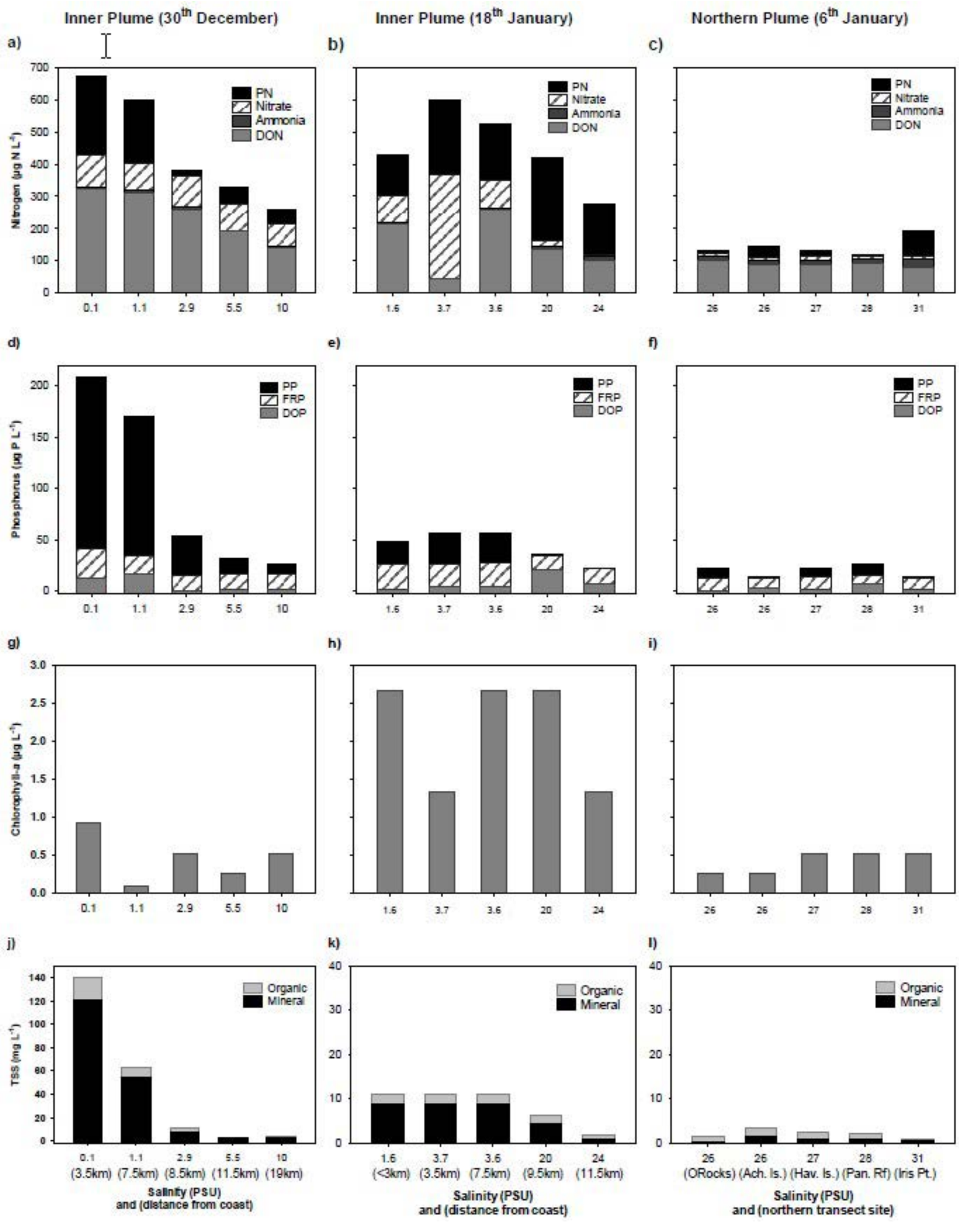

Figure 2.4 Near-surface nitrogen, phosphorus, chlorophyll *a* and TSS concentrations (and organic particulate matter composition) for all sites plotted along the salinity gradient and with distance from the coast for inner Plume Transects 1 (a,d,g,j) and 2 (b,e,h,k), and along the northern Plume Transect 3 (c,f,i,l). Note the change in TSS concentration range for (k) and (l) compared to (j).

2.3.3. Sediment floc types

Table 2.1 describes three types of sediment flocs common in plume waters across the three sampling transects. 'Small mud flocs' (<100 µm) composed of clay and silt particles bound by TEP (Ayukai and Wolanski, 1997; Dagg et al., 2004; Passow et al., 2001) were common in the inner turbid plume surface waters (see Fig. 2.5). 'Larger flocs' (>100 µm) were also observed in turbid plume waters at depths >2 m, suggesting the smaller flocs aggregate as they sink through the water column. Thirdly, 'large floc aggregates' (>200 µm; Figs. 2.5, 2.6d and 2.7), were observed in plume waters with higher PAR and increased biological activity (e.g. diatoms, copepods). Here, small mud flocs had aggregated with algal cells and biological material to form much larger floc aggregates (see Passow et al., 2001).

Table 2.1 Sediment floc types and characteristics identified in this study.

Floc Type	Floc Size	Location	Characteristics/observations
Small mud flocs	<100 µm (commonly seen as <20 µm)	Inner Plume Transects 1 and 3 (surface water only)	• Individual sediment particles (commonly clay and silt) encased by Transparent Exopolymer Particles (TEP) • Observed in inner turbid waters (10–140 mg L^{-1}) with poor light conditions • Largest mud flocs seen in Plume Transect 3 • Floc size decreased along salinity gradients • E.g. 3 and 3.5 km surface water images from both transects (Fig. 2.5) with mineral particles (visible as black dots) encased by transparent mucus
Large flocs	>100 µm	Inner Plume Transect 1 (depth samples only)	• Larger flocs, similar to above but increased presence of larger sediment particles than in small mud flocs seen in the surface waters • Observed in depth samples only; indicating sinking • E.g. Depth sample images in Plume Transect 1 (3.5 and 7.5 km; Fig. 2.5)
Large floc aggregates	>200 µm	Inner Plume Transect 3 (surface and depth) and Northern Plume Transect 2) (surface and depth)	• Fine sediment particles bound by TEP to cellulose/ gelatinous plankton castings or zooplankton (e.g. copepod, see Fig. 2.7) • Observed in plume waters with improved light conditions and increased salinity and biological activity (e.g. diatoms, copepods) • E.g. 2 m depth sample, 3.5 km along Plume Transect 3 (Fig. 2.5); Fig. 2.6d

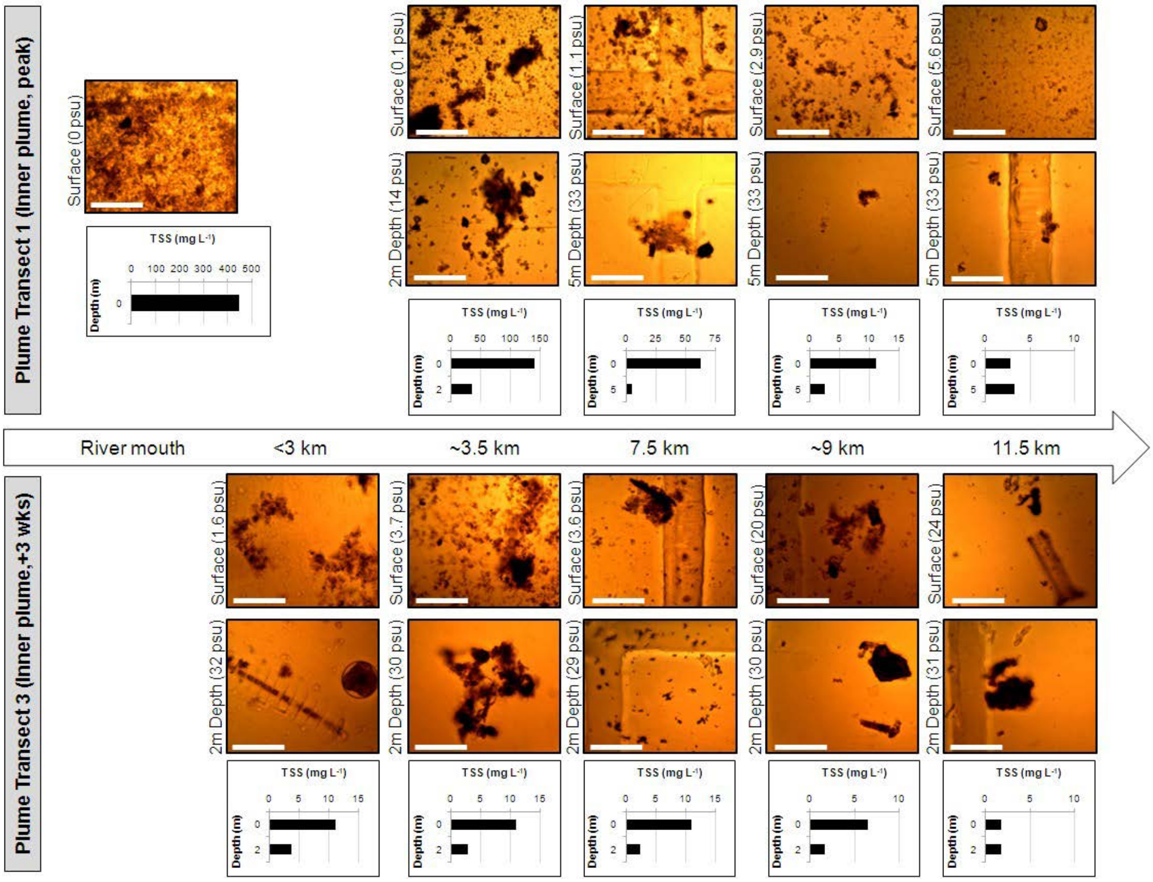

Figure 2.5 Microscope sediment floc images and TSS concentrations for surface and sub-surface water samples collected on 30th December 2010 and 18th January 2011. Surface or depth water samples are indicated on the left side of each image including changes in salinity with time and depth. Scale bars on the floc images indicate 100 µm (0.1 mm) length. A freshwater sample collected at Inkerman during peak discharge (27/12/10) is also displayed (surface water sample only). The freshwater sample shows unflocculated sediment particles prior to mixing with seawater. Particle flocculation in Plume Transect 1 samples (top section of figure) comprise fine sediment particles bound by transparent exopolymer particles (e.g. mucus) forming large mud flocs, with floc size increasing with depth. Samples captured along Plume Transect 3 (bottom section) show an increase in biological production i.e. presence of diatoms and cellulose/gelatinous plankton castings often aggregated with small mud flocs.

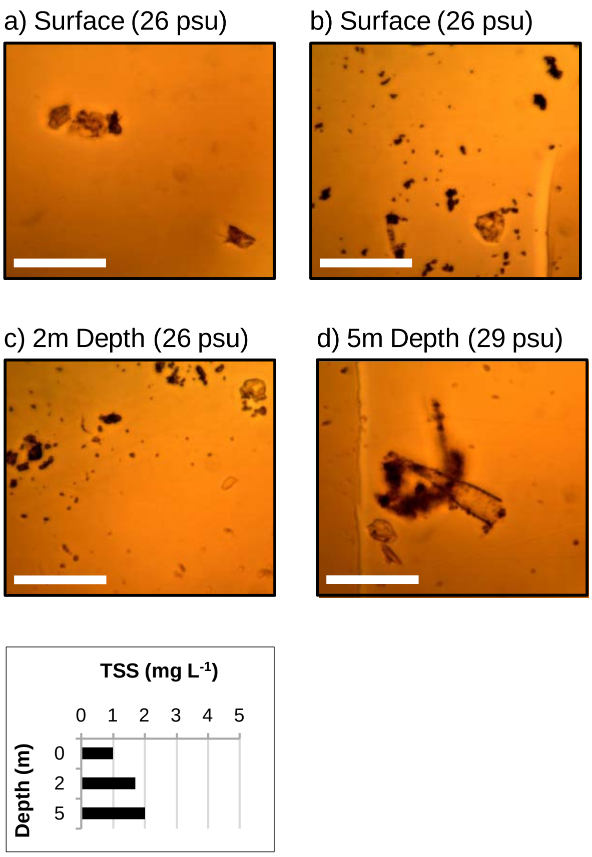

Figure 2.6 Microscope images captured from (a, b) surface, (c) 2 and (d) 5 metres depth in the plume water collected at Orchard Rocks on 06/01/11. Images show individual fine-grained sediment (i.e. clay and silt <16 µm) particles (b–c), large flocs (a) and large floc aggregates of fine particles and plankton remains encased by TEP (d) are still being carried in plume waters as far as Magnetic Island in the weeks after peak discharge. Scale bars represent 100 µm.

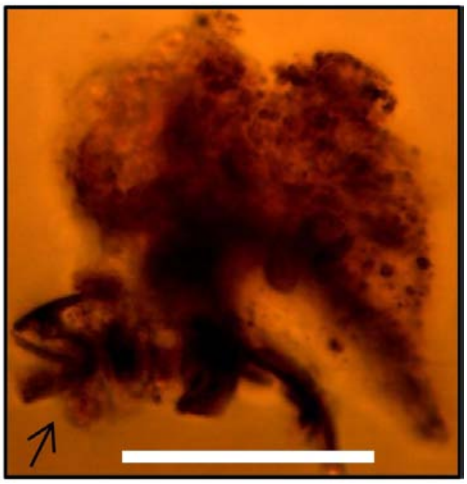

Figure 2.7 Microscope image of a large floc aggregate captured in surface waters off Acheron Is. along Plume Transect 2. Similarly to Fig. 2.6d, the fine-grained sediment particles bound in mucus have formed a large floc aggregate likely including zooplankton (e.g. copepod; see arrow) in the bottom-left corner of the image. Scale bar represents 100 µm length.

2.3.4. Plume Transect 1 (inner plume, peak discharge, 30/12/10)

As the river flood water mixed with seawater, TSS concentrations decreased from 450 mg L^{-1} at the river mouth to <5 mg L^{-1} ~19 km off the coast (Fig. 2.8). This decline along the salinity gradient showed a much faster removal of suspended sediment from the plume surface waters than would be expected for conservative mixing (Appendix Fig. A2.2a). Upon mixing with seawater (i.e. salinity of 0.1 psu) there was rapid settling of the entire sand sized fraction, the majority (>80%) of the fine and coarse silt sized particles, and some (~25%) of the clay particles (Fig. 2.8). The clay fraction dominated (75%) the remaining sediment in suspension along the plume transect, with some (<25%) fine silt and residual coarse silt remaining.

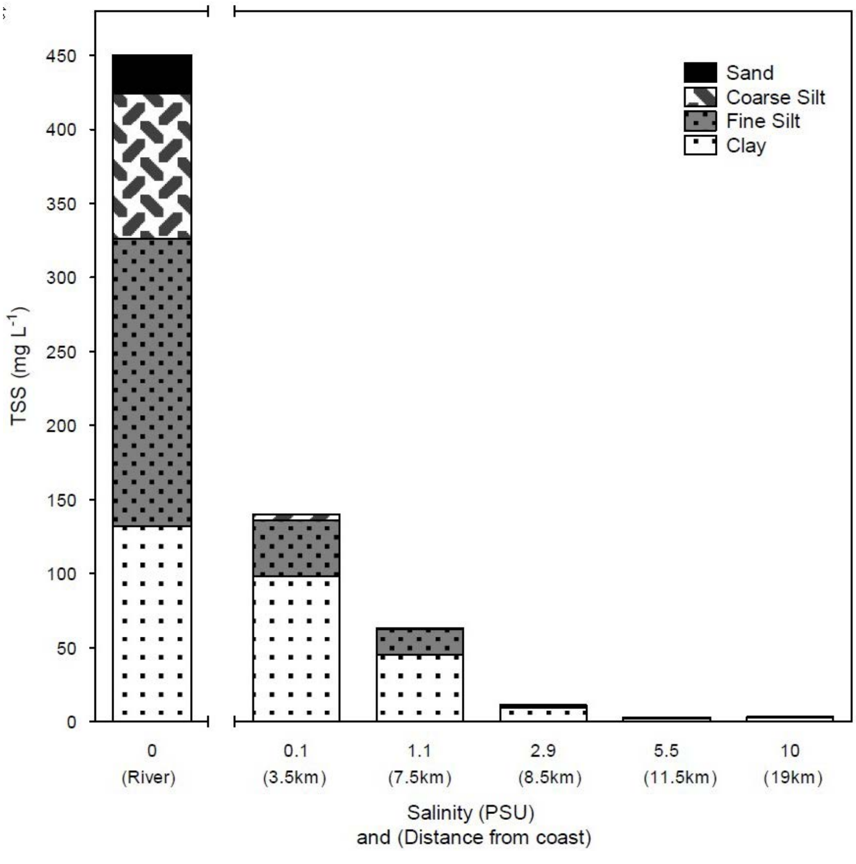

Figure 2.8 Variation along salinity gradient and distance from the coast of TSS concentrations and sediment particle size composition for the Burdekin River at Inkerman (27/12/10:AM) and adjacent plume transect (30/12/10) during peak discharge conditions.

Microphotographs of the samples showed individual sediment particles in the freshwater reaches of the river mouth before aggregating into small mud flocs (<50 µm) at salinity of 0.1 psu (Fig. 2.5), <4 km from the coastline (hereafter referred to as the low salinity depositional zone). The presence of large flocs (>100 µm) as well as individual particles at 2 m depth (Fig. 2.5), coinciding with a rapid decrease in TSS concentrations, indicates settling of these particles from the surface plume. An organic fraction in the suspended particulate matter at this initial low salinity depositional zone (Fig. 2.4j) suggests that there was organic matter available to form these flocs. As TSS concentrations decreased along the salinity gradient, so did the presence of these larger flocs, with only small mud flocs carried away from this low salinity depositional zone (Fig. 2.5). Some deposition of smaller flocs was also evident in sub-surface images captured from samples collected 9.0–11.5 km offshore, however TSS concentrations had decreased to <5 mg L^{-1}.

Particulate nitrogen (PN) and dissolved organic nitrogen (DON) dominated (>70% of TN) the nitrogen species in Plume Transect 1 (Fig. 2.4a). Rapid depletion of PN occurred along the transect from 245 to 15 µg N L^{-1}, as salinity increased from 0.1 to 2.9 psu, respectively (Appendix Fig. A2.2b). In comparison, both nitrate and DON concentrations displayed conservative mixing along the salinity gradient (Fig. 2.4a, Appendix Fig. A2.2c). Particulate phosphorus (PP) behaved similarly to PN, with a rapid decline in the initial low salinity depositional zone from 165 to 10 µg P L^{-1} (Fig. 2.4d). Concentrations of filterable reactive phosphorus (FRP) and dissolved organic phosphorus (DOP) remained relatively unchanged (e.g. <30 µg P L^{-1}) across all three plume transects (Fig. 2.4d–f), whilst chlorophyll *a* concentrations remained <1 µg L^{-1} across Plume Transect 1 (Fig. 2.4g).

2.3.5. Plume Transect 3 (inner plume, +3 weeks, 18/01/11)

Salinity increased from 1.6 to 24 psu along Plume Transect 3 with distance from the river mouth and TSS concentrations decreased from 11 to 2 mg L^{-1} along this salinity gradient (Fig. 2.4k). River TSS concentrations had decreased to ~50 mg L^{-1} after 3 weeks, equivalent to 11% of the initial flood peak concentrations (see Fig. 2.2b). Mucus-bound (i.e. TEP) mud flocs dominated the fine particles present in the inshore plume waters (Fig. 2.5). Diatoms and zooplankton (and their associated feeding structures) were common in both surface and sub-surface samples indicating increased biological activity since the initial transect (Fig. 2.5), and chlorophyll *a* concentrations (1.3–2.7 µg L^{-1}) were the highest measured in this study (Fig. 2.4h). This was also reflected by the increased organic content of particulate matter measured along this transect (Fig. 2.4k). Large floc aggregates (i.e. 100–250 µm) were observed in microphotographs captured from samples collected at 2 m depth at ~3.5, 9.0 and 11.5 km from the coast (Fig. 2.5). Total nitrogen concentrations were similar to Plume Transect 1, with higher PN concentrations compared to the initial transect (e.g. 255–125 µg N L^{-1} in transect 3 compared to 245–15 µg N L^{-1} in transect 1; Fig. 2.4a and b). Nitrate concentrations were higher in the lower salinity waters (i.e. >85 µg N L^{-1}) before decreasing below 20 µg N L^{-1} at the outer two sites, 9.5 and 11.5 km offshore (Fig. 2.4b). Particulate phosphorus concentrations (<30 µg P L^{-1}) were lower than in Plume Transect 1, and now represented equal proportions of total phosphorus with FRP and DOP (Fig. 2.4e).

2.3.6. Plume Transect 2 (Northern plume extent, +10 days, 06/01/11)

Sampled water along the northern Plume Transect 2 were predominately sourced from the Burdekin River with a lesser influence from other localised systems including the small streams flowing into Halifax and Cleveland Bays, and possibly the Herbert River to the north (see Figs. 2.1 and 2.3). Surface TSS concentrations were all <5 mg L^{-1}, with a large proportion (50–70%) composed of organic matter (Fig. 2.4l). Total nitrogen and total phosphorus concentrations had also decreased (<195 µg N L^{-1} and <25 µg P L^{-1}, respectively) compared to inner Plume Transects 1 and 3, where concentrations ranged between 265–675 µg N L^{-1} and 25–210 µg P L^{-1}, respectively (Fig. 2.4a–f). Chlorophyll *a* concentrations (<0.53 µg L^{-1}) were similar to Plume Transect 1 (Fig. 2.4i).

Individual clay and silt-sized particles were suspended in both surface and sub-surface (2 m depth) samples collected at Orchard Rocks off Magnetic Island (Fig. 2.6b and c). Large floc aggregates also occurred in both surface and sub-surface plume waters at this site (Fig. 2.6a and d). Further along this transect plume waters contained negligible ‘mineral’ sediment particles, with an increased presence of large floc aggregates in both surface and sub-surface waters (e.g. Figure 2.7).

2.4. Discussion

2.4.1. Burdekin River discharge and plume movement

The impact of the extended period of low salinity conditions and the continual input of terrestrial contaminants to the GBR lagoon that resulted from the extreme 2010/11 Burdekin River discharge on seagrass and coral reef ecosystems is still under investigation. This study was undertaken during an exceptionally wet year when the Burdekin River discharge exceeded 7,000 ML day^{-1} over a 200–day period (14th November–31st May) compared to base flow conditions of <700 ML day^{-1} (Fig. 2.2b). In addition to the extreme conditions of the 2010/11 wet season, three of the largest Burdekin River discharge years on record (since 1922) have occurred over the past four wet seasons, including 2007/08 (27.5 million ML, 6th largest), 2008/09 (29.4 million ML, 4th largest) and 2010/11 (34.8 million ML, 3rd largest; DERM, 2012). The cluster of these above average wet season events acutely stressed seagrass and corals due primarily to extended periods of low salinity and high turbidity (Brodie and Waterhouse, 2012; McKenzie and Unsworth, 2011).

The extended and high flow conditions of the 2010/11 Burdekin River discharge are reflected in the large area covered by the flood plume, which extended at least as far north as the Palm Island Group and stretched >50 km offshore from the coastline between Cape Upstart and Halifax Bay, impinging on inshore coral reefs and seagrass meadows within Upstart, Bowling Green, Cleveland and Halifax Bays (Fig. 2.3). The true-colour classification technique used in this study provided a valuable technique to track the movement of the plume, particularly where unsuitable atmospheric conditions (e.g. dense cloud cover, sun glint) that commonly occur during wet season flood conditions obscured large areas (Brodie et al., 2010). The classified satellite imagery series of the December 2010–January 2011 Burdekin River flood plume (Fig. 2.3) reveals the plume evolved along a longshore northward trajectory, as has been documented for previous floods (Devlin and Brodie, 2005; King et al., 2001; Wolanski and Jones, 1981; Wolanski and van Senden, 1983). This movement is largely influenced by a combination of south-easterly wind-generated currents and Coriolis forcing. NE/E wind events deviated the flood plume from this northward trajectory to the east, and at such times, the plume waters spread over the mid-shelf including Old and Stanley Reefs (Fig. 2.3f; see also Supp. Video 1 extended image in Bainbridge et al., 2012). In contrast, the Herbert River plume had a much smaller area of influence with the turbid plume constrained within close proximity to the southern Hinchinbrook Channel, and the plume boundary extending <25 km offshore in a NW direction (Fig. 2.2d, see also Supp. Video 1 in Bainbridge et al., 2012).

2.4.2. Burdekin River suspended sediment export and initial low salinity depositional zone

Approximately 2.8 million tonnes of suspended sediments were discharged in the first major flood event during the 2010/11 wet season, accounting for 70% of the suspended sediment load exported in an average year (4 million tonnes: Kroon et al., 2012). The discharge from that water year was ~4–fold higher than the average annual discharge. The finer sediment fractions dominated this load (70%) with equal contributions from clay and fine silt sized fractions. The TSS concentrations in river water decreased during the wet season from >450 mg L^{-1} in the first flood event to <100 mg L^{-1} in the second and third flood events (Fig. 2.2b). This decrease in TSS concentrations and particle size may be due to catchment sediment exhaustion processes (see Amos et al., 2004) or changes in catchment sediment sources. This latter scenario is currently the focus of further investigation.

Satellite imagery visually supports the interpretation that the initial depositional zone of Burdekin River suspended sediment is mostly confined to Upstart Bay (Fig. 2.1 and 2.3c and d). Rapid sediment deposition within this low salinity zone accords with previous studies of Burdekin River flood plumes (Devlin and Brodie, 2005; Wolanski and Jones, 1981), with TSS concentrations declining from 450 in the river to 140 mg L^{-1} as salinity rose to as low 0.1 psu in Plume Transect 1, <4 km from the coast (Fig. 2.8). TSS concentrations declined further along the salinity gradient from the river mouth to <5 mg L^{-1} (salinity of 5.6 psu), within ~10 km of the coastline (Fig. 2.8). The sand and silt fractions measured in Plume Transect 1 were almost completely removed at 0.1 psu (<4 km from the coastline) whilst the clay fraction was mostly removed at ~10 psu (<20 km from the coastline; Fig. 2.8). The Burdekin River plume remained near the surface, mixed little with the underlying seawater and did not reach the seafloor (Appendix Fig. A2.1), a process also observed during previous flood events (Wolanski and Jones, 1981; Wolanski and van Senden, 1983).

Physical and biological flocculation processes accelerated suspended sediment deposition near the Burdekin River mouth (Fig. 2.5), a finding in line with studies on other large turbid river plumes (e.g. Fly River: Ayukai and Wolanski, 1997; Dagg et al., 2004; Amazon River: Gibbs and Konwar, 1986; Eel River: Hill et al., 2000; Po River: Milligan et al., 2007). Previous studies have found a higher abundance of heterotrophic bacteria within this initial mixing zone where low light (i.e. PAR) and salinity conditions may prevent marine plankton blooms (Dagg et al., 2008; Ducklow and Kirchman, 1983; Lohrenz et al., 1999). This bacterial activity has been shown to be responsible for biologically-mediated flocculation, i.e. the formation of muddy marine snow (Ayukai and Wolanski, 1997; Dagg et al., 2004; Passow et al., 2001). Although these studies have primarily focused on the biological uptake of dissolved inorganic nitrogen (in particular nitrate), which dominates nitrogen export from rivers heavily influenced by intensive anthropogenic sources (Seitzinger et al., 2010), terrestrial particulate nitrogen may also fuel these pelagic systems (see Dagg et al., 2004; Mayer et al., 1998). Given particulate nitrogen comprises a large proportion of TN exported by the Burdekin River (Fig. 2.4a), it may play a key role in supporting this heterotrophic bacterial productivity, which have much higher rates in the GBR lagoon than in temperate coastal waters around the world (Alongi and McKinnon, 2005). By contrast the mixing of DON within flood plumes is more difficult to interpret (Fig. 2.4a), and further study needs to characterise the different components of DON and its significance to biogeochemical cycling (Furnas et al., 2011).

Three weeks after peak river discharge, the biologically-mediated flocculation of plume sediment along the inner transect had reduced the TSS concentrations in the plume to <11 mg L^{-1} (Fig. 2.4k), thus improving PAR conditions and enabling increased biological activity, as evidenced by a ~5-fold increase in chlorophyll *a* concentrations (Fig. 2.4g and h). The mud flocs were much larger (>150 µm) than those of the first plume transect, particularly within the initial low salinity depositional zone (see surface images captured 3.0 and 3.5 km, Fig. 2.5). Large floc aggregates (~250 µm; Fig. 2.5) were also commonly observed in samples collected further along this transect in both surface and sub-surface waters, where small mud flocs had coagulated on sticky algal cells and other biological material to form these floc aggregates (see Ayukai and Wolanski, 1997; Fabricius et al., 2003; Passow et al., 2001). PN concentrations along Plume Transect 3 remained relatively consistent along the salinity gradient (125–255 µg

N L^{-1}; Fig. 2.4b), suggesting that during this stage of the plume the PN was mostly suspended particulate matter from organisms generated within the plume rather than PN input from the river. In contrast, the source of PN during peak discharge conditions appeared to be dominated by river input.

2.4.3. Fine sediment transport beyond the initial low salinity depositional zone

Only the clay and some fine silt particles were carried beyond the Burdekin River low salinity depositional zone during peak discharge conditions (Fig. 2.8), and were transported as discrete minerals or small mud flocs (Fig. 2.5). Sampling of the Burdekin River at Inkerman and along the adjacent plume transect during the 2008/09 and 2009/10 flood events found similar sediment transport dynamics, with only finer sediments remaining in suspension upon seawater mixing (Appendix Fig. A2.3). These discrete fine mineral particles also occurred as far north as Cleveland Bay in surface and sub-surface (2 m depth) water collected at Orchard Rocks in Plume Transect 2 (Fig. 2.6), 10 days after the flood peak. This result shows fine sediment particles can be carried at least 100 km within the river plume. However, readily distinguishable mineral particles were not observed in samples collected further along this northern Plume Transect 2; these samples had low TSS concentrations (<5 mg L^{-1}) and high proportions of organic particulate matter, likely generated within the plume (Fig. 2.4l). This resulted in large floc aggregates in both surface and sub-surface waters (e.g. Fig. 2.6d, Fig. 2.7). This organic matter was therefore still accelerating the settling of the last remaining mineral particles considerable distances from the initial low salinity depositional zone. All nutrient and chlorophyll *a* concentrations were lower along this transect compared to the inner Plume Transect 3 (which continued to receive terrestrial nutrients), suggesting that nutrient consumption by phytoplankton communities may have peaked and the terrestrial particulate nutrients had been transformed and incorporated into marine organisms (mainly zooplankton) or settled on the seafloor (Brodie et al., 2012b; Furnas et al., 2005, 2011).

2.4.4. Fate and potential impacts of Burdekin River sediment and nutrients

Burdekin River flood plumes cause direct reductions in the light climate (i.e. PAR) for benthic phototrophic organisms (e.g. coral, seagrass), although this effect is relatively transient in normal years (e.g. 2–3 weeks) compared to the length of light reduction resulting from sediment resuspension in GBR lagoon inshore waters at depths <15 m during the dry season (Larcombe et al., 1995; Orpin et al., 1999). In the 2010/11 wet season, however, plume conditions persisted in inshore waters for at least 10 weeks (Fig. 2.2a) and the effects on benthic light climate may have been severe. The long-term impact of the extended wet season is the subject of current studies (see Brodie and Waterhouse, 2012), including observations of seagrass meadow mortality over large areas of the inshore Burdekin region and an associated increase in the mortality of seagrass specialist feeders including dugongs (*Dugong dugon*) and green turtles (*Chelonia mydas*) (Bell and Ariel, 2011; McKenzie and Unsworth, 2011). The impacts of the extended plume conditions in this region may have been exacerbated by the passage across the region of the Category 5 Tropical Cyclone Yasi (Great Barrier Reef Marine Park Authority, 2011), and separating the effects of each disturbance will be complex when attempted.

Burdekin River sediment **initially** deposits in Upstart Bay, and to a lesser extent Bowling Green and Cleveland Bays (this study, and see also Devlin and Brodie, 2005; Wolanski and Jones, 1981; Wolanski and van Senden, 1983). However, in strong winds (>9 $m\ s^{-1}$; Lambrechts et al., 2010) during the dry season this sediment is subsequently resuspended and transported northward by longshore currents (Lambeck and Woolfe, 2000) to be deposited in Bowling Green (80–90%) and Cleveland (~5–10%) Bays, which are sheltered from the prevailing SE trade winds (Orpin et al., 2004)[1].

Hydrodynamic modelling and satellite imagery suggest that the PN load should remain within Upstart Bay long enough (i.e. ~a few to 30 days) to be mineralised either through bacteria in the plume water column or later in the benthic sediment layer (see Alongi et al., 2007). This mineralised PN would then contribute to the general bioavailable nitrogen pool within the GBR lagoon (Brodie et al., 2012b; Furnas et al., 2011). The PP load behaves similarly to PN, to be ultimately desorbed and/or mineralised and added to the bioavailable P load to the GBR (see McCulloch et al., 2003b).

In contrast, dissolved nutrients were transported well beyond Upstart Bay as far north as Halifax Bay within the plume. In these secondary plume waters, the bioavailable fraction of the dissolved nutrients (all DIN and ~10% of DON, see Furnas et al., 2011)

[1] Note, a recent study since this publication has revealed that the majority of sediment delivered from the Burdekin River is deposited and retained within Upstart Bay (Lewis et al., 2014).

supported primary production (measured as high chlorophyll *a* concentrations) and therefore would have increased the particulate organic matter in the water column (e.g. phytoplankton cells, zooplankton remains). This planktonic material was then available to form large floc aggregates (see Fig. 2.7) with the remaining finer sediment fraction (<16 µm).

Large floc aggregates (with their mud and organic matter content) will have densities lower than those of discrete mineral particles (e.g. clay particles ~2.6 g cm^{-3}) but greater than simple organic matter (~1 g cm^{-3}). This difference in density allows these aggregates to remain in suspension longer than mineral particles, maintaining higher turbidity in the plume water for longer periods and transport further afield. In addition, after these large floc aggregates settle on the seafloor they are potentially more prone to wind-driven resuspension during the dry season (Wolanski et al., 2005). These aggregates were observed across almost the entire plume, including areas with sediment-sensitive benthic organisms (e.g. coral, seagrass). The two major risk factors to these benthic organisms are:

(1) The resuspension of settled sediment flocs during strong winds resulting in increased turbidity and lower PAR levels. During dry season conditions (i.e. negligible river discharge) turbidity is caused by wave-driven resuspension in water depths <15 m (Larcombe et al., 1995; Orpin et al., 1999; Wolanski et al., 2008). The link between increased regional turbidity and increased terrestrial inputs of fine sediment is now more firmly established (Fabricius et al., 2011[2]; Lambrechts et al., 2010) and the results of this study suggest a mechanism – the presence of flocculated fine sediments in the surface sediment layer in places like Cleveland Bay – to substantiate this correlation.

(2) Direct sedimentation of fine sediments and associated nutrients/organic matter cause greater damage to corals than inorganic sediment particles (i.e. sand) due to bacterial growth causing anoxia at the coral surface and subsequent coral mortality (Fabricius et al., 2003; Weber et al., 2006). Corals find it more difficult to remove sticky, muddy marine snow than discrete mineral particles (Fabricius and Wolanski, 2000; Fabricius et al., 2003; Philipp and Fabricius, 2003).

[2] Note the Fabricius et al. (2011) technical report is now published as Fabricius et al. (2013, 2014).

2.5. Conclusion

The 2010/11 Burdekin River flood plume extended >50 km offshore and at least as far north as the Palm Island Group, coinciding with an extended period of river discharge (34.8 million ML) into the GBR lagoon for ~200 days. A major flood event (24th Dec–18th Jan) representing 31% of this wet season discharge exported ~2.8 million tonnes of suspended sediment, which was dominated by clay and fine silt fractions. Sampling of the adjacent turbid flood plume following peak discharge showed rapid deposition of suspended sediment <10 km from the coastline, where all sand and the majority of coarse silt particles (>16 µm) had settled by the time a salinity of 0.1 psu had been reached. This deposition was enhanced by the flocculation of these particles upon mixing with seawater. Clay and fine silt particles and associated nutrients that remained in suspension beyond this initial low salinity depositional zone were observed in plume waters >100 km from the river mouth.

This is the first study in the GBR to investigate particle size partitioning within river flood plumes and confirms the importance of flocculation processes in the dispersion of terrestrial particulate matter in the GBR lagoon. The results highlight the transformation of terrestrial fine sediment and associated nutrients within flood plumes to muddy marine snow (large floc aggregates). These aggregates pose a risk to benthic organisms (e.g. coral and seagrass) due to increased turbidity, enhanced smothering effects on corals due to their sticky nature and are potentially more easily remobilised during subsequent wind-driven resuspension events. Future research (e.g. laboratory-based studies) needs to more thoroughly examine the risk of the different floc types observed in this study to corals, seagrass and other sensitive marine ecosystems.

3. Fine suspended sediment and water budgets for a large, seasonally-dry tropical catchment

Bainbridge Z.T., Lewis S.E., Smithers S.G., Kuhnert P.M., Henderson B.L. and Brodie J.E. 2014. Fine-suspended sediment and water budgets for a large, seasonally-dry tropical catchment: Burdekin River catchment, Queensland, Australia, Water Resources Research 50, 9067-9087.

Abstract

The Burdekin River catchment is a seasonally-dry tropical catchment located in north-east Queensland, Australia. It is the single largest source of suspended sediment to the Great Barrier Reef (GBR). Fine sediments are a threat to ecosystems on the GBR where they contribute to elevated turbidity (reduced light), sedimentation stress and potential impacts from the associated nutrients. Suspended sediment data collected over a five-year period were used to construct a catchment-wide sediment source and transport budget. The Bowen River sub-catchment was identified as the major source of end-of-river suspended sediment export, yielding an average of 530 t km^{-2} yr^{-1} during the study period. Sediment trapping within a large reservoir (1.86 million ML) and the preferential transport of clays and fine silts downstream of the structure were also examined. The data reveal that the highest clay and fine silt loads – which are of most interest to environmental managers of the GBR – are not always sourced from areas that yield the largest total suspended sediment load (i.e. all size fractions). The results demonstrate the importance of incorporating particle size into catchment sediment budget studies undertaken to inform management decisions to reduce downstream turbidity and sedimentation. The data on sediment source, reservoir influence and sub-catchment and catchment yields will improve understandings of sediment dynamics in other tropical catchments, particularly those located in seasonally wet-dry tropical savannah/semi-arid climates. The influence of climatic variability (e.g. drought/wetter periods) on annual sediment loads within large seasonally-dry tropical catchments is also demonstrated in this study.

Keywords: fine sediment; sediment budget; semi arid; Great Barrier Reef; terrestrial runoff

3.1. Introduction

Sediment budgets provide a structured framework for representing river catchment sediment sources, storage and yields (Dunne and Leopold 1978; Walling and Collins, 2008), and provide an effective communication tool for natural resource managers to understand sediment loads and transport (Slaymaker, 2003). In particular catchment-scale sediment budgets have been applied to identify changes in catchment sediment loads and sources associated with anthropogenically-modified land use, including both increases in loads driven by elevated erosion associated with land clearing, agriculture and mining as well as declines in sediment load downstream of depositional areas such as reservoirs (Syvitski, 2003; Walling, 2006). Although this approach is commonly adopted (see reviews by Koiter et al., 2013 and Walling and Collins, 2008), there have been few sediment-budget studies from tropical catchments (see reviews by Nagle et al., 1999 and Tooth, 2000). Further, detailed investigations on the transport of specific sediment size fractions within tropical catchments are rare (e.g. Verbist et al., 2010). This study addresses this knowledge gap by quantifying suspended sediment sources and yields for a large seasonally-dry tropical river catchment with high inter- and intra-annual streamflow variability associated with the arrival and strength of the summer monsoon. The study focused on the finer clay and silt sediment fractions (<16 µm) that are most likely to reach the downstream receiving environment, the GBR lagoon, located on the north-eastern coast of Australia (Chapter 2).

The influence of anthropogenically-increased sediment delivery on inshore GBR turbidity and resuspension regimes has been vigorously debated over the past few decades. Some studies suggest that turbidity levels on the GBR have remained constant over thousands of years due to the availability of abundant terrigenous sediment along the GBR's inner shelf (Larcombe et al., 1995; Orpin and Ridd, 2012). In contrast, recent evidence suggests a strong link between increased inshore turbidity and higher sediment yields to the GBR from streams draining coastal catchments that have been modified by European settlement (Fabricius et al., 2013, 2014). Increased turbidity associated with river plumes and subsequent dry season resuspension events may directly impact GBR coral and seagrass communities by reducing light available for photosynthesis (Collier et al., 2012; Fabricius, 2005). When accompanied by high sedimentation rates smothering may also occur (Weber et al., 2006). Reduced vigour of coral communities affected by elevated turbidity and sedimentation can also result in increased macroalgal cover (De'ath and Fabricius, 2010) and more frequent coral disease outbreaks (Haapkyla et al., 2011). Further, the clay and fine silt-sized sediment particles are easily resuspended (Browne et al., 2012; Davies-Colley and Smith, 2001), and have the greatest effect on corals in the form of increased and persistent turbidity regimes and sedimentation of organic-rich flocs (Chapter 2; Fabricius, 2005; Humphrey et al., 2008; Weber et al., 2006).

To inform targeted and effective management of sediment erosion within the Burdekin catchment, catchment-wide sediment source and transport annual budgets were constructed using empirical field data collected at key river network locations between 2005 and 2010. The contributions of clay (<4 µm), fine silt (4–16 µm) and coarse (>16 µm) sediment fractions were quantified to isolate sediment sources at a relatively coarse 'sub-catchment' scale before 'hot-spot' tributaries were identified and specific environmental drivers for erosion were investigated. This study builds on sediment trapping estimates of a large reservoir within the catchment reported in Lewis et al. (2013), and quantifies the significant influence this impoundment has on downstream sediment transport and end-of-river export. This study reveals that the highest loads of the finer sediment fraction (i.e. clay and fine silt), which are of most interest from a management perspective are not necessarily derived from areas yielding the highest total suspended sediment load, and highlights how climate variability influences sediment loads. For example, elevated loads are typically transported by run-off events following prolonged drought. This study demonstrates that sediment budgets incorporating sediment particle size fractions are far more useful to managers seeking to reduce fine sediment export and inshore turbidity than the traditional 'yield-only' approach.

3.2. Study Area

Refer to Introduction section 1.4 for a detailed description of the Burdekin River catchment.

3.3. Materials and methods

3.3.1. Suspended sediment sample collection

River water samples were collected from existing streamflow gauge locations draining the five major sub-catchments of the Burdekin River (Upper Burdekin, Cape, Belyando and Suttor Rivers, as well as the Bowen River to represent the otherwise ungauged Lower Burdekin sub-catchment), the outflow of the Burdekin Falls Dam (BFD) and the end-of-river freshwater discharge point during streamflow events over five consecutive water years (Oct 1 to Sept 30; 2005/06–2009/10). Site details, locations, and data history for each site are presented in Table 3.1 and shown in Fig. 1.2 and time-series plots of streamflow hydrographs and concentration data are provided in Appendix Fig. A3.1. Surface water 'grab' samples (top 0.5 m of water column) were collected at these sites during flood conditions with a bucket and rope. Where possible, samples were collected over the rising, peak and falling stages of the streamflow hydrograph over multiple streamflow events that occurred each wet season. Samples were collected from the centre of the channel flow where possible, and were well mixed with a stirring rod before being sub-sampled into pre-rinsed 1L polypropylene bottles. Samples were kept on ice prior to laboratory refrigerated storage and subsequent analysis. These water samples were used to measure total suspended solids (TSS) concentrations and to calculate fine suspended sediment loads for the streamflow conditions at each site for each year sampled. Only the washload fractions were examined because the delivery of fine sediments to the GBR is the focus of this study (see Chapter 2).

To increase the spatial density of data, a network of trained landholders was established to collect water samples at ungauged minor tributaries, many of which become inaccessible to external visitors during floods. Twenty-four sites were established, located as close to the bottom of each tributary catchment area as possible, at sites safely accessible to the landholder during floods (see Fig. 1.2). In conjunction with the Queensland Government Community Waterways Program, volunteer water sampling, risk assessment and training procedures were developed and implemented on site with each landholder volunteer (see Appendix Figure A3.2). The importance of capturing the rising and peak stages of each individual flood event were emphasised, with a desire to collect 5–6 samples throughout a typical flow event (e.g. 1–3 samples per day during the event). To ensure adequate sampling took place each wet season, contact with the volunteers was maintained, especially at the onset of each flood event. Between 2004 and 2011, volunteers collected 460 water samples from the 24 sites over rising, peak and falling stages of streamflow events (Appendix Table A3.1). Samples collected by the volunteer network were kept refrigerated until analysed.

Table 3.1 Gauged sample site locations and TSS and particle size analysis (PSA) data collection summary.

Sample site	Gauge station/location	Water years sampled	# TSS samples	PSA Subset	
				# samples	Water years
Upper Burdekin River (Sellheim)	120002C: Burdekin River at Sellheim	2005/06–2009/10	75	32	2005/06–2008/09
Cape River	120302B: Cape River at Gregory Dev. Rd.	2005/06–2009/10	173	24	2005/06–2008/09
Belyando River	120301B: Belyando River at Gregory Dev. Rd.	2005/06–2009/10	155	21	2005/06–2008/09
Suttor River	*120310A: Suttor River at Bowen Dev. Rd.	2005/06–2009/10	117	22	2005/06–2008/09
Burdekin Falls Dam Overflow (capturing above sites)	120015A: Burdekin River at Hydro Site	2005/06–2009/10	348	50	2005/06–2008/09
Bowen (Myuna)	120205A: Bowen River at Myuna	2005/06–2007/08	140**	110	2006/07–2008/09
Burdekin River – Inkerman (End-of-river)	120006B: Burdekin River at Clare (immediately upstream of Inkerman bridge)	2005/06–2009/10	227**	12	2006/07; 2008/09 only***

*120310A gauge was installed after the 2005/06 wet season. Streamflow for this site for the 2005/06 water year was calculated by subtracting the Belyando River gauge (120301B) data from the downstream Suttor River (St Anns) gauge (120303A).

**Individual water year load calculations by the LRE utilise any available preceding wet season TSS data (i.e. develops a site specific TSS concentration/streamflow relationship), which included 40 additional samples from 2002/03 to 2004/05 for the Bowen (Myuna) site and an additional 465 samples from 1986/87 to 2004/05 for the Burdekin River (Inkerman) site (Kuhnert et al., 2012).

***Burdekin River (Inkerman) data was collected by a different authority and not available for PSA. Opportunistic sample collection by the authors at this site during peak flood conditions was conducted specifically for the purposes of PSA.

3.3.2. Laboratory analysis

Total suspended solids analysis

TSS analysis was performed at the TropWATER Laboratory, JCU, Townsville and at the Queensland Department of Science, Information Technology, Innovation, and the Arts (DSITIA) laboratory in Brisbane using standard techniques described in section 2.2.2. It is noted there is a tendency for this method to underestimate the 'true' suspended sediment concentration (SSC) particularly where abundant (i.e. >25%) sand particles are present (see Gray et al., 2000).

Sediment particle size analysis

A subset of water samples collected from the rising, peak and falling stages of the flood hydrograph for each of the gauged sampling sites were selected for particle size analysis. Samples were selected from four of the study water years (2005/06 to 2008/09) where available and include a total of 274 samples. See Table 3.1 for site specific sample numbers and water years represented. These samples were processed from either an additional 1L bottle collected during streamflow events, or a sub-sample of the original water sample. Particle size distributions were determined using the methodology described in section 2.2.2. Sediments were classified as one of three size classes based on the Udden-Wentworth sediment grain size scale (Leeder, 1982): (1) clay (<4 μm); (2) very fine and fine silt (4−16 μm; hereafter referred to as fine silt); and (3) coarse silt and sand (16−2000 μm; hereafter referred to as coarse sediment). Note, as Chapter 2 identified the clay and fine silt fractions are potentially the most damaging to biota in the receiving marine environment, these groups have been refined to combine coarse silt and sand as one category.

3.3.3. Sediment load calculations

Streamflow and corresponding TSS data from each of the gauged locations were entered into a regression style 'Loads Regression Estimator' (LRE) model developed by Kuhnert et al. (2012) to predict suspended sediment loads (in tonnes) with estimates of error for each sub-catchment site and each water year. The LRE uses a generalised additive model (GAM) to incorporate key hydrological processes consisting of:

(1) linear and quadratic terms for streamflow;

(2) the concept of higher TSS concentrations during a 'first flush' and the characterisation of TSS concentrations on the rise and fall of an event;

(3) a discounted flow term that captures historical flows and the exhaustion of sediment supply over the flow period.

The addition of terms such as a rising-falling limb and flow discounting strengthen the predictive capability of the model, as clearly demonstrated by the improved explanatory power achieved by shifting from a simple rating curve style approach to the LRE model that includes these additional terms (Appendix Table A3.2). The discounting flow term provided the greatest increase in the explanatory power of the model, contributing 25–40% of deviance explained for each site. Additional terms (vegetation ground cover and ratio of flow from above and below the BFD (Kuhnert et al., 2012)) were included in the LRE model for the end-of-river (Inkerman) site to accommodate its size and complexity. These terms were not relevant to the sub-catchment sites.

The LRE characterises the loads through a regression modelling relationship for each site that takes into account concentration data collected over multiple water years, with the capacity to predict loads for years that have limited data. Higher confidence is placed on the loads calculated for well-sampled water years, with associated uncertainty ranges <5–10%. In this regard, preceding wet season TSS datasets from the Bowen River (Myuna; 2002/03–2004/05, 40 samples) and Burdekin River (Inkerman; 1986/87–2004/05, 465 samples) were utilised in the calculation of sediment loads for the water years included in this study. Importantly, the number of samples collected in this study increased throughout the monitoring program (Table 3.2), which coincided with larger streamflow events (see Appendix Fig. A3.1), with the LRE (GAM) model developing a strong relationship for each site (with the exception of the Bowen River: see discussion). This, in turn, allowed reasonable confidence in the loads to be generated for the Belyando and Suttor sub-catchments of the Burdekin despite limited sampling carried out in the 2005/06 water year, further highlighting the benefits of applying the LRE model (Kuhnert et al., 2012). The method can detect changes in annual sediment loadings due to catchment condition as the LRE model can characterise the pattern in TSS concentration using the relationship with flow and additional model explanatory terms such as seasonal/annual changes in ground cover over the entire timeframe for modelling (see Kuhnert et al., 2012).

The LRE model quantifies the uncertainty in the load estimate, which is reported in this paper as 80% confidence intervals (Kuhnert et al., 2012). This envelope takes into account uncertainty and variability in TSS concentrations associated with the surface ‘grab’ sampling field method (i.e. variations in TSS concentrations across the stream profile, sub-sampling), errors associated with the laboratory analysis, as well as potential errors associated with opportunistic stream gauge positioning and sampling error. See Kuhnert et al. (2012) for further detail on the LRE, including input data used to quantify the flow error.

Table 3.2 Catchment specific suspended sediment yield contributions (tonnes km^{-2} yr^{-1}) and mean annual concentration (MAC) (mg L^{-1}) during the five monitored water years from 2005 to 2010. Sample size for each site/water year is shown in italics.

Major sub-catchment	**Upstream area (km^2)**	**Sediment yield (t km^{-2} yr^{-1}) and sample size (*n*) for each water year**											**MAC range 2005–2010 (mg L^{-1})**
		2005/06	*n*	2006/07	*n*	2007/08	*n*	2008/09	*n*	2009/10	*n*	Mean	
Upper Burdekin	36,140	60	*12*	85	*14*	130	*15*	415	*26*	47	*8*	147	680–795
Cape	15,860	2	*7*	12	*8*	32	*30*	30	*13*	10	*115*	17	205–360
Belyando	35,055	5	*12*	4	*9*	6	*33*	3	*8*	5	*93*	5	55–650
Suttor	10,870	9	*4*	9	*7*	65	*35*	13	*8*	21	*63*	23	120–370
Burdekin Falls Dam Overflow (capturing above catchments)	114,260	3	*31*	15	*55*	27	*97*	43	*102*	4	*63*	18	81–260
Bowen	7,110	35	*49*	370	*48*	1035*	*43*	670*	*0*	540*	*0*	530*	1780–3600
Burdekin River (End-of-river)	129,600	7	*23*	55	*52*	115	*53*	85	*52*	19	*47*	56	320–730

*Note lower confidence in the Bowen River loads (and therefore sediment yields) in the latter years with wide CV related to lack of monitoring data in these wet seasons.

3.3.4. Catchment-wide discharge and sediment load budgets

Catchment-wide discharge and sediment load budgets were constructed for each of the five monitored water years using streamflow and suspended sediment load data from the gauged study sites. The four gauged sub-catchment sites upstream of the BFD (Upper Burdekin, Cape, Belyando and Suttor Rivers) were used to determine individual sub-catchment discharge and sediment load contributions into the dam for each water year. For whole-of-catchment budget purposes, the ungauged Lower Burdekin contribution to the end-of-river was then determined by subtracting the BFD overflow gauged contribution from the end-of-river gauge. Contributions from the gauged Bowen River (Myuna) site are represented within the Lower Burdekin contribution. Measurements of uncertainty for each of the sediment loads are represented as 80% confidence intervals in parenthesis after each load. Annual dam trapping estimates calculated in Lewis et al. (2013) have also been included within the sediment load budgets. LRE measured uncertainties in annual dam trapping estimates are also reported in parentheses, as 80% confidence intervals. Long-term mean annual discharge based on all available recorded flow years at each gauge, and a five-year mean sediment load for each site calculated over the study period are also provided.

Clay, fine silt and coarse sediment load budget

As sediment particle size data were available over the first four water years (2005–2009), an additional sediment load budget was constructed using four-year averaged sediment load contributions from each of the seven gauged sites including the proportions of clay, fine silt and coarse sediment. This four-year averaged budget is not summative and does not represent a complete mass balance from sub-catchment source to export. However, this four-year period covers a range of rainfall and hydrological regimes, with particle size class contributions from each site relatively similar from year to year, particularly the ratio of the clay/fine silt component to the coarse sediment fraction (data not shown). Therefore it is contended these data are representative of longer term sediment particle size trends within this catchment.

Clay, fine silt and coarse sediment loads were calculated for each of these sites by the following process: (1) linear interpolation was used to calculate daily particle size distribution for days lacking sample data provided data existed prior to and following each interpolated day; (2) the daily suspended sediment load calculated by the LRE tool was multiplied by the corresponding particle size distribution data for that day, and then each day was summed for each water year (2005/06 to 2008/09); (3) these size-fractioned loadings were then scaled-up to represent each full water year using the total annual suspended sediment load for any 'flow/load' period outside of the sample collection dates and (4) the clay, fine silt and coarse sediment load fractions were then calculated for each site, as a sediment load weighted mean of the four water years. The numbers of available particle size samples for each site are displayed in Table 3.1. The Bowen River (Myuna) site had a number of days where multiple samples were collected during a 24-hour period. In this case particle size distribution data for these samples were averaged for that day.

Minor tributary volunteer network sites

Available TSS data for each of the ungauged minor tributary volunteer network sites were averaged over all discrete flood events and water years where water samples were collected to determine a mean TSS concentration per site. The number of wet seasons monitored for each site varied from each location depending on the occurrence of flood events in any given wet season (i.e. wetter versus drier years) and the availability of the landholder to collect samples during such events (see Appendix Table A3.1). Load-based mean annual concentrations (MAC) for each of the end-of-sub-catchment gauged sites from 2005–2010 were also calculated for context with the ungauged minor tributary volunteer network sites located within these sub-catchments. A Burdekin-wide mean TSS concentration was also calculated using compiled TSS data from all Burdekin minor tributary and gauged sub-catchment locations.

3.3.5. Sources of error

Although the sampling techniques applied capture the clay and fine silt sediment fractions of interest in this study, the collection of water samples at the surface may miss the sand fraction transported as suspended, bed and saltation load, resulting in underestimates of this fraction. In an attempt to quantify uncertainties in field collection and laboratory analysis, experimental cross-section transect samples were collected at each gauged site (e.g. triplicate water samples collected at the left bank, centre and right bank of each stream channel). These data confirmed that the surface of each river was laterally well-mixed in relation to TSS concentrations, providing confidence in the surface 'grab' sampling approach and the laboratory methodology; on average, each individual set of triplicate TSS samples were within 10% (RSD). Further statistical analysis of the data show the variation in TSS concentrations across the stream profiles was not significant (see supp. section). This variability in TSS concentration measured through the stream profiles has been incorporated into the LRE model, and contributes to the uncertainty in each load estimate. Belperio (1979) showed the clay and fine silt fractions were well mixed through the water column during flood flows in the Burdekin River, which further confirm the robustness of this sampling approach for the clay and silt fractions, however it is acknowledged that the grab sampling technique may result in the sand-sized fraction being significantly underestimated.

3.4. Results

3.4.1. Catchment-wide discharge and sediment load budgets

Sub-catchment contributions to total catchment discharge

Two of the largest discharge years on the 91-year record at the end-of-river stream gauge occurred during this study, including the 2007/08 (27.5 million ML, 6th largest) and 2008/09 (29.4 million ML, 4th largest) water years. In both water years catchment discharge exceeded three times the mean annual discharge (see Fig. 3.1a). During the 2007/08 water year, streamflow in all major sub-catchments far exceeded mean annual discharge, including 6.2 million ML and 5.9 million ML from the Upper Burdekin and Suttor sub-catchments above the BFD, respectively, and an estimated 9.5 million ML from the ungauged Lower Burdekin (Fig. 3.1b). Overflow from the BFD (18 million ML) dominated end-of-river discharge, with minimal retention of water from the sub-catchments above the BFD.

Streamflow from the Upper Burdekin sub-catchment dominated total Burdekin River discharge volume for the 2008/09 water year, with a near-record 20 million ML (Fig. 3.1b). Approximately 35% of the total annual discharge during 2008/09 occurred in the 6-days following Tropical Cyclone Ellie's path through the upper catchment, and 90% of all discharge in the 2008/09 water year occurred during the two wet season months January and February, 2009 (Bureau of Meteorology, www.bom.gov.au/cyclone/history/index.shtm). The Cape (2.30 million ML) and Bowen (1.38 million ML) Rivers also experienced above average discharge in 2008/09 (Fig. 3.1b). Similarly to 2007/08, end-of-river discharge was dominated by the catchments

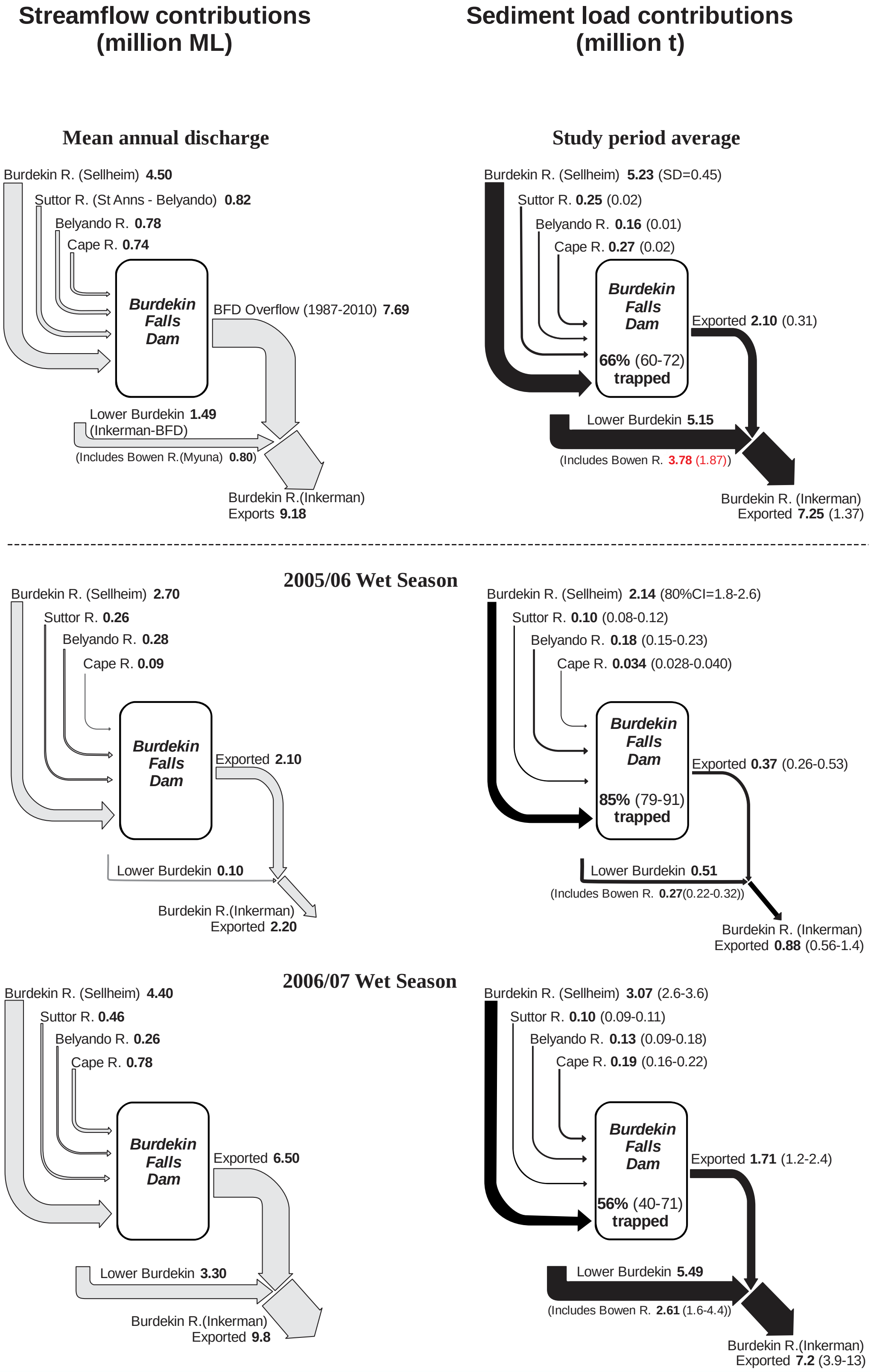
Streamflow contributions (million ML)
Sediment load contributions (million t)
Mean annual discharge
Burdekin R. (Sellheim) 4.50
Suttor R. (St Anns - Belyando) 0.82
Belyando R. 0.78
Cape R. 0.74
Burdekin Falls Dam
BFD Overflow (1987-2010) 7.69
Lower Burdekin 1.49 (Inkerman-BFD)
(Includes Bowen R.(Myuna) 0.80)
Burdekin R.(Inkerman) Exports 9.18
Study period average
Burdekin R. (Sellheim) 5.23 (SD=0.45)
Suttor R. 0.25 (0.02)
Belyando R. 0.16 (0.01)
Cape R. 0.27 (0.02)
Burdekin Falls Dam
66% (60-72) trapped
Exported 2.10 (0.31)
Lower Burdekin 5.15
(Includes Bowen R. 3.78 (1.87))
Burdekin R. (Inkerman) Exported 7.25 (1.37)
2005/06 Wet Season
Burdekin R. (Sellheim) 2.70
Suttor R. 0.26
Belyando R. 0.28
Cape R. 0.09
Burdekin Falls Dam
Exported 2.10
Lower Burdekin 0.10
Burdekin R.(Inkerman) Exported 2.20
Burdekin R. (Sellheim) 2.14 (80%CI=1.8-2.6)
Suttor R. 0.10 (0.08-0.12)
Belyando R. 0.18 (0.15-0.23)
Cape R. 0.034 (0.028-0.040)
Burdekin Falls Dam
85% (79-91) trapped
Exported 0.37 (0.26-0.53)
Lower Burdekin 0.51
(Includes Bowen R. 0.27(0.22-0.32))
Burdekin R. (Inkerman) Exported 0.88 (0.56-1.4)
2006/07 Wet Season
Burdekin R. (Sellheim) 4.40
Suttor R. 0.46
Belyando R. 0.26
Cape R. 0.78
Burdekin Falls Dam
Exported 6.50
Lower Burdekin 3.30
Burdekin R.(Inkerman) Exported 9.8
Burdekin R. (Sellheim) 3.07 (2.6-3.6)
Suttor R. 0.10 (0.09-0.11)
Belyando R. 0.13 (0.09-0.18)
Cape R. 0.19 (0.16-0.22)
Burdekin Falls Dam
56% (40-71) trapped
Exported 1.71 (1.2-2.4)
Lower Burdekin 5.49
(Includes Bowen R. 2.61 (1.6-4.4))
Burdekin R.(Inkerman) Exported 7.2 (3.9-13)

Figure 3.1a

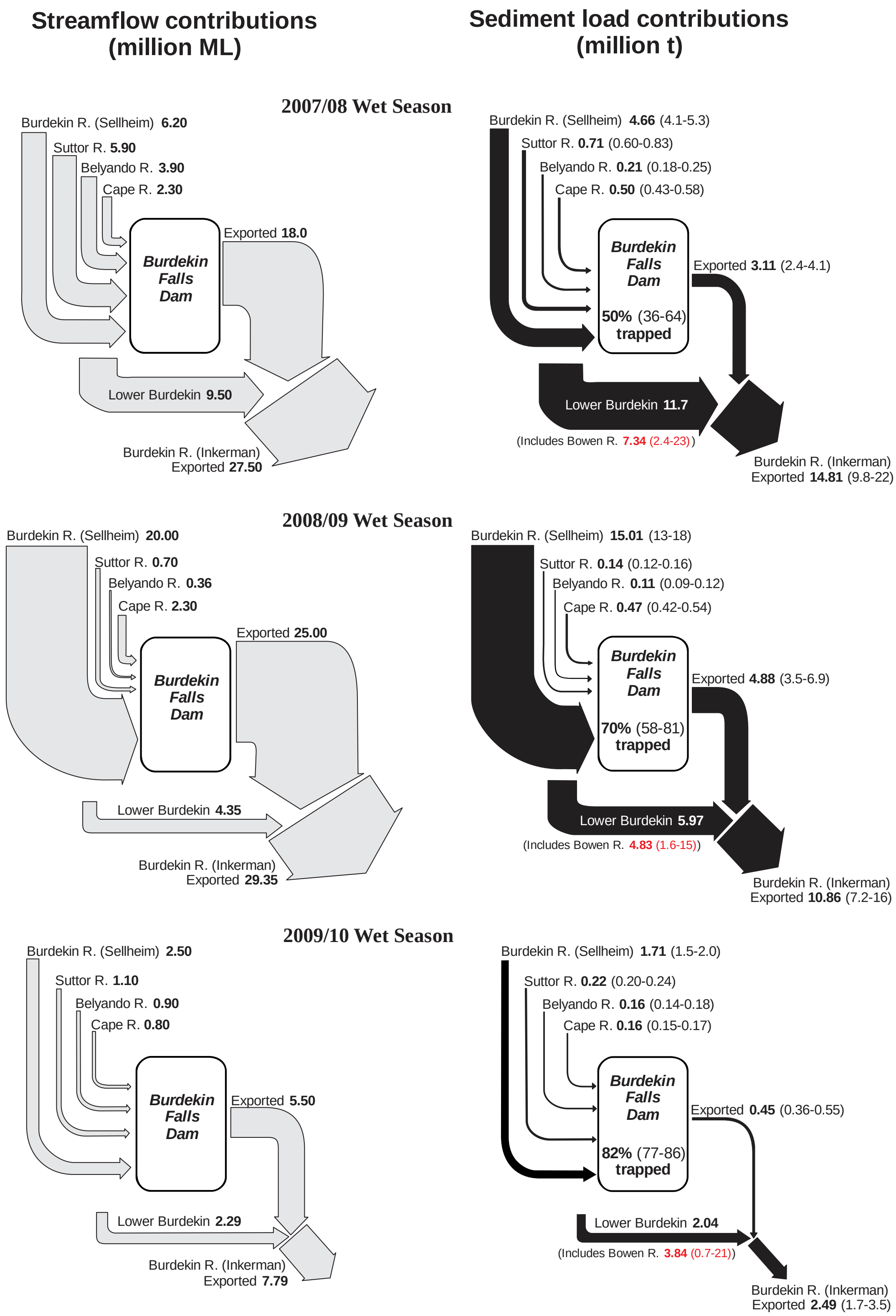

Streamflow contributions (million ML)
Sediment load contributions (million t)
2007/08 Wet Season
Burdekin R. (Sellheim) 6.20
Suttor R. 5.90
Belyando R. 3.90
Cape R. 2.30
Burdekin Falls Dam
Exported 18.0
Lower Burdekin 9.50
Burdekin R. (Inkerman) Exported 27.50
Burdekin R. (Sellheim) 4.66 (4.1-5.3)
Suttor R. 0.71 (0.60-0.83)
Belyando R. 0.21 (0.18-0.25)
Cape R. 0.50 (0.43-0.58)
Burdekin Falls Dam
50% (36-64) trapped
Exported 3.11 (2.4-4.1)
Lower Burdekin 11.7
(Includes Bowen R. 7.34 (2.4-23))
Burdekin R. (Inkerman) Exported 14.81 (9.8-22)
2008/09 Wet Season
Burdekin R. (Sellheim) 20.00
Suttor R. 0.70
Belyando R. 0.36
Cape R. 2.30
Burdekin Falls Dam
Exported 25.00
Lower Burdekin 4.35
Burdekin R. (Inkerman) Exported 29.35
Burdekin R. (Sellheim) 15.01 (13-18)
Suttor R. 0.14 (0.12-0.16)
Belyando R. 0.11 (0.09-0.12)
Cape R. 0.47 (0.42-0.54)
Burdekin Falls Dam
70% (58-81) trapped
Exported 4.88 (3.5-6.9)
Lower Burdekin 5.97
(Includes Bowen R. 4.83 (1.6-15))
Burdekin R. (Inkerman) Exported 10.86 (7.2-16)
2009/10 Wet Season
Burdekin R. (Sellheim) 2.50
Suttor R. 1.10
Belyando R. 0.90
Cape R. 0.80
Burdekin Falls Dam
Exported 5.50
Lower Burdekin 2.29
Burdekin R. (Inkerman) Exported 7.79
Burdekin R. (Sellheim) 1.71 (1.5-2.0)
Suttor R. 0.22 (0.20-0.24)
Belyando R. 0.16 (0.14-0.18)
Cape R. 0.16 (0.15-0.17)
Burdekin Falls Dam
82% (77-86) trapped
Exported 0.45 (0.36-0.55)
Lower Burdekin 2.04
(Includes Bowen R. 3.84 (0.7-21))
Burdekin R. (Inkerman) Exported 2.49 (1.7-3.5)

Figure 3.1b

Figure 3.1 (Previous page) Streamflow (left) and suspended sediment (right) budgets for the Burdekin River catchment over five monitored water years 2005/06 to 2009/10. Arrows represent the respective contributions from each of the Burdekin River major sub-catchments, the Burdekin Falls Dam spillway, Lower Burdekin (includes a contribution from the gauged Bowen River), and end-of-river export (Inkerman), where the width of each arrow indicates contribution size. Each load estimate in million tonnes is accompanied by 80% confidence intervals as a measure of uncertainty. Four of the major sub-catchments flow into the Burdekin Falls Dam, and an estimate of suspended sediment trapped within this reservoir is also represented (% trapped accompanied with 80% CI) for each water year, as reported in Lewis et al. (2013). The Lower Burdekin sub-catchment contribution is calculated by subtracting the BFD overflow discharge/sediment load from the end-of-river (Inkerman) discharge/sediment load. The Bowen River loads in the 2007/08, 2008/09 and 2009/10 water years have low confidence due to a lack of monitoring data available for this site in the latter years. Mean annual discharge (long-term based on available flow data at each gauge) and a five-year mean sediment load (including SD in brackets) for each site over the study period are also shown.

above the BFD. Discharge in the 2006/07 and 2009/10 water years were comparable to average annual discharge volumes (Fig. 3.1a). The 2005/06 water year was well below average across the entire Burdekin catchment, with an annual discharge of just 2.2 million ML. The BFD was well below capacity at the start of this wet season due to drought, allowing around 40% of inflow from upstream sub-catchments to be captured before water spilled over the dam wall and flowed downstream (Fig. 3.1a).

Sub-catchment contributions to total catchment sediment export

Application of the LRE model indicates that the Upper Burdekin sub-catchment was the source of between 76 and 95% of suspended sediment influx to the BFD over each water year from 2005/06 to 2009/10 (Fig. 3.1). In comparison, the Cape, Belyando and Suttor sub-catchments each contributed between just 1 and 11% of the suspended sediment loads delivered to the dam during each of the monitored water years. Suspended sediment trapping within the BFD ranged from 50 to 85% over the five water years, with the highest trapping occurring in 2005/06 (85%) and 2009/10 (82%) (Lewis et al., 2013). In both of these years, similar sediment load inputs and export from the dam occurred (Fig. 3.1). During the five-year study period, the Lower Burdekin sub-catchment area contributed 55–82% to the end-of-river suspended sediment export. The bulk of this sediment was derived from the Bowen River sub-catchment (7,110 km^2 at

Myuna gauge), which includes approximately 50% of the total Lower Burdekin sub-catchment area (Fig. 3.1).

3.4.2. Sub-catchment annual sediment yields

The Bowen River had the largest annual sediment yield of all Burdekin sub-catchments when sediment loads were normalised to catchment area, with a mean annual yield of 530 t km^{-2} yr^{-1} over the five water years (Table 3.2). The mean annual sediment yield from the Upper Burdekin sub-catchment, five times the size of the Bowen sub-catchment, was 147 t km^{-2} yr^{-1}; with the highest yield (415 t km^{-2} yr^{-1}) occurring during the above average 2008/09 water year. Sediment yields from the Cape, Belyando and Suttor sub-catchments were markedly lower, with the study period means ranging between 5 and 23 t km^{-2} yr^{-1} (Table 3.2). An exception occurred in the Suttor sub-catchment during the wet 2007/08 water year which resulted in a sediment yield of 65 t km^{-2} yr^{-1}.

3.4.3. Minor tributary 'hot-spot' sources

Site-averaged TSS concentrations over the study period ranged from 115 to 4,075 mg L^{-1} across the minor tributary volunteer network sites, providing a reliable indication of sediment source or 'hot spot' areas to target remedial efforts (Fig. 3.2). The tributaries with the highest mean TSS concentrations were observed within the Upper Burdekin and Bowen sub-catchments, reflecting the large sediment load contributions from these two sub-catchments (section 3.4.1). The Dry River and Camel Creek tributaries of the Upper Burdekin sub-catchment had the highest average TSS concentrations across the entire Burdekin (3,395 and 4,075 mg L^{-1}, respectively) (Fig. 3.2). These sites are located in the northern area of this sub-catchment, and all monitored tributaries in this region had elevated TSS concentrations including Grey Creek (2,465 mg L^{-1}) and the Clarke River (1,230 mg L^{-1}). The Clarke River is the largest tributary (~6,400 km^2) draining into the Upper Burdekin River (Fig. 3.2). The other tributaries of the Upper Burdekin had much lower TSS concentrations, particularly Fletcher Creek (130 mg L^{-1}) within the basalt country and the two eastern tributaries that drain the wet coastal range, the Star and Running Rivers (210 and 235 mg L^{-1}, respectively). The five-year average mean annual concentration (MAC) for the Upper Burdekin (735 mg L^{-1}) was below the Burdekin-wide average of 980 mg L^{-1}.

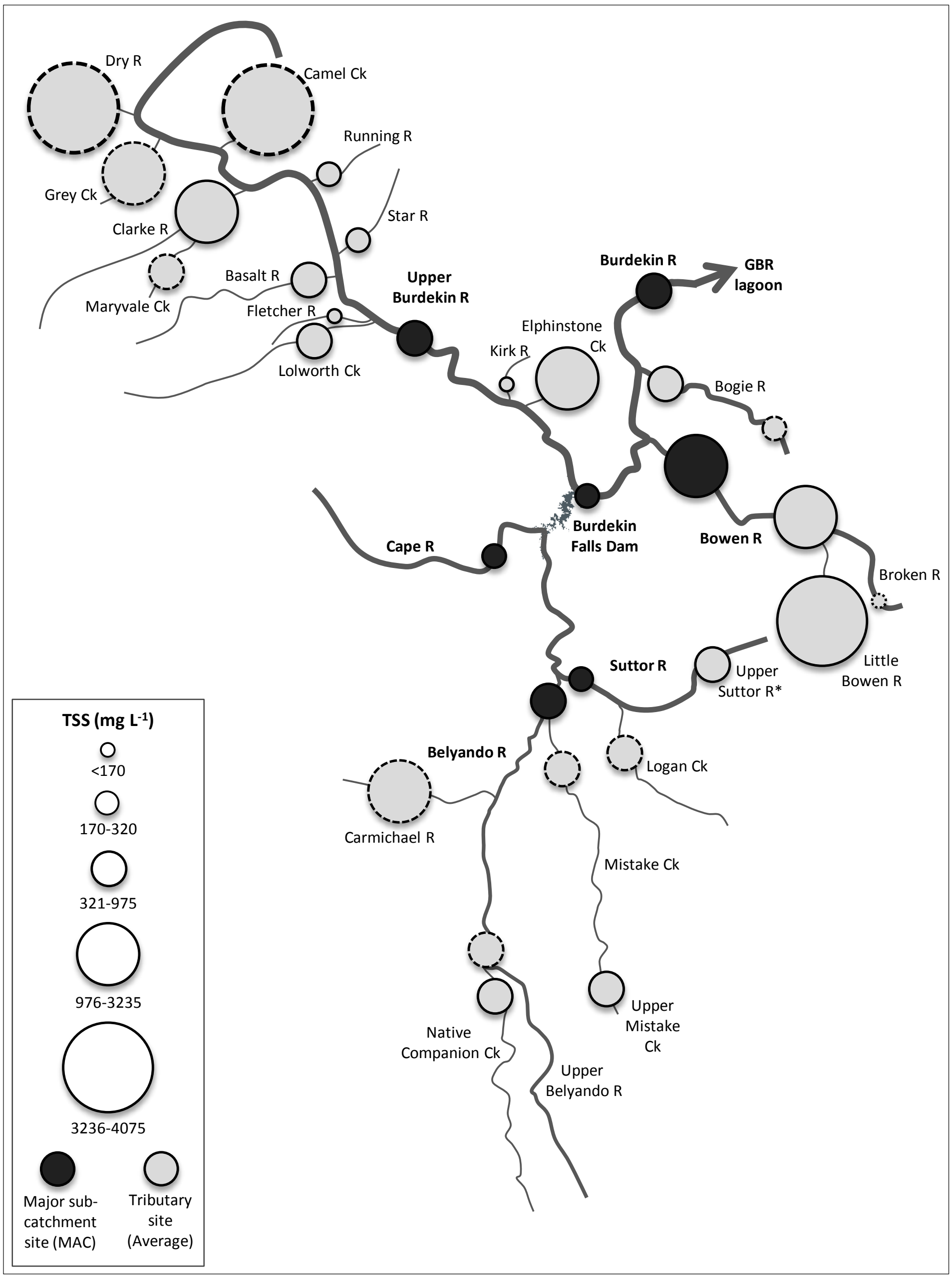

Figure 3.2 Average suspended sediment concentration (light grey circles) for each tributary network site across the Burdekin over seven water years (2004–2011) of data collection. Load-based mean annual concentrations (MAC) for the seven gauged sites (2005–2010) are also displayed for reference, shown as dark grey circles. Circle size represents mean TSS concentration in mg L^{-1} for each site, with the sizing scale representing increasing TSS concentration based on percentiles (<10%, 10–30%, 30–70%, 70–90% and >90%) of all site averages. Dotted circles indicate lower data confidence, with either <3 wet seasons monitored or <20 TSS samples collected in total. *Samples collected 2002/03 to 2008/09.

In comparison, the Belyando, Suttor and Cape River sub-catchments all had lower end-of-catchment MAC's (335, 220, 245 mg L^{-1}, respectively), despite elevated TSS concentrations in some tributaries of the Belyando and Suttor sub-catchments, including the Carmichael (1,100 mg L^{-1}), upper Belyando (925 mg L^{-1}) and upper Suttor (850 mg L^{-1}) Rivers. All sites in the Bowen River sub-catchment had TSS concentrations well above the Burdekin-wide average, except for the small (36 km^2) rainforest headwater site on the upper Broken River (115 mg L^{-1}). The Little Bowen River had the highest average TSS concentration (3,270 mg L^{-1}) within the Bowen. The gauged site (Myuna) had the highest five-year average MAC of the five Burdekin sub-catchments (2,880 mg L^{-1}; Fig. 3.2). The Bogie River, the second largest tributary of the Lower Burdekin had TSS concentrations below the Burdekin-wide average at both upper (305 mg L^{-1}) and lower (510 mg L^{-1}) locations (Fig. 3.2).

3.4.4. Clay, fine silt and coarse sediment load budget

The clay and fine silt sediment fractions (<16 μm) dominated (>70%) suspended sediment at all Burdekin sub-catchment sites over the four water years (2005–2009) where sediment particle size data were available (Fig. 3.3). The Upper Burdekin sub-catchment was the dominant (90%) source of all clay, fine silt and coarse sediment fraction loads into the BFD (Fig. 3.3). Minor sediment load contributions into the dam from the other three upstream sub-catchments were dominated (78–91%) by the clay and fine silt fractions; the clay-only component dominates the sediment fraction contributed by the Belyando (50%) and Suttor (61%) sub-catchments (Fig. 3.3). The efficiency with which different particle size fractions are trapped within the BFD was considered by Lewis et al. (2013), but they did not directly report the specific trapping of the clay and fine silt-sized fractions. The reanalysis of these data averaged over the four water years show that 31% of the clay, 66% of the fine silt and 92% of the coarse sediment fractions were trapped by the BFD, with an overall average trapping efficiency of 66% (Figs. 3.1 and 3.3). The BFD overflow and Bowen River sub-catchment sites contributed a similar clay load of 1.32 and 1.03 million tonnes, respectively, to the end-of-river over the four-year average (Fig. 3.3). Export at the end-of-river was dominated (81%) by the clay and fine silt sediment fractions (Fig. 3.3).

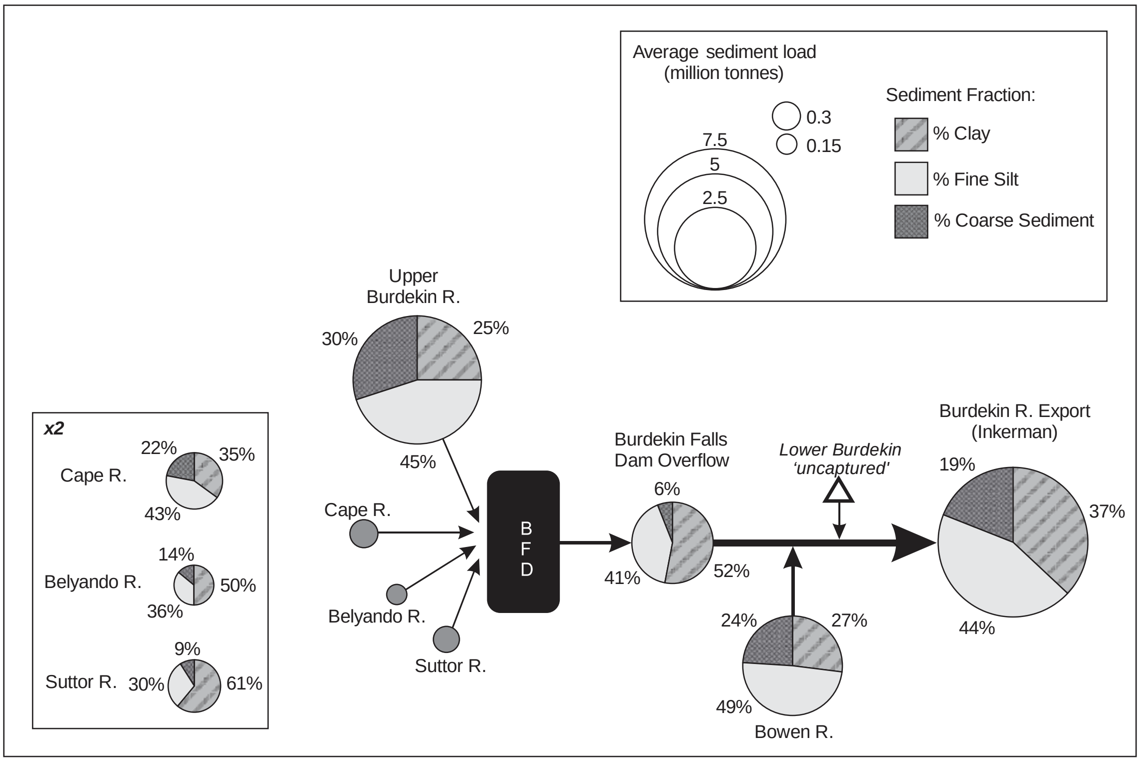

Figure 3.3 Four-year (2005–2009) mean suspended sediment load contributions from each of the major sub-catchments (Upper Burdekin= 6.22 million tonnes; Cape= 0.30 Mt; Belyando= 0.16 Mt; Suttor= 0.26 Mt, Bowen= 3.76 Mt), Burdekin Falls Dam (2.52 Mt), and end-of-river export (Inkerman= 8.44 Mt), with volume (million tonnes) represented by circle area. The proportions of clay, fine silt and coarse sediment fractions contributed by each of these sites are also shown, within each circle. A triangle denotes an 'uncaptured' sediment load (2.16 Mt) contributed to the end-of-river from the ungauged component of the Lower Burdekin sub-catchment.

3.5. Discussion

3.5.1. Catchment-wide discharge and sediment load budgets

The Upper Burdekin sub-catchment was the dominant source of streamflow to the end-of-river over the five water years (Fig. 3.1). Roth et al. (2002) calculated that the Upper Burdekin on average contributes 50% of total annual end-of-river discharge despite comprising only ~30% of the Burdekin catchment area, suggesting the flows measured in the study period are representative of longer-term patterns. The study period captured below average, average and above average discharge years in all Burdekin sub-catchments (Fig. 3.1). This included the largest gauged annual discharge recorded for the Belyando River (2007/08; recurrence interval (RI) =58) and second largest for the Upper Burdekin (2008/09; RI=33). Very little discharge from sub-catchments upstream of the BFD was trapped in the reservoir during the study period, except for 2005/06, when drought had reduced reservoir water levels to ~60% of capacity (Fig. 3.1a). Otherwise the dam was almost full prior to each wet season; despite its considerable volume (1.86 million ML), full capacity is <25% of the average annual inflow. BFD overflow waters were the primary source (i.e., 65–95%) to end-of-river discharge over the study period, with the remainder contributed from the Lower Burdekin sub-catchment, including the Bowen River (Fig. 3.1).

An important finding of this study is that the Upper Burdekin is the dominant sediment source to the BFD under all streamflow conditions, contributing 76–95% of the total sediment influx in each of the five water years studied. The Cape, Belyando and Suttor sub-catchments each contributed only 1–11% of the total sediment load into the dam in any water year during the study period (Fig. 3.1). The contrast between the Upper Burdekin and these other sub-catchments was greatest in the 2007/08 water year when the Belyando and Suttor sub-catchments combined contributed ~54% of total inflow into the dam due to above average events across their catchment areas, but contributed only 15% of the total sediment load (0.92 million tonnes) into the dam (Fig. 3.1b). In comparison, the Upper Burdekin contributed 4.66 million tonnes, or 77% of the sediment load into the BFD, while contributing only ~33% of total inflow (Fig. 3.1b). The BFD reservoir trapped an average of 66% (80% CI = 60–72) of annual suspended sediment influx over the five study years (Fig. 3; Lewis et al., 2013). The importance of the Upper Burdekin sub-catchment as a major sediment source to end-of-river export has been diminished by the construction of this reservoir and its sediment trapping efficiency. Assuming equal trapping of sediment within the reservoir contributed from all upstream sub-catchments, the Upper Burdekin contributed ~14–43% to annual end-of-river sediment export during this study period. The Lower Burdekin sub-catchment, including the Bowen River, is now the major sediment source of suspended sediment discharged into the GBR lagoon, despite representing only 12% of the entire Burdekin catchment area (Fig. 3.1). The Bowen River contribution to end-of-river sediment export ranged from 31–50% over the study period, representing 48–81% of the Lower Burdekin sub-catchment contribution (Fig. 3.1). However these Bowen River contributions do not include the 2009/10 water year due to a high uncertainty in the load estimate; high uncertainties for the Bowen River were also calculated for the 2007/08 and 2008/09 load estimates (see load estimates in red, Fig. 3.1b). The high uncertainties result from a lack of TSS concentration data available during these above average discharge years and the difficulties developing discharge-TSS concentration relationships using TSS data collected only in below average and average water years. In particular, TSS data were not available for the largest streamflow event in the above average (RI=13) 2007/08 water year (see Appendix Fig. A3.1f). Uncertainties in the Bowen load outputs highlight the importance of (1) prioritising critical water quality monitoring sites to inform management decision-making and (2) prioritising the capture of larger discharge events in sampling regimes for more precise load calculations.

Our results demonstrate the importance of measured stream TSS concentration and flow data to accurately estimate loads and source areas of suspended sediment in comparison to catchment modelling-only studies. The study of McKergow et al. (2005) (see also Brodie et al., 2003) based on the SedNet model showed delivery of a large proportion of the suspended sediment from a small proportion of the catchment, although their findings were limited to an assessment of the entire GBR catchment area (i.e. no specific numerical data for the Burdekin catchment were presented). Furthermore inaccurate and unrealistic assumptions in the modelling approach at the time, such as overestimates of dam trapping (see Lewis et al., 2013) and underestimates of gully and streambank erosion (see Wilkinson et al., 2013) are now known to have produced poor estimates of actual sub-catchment spatial sources of suspended sediment. In contrast, the use of measured field data for suspended sediment and particle size in this study provides far more accurate estimates which can be compared and used to calibrate recently improved modelling estimates using the Source Catchments model (unpublished data) and updated versions of SedNet (Wilkinson et al., 2014).

3.5.2. Sub-catchment annual sediment yields: a comparison with other tropical river studies

End-of-river sediment yields for the Burdekin are low (<115 t km^{-2} yr^{-1}) when compared to published yields from other tropical catchments around the world (Table 3.3). Most catchment studies across the tropical belt have been conducted in wet tropical rainforest (*Af*), monsoon (*Am*) and savannah (*Aw*) climates (Peel et al., 2007) within South America and South-East Asia, where annual rainfall typically exceeds 2000 mm y^{-1} and yields exceed 500 t km^{2} yr^{-1} (Table 3.3). Although the Burdekin catchment is defined largely as semi-arid (*Bsh*), it is the higher rainfall and steeper terrain of the coastal areas

(*Aw* and *Cwa*) that are the primary hydrological drivers of this catchment where climatic conditions are between wet tropical and the more temperate semi-arid or 'dryland' regions (see Tooth, 2000). Indeed, sediment yields from the Bowen River reflect its wet coastal location, particularly in 2006/07, 2007/08 and 2008/09 where mean annual discharge (0.80 million ML) was well exceeded (1.03, 2.49 and 1.38 million ML, respectively). Bowen sediment yields (370–1035 t km^{-2} yr^{-1}) in these years are comparable with rates generated in much wetter tropical rainforest studies of the Andes (Restrepo and Kjerfve, 2000) and NW Amazon basin in South America (Laraque et al., 2009), Borneo (Chappell et al., 2004) and northern Vietnam in South-East Asia (Ha Dang et al., 2010; Table 3.3). In contrast, sediment yields generated from all other Burdekin sub-catchments and the end-of-river are more comparable to those generated in north-eastern Africa and India (Dunne, 1979; Nyssen et al., 2009; Panda et al., 2011), where wet-dry tropical conditions also prevail (i.e., high variability, rare but extreme runoff events). Thus data generated in this study and the sediment budget approach utilised might be most applicable for use in such climatic regions, where few sediment sourcing and yield studies have been conducted.

3.5.3. Minor tributary 'hot-spot' sources

Across the Burdekin sub-catchments variations in sediment load contributions are driven by their varied topography, geology, rainfall and vegetation. The Upper Burdekin and Bowen sub-catchments have steep terrain, with highly incised river channels (>18 m channel depths) that are highly efficient in streamflow and sediment transport (Fielding and Alexander, 1996; Roth et al., 2002). The tributaries with the highest average TSS concentrations are located within these two sub-catchments, including the north-western region of the Upper Burdekin, a relatively steep landscape hosting old sedimentary rock deposits prone to erosion. Tributaries monitored in this region include the Dry and Clarke Rivers, and Camel and Grey Creeks (Fig. 3.2). The Little Bowen River was also identified as a 'hot-spot' within the Bowen River sub-catchment, with large areas of exposed soils and gullying, also containing old sedimentary rock deposits, and TSS concentrations peaking >10,000 mg L^{-1} in both 2006/07 and 2008/09. Recent sediment tracing by Wilkinson et al. (2013) also identifies the Little Bowen River as a major sediment source, together with large areas of gully erosion immediately upstream of the Myuna gauge. Tributaries within both the Bowen

Table 3.3 Comparison of Burdekin sediment yields (bold type) with other tropical river sediment studies.

Wet or dry tropical climate	Köppen climate classification [*Peel et al.,* 2007]	Mean annual rainfall (mm yr^{-1})	Study location	River	Study reference	Upstream catchment area (km^2)	Dominant land use	Average annual sediment load (Million tonnes yr^{-1})	Annual sediment load for study period (Mt)	Sediment yield (t km^{-2} y^{-1})
Wet	*Af* Tropical rainforest	3200	Ecuador/ Peru, South America	Napo River, Amazon basin	*Laraque et al.,* [2009]	26,860/ 100 520	Forest	-	26,860 km^2: 22.6 Mt (2002–2005) 100,520 km^2: 46 Mt (2004/2005)	463–998
Wet	*Af, Am, Aw* Tropical rainforest, monsoon,savannah	2050 (basin mean variation 1200–3100)	Columbia, South America	Magdalena River, Andes	*Restrepo & Kjerfve* [2000]	257,440	Agriculture, forest	143.9 (1975–1995)	-	560
Wet	*Af* Tropical rainforest	2500	Indonesia, SE Asia	upper Way Besai catchment, West-Lambung, Sumatra	*Verbist et al.,* [2010]	6.7–360	Coffee, forest, paddy rice	-	-	110–1730
Wet	*Am* Tropical monsoon climate	2765	Borneo, SE Asia	Baru catchment	*Chappell et al.,* [2004]	0.44	Forest, selective logging	-	0.00026 Mt (12 mths to 30/06/96)	592
Wet/Dry	*Aw* Tropical savannah (wet and dry)	2125–2700	Indonesia, SE Asia	Upper Konto catchment, East Java	*Rijsdijk* [2005]	233	Natural forest, agroforestry (steep area), intensive agriculture, rice	-	0.29 Mt (average of 1988–1989) *includes bed load	1200
Wet/Dry	*Cwa* Humid Subtropical	1600	Vietnam, SE Asia	Red River watershed, China, Laos, Vietnam	*Ha Dang et al.,* [2010]	169,000	Forestry/natural forest, agriculture	90	24–200 Mt (1960–2008)	600
Wet/Dry	*Aw* tropical savannah (wet and dry)	800–1360	India (draining east into Bay of Bengal)	8 tropical (Peninsular) river basins	*Panda et al.,* [2011]	35,000–313,000	Agriculture, forest	1.5–170 (1986–2006)	-	17–704
Wet/Dry	*Aw* tropical savannah; *BSh* Hot semi-arid	250–3500	Kenya, Africa	multiple catchments, southern Kenya	*Dunne* [1979]	<2000	Forest, rangeland, agriculture	-	-	20–200
Dry	*BSh* Hot semi-arid	600	Ethiopian highlands, Africa	May Zeg-zeg, Tigray, north Ethiopia	*Nyssen et al.,* [2009]	1.87	Agriculture, exclosure, rangeland, grassland	-	0.00036 Mt (2006)	190
Dry	**Predominately *BSh* Hot semi-arid, coastal areas *Aw/Cwa***	**500–2500**	**Australia**	**Burdekin River, north Queensland**	***This study; Kuhnert et al.,* [2012]**	**133,400**	**Grazing**	**3.93**	**0.88–14.81 Mt (range 2005–2010 water years)**	**7–114**
Dry	*BSh* Hot semi-arid	630 (basin mean variation 530–2000)	Australia	Fitzroy River, neighbouring basin	*Packett et al.,*[2009]	142,600	Grazing, dryland cropping	-	0.03–4.24 Mt (range 1994–98 & 2002–2008)	0.23–30

(Broken River) and Upper Burdekin (Star and Running Rivers) sub-catchments with coastal rainforest headwaters contribute considerable streamflow to the end of each sub-catchment, but have low sediment concentrations compared to other tributaries within these sub-catchments (Fig. 3.2). For example, the Star and Running Rivers contributed ~30% of Upper Burdekin discharge in the 2005/06 water year, but only ~3% of the total sediment load exported by this sub-catchment. The tributaries draining these wetter coastal catchments are naturally forested. The western tributaries of the Upper Burdekin and Bowen sub-catchments are less densely vegetated and widely composed of weathered and erodible lithologies (Fig. 1.4).

In contrast, the south-western Cape, Belyando and Suttor sub-catchments have low relief, expansive anastomosing floodplains (overbank flooding at gauged site depths of 8, 8 and 4.5m, respectively), less stream power for entraining coarser material and greater opportunity for sediment deposition before it is exported from these sub-catchments. Thus, although the steeper headwater tributaries within these western sub-catchments produce high sediment concentrations (e.g. Carmichael and upper Suttor Rivers), mean end of sub-catchment yields remain low (<23 t km^{-2} yr^{-1}) compared to the Upper Burdekin (147 t km^{-2} yr^{-1}) and Bowen (530 t km^{-2} yr^{-1}) sub-catchments (Table 3.2), both of which have greater sediment availability and transportability.

3.5.4. Clay, fine silt and coarse sediment load budget

Suspended sediment loads exported by all Burdekin sub-catchment sites were dominated by the clay (<4 µm) and fine silt (4–16 µm) sediment fractions over the four water years 2005/06 to 2008/09 (Fig. 3.3). As noted in the methods, the coarser sand fraction may be underestimated in the results. Clay, fine silt and coarse sediment loads into the BFD were all dominated by the Upper Burdekin sub-catchment, including 4.35 million tonnes of clay and fine silt per year on average over this four year period. In comparison, the Cape, Belyando and Suttor sub-catchments combined contributed an average of 0.60 million tonnes of clay and fine silt per year (Fig. 3.3). Although the BFD traps an average of 66% of incoming sediment and considerably reduces sediment delivery to the end-of-river from these four upstream sub-catchments, it is the coarser sediment fraction that is preferentially trapped. As a result, the clay-sized fraction dominates all sediment carried over the dam spillway (Fig. 3.3; Lewis et al., 2013). While the Bowen River was a much larger source of suspended sediment loads to the end-of-river when compared to the BFD source, the mean particle size specific loads over this period reflect the increasing proportional importance of the BFD source with respect to the contribution of fines to the end-of-river. Indeed the proportional contribution from the Bowen River to BFD source reduces from 1.5:1.0 for the bulk sediment fraction (3.76 and 2.52 million tonnes from the Bowen River and BFD sources, respectively), to 1.2:1.0 when the combined clay and fine silt fractions are considered (i.e. 2.86 and 2.36 million tonnes, respectively) and further to 0.8:1.0 when the clay-only fraction is considered (1.03 and 1.32 million tonnes, respectively). However, the clay-only sediment yield from the smaller Bowen River sub-catchment (145 t km^{-2} yr^{-1}) is 10-fold higher than the BFD overflow source (11 t km^{2} yr^{-1}). Despite the influence of the BFD in reducing sediment export from the upstream catchment area (114,260 km^2), and the increased importance of the Lower Burdekin sub-catchment area as the major sediment source, management efforts targeting the finer sediment fractions still need to consider this large source area above the BFD.

Further geochemical and clay mineralogy tracing analyses may also highlight the relative importance of apparent minor sediment sources such as the Belyando and Suttor Rivers, which contribute almost exclusively the clay and fine silt fractions (86% and 91%, respectively, Fig. 3.3). Waterholes within these two sub-catchments are constantly turbid (Burrows et al., 2007), and fine dispersible clay particles are known to be contributed to the BFD by the Suttor arm (Fleming and Loofs, 1991), with the reservoir often remaining turbid long after flood conditions recede (author per. obs.; Fleming and Loofs, 1991; Griffiths and Faithful, 1996). Such tracing may discriminate these dispersive clay types from other potential clay sources across the Burdekin and determine which clay mineral types are preferentially transported through the catchment and further into the adjacent marine environment. A further research gap is the quantification of the relative contributions of suspended clays washed as surface runoff into tributaries compared to those yielded from lower in the soil profile by gully and streambank erosion. This quantification will help to further target erosion management efforts. Recent research has identified sub-surface erosion processes as major sediment sources in the larger Australian tropical catchments, including the Burdekin, under current climatic and land management conditions (see reviews by Bartley et al., 2014 and Caitcheon et al., 2012).

3.5.5. Burdekin River discharge and sediment export to the GBR lagoon

Above average discharge across the Burdekin sub-catchments in the 2007/08 and 2008/09 water years resulted in total Burdekin discharge to the GBR lagoon that were three times the mean annual discharge, and are ranked as the sixth (2007/08) and fourth (2008/09) largest years on record (Fig. 3.1b). These wetter years were followed by the third largest discharge year on record in 2010/11 (34.8 million ML), which saw an extended period of river discharge into the GBR lagoon for ~200 days (Chapter 2). This study has fallen within a 'wet cycle' in the longer term inter-decadal cycling of wet and dry conditions in the Burdekin, where rainfall and streamflow trends coincide with the Pacific Decadal Oscillation cool phases, which influence strong ENSO La Niña events (Lough, 2007; Lough et al., in press). The current wet conditions followed a period of drought in the mid-late 1990's/early 2000's and preceding wetter cycles in the 1950's, 1970's and the late 1980's/early1990's. Reconstructed streamflow using coral luminescence showed an increase in the cyclic variability of rainfall and streamflow in the 20th century, as well as the extent of both wet and dry conditions (Lough, 2007). The tight cluster of very wet years highlighted in this study are projected to occur more regularly as climate change progresses (Lough, 2007; Lough et al., in press), increasing the frequency and volume of terrestrial sediment discharged to the inshore GBR.

As part of a broader research effort focused on managing Burdekin River export to the GBR lagoon, Kuhnert et al. (2012) calculated annual Burdekin suspended sediment export using the Loads Regression Estimator (LRE) on 24-years of available suspended sediment data (1986–2010). This data analysis incorporated key controlling features of Burdekin sediment export including covariates representing (1) ratio of streamflow sourced from above the BFD, and (2) annual dry season vegetation ground cover figures, representing the influence of cover on sediment erosion (Kuhnert et al., 2012). Using these explanatory terms they were able to produce an average load of 3.93 (80% CI=3.41–4.45) million tonnes, with tight uncertainty bounds representing errors associated with the input data, thus providing resource managers with our current best estimate of present day Burdekin sediment export. When compared to this study period, three of the five water years far exceeded this long-term average, including 7.2 million tonnes in 2006/07, 14.81 million tonnes in 2007/08 and 10.86 million tonnes in 2008/09 (Fig. 3.1), illustrating the variability of suspended sediment export from this river catchment and the influence of wetter climatic cycles.

The influence of drought breaking years and sediment supply availability on Burdekin River annual suspended sediment export has also been highlighted in this study. For instance, end-of-river export was ~30% greater in 2007/08 than 2008/09, despite both water years having discharges of similar volumes; 27.50 and 29.35 million ML, respectively. The earlier year had a larger sediment contribution from the catchment area below dam, with higher sediment yields per unit area (Table 3.2). The Burdekin has been described as a supply-limited catchment (Amos et al., 2004) and given that above average discharge occurred across the entire catchment in 2007/08 (Fig. 3.1), it is also likely there was a depletion in available sediment supply for runoff in the subsequent year. Previous studies have highlighted the increased sediment loads delivered during drought-breaking floods (Amos et al., 2004; McCulloch et al., 2003a; Mitchell and Furnas, 1996), which was also observed in this study with a drought breaking flood year in 2006/07 which followed a series of relatively dry years, including 2005/06 (Fig. 3.1). Total discharge in the 2006/07 and 2009/10 water years were similar to average annual discharge, however, the sediment load exported in 2006/07 (7.2 million tonnes) was double the annual average and three times greater than the sediment load exported in 2009/10 (2.49 million tonnes; Fig. 3.1). The 2009/10 sediment load also reflects the depleted sediment supply after the two record flood years, and improved ground cover across the entire catchment resulting from this wetter period, which results in decreased soil loss (Bartley et al., 2014). Indeed Kuhnert et al. (2012) found a significant decrease in sediment loads at the end-of-river site as ground cover increases.

3.5.6. Implications for Great Barrier Reef management

The Upper Burdekin and Bowen River sub-catchments have the highest suspended sediment yields of all Burdekin sub-catchments and were the major sediment sources during this study. Their wetter coastal locations, steeper topography and weathered geology result in high streamflow and sediment transport efficiency. The Upper Burdekin is the major source of discharge to both the BFD and end-of-river, and the dominant source of all sediment fractions (i.e. clay, fine silt and coarse sediment) into the BFD. The BFD reservoir is an efficient sediment trap, and has reduced the suspended sediment load supplied from the large upstream catchment area (88% of the entire catchment) to end-of-river export, including the Upper Burdekin source. The reservoir has also influenced the sediment size fractions transported from this upstream catchment area, with the finer clay fraction now dominating all sediment exported over the dam spillway to the river mouth and adjacent GBR lagoon. This study identified the Bowen River as the major source of end-of-river suspended sediment export. This catchment has a comparatively small upstream area and the highest sediment yields (mean of 530 t km^{-2} yr^{-1}) across the Burdekin, providing a clear focus area for management efforts aimed at reducing the export of all sediment size fractions. However, the study findings show that similar load contributions of both the clay and fine silt fractions were delivered from the two major source areas: the Bowen River and the BFD overflow. Targeted source area remediation of the clay and fine silt sediment fractions of increased ecological risk should first be confined to the Bowen River sub-catchment if assessed on a per unit area contribution; however, further investigation into the geochemical and clay mineralogy characteristics of these different clay/fine silt sources is suggested, and their subsequent transport in and likely impact on the marine environment is required. The sediment sourcing, reservoir influence on sediment size transport and yield data generated across the Burdekin has broader application in other dry tropical river catchments, particularly those located in wet-dry tropical savannah climates. This study also highlights the importance of incorporating sediment particle size into catchment sediment budget studies where management goals are aimed at reducing downstream turbidity and sedimentation on marine ecosystems such as seagrass meadows and coral reefs.

The influence of this terrigenous fine sediment within the GBR has been recently highlighted by Fabricius et al. (2014), who correlated increased inshore turbidity with rainfall and runoff events from GBR rivers such as the Burdekin. Finer sediment particles, often with an attached organic component once in the marine environment, are easily resuspended and transported along the GBR shelf (Brodie et al., 2012; Orpin et al., 1999; Webster and Ford, 2010; Wolanski et al., 2008) and are the most harmful sediment type to GBR receiving ecosystems such as corals (Fabricius and Wolanski, 2000; Humphrey et al., 2008; Weber et al., 2006), seagrass (Collier et al., 2012) and other associated communities such as reef fish (Wenger and McCormick, 2013). The combined influence of increased fine sediment particles with decreased salinity (i.e. synergistic effects on coral fertilisation; see Humphrey et al., 2008) during extended flood plume conditions in above average Burdekin discharge years also requires further investigation. While this study shows a clear partitioning of sediment fractions through the BFD (this Chapter) and into the marine environment (Chapter 2), there is still a need to delineate the marine areas of most risk to the increased sediment loads delivered from the Burdekin River (Bartley et al., 2014). For example, coral reefs that have developed and thrived in naturally turbid areas such as Paluma Shoals and Middle Reef (Browne et al., 2013; Perry et al., 2012) are unlikely to be as adversely affected by increased sediment loadings as clear water reefs, such as off Pelorus Island where elevated sediment inputs and associated increased turbidity are argued to have negatively affected coral reefs (Roff et al., 2013).

4. Clay mineral source tracing and characterisation of Burdekin River and flood plume fine sediment

Bainbridge Z., Lewis S., Smithers S., Wilkinson S., Douglas G., Hillier S., Brodie J. Accepted. Clay mineral source tracing and characterisation of Burdekin River (NE Australia) and flood plume fine sediment. Journal of Soils and Sediments, doi: 10.1007/s11368-015-1282-4.

Abstract

Purpose To define the relative contributions of tributaries within the Burdekin River catchment to fine suspended sediment delivered to the Great Barrier Reef (GBR) lagoon, and investigate the temporal variability in these contributions.

Materials and Methods Sediments in river and flood plume water samples were analysed for particle size and clay mineral abundance at 31 sites across the Burdekin catchment. Sampling sites included minor tributaries, sub-catchment, reservoir and end-of-river outlets, and the adjacent coastal flood plume. Samples were collected during multiple wet season streamflow events from 2005−2011. Particle size data were used to calculate catchment-wide fine sediment (<10 μm) and clay-only (<4 μm) budgets and a clay mineral ratio was used to distinguish geological source areas.

Results and discussion This sediment source tracing study identified basaltic, granitic and sedimentary geologies as the dominant sources of end-of-river and flood plume fine sediments (<10 μm) across the Burdekin. A clay mineral ratio (illite/illite+expandable clays) clearly distinguished between the two main catchment source areas, highlighting the importance of considering both of these sources for management of the finer sediment fractions that are potentially more ecologically damaging in the marine environment. This ratio also highlighted the relative enrichment of expandable (smectite-rich 'shrink-swell') clays along the salinity gradient within remaining flood plume fine sediment.

Conclusions The distinctive geological source-related "fingerprints" found in this study validate the relative proportions of clay minerals as a valuable tracing tool in large and geologically complex catchment settings, and across freshwater-marine continuums.

Keywords: turbidity; erosion; catchments; Great Barrier Reef; sediment budget; sediment fingerprinting; clay mineral ratios

4.1. Introduction

Increased turbidity and sedimentation associated with the delivery of greater quantities of fine sediments to the coast due to anthropogenic modification of catchments have seriously degraded many near-shore marine ecosystems around the world (Fabricius, 2005; Golbuu et al., 2011; Lotze et al., 2006; Restrepo et al., 2006; Risk, 2014; Rogers, 1990). Within the Great Barrier Reef (GBR), Australia, there is growing evidence that increased turbidity and sedimentation associated with agricultural development of the coastal catchments have negatively impacted valuable ecosystems (Brodie and Waterhouse, 2012), including seagrass meadows (Collier et al., 2012; Petus et al., 2014) and coral reefs (Fabricius and De'ath, 2001; Fabricius et al., 2005; Roff et al., 2013). Indeed, sediment yields to the GBR from coastal catchments (with a total area of 426,000 km^2) have increased by ~5.5 fold since they were cleared for agricultural development (c. 1850) (Kroon et al., 2012). While only a fraction of this material is generally delivered directly to the GBR (Chapter 2; Lewis et al., 2014), significant quantities of nitrogen and other contaminants are delivered to the coast attached to fine sediment. Identifying major catchment source areas of this sediment and an improved understanding of how it is transported through the catchment and dispersed within GBR coastal waters are required to better manage this threat (see Bartley et al., 2014 for review).

Sediment fingerprinting uses one or more physical or biochemical properties of sediment to identify the upstream origin(s) of this sediment, and investigates river catchment sediment dynamics at varying spatial and temporal scales (Koiter et al., 2013). Clay mineral properties of sediment are dependent on parent rock material, time and environmental conditions that influence weathering (McKenzie et al., 2004; Viscarra Rossel, 2011). Therefore, the presence and relative abundance of common clay minerals within a suspended sediment sample may provide a unique 'fingerprint' that can be traced to an individual river or source area (Gingele and De Deckker, 2004). However, the success of this technique is dependent on the source area fingerprints being sufficiently different from each other, and limited mixing of multiple upstream sources at the point of sampling. Clay mineral fingerprinting has been applied as a sediment-tracing technique to inform palaeoclimatic reconstructions from marine sediment cores (Gingele and De Deckker, 2004; John et al., 2006; Limmer et al., 2012) and to trace contemporary sediment sources within fluvial catchments (Douglas et al., 2006b; Gingele and De Deckker, 2005; Guyot et al., 2007; Sionneau et al., 2008). Studies commonly focus on four clay mineral groups including illite, smectite, kaolinite and chlorite. Kaolinite is typically associated with leached soils under tropical weathering conditions, and smectite forms from volcanic parent rocks or may authigenically form in poorly-drained environments. In contrast, illite and chlorite are typically inherited from parent materials through physical weathering processes in drier and cooler environments (Gingele and De Deckker, 2005; Viscarra Rossel, 2011).

In an Australian context, clay mineral assemblages have been used to characterise discharge from large Australian rivers and to examine the spatial distribution of sediment delivered to offshore marine environments through tracing in sediment cores collected around the continental margin (Gingele and De Deckker, 2004). Clay mineral fingerprinting has also revealed how fine suspended sediments with different clay mineralogies may be strongly fractionated in the marine environment. For example, smectite-rich clays are preferentially entrained and transported further relative to other minerals in flood plume waters of the Fitzroy River discharging into the GBR lagoon (Douglas et al., 2006a). This finding has important implications for understanding the transport and resuspension potential of fine sediments composed of different clay minerals in marine settings. For example, Chapter 2 identified clay and fine silts (i.e. <16μm) to be preferentially transported in Burdekin River primary flood plume waters, with greater dispersal potential and characteristics (i.e. organic and nutrient-rich) likely to be most damaging to marine receiving environments. However, there is a need to further characterise this sediment fraction in terms of its catchment origins and source processes.

This study uses sediment particle size and clay mineral fingerprinting to characterise the spatial and temporal variability of suspended sediment collected across Burdekin River tributaries, larger sub-catchments and coastal flood plumes during consecutive wet seasons from 2005 to 2011. The clay mineral component focuses only on the finer, <10 μm sediment fraction, of most risk to downstream receiving ecosystems (Chapter 2). A fine (<10 μm fraction) sediment load budget is constructed to identify the major sources of clay and very fine silt sized-sediments from within this large catchment (130,400 km^2), and to trace their transport and dispersal in resultant coastal flood plumes. The preferential transport of fine sediments composed of different clay minerals through a reservoir and within coastal flood plumes are also examined. These findings are discussed in the context of best managing sediment erosion in the Burdekin catchment to reduce the export to the GBR of the most damaging fine fractions. The comprehensive clay mineral abundance dataset (231 samples) is used to link river and coastal flood plume sediment to the source area geology of upstream tributaries and to define the contributions to downstream sediment loads of particular geological areas. The results show that the expandable clays are preferentially transported within flood plumes, which are likely derived from the Bowen River source. The study approach highlights the potential of the clay mineral fingerprinting technique for use in other large and seasonally-dry tropical, or semi-arid catchments.

4.2. Materials and methods

4.2.1. Catchment characteristics

Refer to Introduction section 1.4 for a detailed description of the Burdekin River catchment. Further geological description of the Burdekin catchment relevant to this Chapter is provided below.

The near-coastal Upper Burdekin and Bowen sub-catchments are bordered by steep mountain ranges, dominated by igneous and sedimentary rock types (Fig. 4.1). The Nulla Basalt Province occupies a large proportion of the western Upper Burdekin sub-catchment, and includes basalts ranging from 13,000 years (Toomba basalt flow) to 5 million years in age (Whitehead and Stephenson, 1998). Permian basalts (252–300 Ma) are located in the Bowen catchment within its lower reaches and within the Little Bowen River tributary (Lizzie Creek Volcanics; Malone et al., 1966), and highly weathered Tertiary basalts (20–30 Ma) also occur in the upper section of the Bowen River sub-catchment (Dickins and Malone, 1973). The drier western sub-catchments (Cape, Belyando and Suttor) are mostly formed over remnant sedimentary basins, with small areas of volcanic (Tertiary basalts) and metamorphic rocks in the headwaters of the Suttor and Belyando (Mistake Creek tributary only) sub-catchments (Fig. 4.1).

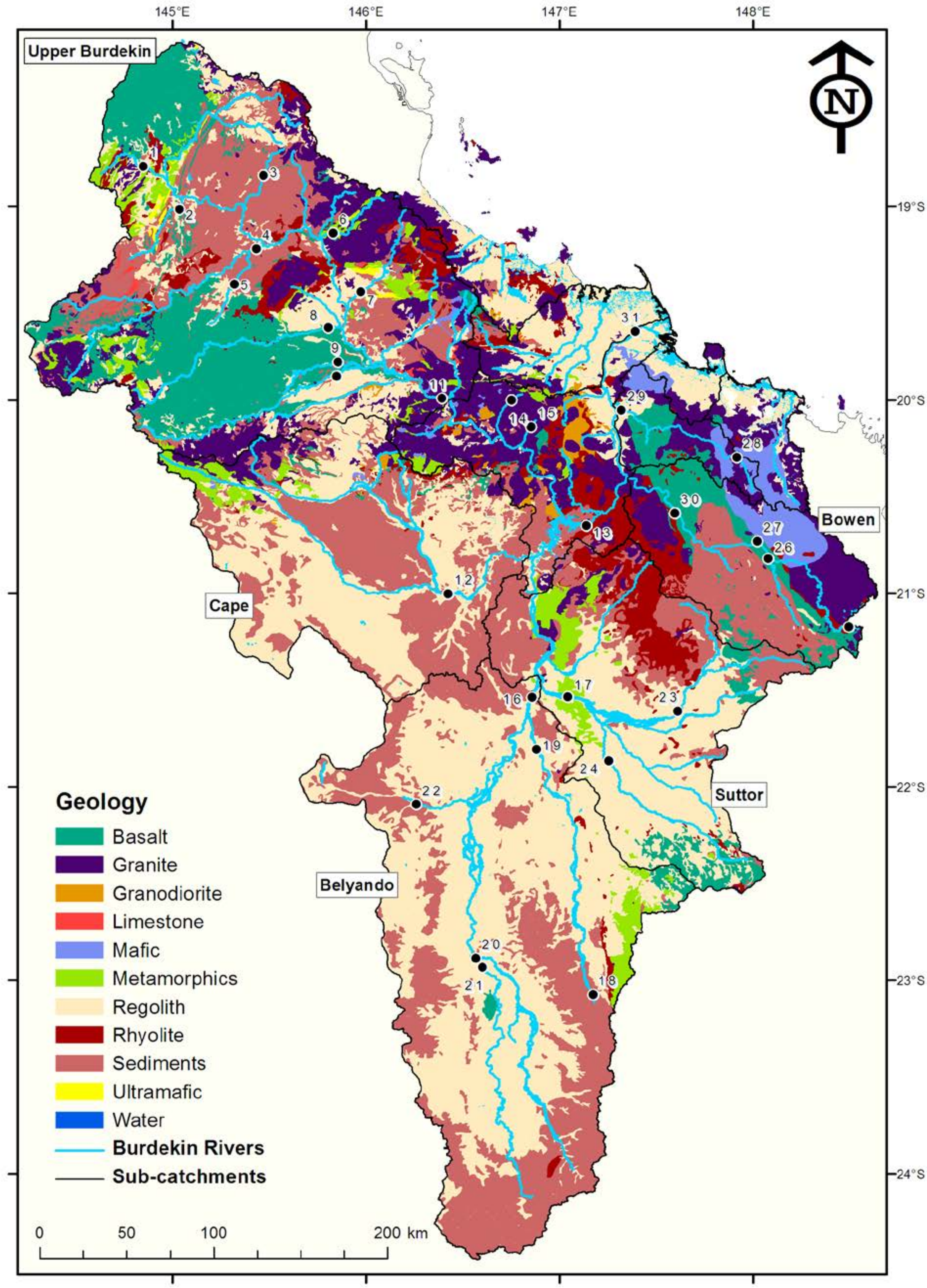

Figure 4.1 Major geologies of the Burdekin River catchment. Site numbers relate to Table 4.1 (Source: GeoScience Australia).

4.2.2. Sample collection

Flood water surface 'grab' samples (top 0.5 m of water column) were collected at 31 locations across the Burdekin River catchment, capturing all stages of the hydrograph over multiple streamflow events that occurred each wet season (Fig. 1.2). The study period included six consecutive water years (Oct 1 to Sept 30) from 2005/06 to 2010/11. Sampling sites included seven streamflow gauge locations draining the five major sub-catchments of the Burdekin River (Upper Burdekin, Cape, Belyando, Suttor and Bowen Rivers), the Burdekin Falls Dam (BFD) outlet and the end-of-river freshwater discharge point (Inkerman). In addition, a network of 24 landholders was established and formally trained to collect water samples at ungauged minor tributary locations across the Burdekin (Fig. 1.2; see also Appendix Table A3.1). These sites were established to increase the spatial density of the dataset collected across this large and sparsely populated (~25,000 people) river catchment, and included locations inaccessible by road during flood events. Further details about sample collection can be found in 3.3.1. It is acknowledged that the surface sampling techniques applied in this study likely underestimate the sand fraction but nonetheless provide a large, internally consistent spatial and temporal dataset for assessing catchment fine sediment sources.

Total suspended solids (TSS) concentrations were measured from the water samples collected across all sites (Chapter 3). Here further analysis of a subset of these samples for particle size and clay mineralogy is described. Particle size analysis was conducted on 504 samples selected from the rising, peak and falling stages of the streamflow hydrograph (Table 4.1). A smaller subset of 231 samples was analysed for clay mineralogy, with representative samples selected mostly from the rise and peak flood stages of larger streamflow events to best capture periods where the majority of suspended sediment was transported through the catchment.

Surface samples from coastal flood plumes adjacent to the Burdekin River mouth were also collected for each wet season from 2007/08 to 2010/11 (22/01/08; 9/02/09; 24/02/10; 25/03/10; 30/12/10). These samples were collected from the turbid inner plume (i.e. 'Primary' water type; see Petus et al., 2014, Appendix A) immediately following peak discharge at the end-of-river site. Samples were collected along the central plume axis within 10 km of the river mouth, following the suspended sediment-salinity gradient. The two major flood peaks in the 2009/10 wet season were sampled.

Table 4.1 Study site details (water years sampled, upstream catchment area, *n*, number of samples collected), mean TSS concentrations (mg L^{-1}), average (mean ± standard deviation) sediment particle size and clay mineralogy proportions and proportion of basalt in the upstream catchment area.

Site (Site ID on Fig. 4.1)	Major sub-catchment	Upstream catchment area (km^2)	% upstream basalt (mafic-ultramafic)	Wet seasons data collected	Mean TSS ** (mg L^{-1})	Sediment particle size (TSS weighted) (mean ± 1 s.d.)					Clay mineralogy (TSS weighted) (mean ± 1 s.d.)				
						n	<10 µm Fraction (%)	Clay (%)	Fine silt (%)	Coarse (%)	*n*	Kaolin (%)	Illite (%)	Expandables (%)	I/I+E ratio
(1) Dry River	Upper Burdekin	680	31	2006/07	3,395	1	97	70	30	0	1	57	5	38	12
(2) Grey Creek		1,005	11	2006/07–2007/08	2,465	5	59 ± 12	25 ± 7	49 ± 4	27 ± 11	4	21 ± 7	15 ± 2	64 ± 8	18
(3) Camel Creek		260	2	2005/06–2006/07	4,075	4	54 ± 6	23 ± 3	47 ± 6	30 ± 6	3	22 ± 5	40 ± 5	38 ± 4	52
(4) Clarke River		6,425	33	2006/07–2008/09	1,230	19	64 ± 10	27 ± 5	52 ± 5	21 ± 10	13	17 ± 3	41 ± 18	42 ± 19	50
(5) Maryvale Creek		900	61	2006/07; 2008/09	910	4	na	40 ± 20	42 ± 4	17 ± 18	3	9 ± 2	2 ± 2	89 ± 3	2
(6) Running River		680	3	2005/06–2008/09; 2010/11	235	9	52 ± 6	20 ± 4	48 ± 4	32 ± 6	4	16 ± 0.8	24 ± 2	60 ± 2	28
(7) Star River		1,690	6	2006/07–2010/11	210	11	69 ± 21	32 ± 15	51 ± 9	18 ± 19	3	9 ± 2	43 ± 11	48 ± 10	47
(8) Basalt River		2,050	70	2006/07; 2008/09–2010/11	620	19	56 ± 10	25 ± 8	46 ± 6	29 ± 10	8	14 ± 5	6 ± 5	80 ± 8	7
(9) Fletcher Creek		885	95	2005/06–2008/09	130	12	57 ± 15	30 ± 19	37 ± 9	33 ± 13	2	7 ± 0	0 ± 0	93 ± 0	0
(10) Lolworth Creek		2,295	47	2005/06–2008/09	445	5	55 ± 10	23 ± 9	46 ± 3	30 ± 9	3	25 ± 4	30 ± 6	46 ± 2	39
(11) Upper Burdekin@ Sellheim		**36,140**	**28**	**2005/06–2008/09**	**735**	**32**	**56 ***	**25 ***	**45 ***	**30 ***	**22**	**18 ± 3**	**29 ± 5**	**53 ± 5**	**35**
(12) Cape@Taemas	Cape	**15,860**	**0**	**2005/06–2008/09**	**245**	**24**	**65 ***	**35 ***	**43 ***	**22 ***	**8**	**25 ± 9**	**35 ± 14**	**40 ± 10**	**46**
(14) Kirk River		210	1	2006/07–2010/11	170	8	53 ± 16	21 ± 6	48 ± 15	31 ± 19	2	14 ± 0	24 ± 1	62 ± 1	28
(15) Elphinstone Creek		50	0	2006/07, 2008/09–2010/11	1,405	7	67 ± 8	30 ± 5	50 ± 4	19 ± 8	5	19 ± 3	21 ± 7	60 ± 8	26
(18) Upper Mistake Creek	Belyando	75	0	2005/06–2007/08, 2009/10–2010/11	370	22	88 ± 13	60 ± 17	34 ± 11	6 ± 9	5	3 ± 1	41 ± 5	56 ± 6	42
(19) Mistake Creek		8,770	3	2005/06–2006/07	555	4	90 ± 3	64 ± 6	32 ± 5	4 ± 2	2	13 ± 0.7	24 ± 1	64 ± 0.7	27
(20) Upper Belyando River		11,260	0	2005/06–2007/08	925	5	89 ± 13	64 ± 14	30 ± 6	6 ± 9	5	15 ± 11	30 ± 11	56 ± 5	35

(21) Native Companion Creek		5,445	1	2005/06–2007/08, 2009/10–2010/11	450	10	75 ± 18	49 ± 22	35 ± 13	16 ± 14	5	28 ± 7	23 ± 5	49 ± 10	31
(22) Carmichael River		2,280	0	2006/07	1,100	5	85 ± 7	51 ± 16	42 ± 14	7 ± 4	5	41 ± 8	9 ± 4	51 ± 11	14
(16) Belyando@ Belyando Crossing		**35,055**	**1**	**2005/06–2008/09**	**335**	**21**	**76 ***	**50 ***	**36 ***	**14 ***	**11**	**28 ± 6**	**19 ± 5**	**53 ± 6**	**26**
(23) Upper Suttor River		2,1 00	10	2006/07–2008/09	850	10	81 ± 13	46 ± 27	44 ± 21	10 ± 7	8	25 ± 12	5 ± 2.9	70 ± 14	6
(24) Logan Creek	Suttor	3,325	23	2006/07–2007/08	350	4	93 ± 17	65 ± 25	32 ± 14	3 ± 13	2	18 ± 5	5 ± 0	78 ± 5	6
(17) Suttor@ BowenDevRd		**10,870**	**10**	**2005/06–2008/09**	**220**	**22**	**84 ***	**61 ***	**30 ***	**9 ***	**13**	**25 ± 8**	**7 ± 6**	**67 ± 12**	**10**
(25) Upper Broken River		35	21	2006/07, 2010/11	115	3	33 ± 15	11 ± 5	37 ± 10	52 ± 15	-	-	-	-	-
(26) Little Bowen River		1,490	33	2006/07–2008/09	3,270	11	72 ± 8	32 ± 7	51 ± 4	17 ± 8	9	12 ± 2	13 ± 3	76 ± 4	14
(27) Bowen River (Dartmoor)	Bowen Bogie	3,890	35	2006/07, 2008/09	1,055	6	73 ± 16	36 ± 11	49 ± 4	15 ± 13	5	11 ± 3	13 ± 13	76 ± 15	14
(28) Upper Bogie River		255	40	2006/07–2007/08	305	3	43 ± 7	15 ± 4	43 ± 2	42 ± 7	1	21	62	17	78
(29) Bogie River		1,740	52	2006/07–2008/09	510	15	61 ± 16	31 ± 16	48 ± 9	21 ± 13	7	13 ± 4	5 ± 4	82 ± 5	6
(30) Bowen@Myuna		**7,110**	**28**	**2006/07–2008/09**	**2,880**	**110**	**63 ***	**27 ***	**49 ***	**24 ***	**9**	**14 ± 3**	**10 ± 7**	**76 ± 9**	**11**
(13) BFD@Overflow	**Reservoir**	**114,620**	**10**	**2005/06–2008/09**	**180**	**50**	**86 ***	**52 ***	**41 ***	**6 ***	**17**	**20 ± 2**	**28 ± 5**	**53 ± 6**	**34**
(31) BurdekinR@ Inkerman	**End-of-river**	**129,600**	**13**	**2006/07–2010/11***	**475**	**34**	**71 ***	**37 ***	**44 ***	**19 ***	**12**	**18 ± 3**	**23 ± 4**	**59 ± 6**	**28**
Plume Group1 (0.1—10 psu)	**Primary flood plume**	**na**	**na**	**2007/08–2010/11**	**65—220**	**7**	**-**	**53 ± 19**	**41 ± 15**	**6 ± 5**	**8**	**20 ± 2**	**21 ± 3**	**59 ± 4**	**26**
Plume Group2 (2—24 psu)		**na**	**na**	**2007/08–2010/11**	**3—45**	**5**	**-**	**66 ± 21**	**27 ± 15**	**7 ± 7**	**7**	**20 ± 4**	**17 ± 5**	**63 ± 7**	**22**
Old Reef Grab Sample		na	na	Apr-2012	-	-	-	-	-	-	1	21	9	71	11

* From Fig. 3.2/4.1 sediment budgets, based on 2005/06–2008/09 PSA data only.
** From Chapter 3

Overall, 15 plume samples contained sufficient sediment for TSS and clay mineralogy analyses, while only 14 samples contained enough sediment for particle size analysis. Flood plume particle size analysis was restricted to samples collected within the more turbid plume boundaries (generally >10 mg L^{-1}). Opportunistically, an additional benthic sediment sample of terrigenous origin was collected from Old Reef, ~65 km off the Burdekin coast with a Van Veen grab sampler, in April 2012. This sample was collected as part of a separate study and was analysed to see if terrigenous sediments could be detected.

4.2.3. Sediment particle size analysis

Particle size distributions for the water samples were determined using the methodology described in section 2.2.2. Following Chapter 3, sediments were classified as one of three size classes: (1) clay (<4 µm); (2) fine silt (4–16 µm); and (3) coarse sediment (16–2000 µm). Clay, fine silt and coarse sediment contributions from each of the Burdekin major sub-catchments provided in Chapter 3 have been reanalysed to calculate a catchment-wide sediment budget for the <10 µm sediment fraction (i.e. very fine silt and clay), representing the fraction recovered for the clay mineral analysis. The clay-only sediment budget is also provided for comparison. This four-year averaged budget over the study period (2005/06–2008/09) represents an average for each individual site and is therefore not summative and does not represent a complete mass balance from sub-catchment source to the end-of-river. For a full method description see section 3.3.4, including average BFD trapping estimates of the <4 µm sediment fraction. The same methodology was applied to the calculation of the <10 µm fraction.

4.2.4. Clay mineralogy

The <10 µm fraction is increasingly favoured in geochemical sediment tracing studies (Douglas et al., 2003, 2006b, 2010; Hughes et al., 2009; Olley et al., 2013), to avoid the need for particle size correction between source and sediment (Wilkinson et al., 2013). This fine fraction also captures the larger clay minerals (i.e. illite) with individual particles often larger than the clay (<4 µm) fraction (Gibbs, 1977). Collected water samples of 1–5 L were placed in a beaker in an ultrasonic bath for 20 minutes and then wet sieved through a 38 µm mesh. Samples were transferred into a measuring cylinder and shaken before following Stoke’s law of settling to recover the <10 µm sediment fraction (Moore and Reynolds, 1997). This process was repeated 4–5 times per sample to ensure adequate separation and recovery of this size fraction, which then was syphoned into a clean beaker and oven dried at 50°C to a thick slurry. The samples were then prepared for X-ray diffraction (XRD) using the oriented glass slide method described by Moore and Reynolds (1997).

Clay mineral assemblages were determined using the semi-quantitative method of Moore and Reynolds (1997). The samples were analysed at the Advanced Analytical Centre, James Cook University on a Bruker X-ray Diffractometer with a set of four diffraction patterns run for each sample, including untreated air-dried; solvated in ethylene glycol by vapour pressure at 60°C for 16 hours; heated to 400°C for 2 hours; and heated to 550°C for 2 hours. Scans were run at 0.02 steps (counting for 1.2 s $step^{-1}$) through the range 2–70Å for the initial air-dried sample, and a shorter range from 2–32Å for the subsequent treated runs.

The diffraction data were analysed using the Bruker Diffrac Plus EVA software by measuring peak intensity (as peak area) as described in Hillier (2003). The normalised reference intensity ratio (NRIR) method was used to estimate relative weight percentages of the clay mineral groups kaolin, illite and 'expandables'. The expandables clay group includes smectites (e.g. montmorillonite) as well as other mixed-layer clay minerals with a smectitic (expandable) component, all of which have a high capacity to 'shrink-swell' through water and cation exchange. This classification emphasises that the expandable clays are not necessarily pure smectites and may vary in composition from place to place. Kaolin is used in preference to kaolinite since the kaolin group mineral halloysite is likely present in some sources and this study has not attempted to distinguish between kaolinite and halloysite. The NRIR approach is semi-quantitative and does not account for any non-clay minerals also present in the <10 µm sediment fraction. Quartz was used as an internal peak position standard as it was present in all samples and produced the largest peak of the non-clay minerals. Individual clay mineral relative abundance uncertainty is ±5% (Hillier, 2003). The ratio of illite to illite + smectite (I/I+S) used by Douglas et al. (2006a, 2006b) as a surrogate of basaltic to non-basaltic sources and to investigate enrichment in smectitic-rich clays was also calculated. As smectite is represented in this study by the expandable (E) clays grouping, I/I+E is used.

Chlorite was rarely present in the study samples. Chlorite was only present as a minor trace mineral (i.e. ≤2 wt.%) in the Upper Burdekin sub-catchment site (and upstream tributaries #2, 3, 4, 7), Bowen sub-catchment site (and upstream tributaries #26, 27), the BFD, end-of-river (Inkerman) and flood plume sites. Chlorite was excluded from further analysis due to this low abundance.

4.2.5. Data processing and analysis

It was desired that the source contribution results best represent sediment loads, which is a function of suspended sediment concentration and flow volume. Therefore the degree to which the samples represented the long-term mean particle size and clay mineral abundances was improved by weighting the properties of samples with higher TSS concentrations. Weighting samples by concentration was used as an alternative to weighting by load for the ungauged sampled tributary sites. Load-based weightings were applied to the gauged major sub-catchments, reservoir outlet and end-of-river sites. It is argued that concentration weighting provides a reasonable estimate of load weighting, because the highest TSS concentrations during streamflow events occur during the rising/peak stages of the hydrograph (Amos et al., 2004; Belperio, 1979; Kuhnert et al., 2012). Tributary samples chosen for particle size analysis were thus screened to represent the larger streamflow events of each wet season. This avoids problems associated with using data from early wet season ‘first flush’ events that often have higher TSS concentrations but small discharge volumes not representative of the wider upstream catchment area. To best capture and weight the dataset towards these larger flow volume stages, the mean sediment particle size groupings (clay, fine silt, coarse sediment and <10μm fractions) for each tributary site were calculated by applying a TSS weighting factor, represented as

$$WPS_y = \sum TSS^*_{n_1 - n_x} \times PS_{n_1 - n_x} \qquad (1)$$

where WPS_y = weighted particle size for site y, TSS* = normalised TSS concentration (mg L^{-1}) (individual sample proportion of summed TSS concentrations for that site i.e. n_1/n_i where $n_i = \sum n_{1} + n_{2} + n_{3}$)) for samples n_1 to n_x and PS = particle size (calculated as clay, fine silt, coarse and <10 μm fractions) of samples n_1 to n_x.

A similar TSS-weighted approach was utilised to determine mean clay mineral proportions, although a smaller dataset was available to represent each site, especially at the tributary scale. One to thirteen mineralogy samples were analysed to represent each of the ungauged tributary sites (see Table 4.1), with less confidence placed on the sites where only one or two clay mineralogy samples were analysed (i.e. Dry River, Upper Bogie River). Highest data confidence is placed on the seven gauged sites where 9–22 samples were analysed per site for clay mineralogy. The variability of clay mineral assemblages over the streamflow hydrograph and with different streamflow events were investigated using the Upper Burdekin sub-catchment site as a case study during the second largest annual discharge water year (2008/09) recorded at the Sellheim gauge (20 million ML; Fig. 3.1b).

End-of-river freshwater discharge volumes and TSS concentrations varied each wet season, related to upstream sub-catchment sources, rainfall volumes and intensity, climatic variability and annual ground cover. Therefore salinity and maximum TSS concentrations varied along the flood plume transect for each sampled wet season. Clay mineralogy data for all years sampled (2007/08–2010/11) were categorised into two groups (Plume Groups 1 and 2) based on decreasing TSS concentration with increasing salinity and distance from the river mouth (i.e. 65–220 mg L^{-1} and 3–45 mg L^{-1}). This category best represented the transition across the initial depositional zone within Upstart Bay (see Fig. 2.8 and Appendix Fig. A2.3).

Ternary graphs were constructed to display the clay mineral data in the context of the upstream geology of each of the tributary sites and to further examine the relationship between the major sub-catchments and end-of-river/flood plume sites. In that regard, ‘end member’ tributary sites were identified as basalt (>60% basalt comprised the upstream catchment area), sedimentary (>80%) and granite (>70%) and plotted separately to the other sites containing mixed geology (Table 4.2). Sites 1 (Dry River) and 28 (Upper Bogie River) were excluded from this analysis due to limited clay mineralogy data.

Table 4.2 Tributary site upstream catchment area geology, with grey shading indicating major geology represented in Figure 4.3.

Sites	Basalt	Mafic	Ultramafic	Combined Basalt, Mafic, Ultramafic	Rhyolite	Sediments	Granite	Regolith	Metamorphics
(1) Dry River	31%	0%	0%	31%	11%	2%	10%	19%	26%
(2) Grey Creek	3%	0%	7%	10%	7%	47%	2%	22%	7%
(3) Camel Creek	2%	0%	0%	2%	0%	**81%**	7%	10%	0%
(4) Clarke River	33%	0%	0%	33%	5%	30%	14%	10%	6%
(5) Maryvale Creek	**61%**	0%	0%	61%	0%	15%	0%	24%	0%
(6) Running River	1%	0%	2%	3%	0%	1%	**78%**	0%	17%
(7) Star River	0%	0%	6%	6%	18%	20%	34%	8%	13%
(8) Basalt River	**70%**	0%	0%	70%	9%	0%	8%	10%	3%
(9) Fletcher Creek	**95%**	0%	0%	95%	0%	2%	0%	4%	0%
(10) Lolworth Creek	47%	0%	0%	47%	0%	10%	28%	14%	2%
(14) Kirk River	0%	1%	0%	1%	0%	6%	**70%**	0%	23%
(15) Elphinstone Creek	0%	0%	0%	0%	0%	0%	**100%**	0%	0%
(18) Upper Mistake Creek	0%	0%	0%	0%	0%	**100%**	0%	0%	0%
(19) Mistake Creek	3%	0%	0%	3%	2%	20%	0%	68%	8%
(20) Upper Belyando River	0%	0%	0%	0%	0%	51%	0%	49%	0%
(21) Native Companion Creek	1%	0%	0%	1%	0%	50%	0%	49%	0%
(22) Carmichael River	0%	0%	0%	0%	0%	50%	0%	50%	0%
(23) Upper Suttor River	10%	0%	0%	10%	10%	59%	1%	21%	0%
(24) Logan Creek	23%	0%	0%	23%	2%	2%	0%	72%	1%
(25) Upper Broken River	21%	0%	0%	21%	0%	0%	80%	0%	0%
(26) Little Bowen River	33%	0%	0%	33%	2%	58%	4%	3%	0%
(27) Bowen River (Dartmoor)	16%	19%	0%	35%	5%	22%	37%	1%	0%
(28) Upper Bogie River	0%	40%	0%	40%	0%	0%	59%	2%	0%
(29) Bogie River	34%	18%	0%	52%	2%	0%	41%	4%	0%

4.3. Results

4.3.1. Sediment source tracing using <10 μm fraction and clay mineral fingerprints

The clay mineral fingerprints of the Upper Burdekin study site samples were remarkably consistent over all stages of the flow hydrograph and multiple streamflow events that occurred in the 2008/09 wet season, despite large variations in TSS concentrations and sediment particle size distribution (Fig. 4.2b and c). The relative abundance of expandable clays, of most interest in this study, ranged from 43% to 56% (CV=0.07) and the <10 μm fraction comprised an average of 52% (CV=0.02) across the wet season samples. In contrast, the proportion of coarse sediment varied between 16–43% (CV=0.24) and was greatest during the largest rises in streamflow (e.g. 14/01, 27/01, 03/02, Fig. 4.2a).

More broadly across the study sites, the variation in relative clay mineral abundance between samples from each site across all years were generally within the analytical error margin (±5%), especially for kaolin (Table 4.1). Relative clay mineral abundances were most variable in sediments collected at sites with large areas of sedimentary geology within their upstream catchment (e.g. 30–60%); for example, the Clarke, Star, Upper Suttor, Suttor and Belyando tributary sites (Table 4.1). Variability was greatest in suspended sediments from the Clarke River, a large and geologically complex tributary of the Upper Burdekin (1 s.d.= ±18% and ±19% for illite and expandable clays, respectively). In contrast, clay mineral abundances were least variable (SD for all clay minerals <2%) in samples from the granite-dominated (>70%) tributaries including the Running and Kirk Rivers.

4.3.2. Tributary sediment characteristics and geological influences

All Belyando and Suttor tributary site samples are dominated by the clay fraction (46–65%), and due to low coarse fraction components (3–16%) have the largest proportion of combined clay/fine silt (84–97%) across the Burdekin (Appendix Fig. A4.1). Fine silt dominates suspended sediment contributed by Bowen and Bogie River tributary sites (48–51%), except for the smaller, headwater tributary sites hosted within granite rock areas (sites #25, 28 in Fig. 4.1 and Table 4.1). The suspended sediment within the tributaries of the Upper Burdekin sub-catchment were dominated by the fine silt (>45%) and coarse (15–30%) sediment fractions (Appendix Fig. A4.1).

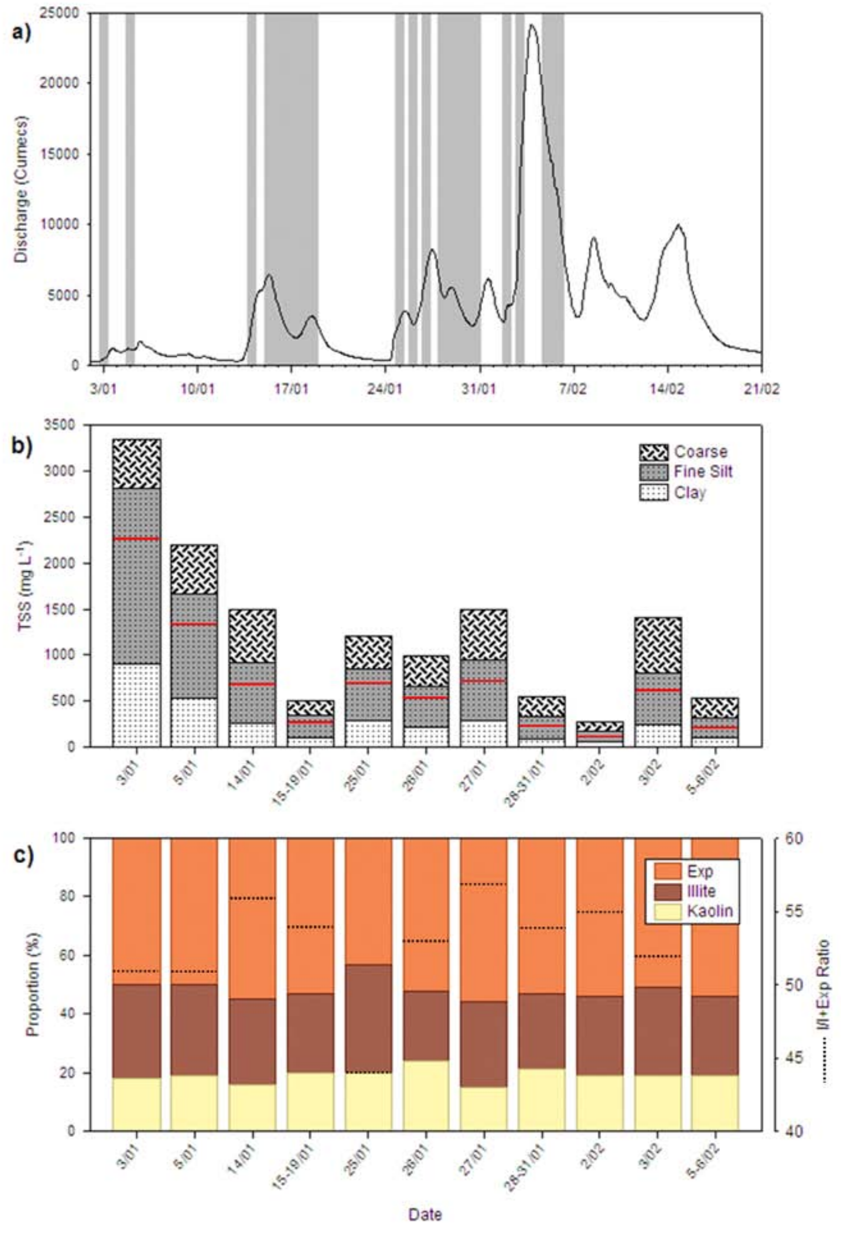

Figure 4.2 (a) Discharge at the Upper Burdekin River (Sellheim) gauge during the 2008/09 wet season (03-Jan–06-Feb). River water sample collection periods are overlayed as grey vertical lines. (b) Graph of TSS concentrations for the Upper Burdekin River (Sellheim) surface water samples with sediment particle size composition of each sample represented as clay (<4 μm), fine silt (<16 μm) and coarse (>16 μm) sediment. Red line on each sample indicates the <10 μm fraction analysed for clay mineralogy. (c) Relative proportions of expandables, illite and kaolin clay mineral groups for each of the water samples represented in (a). The I/I+E ratio for each sample is represented as a dashed line (ratio for the 5-6/02 is 55).

The clay mineral fingerprints of samples collected at the end-of-sub-catchment for the Bowen and Suttor sites sit within their respective upstream tributary samples, with similar fingerprints for the Upper Suttor (#23)–Suttor (#17) and the Little Bowen (#25)–Bowen@Dartmoor (#27)–Bowen@Myuna (#30) downstream transects, respectively (Table 4.1). All suspended sediment collected at these sites had a higher proportional abundance of expandable clays (67–78%), with kaolin relatively more abundant along the Suttor transect (25%), at the expense of illite (Fig. 4.3a). The Bogie River (#29), which drains directly into the Burdekin River downstream of the BFD also had a high abundance of expandable clays (82 ±5%; mean ±1 s.d.) in all sediment samples. I/I+E ratios were low (i.e. <14) in sediments across all Suttor and Bowen sub-catchment sites, with the Suttor and Bogie River sites (ratios of 6–10) distinguishable from the Bowen River sites (11–14) (Table 4.1).

Clay mineral relative abundances in sediment collected at each of the Belyando tributary sites were more variable, with increasing kaolin abundance and decreasing illite related to the proportion of upstream sedimentary and regolith (i.e. channel and flood plain alluvium and sand plain) geologies (sites #18–22; Fig. 4.3a). The abundance of expandable clays in sediment from each of these sites varied from 49 to 64%, and the ratio of I/I+E ranged from 14 to 42 (Table 4.1). Mistake Creek (#19) sediment had the highest abundance of expandable clays (64 ±0.7%) and the small amount of upstream basalt (3%) had an influence on its position compared to the other Belyando tributaries (Fig. 4.3a). The Belyando end-of-sub-catchment plots closest to sediment collected at the Native Companion Creek tributary (#21, Fig. 4.3a), with similar abundances of expandable clays (49–53%), kaolin (28%) and illite (19–23%). In contrast, the Mistake Creek tributary sediment had a I/I+E ratio of 27, similar to the end-of-sub-catchment site (ratio of 26).

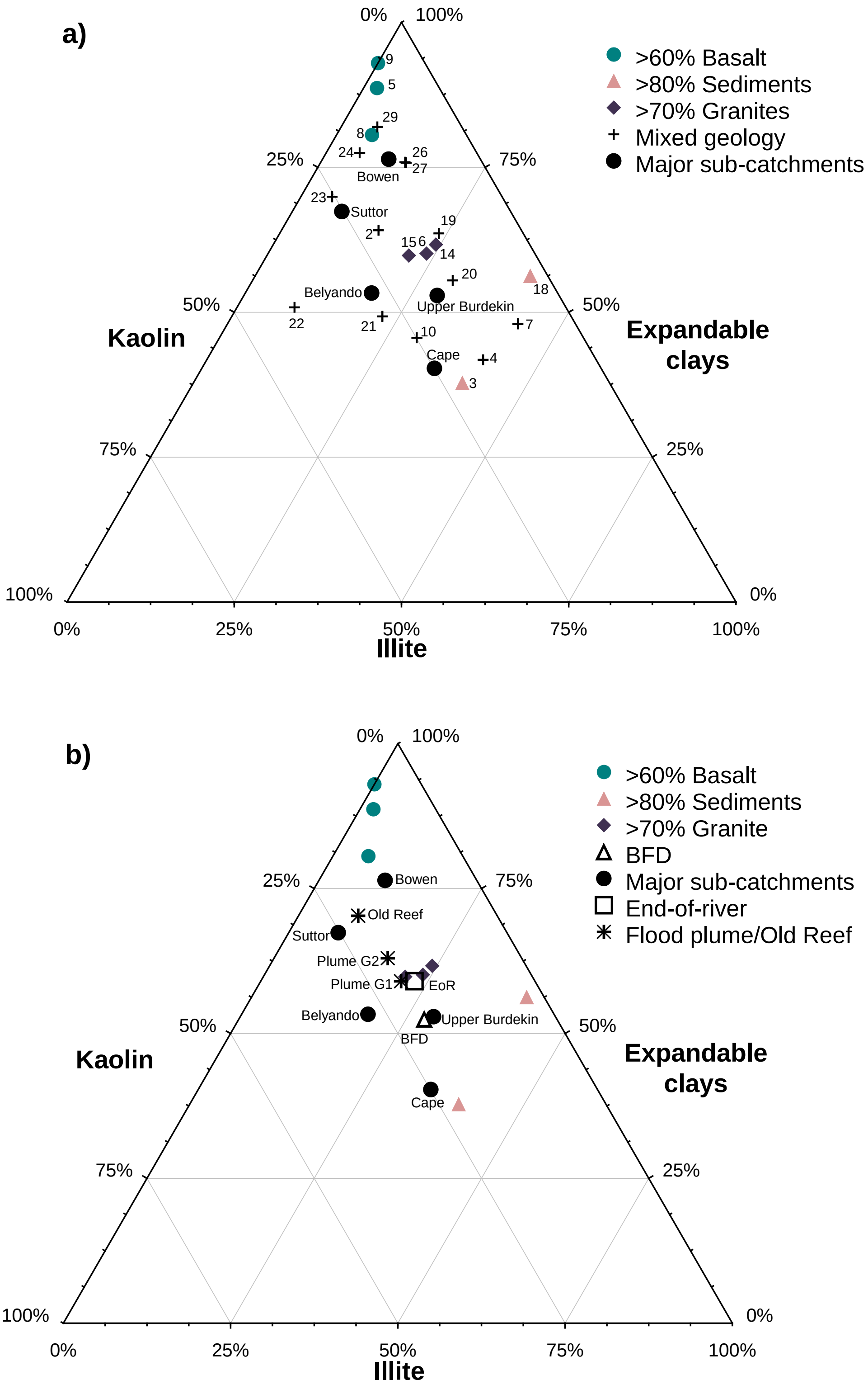

Figure 4.3 Clay mineral ternary diagrams related to source geologies: (a) River sediment for each sub-catchment outlet and for tributary locations with dominant geologies occupying either >60% basalt, >70% granite or >80% sedimentary of upstream catchment area (locations are numbered as per Fig. 4.1). (b) Major sub-catchments, Burdekin Falls Dam outlet, End-of-river, flood plume (Plume Group 1 denoting the location nearest to the coast) and Old Reef sediments related to upstream geological sources.

The relative abundances of clay minerals were most spatially variable across the Upper Burdekin tributary sites, the largest (36,140 km^2) and most geologically complex major sub-catchment (Fig. 4.1). Samples from the basalt dominated (i.e. >60%) western tributaries (Maryvale Creek (#5), Basalt River (#8), Fletcher Creek (#9)) were most abundant (80–93%) in expandable clays (Table 4.1, Fig. 4.3a). Illite content was negligible (0–6%) in sediment collected at these sites, and consequently I/I+E ratios were 0–7, and were the lowest across the Burdekin. However, the clay mineral signature of Upper Burdekin end-of-sub-catchment sediments more closely reflected sites influenced by sedimentary and granitic landscapes (Fig. 4.3a). These included mixed geology tributaries showing the strong influence of sedimentary geology (e.g. Clarke River (#4), Star River (#7), Lolworth Creek (#10)), despite comparatively larger upstream catchment areas of basalt (#4, #10) and granite (#7) geologies (see Table 4.2). I/I+E in sediment collected at these sites ranged from 39–52 and were the highest across the Burdekin (Table 4.1). The granite dominated (>70% upstream area) Running (#6) and Kirk (#14) Rivers and Elphinstone Creek (#15) sites all contained abundant expandable clays (60–62%), and tightly cluster on the ternary diagram separating the basaltic, granitic and sedimentary tributaries (Fig. 4.3a). An I/I+E ratio of ~28 was characteristic of sediments from these granitic sites.

The expandable clays were least common in suspended sediments collected from the Cape River sub-catchment (40 ±10%), and similar characteristics were observed for the other western tributaries draining the Great Dividing Range (e.g. Sites #1, 10, 22). Cape River suspended sediment had a relatively high abundance of kaolin (25 ±9%) compared to most study sites, and its I/I+E ratio of 46 was the highest end-of-sub-catchment value calculated (Table 4.1).

4.3.3. Sub-catchment sediment characteristics and sources of end-of-river fine (<10 μm) sediment

The Upper Burdekin sub-catchment was the major contributor of finer sediment fractions into the BFD, contributing an average of 87% and 82% of the <10 μm fraction and clay-only (<4 μm) loads, respectively, delivered into the dam over the four-year period (Fig. 4.4). Over this study period the BFD trapped on average ~47% of all <10 μm fraction sediment entering the dam from upstream catchments. Only 31% of the clay-only fraction was trapped. The <10 μm sediment fraction and clay-only budgets show almost equal contributions to end-of-river export from the two main source areas identified in Chapter 3, including (1) overflow sediment from the BFD and (2) the Bowen River sub-catchment which enters below the dam. The average clay-only end-of-river load (3.14 million tonnes) comprises approximately half of the <10 µm fraction load (5.99 million tonnes).

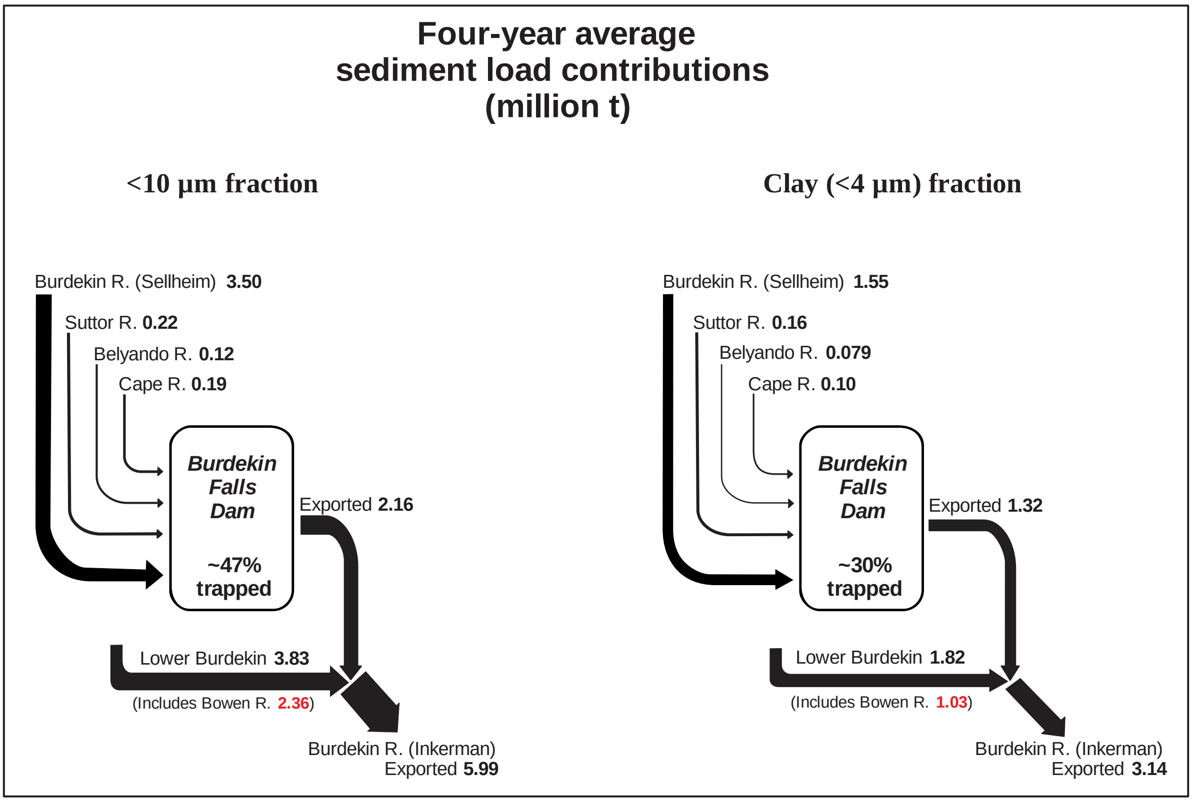

Figure 4.4 Four-year (2005/06–2008/09) average fine sediment (<10 µm fraction) and clay-only (<4 µm) budgets for the Burdekin River catchment. Arrows represent the respective contributions from each of the Burdekin River major sub-catchments, the Burdekin Falls Dam spillway, Lower Burdekin (includes a contribution from the gauged Bowen River), and end-of-river export (Inkerman), where the width of each arrow indicates contribution size in million tonnes. The Lower Burdekin sub-catchment contribution is calculated by subtracting the BFD overflow sediment load from the end-of-river sediment load. Bowen River loads have lower confidence due to a lack of monitoring data available for this site in the latter years (see 3.5.1).

The expandable clays were the most abundant clay minerals in suspended sediments collected across the Burdekin's major sub-catchments, with the greatest abundance measured at the Bogie (82 ±5%), Bowen (76 ±9%) and Suttor (67 ±12%) River sites

(Fig. 4.5). These sub-catchment fingerprints can be discriminated by a greater abundance of kaolin in Suttor sediment (25 ±8%) compared to the Bowen (14 ±3%) and Bogie (13 ±4%). The Upper Burdekin sub-catchment suspended sediment was characterised by a dominance of both expandable clays (53 ±5%) and illite (29 ±5%), and BFD overflow sediment reflected this Upper Burdekin clay mineral signature (i.e. <2% variation between sites for each mineral which was within the analytical error margin) (Fig. 4.5). The I/I+E ratio discriminates this Upper Burdekin-BFD overflow sediment source signature (ratios of 35 and 34, respectively) from the basaltic and expandable-rich sediment in the Bowen (ratio of 11) and Suttor (ratio of 10) sub-catchments. End-of-river (Inkerman) fine sediment also contains abundant expandable clays (59 ±6%), with an average end-of-river I/I+E ratio of 28 (range of 18–36). This site was one of the most variable, reflecting wet season variations amongst the two large, upstream source areas.

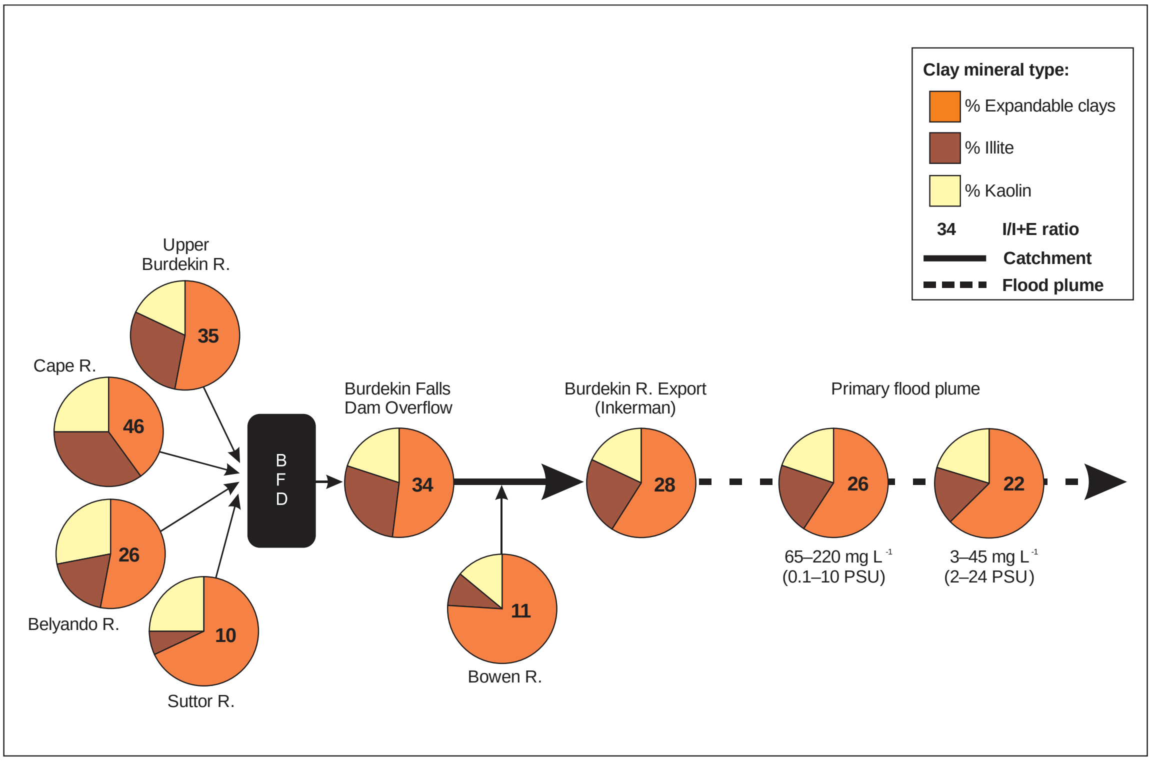

Figure 4.5 Five-year (2006/07–2010/11) average clay mineralogy for the Burdekin River major sub-catchments, Burdekin Falls Dam, end-of-river (Inkerman) export, and inshore Burdekin River primary flood plume, <25 km from the river mouth. Pie charts represent mean proportions of the three clay mineral groups kaolin, illite and expandables, with the average I/I+E ratio for each site also displayed. The flood plume data are grouped into two categories based on decreasing TSS concentration (65–220 mg L^{-1} and 3–45 mg L^{-1}) with increasing salinity (0.1–10 psu, and 2–24 psu) and distance from the river mouth.

4.3.4. Flood plume sediment characteristics and fractionation

End-of-river flood peak TSS concentrations (290–750 mg L^{-1}) decline rapidly upon seawater mixing within Upstart Bay, where concentrations fell to 65–220 mg L^{-1} in the turbid inner Plume Group 1, with salinity ranging between 0.1–10 psu across all flood plumes sampled (Table 4.3). Further along the flood plume transect, Plume Group 2 samples had sediment concentrations <45 mg L^{-1} and salinity between 2–26 psu. The proportion of the clay sized-sediment fraction increased along each sampled flood plume transect, with the largest increase in the 2010/11 transect from 29% to 82% of all sediment-size fractions (Table 4.3; see also Fig. 2.8 and Appendix Fig. A2.3).

Table 4.3 Suspended sediment characteristics across the river flood peak and adjacent primary flood plume over five river flood events (2007/08–2010/11), including TSS concentration (mg L^{-1}), proportion of clay sized-sediment fraction (%) and I/I+E ratio.

Water year	Location	*n*	Sediment characteristics		
			TSS (mg L^{-1}) (range)	% Clay fraction (mean ± 1 s.d.)	I/I+E ratio (mean ± 1 s.d.)
2007/2008	End-of-river flood peak (Freshwater)	1	345	18	28
	Plume Group 1 (0.1—10 psu)	3	85–200	30 ± 1.4	24 ± 1
	Plume Group 2 (2—24 psu)	1	25	-	18
2008/2009	End-of-river flood peak (Freshwater)	1	430	32	32
	Plume Group 1 (0.1—10 psu)	2	180—220	49 ± 5.7	27 ± 2.4
	Plume Group 2 (2—24 psu)	0	3	-	-
2009/2010 (Feb'10)	End-of-river flood peak (Freshwater)	1	290	50	31
	Plume Group 1 (0.1—10 psu)	1	65	71	21
	Plume Group 2 (2—24 psu)	2	6.5—25	77	28 ± 0.6
2009/2010 (March'10)	End-of-river flood peak (Freshwater)	1	750	20	21
	Plume Group 1 (0.1—10 psu)	0	-	-	-
	Plume Group 2 (2—24 psu)	2	11—45	44 ± 13	13 ± 3.2
2010/2011	End-of-river flood peak (Freshwater)	1	450	29	27
	Plume Group 1 (0.1—10 psu)	2	65—140	70 ± 0.7	32 ± 1.2
	Plume Group 2 (2—24 psu)	2	2.8-11	82 ± 2.1	24 ± 2.1

The average clay mineral fingerprints of the two Plume Groups closely resemble that of the end-of-river, and were not statistically different (i.e. within 1 standard deviation). However, declining I/I+E ratio values with increasing salinity along each individual end-of-river/flood plume transect supports the hypothesis that the smectite-rich expandable clays are enriched within the plume waters (Table 4.3). The largest declines were observed in the 2007/08 and March 2010 transects, where I/I+E fell from 28 to 18 and from 21 to 13 along each transect, respectively, with corresponding declines in TSS concentrations to <50 mg L^{-1}. These two transects also captured the largest increases in salinity (i.e. Plume Group 2 samples had a salinity of 7.7 psu in 2007/08 and 16–24 psu in March 2010). Further offshore the Old Reef benthic sediment sample had an I/I+E ratio of 11.

4.4. Discussion

4.4.1. Sediment source tracing using <10 μm fraction and clay mineral fingerprints

Most clay mineral catchment tracing studies report results using only 1–2 samples to represent each site (e.g. Gingele and De Deckker, 2005; Guyot et al., 2007) and samples are often collected from river bed lag deposits, after flood events have occurred. As such, the utility of this approach may be limited as it is assumed that the residual deposit is representative of all material transported during the preceding flood event(s). In this study a comprehensive clay mineral dataset has been produced for >31 sites across the Burdekin and adjacent coastal flood plume, representative of the rise and peak flood stages of multiple streamflow events over a six-year period. The spatial and temporal span of clay mineral relative proportions used to develop often unique source-related fingerprints achieved in this study demonstrate the value of clay mineralogy for tracing sediment source and fluxes in large and geologically complex catchments. Clay mineral fingerprinting has previously been little-used in sediment tracing studies and this study has shown the stability of these fingerprints in comparison to other techniques such as geochemical tracing which can display non-conservative behaviour, and thus produce results that may be difficult to confidently interpret (see Koiter et al., 2013). In the Upper Burdekin (36,140 km^2) the relative abundance of clay minerals remained within 4% across a large runoff event despite large fluctuations in TSS concentrations, sediment particle size, stages of the flow hydrograph and tributary sources (Fig. 4.2), and within 5% variation across all study years (Table 4.1). Clay mineral assemblages for most sites showed similar consistency and were also within the ±5% error margin. In that regard, the data indicate that in many cases only 1–2 samples from an area may be sufficient to develop a reproducible signature for clay tracing studies. The study results also validate the use of the clay mineral tracing approach for use in similar catchments elsewhere, and in studies reconstructing climate change from marine deposits of clays exported from terrestrial catchments.

It should be expected that sites with large areas of sedimentary geology upstream may have more temporally-variable mineral abundances relating to the parent-rock material, or the type of sediments (i.e. shale, limestone etc.). Indeed, this study found greater variation (typically 10% up to 15%) at tributary sites with two geologies in separate areas of the upstream catchment. For example, the large (6,425 km^2) Clarke River tributary displayed the greatest variability in clay mineral abundance (i.e. 19% for expandable clays), reflecting contributions from two dominant geologies with different mineral signatures (i.e. 33% basalt and 30% sedimentary geology in upstream area; Table 4.2). Granite (>70%) and basalt (>60%) dominated smaller tributaries (i.e. <1,000 km^2) had the least variability in relative abundances of clay minerals over the study period (i.e. 0–3%).

The consistency in clay mineral assemblages across runoff events and water years for most study sites also validates the use of the <10 µm sediment fraction for source tracing (Wilkinson et al., 2013). Despite the large variability in TSS concentration and the proportion of the coarse sediment fraction over individual hydrograph stages and separate streamflow events at the Upper Burdekin site (Fig. 4.2), the abundance of expandable clays and the proportion of the <10 µm sediment fraction of total suspended sediment remained consistent (CV of 0.07 and 0.02, respectively). This reflects the predominance of the clay minerals in the <10 um fraction whilst tracing of coarser size fractions (i.e. <63 µm), quartz and to a lesser extent primary minerals (e.g. feldspars or micas) serve to act as a diluent on the clay mineral fraction. The differences in the coarse sediment fraction across the Burdekin catchment validates the <10 µm fraction approach used in this study. In particular the Upper Burdekin sub-catchment and tributary sediments contain a higher proportion of coarse material (i.e. ~30%) than the other Burdekin sub-catchments, where the <10 μm fraction represents most suspended sediment transported (63–90%) (Table 4.1, Appendix Fig. A4.1).

4.4.2. Tributary sediment characteristics and geological influences

This study builds on the earlier application of the I/I+S ratio by Douglas et al. (2006a, 2006b, 2007) and confirms the reliability of this measure of the influence of basalt geology (and to a lesser extent granite) on river sediment relative to sedimentary landscapes. Clay mineral ratios have been used previously as proxies of chemical weathering and to examine environmental trends (Alizai et al., 2012; Limmer et al., 2012), but have received less attention in contemporary erosion sourcing studies. This measure deserves broader application to catchments containing these rock types, through clearly distinguishable geologic source identification across tributary (this study), reservoir (this study; Douglas et al., 2006b, 2007) and flood plume (this study; Douglas et al., 2006a) scales. Douglas et al. (2006b) used the I/I+S ratio to discriminate basaltic source areas (i.e. ratios of 4–10) in the neighbouring Fitzroy River from those comparatively enriched in illite (i.e. ratio of 47). The results also reveal that the clay mineralogy of <10 μm suspended sediment is heavily influenced by the geological signature of upstream catchment areas. Expandable (i.e. smectitic) clays were most abundant where basalt and other mafic/ultramafic rocks of similar composition comprised greater than 10% of the upstream catchment area (Fig. 4.3a and 4.6; Table 4.2) resulting in the lowest I/I+E ratios (i.e. 0–18) across the Burdekin and thus providing a distinctive 'basalt source' clay mineral signature (Table 4.1, Fig. 4.6). This fingerprint was strongest for the Upper Burdekin tributaries (sites #5, 8, 9 in Fig. 4.3a) which drained large areas (i.e. >60%) of the Nulla Basalt Province (i.e. ratios of 0–7). In comparison, I/I+E ratio values of Clarke River and Lolworth Creek tributary sediments were much higher (50 and 39, respectively) despite also containing Nulla Basalt in the upper catchments; these discrepancies are discussed below. The influence of basaltic landscapes as the source of downstream fine sediment was greatest in the Bowen and Suttor sub-catchments, where the expandable clay-rich 'basalt source' signature (I/I+E ratios of 6–14) was evident in sediment collected throughout both sub-catchments from tributary to the outlet, despite comprising relatively smaller areas (10–33%) of the upstream catchment (Table 4.1). The Tertiary basalts in these sub-catchments are much older (20–30 Ma) than those of the Upper Burdekin (0.013–5 Ma; Dickins and Malone, 1973) and hence have had much longer to develop deep weathering profiles. In particular, soils derived from Tertiary basalts (35.2–27.4 Ma; Jones and Verdel, 2015) in the neighbouring Theresa Creek catchment of the Fitzroy River, which borders the Suttor River and Mistake Creek tributaries (Belyando) were found to be highly erodible once cultivated (Hughes et al., 2009). Permian basalts (252–300 Ma) and other mafic geologies may also be sources of fine sediments in the Bowen sub-catchment. Hence, this higher relative contribution of basalt along the Suttor and Bowen downstream continuums suggest that soils developed over basalt (and other mafics) are eroding at a higher rate relative to soils on other geological sources in these catchments. Indeed, previous studies in the Bowen sub-catchment have identified that mafic (basalt) geological sources produce higher sediment yields (Wilkinson et al., 2013). However, further discrimination is required to determine if the Tertiary basalts in the upper reaches of the Little Bowen tributary are the primary source of fine (<10 µm) sediments within this tributary, or whether the soils developed on sedimentary rocks contribute most, as suggested in Chapter 3.

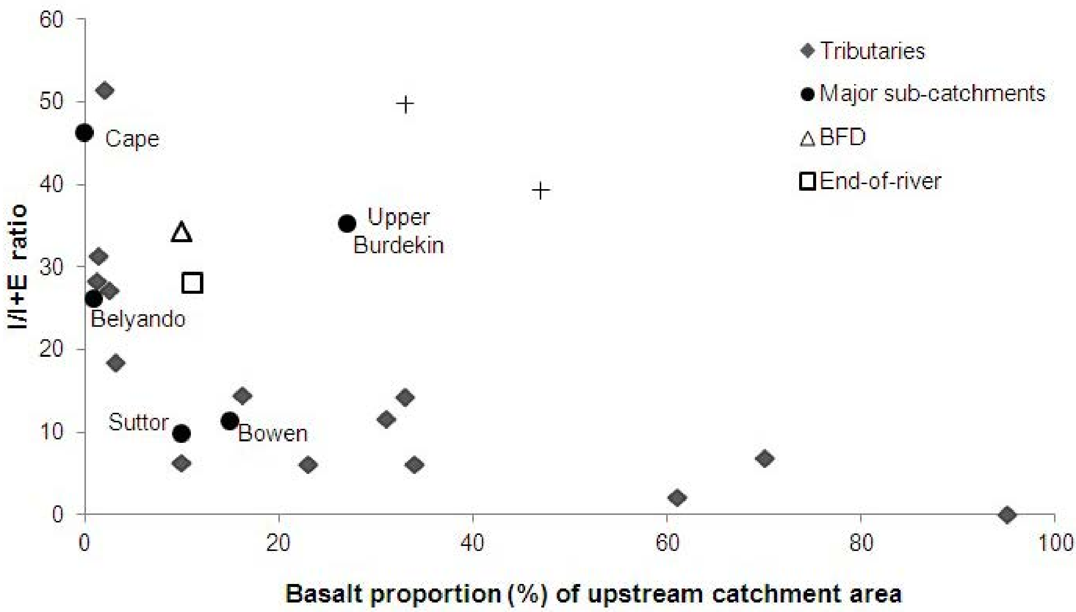

Figure 4.6 I/I+E ratio relationship with the proportion of basalt in the upstream catchment area. The outliers of the Clarke River and Lolworth Creek tributary sites are highlighted as crosses and discussed in the text.

The distinctive 'basalt source' clay mineral signatures seen in the basalt-dominated tributaries of the Upper Burdekin are not reflected downstream at the outlet of this major sub-catchment (Fig. 4.3a). Here, the end-of-sub-catchment signature reflects the larger volume of fine sediment contributed from tributaries with more erosive sedimentary derived-soils, such as the Clarke River and Camel Creek, which contain average TSS concentrations ranging between 1,200–4,000 mg L^{-1} (Fig. 3.2), and high I/I+E ratios >50. In comparison, average TSS concentrations of the basalt dominated tributaries ranged from 130–900 mg L^{-1} with I/I+E ratios between 0 and 7. This pattern is also replicated at a smaller scale for the Clarke River sub-catchment, where the strong basalt signature of the Maryvale Creek tributary is not carried through to the end of the Clarke River, with I/I+E ratios of 2 and 50, respectively (Fig. 4.3a; Table 4.1). In this instance the larger sediment volumes (using average TSS concentrations as a proxy; also see Ciesiolka, 1976) delivered from this catchment are derived from the sedimentary landscapes. Similarly, the clay mineral fingerprint of the Lolworth Creek tributary (#10 in the Upper Burdekin) also reflects a greater influence from the lesser area of upstream sedimentary geology, with a high I/I+E value (ratio of 39) despite an upstream basalt area of almost 50%. Lolworth Creek contains the Toomba basalt flow, the youngest basalt feature of the Nulla Basalt Province (~13,000 years) which comprises large areas of unweathered rock (Whitehead and Stephenson, 1998).

4.4.3. Sub-catchment sediment characteristics and sources of end-of-river fine (<10 μm) sediment

The clay mineral tracing data found the Upper Burdekin sub-catchment was the dominant upstream sediment contributor to the BFD overflow, with similar clay mineral signatures at these two sites (i.e. within 2% for each mineral), which was consistent with all sediment size budgets i.e. 'bulk', fine (<10 µm) and clay (<4 µm) fractions (Fig. 4.2, Chapter 3). Upper Burdekin-BFD overflow fine sediment is characterised by an abundance of both expandable and illite clays, and this sediment is related most closely to sedimentary and granitic sources (Fig. 4.3b). The ternary plot also suggests the Belyando sub-catchment has the next greatest influence on BFD overflow fine sediments.

Expandable clays dominated (40–76%) fine sediment (<10 µm) across the major sub-catchments of the Burdekin with varying contributions of kaolin (14–28%) and illite (7–

35%; Fig. 4.5). The clay mineral abundance ternary diagram plots the end-of-river site closer to the Upper Burdekin-BFD source, suggesting end-of-river fine sediment originates from sedimentary and granitic sources, with an additional influence from some basalt/expandable clay-rich source area(s), including within the Bowen and Bogie Rivers downstream of the reservoir (Fig. 4.3b). The end-of-river I/I+E ratio discriminates between these two major source areas to the end-of-river, and the high variability of this ratio (range of 18–36) reflects the variable contributions from the Upper Burdekin-BFD (ratios of 35–34) and Bowen River (ratio of 11) sources. These influences are wet season source dependant, and individual flood peak end-of-river I/I+E ratios do show variation between these two sources consistent with variation in sub-catchment rainfall and streamflow event magnitudes. For example, the 2008/09 and February 2010 end-of-river peak ratios were highest (32 and 31, respectively), reflecting the Upper Burdekin-BFD source due to major streamflow events in the Upper Burdekin sub-catchment (see Fig. 3.1). The peak end-of-river I/I+E ratio was lowest (21) in the March 2010 streamflow event, where the flood peak occurred within 24 hours of Tropical Cyclone Ululi’s passage over the Bowen River sub-catchment. The 2007/08 streamflow event provides a third example where the I/I+E ratio (28) reflected sediment contributions from all major sub-catchments of the Burdekin (Table 4.3). Such variability at a large (133,400 km^2), end-of-river site reflecting two distinctive source contributions is expected at this scale, and this study highlights the importance of capturing multi-year datasets to identify these variations in annual wet season rainfall and source contributions. Importantly for end-of-river sediment source identification, the clay mineral fingerprints provide additional evidence that both major source areas need to be considered for management of the finer sediment fraction.

4.4.4. Flood plume sediment characteristics and fractionation

Sampling of primary type flood plume waters following Burdekin River streamflow events reveal that sediment concentrations rapidly decrease upon seawater mixing (from 0.1 psu), with mean end-of-river TSS concentrations declining from 475 to <25 mg L^{-1} within 10 km of the river mouth (Table 4.3). With the deposition of coarser sediment fractions at the river mouth, the proportion of clay sized-sediments increased by between 1.5 and 3-fold within the plume. Declining I/I+E ratios along each sampled transect with increasing salinity provides evidence for relative enrichment of the expandable (smectite-rich) clays within this remaining fine sediment (Table 4.3), as also seen in the flood plume waters of the neighbouring Fitzroy River (Douglas et al., 2006a) and other large rivers globally (Gibbs, 1977; Sionneau et al., 2008). In a study of Mississippi River sediment transport, Sionneau et al. (2008) found three factors control the clay mineral distribution in the Gulf of Mexico with the most important factor being the relative contributions from upstream fluvial sources, as observed in this study. The differential settling of illite along the gradient from the coast, and surface-ocean currents were also identified as contributing factors. The physical sorting of larger sediment particles (Hillier, 1995), including all coarse sediment fractions (i.e. fine silt to sand) and the larger clay mineral particles within the <10 μm fraction (i.e. illites and kaolins; Gibbs, 1977; Hillier, 1995) also appears to be an important control on sediment fractionation and deposition in Burdekin flood plumes.

The study findings suggest that fine sediments derived from sedimentary and granitic terrains delivered by the Upper Burdekin strongly influence both BFD and end-of-river sediment composition, but are preferentially deposited inshore upon seawater mixing (Fig. 4.3b). Other GBR studies have found basaltic-derived fine sediment abundant in both flood plume (Douglas et al., 2006a) and offshore marine deposits (McCulloch et al., 2003b). However, within the Burdekin flood plume the clay mineral data do not distinguish between a general enrichment of expandable clays from this Upper Burdekin-BFD source or an increase in the relative contribution of expandable clay-rich fine sediment originating from basalt areas in other catchments, such as the Bowen River. Further study is required to confirm these basaltic-sediments as the primary source of Burdekin fine sediment transported offshore, perhaps by involving more detailed XRD investigation of the expandables category, or by using geochemical and isotopic sourcing techniques. Characterisation of reef flat and other benthic sediment deposited along the known Burdekin River flood plume trajectory also requires investigation, with evidence of further enrichment of the expandable clays within the marine environment seen in the benthic sediment sample collected from Old Reef, 65 km east of the Burdekin River mouth.

4.5. Conclusions

In summary, the distinctive geological source-related "fingerprints" found in this study prove the applicability of clay mineral-based tracing within large, dry tropical catchments, and across the freshwater to marine continuum. Further, this study highlights the suitability of a clay mineral ratio (I/I+E) for broader application across the GBR catchment area, and other similar environments, to discriminate basaltic sources of fine sediments. Analysis of individual site sediments collected over multiple streamflow events and water years found consistency in clay mineral relative abundances, and the I/I+E ratio distinguished basaltic (ratio of 0–7), granitic (28) and sedimentary (42–52) geological sources. These ratios also clearly distinguished the Upper Burdekin-BFD reservoir source (34–35) from the expandable clays-rich Bowen River source (11), and were used in conjunction with the catchment-wide fine sediment (<10 µm) budget to provide multiple lines of evidence to guide the remediation of fine sediment sources. This study found annual wet season rainfall distribution and resulting contributions from the two main source areas to be a dominant factor controlling Burdekin end-of-river sediment characteristics each year, with varying contributions from sedimentary and granitic landscapes (Upper Burdekin-BFD reservoir source) as well as basaltic/expandable clay-rich sources, such as the Bowen River downstream of the reservoir. Finally, despite this annual variability in end-of-river sediment sources, an examination of flood plume sediments over consecutive water years found consistency in the physical sorting and settling of all coarse sediment and larger clay mineral particles upon mixing with seawater (i.e. 0.1 psu). Further, the I/I+E ratio provided evidence of relative enrichment of the expandable (smectite-rich) clays within remaining flood plume sediment after this bulk deposition near the river mouth.

5. Discussion and Conclusions

5.1. Overview

Increased turbidity and sedimentation associated with greater terrestrial runoff following agricultural development of coastal catchments has resulted in the degradation of near-shore tropical marine ecosystems around the globe (Fabricius, 2005; Risk, 2014). Over the past decade, research has determined fine (<63 µm), organic and nutrient-rich terrigenous sediments have the greatest negative effects on tropical marine ecosystems (Fabricius and Wolanksi, 2000; Perez et al., 2014; Philipp and Fabricius, 2003; Weber et al., 2006, 2012). Moreover, the role of fine terrigenous sediments on resuspension regimes and increased turbidity in inshore marine and estuarine environs has also been examined (Davies-Colley and Smith, 2001; Fabricius et al., 2014; Wolanski et al., 2008). However, there have been limited field studies to date examining the size, composition, transformation processes and dispersal of terrigenous sediments in tropical estuarine and marine environments, or tracing the sediment of greatest threat back to upstream catchment source areas. Within the Great Barrier Reef (GBR), suspended sediment export from the Burdekin River, the largest discrete source, has increased since European settlement of the catchment (Bartley et al., 2014; Kroon et al., 2012). Increased turbidity and decreased clarity in GBR waters off the Burdekin can persist for several months following flood plume formation, as material delivered in those events is resuspended by waves and currents (Fabricius et al., 2014). Importantly, detailed examination of the composition of this sediment within these GBR waters, or the identification of its upstream catchment source has not yet been undertaken. Hence, the primary aim of this thesis is *to characterise and source Burdekin River flood plume suspended sediment, which is most likely to directly affect coral reef and seagrass ecosystems of the central GBR.*

Historically, large seasonally-dry tropical catchments (e.g. >100,000 km^2) have been poorly studied, in part due to the logistical and financial constraints of covering such extensive scales, and the difficulties in adequately capturing streamflow events in such highly variable and seasonal climates. However, tropical rivers export large volumes of suspended sediments into adjacent marine environments during seasonal rainfall and discharge events, including those associated with cyclonic activity. An increased understanding of sediment yields and rates of delivery is especially important where suspended sediments are transported to environmentally, socially, economically and culturally important and sensitive marine ecosystems.

This thesis pursues a multi-disciplinary approach to determine the key sources and transport pathways of suspended sediments across the large Burdekin catchment and adjacent coastal waters. The study utilises an integrated suspended sediment, particle size and clay mineralogy dataset consisting of data collected at high spatial and temporal resolution across the catchment and flood plume waters (see section 1.6). Burdekin River flood plume dynamics controlling the fractionation, transformation and dispersal of suspended sediment within the GBR lagoon were examined (Chapter 2), and used to guide subsequent investigations of catchment sources using sediment budgets (Chapter 3) and source tracing (Chapter 4). This study confirms the applicability of these sediment budget and clay mineral-based source tracing techniques to better understand sediment dynamics in seasonally-dry tropical environments, and for large catchments. Further the development of particle size specific yields provides a novel approach to identify key locations within a catchment from which the most ecologically damaging grainsize fractions are exported. Here I discuss the key findings of this study within the context of four key research objectives, designed to achieve the broader research aim outlined above.

Objective 1: *Identify and describe the hydrodynamic, biological and chemical processes controlling the transformation and dispersal of suspended sediments and particulate nutrients in flood plumes delivered to the GBR from the Burdekin River*

River flood plume hydrodynamic and chemical processes that control the transformation and delivery of terrigenous sediments and nutrients in the immediate near-shore marine environment have been the subject of considerable international research (e.g. Ayukai and Wolanski, 1997; Dagg et al., 2004; Gibbs and Konwar, 1986; Golbuu et al., 2003; Hill et al., 2000; Lohrenz et al., 1999; Milligan et al., 2007; Wolanski and Gibbs, 1994). Within the GBR lagoon, the influence of these processes on the size and composition of suspended sediment and associated nutrients and organic matter that can be most readily dispersed offshore to sensitive habitats (Coles et al., 2011; Erftermeijer et al., 2012) remain poorly understood. This study provides a comprehensive flood plume dataset for the Burdekin River, including five discrete flood events sampled from 2007/08 to 2010/11 as presented in Chapters 2 and 4. An examination of flood plume sediment dynamics during peak discharge conditions found suspended sediment was rapidly deposited once the floodwaters mixed with seawater and salinity rose above 0.1 psu (Fig. 2.8, Table 4.2). Suspended sediment concentrations typically decreased to around one percent of the river mouth concentration within the 0 to 10 psu salinity zone (e.g. 450 to 5 mg L^{-1}), typically extending no further than 20 km from the coast (Chapters 2 and 4). While these findings support the conclusions of earlier Burdekin River flood plume studies (e.g. Devlin and Brodie, 2005; Wolanski and Jones, 1981), this thesis contributes significantly to the detail and knowledge of the origin and dynamics of flood plume sediments discharged into coastal waters. Further, this study coincided with a wetter climatic cycle in the historical rainfall record for the Burdekin catchment, correlated to the Pacific Decadal Oscillation (Lough, 2011; Rodriguez-Ramirez et al., 2014). Thus, this study examined a series spanning low annual flows to unusually large rainfall and river discharge years, including the 3rd, 4th and 6th largest discharge years on record (Fig. 5.1; Lough et al., in press) and uniquely captures runoff and associated sources of suspended sediment from all areas of this large catchment (Chapter 3).

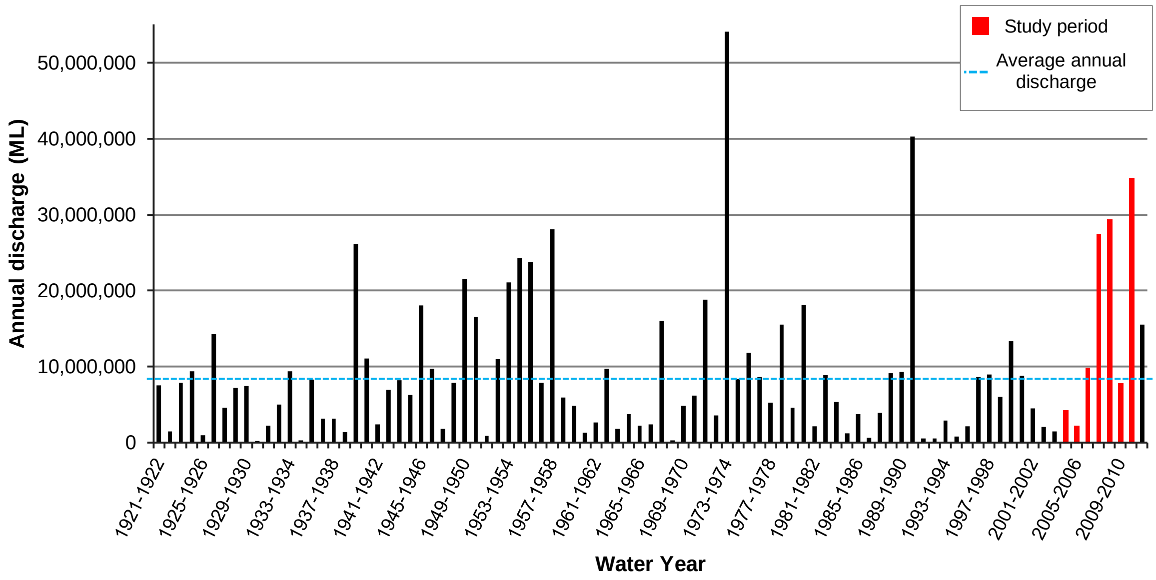

Figure 5.1 Historical Burdekin River annual discharge at the Clare gauge from 1921 to 2012 (DERM, 2012), highlighting the study water years (red), and long-term average annual discharge (9.18 million ML) for this 91-year period (blue-dotted line).

Earlier research has shown suspended sediment from the Burdekin River and other GBR dry tropical rivers, such as the Fitzroy River, mostly settles close to the river mouths (Devlin and Brodie, 2005; Lewis et al., 2014; Radke et al., 2010; Webster and Ford, 2010; Wolanski and Jones, 1981). Importantly for the first time in the GBR, Chapter 2 found all sand (>63 µm) and the majority (>80%) of clay and silt (<63 µm) sized-sediment exported from the Burdekin River to rapidly settle by the time the freshwater plume mixed with the receiving seawater, and salinities had increased to just 0.1 psu, normally within 10 km of the coast (Fig. 2.8). Microphotographs of sub-surface plume water within this zone revealed flocs of sediment particles were settling bound by organic matter, with floc sizes >100 µm in diameter. The influence of both physical and biological flocculation processes (e.g. size sorting and settling, salinity, production of binding 'glues') in accelerating settling of river suspended sediment as it encounters seawater have been well documented in other coastal settings internationally (e.g. Ayukai and Wolanski, 1997; Fox et al., 2004; Gibbs and Konwar, 1986; Hill et al., 2000; Hillier, 1995). This study provides the first evidence of this process occurring in the flood plumes of the large, sediment-laden, dry tropical rivers discharging into the GBR, with the preferential deposition of coarse suspended sediment shown to be accelerated through biologically-mediated flocculation.

Biologically-mediated flocculation of sediment within turbid coastal waters has been shown to be driven by heterotrophic bacterial activity, where the low light and salinity conditions can prevent marine phytoplankton blooms (Dagg et al., 2008; Lohrenz et al., 1999). Most previous studies have focused on the influence of dissolved inorganic nitrogen which dominates global nitrogen export (Seitzinger et al., 2010). The results in Chapter 2 demonstrate that particulate nitrogen and phosphorus are non-conservatively mixed in this initial turbid, low salinity area of the flood plume. Although some of the nutrient loss from surface waters is due to physical settling, it is hypothesized these particulate nutrients also drive bacterial activity in this zone leading to the formation and subsequent settling of these large organic-rich sediment flocs. In short, the evidence suggests that particulate nutrients may accelerate suspended sediment deposition close to the river mouth. As microphotographs of the samples taken from the end-of-river (freshwater) showed that these sediments were unflocculated, the formation of flocs must occur upon estuarine mixing where conditions become favorable for bacteria. A detailed examination of the dynamics and drivers of the particulate nutrients and their interactions with suspended sediments in coastal estuaries was beyond the scope of the present study. Great Barrier Reef flood plume research to date has primarily focused on the secondary plume water types (i.e. intermediate salinity, reduced TSS; Petus et al., 2014) further offshore, and the uptake of dissolved inorganic nitrogen by marine phytoplankton where growth is no longer light limited (e.g. Brodie et al., 2010; Davies and Eyre, 2005; Devlin and Brodie, 2005; Radke et al., 2010). Hence, the influence of particulate nutrients in driving biogeochemical cycles during initial flood plume conditions, and redistribution and potential mineralization within the coastal waters in subsequent dry season months (see Radke et al., 2010) may currently be underestimated for seasonally-dry tropical rivers. Again, further investigation to resolve this should be a priority.

Objective 2: *Identify and characterise the sediment types that are likely to affect the greatest area of the GBR and have the most severe direct impacts on GBR ecosystems*

The types of sediment that are most readily dispersed in plume waters beyond the initial turbid zone must be identified to develop effective management priorities to reduce the direct impact of terrigenous sediments on sensitive tropical marine ecosystems. Although the transport and transformation of terrigenous sediment and associated particulate matter in marine waters by flood plumes has been studied for a number of the world's largest rivers (see Dagg et al., 2004), few studies have examined flood plumes generated by seasonally-dry tropical rivers, or those located along the GBR coast. The extensive areas over which flood plume waters disperse across the inner and mid-shelf regions of the GBR have now been mapped in detail, including frequency of spatial exposure (e.g. Fig 9 in Devlin et al., 2013; Fig. 9 in Álvarez-Romero et al., 2013), using a combination of satellite imagery and *in situ* measurements of salinity, chlorophyll *a*, TSS and nutrients (Álvarez-Romero et al., 2013; Brodie et al., 2010; Devlin et al., 2012, 2013; Petus et al., 2014; Schroeder et al., 2012). However, to date the sediment entrained in these plumes has been poorly characterised. Thesis Objective 2 sought to address this knowledge gap. This chapter revealed clay (<4 µm) and fine silt (4–16 µm) sediment fractions are dispersed furthest in flood plumes discharged from the Burdekin River. Thus, further research should focus on the dynamics of these fractions in terms of their physical behaviour in flood plumes and subsequent resuspension events, as well as the nutrient and contaminant content of these different size fractions. The identification of these size fractions most widely dispersed in flood plumes can also be used to isolate the catchment source(s) of these clay and fine silt sediments to most effectively implement catchment management actions to mitigate downstream impacts. Hence, the results of Chapter 2 guided the focus of investigations for the later chapters of this thesis.

Clay and fine silt sized-sediments were observed during peak flood conditions as discrete mineral particles or, once suspended sediment had reduced to <10 mg L^{-1}, small flocs in plume waters adjacent to the coast (Chapter 2). With improving light conditions as sediment concentrations and associated turbidity decreased in the weeks following discharge events, biological activity increased in the coastal plume waters (i.e. <20 km from the mouth), indicated by higher chlorophyll *a* concentrations, and the presence of diatoms and zooplankton (observed in microphotographs e.g. Fig. 2.5). During this phase microphotographs showed suspended sediments encased in biological matter as large, low-density, floc aggregates (100–200 µm; Fig. 2.6), with sampling indicating that they maintain this state after seaward propagation at least 100 km from the river mouth. Thus for the first time in the GBR, this study has identified flood plume fine sediment (<16 µm) is dispersed into the lagoon as organic-rich flocs. These specific sediment characteristics are those identified to be most damaging to corals (i.e. organic and nutrient-rich, fine (<63 µm) sediment (Weber et al., 2006, 2012)), that is readily resuspended and causes enhanced smothering effects due to its propensity to adhere to coral surfaces (Fabricius and Wolanski, 2000). As the other large rivers discharging into the GBR are also characterised by high suspended sediment and nutrient loadings it is hypothesised that nutrient-enhanced biological encasement of fines to form flocs may be a key mechanism influencing the dispersal of fine terrigenous sediment across most of the GBR.

The publication arising from Chapter 2 (Bainbridge et al., 2012) was the first to describe the extent and duration of flood plume conditions resulting from significant rainfall and river discharge in the extreme 2010/11 water year, associated with one of the strongest La Niña events on record (Lough et al., in press). This study identified the likely impact of such flood plumes resulting from extreme discharge events (i.e. >90th percentile; Lough et al., in press), carrying suspended sediments, nutrients and other contaminants that may persist within inshore GBR waters for weeks, and continue to be resuspended in the months following such events (e.g. Fabricius et al., 2014). For example, the 2010/11 Burdekin River flood plume persisted for at least 10 weeks within the GBR. Prior to this extreme rainfall and discharge event, flood plumes had generally been considered to be short-lived phenomena that quickly become well-mixed with seawater in the strong winds and currents often prevalent during the wet season months (Devlin et al., 2001). The interactive effects of reduced salinity and poor water quality on marine ecosystems has been shown experimentally (Humphrey et al., 2008), and the detrimental effects on inshore coral reef and seagrass communities attributed to flood plumes discharged by coastal rivers along the GBR in the extreme 2010/11 water year have been documented in an array of recent publications (Berkelmans et al., 2012; Butler et al., 2013; Coles et al., 2014; Fabricius et al., 2014; Jones and Berkelmans, 2014; Thompson et al., 2014; Petus et al., 2014). Further, recent inshore GBR coral reef health monitoring found increasing volumes of clay and silt sized-sediments settled on inshore reefs from 2005 to 2012 (Thompson et al., 2013), in addition to regionally increasing turbidity due to the above average rainfall and river discharge conditions experienced over this time. These findings support the thesis that finer sediment particles are being preferentially transported to inshore reef environments during large river discharge and flood plume events and influence subsequent resuspension events (Fabricius et al., 2014).

Objective 3: *Identify major sources of suspended sediment in the Burdekin catchment, including the spatial and temporal variability of suspended sediment sub-catchment contributions, by constructing a catchment-wide budget and partition the budget into defined (Objective 2) suspended sediment particle size fractions.*

Internationally, suspended sediment source and transport processes in seasonally-dry tropical rivers have received limited attention. However, large seasonally-dry tropical rivers contribute the highest loads exported from the GBR catchment area and as such identifying sediment source areas and an improved understanding of how this suspended sediment is transported through these catchments are imperative to manage the threat to GBR marine ecosystems. This thesis is the first catchment-wide, empirical-based approach to construct budgets of sub-catchment discharge and suspended sediment load contributions for the Burdekin River, and includes the compilation and analysis of one of the most comprehensive suspended sediment datasets collected across all GBR catchments. The data presented in Chapter 3 were collected during wet season streamflow events, and include five consecutive water year budgets represented by seven strategic sub-catchment, reservoir outlet and end-of-river streamflow gauging station locations. These budgets are complemented by data from 24 additional tributary sites sampled during streamflow events between 2004 and 2011 by a trained volunteer network. This study illustrated catchment-wide suspended sediment budgets for large seasonally-dry tropical catchments can readily distinguish consistent, dominant sub-catchment sources of end-of-river suspended sediment export. The budget approach was also useful in quantifying the influence of a reservoir (which captures 88% of the entire catchment area) on end-of-river discharge and suspended sediment export.

Variability in the contributions of suspended sediment from sub-catchments across the Burdekin catchment can be distinguished by key geomorphic features. The Bowen and Upper Burdekin sub-catchments were identified as the main sediment contributing sub-catchments, dominating end-of-river suspended sediment supply throughout the study period, including water years where rainfall and discharge were larger in the drier inland sub-catchments. These sub-catchments are characterised by steeper topography, erosive soils, and wetter climates due to proximity to the coast. The drier inland sub-catchments (Belyando, Suttor and Cape), characterised by low relief and expansive anastomosing floodplains were found to generate sediment yields <23 t km^{-2} yr^{-1}, an order of magnitude lower than their coastal counterparts (147–530 t km^{-2} yr^{-1}; Table 3.2). This characterisation of sub-catchments by geomorphic attributes and associated sediment yields provides a rare and valuable sediment yield dataset that can be utilised for other seasonally-dry tropical or semi-arid studies with similar geomorphic conditions.

The sediment budget analyses in Chapter 3 identified a sub-catchment representing only 12% of the total catchment area to be the dominant contributor (55–82%) of end-of-river suspended sediment export, providing a well-defined and constrained geographical area to target on-ground remedial investment. These results highlight the effectiveness of the sediment budget technique at this large scale, and provide an empirical approach to sediment source identification both within large river catchments and dry tropical environments. For studies of ephemeral river systems such as the Burdekin, this research also highlighted the importance of intensive sampling regimes that target and capture larger streamflow events at key sub-catchment locations in order to reduce uncertainty in calculated suspended sediment loads and accurately quantify sub-catchment contributions. This can be logistically difficult in such catchments with spatially and temporally variable hydrological regimes (e.g. Alexander et al., 2001). The benefits of establishing a trained, technically proficient volunteer sampling network to overcome the logistical constraints of 'event' field sampling across large river catchments with remote tributaries were also confirmed by this study.

Numerical catchment models have been previously relied upon to identify catchment sediment sources and sub-catchment load contributions. However, these models have rarely been validated for the seasonally-dry tropical conditions of the large GBR river catchments. This thesis has generated a valuable dataset that will support the calibration and validation of such models for these environments; including suspended sediment sub-catchment yield rates, catchment-wide sediment budgets under a range of discharge conditions, and estimates of suspended sediment trapping within reservoirs located in the catchment. This study included error margins for sub-catchment suspended sediment loads and reservoir sediment trapping estimates for the first time in the GBR (Chapter 3; Kuhnert et al., 2012; Lewis et al., 2013), improving data confidence and providing confidence intervals for model comparison. The highly seasonal and variable nature of streamflows within seasonally-dry tropical catchments means that models based on forecasting 'average annual loads' will not adequately capture the wide range of potential annual sediment yields (e.g. 0.004 to 15.7 million tonnes at the end-of-river site over a 24-year period). Temporal variations in suspended sediment yields associated with drought breaking floods, or sediment supply-limited years are also not captured in most forecast models. These constraints should be better acknowledged as a limitation to the application of numerical catchment models to seasonally-dry tropical catchments.

Catchment sediment budget studies often represent the <63 µm fraction as a single entity, focusing on the different fluvial transport efficiency of this material which is transported as suspended sediment, relative to that of bed material which is predominantly transported along, or close to, the bed (Koiter et al., 2013; McKergow et al., 2005). In Chapter 3 this study takes a higher-resolution approach and divides this fraction into clay (<4 µm), fine silt (4−16 µm) and coarse (i.e. >16 µm) sediment fractions (Fig. 3.3), to identify the sub-catchment sources of clay and fine silt sediments which can be transported with different efficiencies through impoundments such as the Burdekin Falls Dam (BFD), and which have most relevance to sustainably managing the GBR ecosystem (Chapter 2). This component of the thesis provides a unique approach for application in other tropical river studies, including studies seeking to determine sub-catchment sources of clay or silt fractions, or reservoir influence on the transport and deposition of different sediment size fractions. Although the BFD has minimal influence on end-of-river discharge, the reservoir did significantly reduce suspended sediments contributed from the upstream catchment area to the end-of-river (Fig 3.1). Indeed, annual reservoir trapping efficiency of suspended sediments ranged from 50–85% of total incoming suspended sediments during the study period. Significantly, the revised sediment budget based on the specific sediment size fractions found the reservoir preferentially trapped the coarser (>16 µm) sediment fractions (92%), increasing the proportion of clays and fine silts in the sediment loads being carried over the dam wall (Fig. 3.3; Lewis et al., 2013). The data also revealed the highest clay and fine silt loads, of most interest to environmental managers of the GBR, are not always sourced from areas that yield the largest 'bulk' suspended sediment load (i.e. all size fractions). Whilst the Bowen River was identified as the major source of 'bulk' suspended sediments across the Burdekin catchment, when the clay-only fraction is considered, almost equal loads are contributed from the Bowen River and BFD overflow sources (e.g. 1.03 and 1.32 million tonnes, respectively, over the study period average; see section 3.5.4). However, the clay-only specific sediment yield from the Bowen River (145 t km^{-2} yr^{-1}) is 10-times higher than the BFD overflow source (11 t km^{-2} yr^{-1}). Thus, this chapter demonstrated the importance of incorporating sediment particle size into catchment sediment budget research targeting remediation of source areas for the finer sediment fractions of most concern to marine park managers.

Objective 4: *Examine the potential of clay mineralogy-based tracing to discriminate discrete sediment sources and trace flood plume suspended sediment within a large, geologically complex catchment.*

The applicability of clay mineralogy as a sediment tracing technique for catchment studies with a specific focus on tracing terrigenous sediment in flood plumes back to a catchment origin was evaluated in Chapter 4. Studies linking catchment sources to the downstream transport and dispersal of this sediment within the adjacent marine environment are rare (Risk, 2014), particularly those that seek to both characterise and source sediment carried beyond inshore turbid zones. To address this knowledge gap, the clay and fine silt sized-sediments carried in secondary plume waters (as identified in Chapter 2) were traced to geological source areas within high sediment-yielding sub-catchments of the Burdekin identified in Chapter 3. Clay mineral abundance data were also used to further characterise flood plume fine sediment most readily dispersed offshore. Using key clay minerals identified in sediments collected across tributary to flood plume scales, sedimentary, granitic and basaltic geologies were identified as the main sources of end-of-river fine (<10 µm) sediment (Fig. 4.3). Sediments derived from basaltic sources were most clearly distinguishable from other geological sources using a clay mineral ratio (I/I+E; see 4.2.4; Fig. 4.3a), which highlighted the dominance of basaltic sources of sub-catchment outlet sediments (e.g. Bowen and Suttor Rivers) despite comprising relatively small areas (10–33%) of the upstream catchment. Expandable (smectite-rich) clays also appear to be relatively enriched in flood plume waters upon seawater mixing (Fig. 4.5), as the coarser sediment (>16 µm) is deposited within the initial turbid zone. Douglas et al. (2006a) and Smith et al. (2008) found smectites were also enriched in the Fitzroy River estuary, and concluded they contained a substantial Tertiary basalt component. Hence, there is now evidence suggesting flood plume sediments most readily dispersed offshore from the two largest sediment sources to the GBR (i.e. Burdekin and Fitzroy Rivers) are characterised by fine clay originating from basaltic lithologies within the catchment.

This thesis has utilised complementary, multiple lines of evidence to identify sediment sources across a large, seasonally-dry tropical catchment, including (i) a series of annual catchment-wide discharge and sediment budgets using empirical suspended sediment loads data over a five-year period; (ii) a refined version of this budget incorporating specific sediment size fractions from four years of available particle size data; and (iii) tracing of end-of-river and coastal flood plume fine (<10 µm) sediment using clay mineral abundance data collected over six water years from 31 sites across the catchment. Recent reviews (Fu et al., 2013; Koiter et al., 2013) have highlighted the benefits of a ‘multiple lines of evidence’ approach to sediment source investigation, given the limitations and uncertainties associated with individual monitoring, tracing or modelling techniques (also discussed above (Objective 3) and sections 3.3.5 and 4.4.1).

In this study clay mineral tracing provided additional evidence to confirm the sub-catchment contributions of clay and very fine silt (i.e. <10 μm) as identified in the sediment budget approach. Further, the use of a ratio of common clay minerals enabled geological source areas within identified sub-catchments to be further discriminated for targeted landscape rehabilitation. Such approaches to source investigation have been applied in several northern Australia river catchments (e.g. Ord River (Wasson et al., 2002), Fitzroy River (Douglas et al., 2008), Mitchell River (Rustomji et al., 2010) and Normanby River (Brooks et al., 2013)), using a combination of sediment flux/load data, multiple tracers (e.g. isotopes, geochemistry), gully sediment yield rates and/or numerical catchment models. This combined approach provides greater confidence in management recommendations to Government and regional Natural Resource Management (NRM) organisations commissioning research to target substantial investment in on-ground remedial efforts. As shown in this thesis, the multiple lines of evidence approach has particular usefulness and broader global application in poorly studied catchments, such as those located in dry tropical environments.

The often distinctive geological source-related “fingerprints” found in this study suggest the relative proportions of clay minerals to be a valuable tracing tool in large and geologically complex catchments. This technique has particular utility in such catchments to examine broad trends in fine sediment sources to guide the focused application of more expensive and time consuming geochemical and/or isotopic tracing techniques within specific sub-catchment areas. Further, this study found 1-2 samples from any given source area may be sufficient to generate reproducible signatures, highlighting the efficacy of this technique and its potential application for similar sediment tracing and climatic studies in other catchments. It has also been argued that clay minerals may provide a more suitable tracer that geochemistry, especially in studies across the saline mixing zone where interference of geochemical tracers can occur (Koiter et al., 2013). However, geochemical and isotopic fingerprinting techniques have the advantage of providing quantification of multiple upstream source area contributions (e.g. Douglas et al., 2008; Wilkinson et al., 2013). Thus a combination of methods for use within catchments of this scale is likely the most suitable approach, where these latter techniques may be used to target areas identified as most relevant by the clay mineral-based approach. The advantages of an intensive, multi-year sampling approach to the study of highly variable seasonally-dry tropical catchments have also been highlighted in this thesis, especially to capture annual variability in source contributions to the end-of-river for larger catchments.

5.2. Concluding remarks and future research directions

This is the first study to examine sediment particle size fractionation within flood plumes and adjacent catchments of the GBR and confirms the importance of biologically-mediated flocculation processes in influencing both the deposition and dispersion of terrestrial particulate matter within the GBR lagoon. The identification of both the specific sediment size fractions (<16 µm) and mode of dispersal of this sediment as organic-rich flocs in initial plume waters provide a significant advancement in our understanding of terrigenous sediment dispersal and transformation within the lagoon, and the nature of this sediment as it reaches GBR ecosystems across and along the shelf. Further, sub-catchment sources of these clay (<4 µm) and fine silt (4–16µm) sediments were identified across this large river catchment using particle size specific catchment sediment budgets. These source areas were further refined to geological sources using a clay mineral-based tracing technique with great success. This study highlights the importance of examining the particle size of suspended sediments exported from the large, dry tropical rivers of the GBR and similar coastal settings, and should guide further research examining the ecological effects of terrigenous sediment (and associated nutrients and other contaminants) on coral reefs, seagrass meadows and other marine ecosystems.

The approach to sediment source identification presented in this thesis for the Burdekin River catchment is suitable for broad application across the GBR catchment area and lagoon to aid in further identification of (i) terrigenous sediment sources for on-ground investment strategies, (ii) the characteristics of this sediment dispersed in flood plumes, and (iii) the final fate of this sediment and impact within the GBR lagoon. Further research areas include:

- Much of the research to date examining the ecological effects of terrigenous sediment on marine ecosystems such as seagrass meadows and coral reefs has focused on the <63 µm ‘mud’ sediment fraction as a single homogenous fraction. This thesis has demonstrated that <16 um sediment is transported in organic-rich flocs whilst coarser sediment deposits near the river mouth. These findings strongly indicate that the finer clay (<4 µm) and fine silt (4–16 µm) fractions should be analysed separately in future investigations. However, it remains likely that nutrients in all particle sizes can contribute to reduced light clarity and dispersal of fine sediment fractions within the lagoon, by their dissociation into the water column and subsequent contribution to algal growth, on sediment flocs or separately. Therefore, it has also become important to better understand the particulate nutrient content, and the degree and rates of bioavailability of different size fractions delivered to coastal waters.

- Refinement of the clay mineral ratio as a tool to trace and assign plume sediment to its geological origin. Strengthening of this tool in combination with geochemical and/or isotopic tracers to further identify multi-sourced basaltic-derived sediment is currently under further investigation, with several tracing projects recently completed in the Burdekin catchment (Burton et al., 2014). Such tracing could also be extended further within the receiving marine environment to trace the origin of resuspended sediments and/or deposited sediment on reef flats and seagrass meadows.

- Confirmation of sediment particle size and floc formation processes within secondary plume waters of other important GBR rivers. In the discussion (Objective 2) it was hypothesised that sediments discharged from the other large, sediment-laden rivers of the GBR are also dispersed as organic-rich flocs, however this depends on the characteristics of sediments (e.g. particle size, organic content) and associated nutrient loads (e.g. quantity, bioavailability, species present) carried within these plume waters, which requires further investigation. The fractionation and transformation processes influencing sediment contributed from the smaller, wetter catchments of the GBR, characterised by smaller sediment loads and high dissolved nutrient loadings (i.e. more intensive fertilizer use; Bainbridge et al., 2009) also requires further research.

- Recent research across northern Australian rivers has identified sub-surface (e.g. gullies, channel bank) erosion processes as the dominant source of sediment yields from most large, dry tropical catchments (e.g. Caitcheon et al., 2012; Olley et al., 2013; Wilkinson et al., 2013). Research to date on sub-surface erosion in catchments draining to the GBR has focused on the <63 µm sediment fraction as a single homogenous fraction. The findings of this thesis strongly support further examination of the specific clay and fine silt (<16 µm) fraction contributions across key source erosion processes.

References

Alexander, J., Fielding, C.R., Wakefield, S.J., George, M.T., Cottnam, C.F. 2001. Fluvial geochemistry through a short-duration, Tropical-Cyclone induced discharge event in the Burdekin River and Hann Creek, North Queensland, Australia. Aquatic Geochemistry 7, 275-293.

Alizai, A., Hillier, S., Clift, P.D., Giosan, L., Hurst, A., VanLaningham, S., Macklin, M. 2012. Clay mineral variations in Holocene terrestrial sediments from the Indus Basin. Quaternary Research 77, 368-381.

Alongi, D.M., McKinnon, A.D. 2005. The cycling and fate of terrestrially-derived sediments and nutrients in the coastal zone of the Great Barrier Reef shelf. Marine Pollution Bulletin 51, 239-252.

Alongi, D.M., Trott, L.A., Pfitzner, J. 2007. Deposition, mineralisation, and storage or carbon and nitrogen in sediments of the far northern and northern Great Barrier Reef shelf. Continental Shelf Research 27, 2595-2622.

Álvarez-Romero, J.G., Devlin, M., Teixeira da Silva, E., Petus, C., Ban, N.C., Pressey, R..L. Kool, J., Roberts, J.J., Cerdeira-Estrada, S., Wenger, A.S., Brodie, J. 2013. A novel approach to model exposure of coastal-marine ecosystems to riverine flood plumes based on remote sensing techniques. Journal of Environmental Management 119, 194-207.

Amos, K.J., Alexander, J., Horn, A., Pocock, G.D., Fielding, CR. 2004. Supply limited sediment transport in a high-discharge event of the tropical Burdekin River, North Queensland, Australia. Sedimentology 51, 145-162.

Andréfouët, S., Mumby, P., McField, M., Hu, C., Muller-Karger, F. 2002. Revisiting coral reef connectivity. Coral Reefs 21,43-48.

APHA. 2005. Standard methods for the examination of water and wastewaters. 21st edn. American Public Health Association, American Water Works Association and Water Environment Federation, Washington, USA.

Ayukai, T., Wolanski, E. 1997. Importance of biologically mediated removal of fine sediments from the Fly River plume, Papua New Guinea. Estuarine, Coastal and Shelf Science 44, 629-639.

Bainbridge, Z., Brodie, J., Faithful, J., Sydes, D., Lewis, S. 2009. Identifying the land-based sources of suspended sediments, nutrients and pesticides discharged to the Great Barrier Reef from the Tully Basin, Queensland, Australia. Marine and Freshwater Research 60, 1081-1090.

Bainbridge, Z.T., Wolanski, E., Álvarez-Romero, J.G., Lewis, S.E., Brodie, J.E. 2012. Fine sediment and nutrient dynamics related to particle size and floc formation in a Burdekin River flood plume, Australia. Marine Pollution Bulletin 65, 236-248.

Bainbridge, Z.T., Lewis, S.E., Smithers, S.G., Kuhnert, P.M., Henderson, B.L., Brodie, J.E. 2014. Fine-suspended sediment and water budgets for a large, seasonally dry tropical catchment: Burdekin River catchment, Queensland, Australia. Water Resources Research 50, 9067-9087.

Bannister, R.J., Battershill, C.N., de Nys, R. 2012. Suspended sediment grain size and mineralogy across the continental shelf of the Great Barrier Reef: Impacts on the physiology of a coral reef sponge. Continental Shelf Research 32, 86-95.

Bartley, R., Wilkinson, S.N., Hawdon, A.A., Abbott, B.N., Post, D.A. 2010. Impacts of improved grazing land management on sediment yields. Part 2: Catchment response. Journal of Hydrology 389, 249-259.

Bartley, R., Bainbridge, Z., Lewis, S., Kroon, F., Wilkinson, S., Brodie, J., Silburn, M. 2014. Relating sediment impacts on coral reefs to watershed sources, processes and management: A review. Science of the Total Environment 468-469, 1138-1153.

Bell, I., Ariel, E. 2011. 2011. “Dietary shift in green turtles” In McKenzie, L.J., Yoshida, R.L., Unsworth, R. (Eds). Seagrass-Watch News. Issue 44, November 2011. Seagrass-Watch HQ. 32pp.

Belperio, A.P. 1979. The combined use of wash load and bed material load rating curves for the calculation of total load: An example from the Burdekin River, Australia. Catena 6, 317-329.

Belperio, A.P. 1983. Terrigenous sedimentation in the central Great Barrier Reef lagoon: A model from the Burdekin Region. BMR Journal of Geology and Geophysics 8, 179-190.

Berkelmans, R., Jones, A.M., Schaffelke, B. 2012. Salinity thresholds of Acropora spp. on the Great Barrier Reef. Coral Reefs 31, 1103-1110.

Bianchi, M., Marty, D., Teyssie, J.-L., Fowler, S.W. 1992. Strictly aerobic and anaerobic bacteria associated with sinking particulate matter and zooplankton fecal pellets. Marine Ecological Progress Series 88, 55-60.

Bianchi, M., Bonin, P., Feliatra. 1994. Bacterial nitrification and denitrification rates in the Rhone River plume (northwestern Mediterranean Sea). Marine Ecological Progress Series 103, 197-202.

Brinkman, R., Wolanski, E., Spagnol, S. 2004. Field and model studies of the nepheloid layer in coastal waters of the Great Barrier reef, Australia. pp. 225-229 in Jirka, G.H., and Uijttewaal, W.S.J. (eds.) “Shallow Flows”, A. Balkema Publishers, Leiden.

Brinkman, R., Tonin, H., Furnas, M., Schaffelke, B., Fabricius, K. 2014. Targeted analysis of the linkages between river runoff and risks for crown-of-thorns starfish outbreaks in the Northern GBR. Australian Institute of Marine Science Report June, 2014.

Brodie, J., Waterhouse, J. 2012. A critical review of environment management of the ‘not so Great’ Barrier Reef. Estuarine, Coastal and Shelf Science 104-105, 1-22.

Brodie, J., McKergow, L.A., Prosser, I.P., Furnas, M., Hughes, A.O., Hunter, H. 2003. Sources of sediment and nutrient exports to the Great Barrier Reef World Heritage Area. ACTFR Report No. 03/11, Australian Centre for Tropical Freshwater Research, James Cook University, Townsville, 208 pp.

Brodie, J.E., Schroeder, T., Rohde, K., Faithful, J.W., Masters, B., Dekker, A., Brando, V., Maughan, M. 2010. Dispersal of suspended sediments and nutrients in the Great Barrier Reef lagoon during river discharge events: conclusions from satellite remote sensing and concurrent flood plume sampling. Marine and Freshwater Research 61, 651-664.

Brodie, J.E., Devlin, M., Haynes, D., Waterhouse, J. 2011. Assessment of the eutrophication status of the Great Barrier Reef lagoon (Australia). Biogeochemistry 106, 281-302.

Brodie, J.E., Kroon, F.J., Schaffelke, B., Wolanski, E.C., Lewis, S.E., Devlin, M.J., Bohnet, I., Bainbridge, Z.T., Waterhouse, J., Davis, A.M. 2012a. Terrestrial pollutant runoff to the Great Barrier Reef: An update of issues, priorities and management responses. Marine Pollution Bulletin 65, 81-100.

Brodie, J., Wolanski, E., Lewis, S., Bainbridge, Z. 2012b. An assessment of residence times of land-sourced contaminants in the Great Barrier Reef lagoon and the implications for management and reef recovery. Marine Pollution Bulletin 65, 267-279.

Brooks, A., Spencer, J., Olley, J., Pietsch, T., Borombovits, D., Curwen, G., Shellberg, J., Howley, C., Gleeson, A., Simon, A., Bankhead, N., Klimetz, D., Eslami-Endargoli, L., Bourgeault, A. 2013. An empirically-based sediment budget for the Normanby basin: Sediment sources, sinks and drivers on the Cape York Savannah. Griffith University, Brisbane, 506pp.

Browne, N.K., Smithers, S.G., Perry, C.T., Ridd, P.V. 2012. A field-based technique for measuring sediment flux on coral reefs: application on turbid reefs on the Great Barrier Reef. Journal of Coastal Research 28 (5), 1247-1262.

Browne, N.K., Smithers, S.G., Perry, C.T. 2013. Spatial and temporal variations in turbidity on two inshore turbid reefs on the Great Barrier Reef, Australia. Coral Reefs 32, 195-210.

Bruno, J.F., Selig, E.R. 2007. Regional decline of coral cover in the Indo-Pacific: timing, extent, and subregional comparisons. PLoS ONE 2(8), e711.

Burrows, D., Maughan, M., Butler, B., Lymburner, L. 2007. Assessing the condition of wetlands in the Burdekin catchment using existing GIS data and field knowledge for the Coastal Catchments Initiative. ACTFR Report 06’20, TropWATER, JCU, Townsville, 91pp.

Burton, J., Furuichi, T., Lewis, S., Olley, J., Wilkinson, S. 2014. Identifying erosion processes and sources in the Burdekin Dry Tropics catchment - synthesis report. Department of Science, Information Technology, Innovation and the Arts, Brisbane.

Butler, I.R., Sommer, B., Zann, M., Zhao, J.X., Pandolfi, J.M. 2013. The impacts of flooding on the high-latitude, terrigenoclastic influenced coral reefs of Hervey Bay, Queensland, Australia. Coral Reefs 32, 1149-1163.

Caitcheon, G.G., Olley, J.M., Pantus, F., Hancock, G., Leslie, C. 2012. The dominant erosion processes supplying fine sediment to three major rivers in tropical Australia, the Daly (NT), Mitchell (Qld) and Flinders (Qld) Rivers. Geomorphology 151-152, 188-195.

Chappell, N.A., Douglas, I., Hanapi, J.M., Tych, W. 2004. Sources of suspended sediment within a tropical catchment recovering from selective logging. Hydrological Processes 18, 685-701.

Ciesiolka, C. 1976. Erosion and Sedimentation. pp. 605-657 in Resources and Potential of the Burdekin River basin, Queensland. Burdekin Project Committee. Australian Government Publishing Service, Canberra.

Coles, R., Grech, A., Rasheed, M., McKenzie, L., Unsworth, R., Short, F. 2011. Seagrass ecology and threats in the tropical Indo-Pacific Bioregion. In R.S. Pirog (Ed) Seagrass: Ecology, uses, and threats. Nova Science Publishers, New York, 225-239.

Coles, R.G., Rasheed, M.A., McKenzie, L.J., Grech, A., York, P.H., Sheaves, M., McKenna, S., Bryant, C. 2015. The Great Barrier Reef World Heritage Area seagrasses: Managing this iconic Australian ecosystem resource for the future. Estuarine, Coastal and Shelf Science 153, A1-12.

Collier, C.J., Waycott, M., McKenzie, L.J. 2012. Light thresholds derived from seagrass loss in the coastal zone of the northern Great Barrier Reef, Australia. Ecological Indicators 23, 211-219.

Cooper, T.F., Uthicke, S., Humphrey, C., Fabricius, K.E. 2007. Gradients in water column nutrients, sediment parameters, irradiance and coral reef development in the Whitsunday Region, central Great Barrier Reef. Estuarine, Coastal and Shelf Science 74, 458-470.

Dagg, M., Benner, R., Lohrenz, S., Lawrence, D. 2004. Transformation of dissolved and particulate materials on continental shelves influenced by large rivers: plume processes. Continental Shelf Research 24, 833-858.

Dagg, M.J., Bianchi, T., McKee, B., Powell, R. 2008. Fates of dissolved and particulate materials from the Mississippi River immediately after discharge into the northern Gulf of Mexico, USA, during a period of low wind stress. Continental Shelf Research 28, 1443-1450.

Davies, P. 2004. Nutrient processes and chlorophyll in the estuaries and plume of the Gulf of Papua. Continental Shelf Research 24, 2317-2341.

Davies, P.L., Eyre, B.D. 2005. Estuarine modification of nutrient and sediment exports to the Great Barrier Reef Marine Park from the Daintree and Annan River catchments. Marine Pollution Bulletin 51, 174-185.

Davies-Colley, R.J., Smith, D.G. 2001. Turbidity, suspended sediment and water clarity: a review. Journal of the American Water Resources Association 37, 1085-1101.

De'ath, G., Fabricius, K.E. 2010. Water quality as regional driver of coral biodiversity and macroalgal cover on the Great Barrier Reef. Ecological Applications 20, 840–850.

De'ath, G., Fabricius, K.E., Sweatman, H., Puotinen, M. 2012. The 27-year decline of coral cover on the Great Barrier Reef and its causes. PNAS 109, 17995–17999.

DERM. 2012. Streamflow discharge data provided by the State of Queensland (Department of Environment and Resource Management).
Available at: www.watermonitoring.derm.qld.gov.au/host.htm, accessed 15 July 2012.

DeVantier, L., De'ath, G., Turak, E., Done, T. Fabricius, K. 2006. Species richness and community structure of reef-building corals on the nearshore Great Barrier Reef. Coral Reefs 25, 329-340.

Devlin, M.J., Brodie, J. 2005. Terrestrial discharge into the Great Barrier Reef lagoon: nutrient behaviour in coastal waters. Marine Pollution Bulletin 51, 9-22.

Devlin, M., Waterhouse, J., Taylor, J., Brodie, J. 2001. Flood plumes in the Great Barrier Reef: spatial and temporal patterns in composition and distribution. GBRMPA Research Publication No. 68, Great Barrier Reef Marine Park Authority, Townsville.

Devlin, M.J., McKinna, L.W., Alvarez-Romero, J.G., Petus, C., Abbott, B., Harkness, P., Brodie, J. 2012. Mapping the pollutants in surface river plume waters in the Great Barrier Reef, Australia. Marine Pollution Bulletin 65, 224-235.

Devlin, M., Da Silva, E., Petus, C., Wenger, A., Zeh, D., Tracey, D., Álvarez-Romero, J. G., Brodie, J. 2013. Combining in-situ water quality and remotely sensed data across spatial and temporal scales to measure wet season chlorophyll-a variability: Great Barrier Reef lagoon (Queensland, Australia). Ecological Processes 2, 31.

Dickins, J.M., Malone, E.J. 1973. Geology of the Bowen Basin, Queensland. Bureau of mineral resources, geology and geophysics. Australian Government Publishing Service, Canberra. ISBN 0 64200228 2.

Douglas, G.B., Palmer, M.J., Caitcheon, G. 2003. The provenance of sediments in Moreton Bay, Australia: A synthesis of major, trace element and Sr-Nd-Pb isotopic geochemistry, modelling and landscape analysis. Hydrological Processes 494, 145-152.

Douglas, G.B., Ford, P.W., Palmer, M., Noble, R.M., Packett, R. 2006a. Fitzroy River Basin, Queensland, Australia. II. Identification of sources of estuary bottom sediments. Environmental Chemistry 3, 377-385.

Douglas, G.B., Ford, P.W., Palmer, M., Noble, R.M., Packett, R. 2006b. Fitzroy River Basin, Queensland, Australia. I. Identification of sediment sources in impoundments and flood events. Environmental Chemistry 3, 364-376.

Douglas, G., Palmer, M., Caitcheon, G., Orr, P. 2007. Identification of sediment sources to Lake Wivenhoe, south-east Queensland, Australia. Marine and Freshwater Research 58, 793-810.

Douglas, G.B., Ford, P.W., Palmer, M.R., Noble, R.M., Packett, R.J., Krull, E.S. 2008. Fitzroy River Basin, Queensland, Australia. IV. Identification of flood sediment sources in the Fitzroy River. Environmental Chemistry 5, 243-257.

Douglas, G.B., Kuhnen, M., Radke, L.C., Hancock, G., Brooke, B., Palmer, M.R., Pietsch, T., Ford, P.W., Trefry, M.G. and Packett, R. 2010. Delineation of sediment sources to a coastal wetland in the Great Barrier Reef catchment: influence of climate variability and land clearing since European arrival. Environmental Chemistry 7, 190-206.

Duane Nellis, M., Harrington Jr, J.A., Wu, J. 1998. Remote sensing of temporal and spatial variations in pool size, suspended sediment, turbidity, and Secchi depth in Tuttle Creek Reservoir, Kansas: 1993. Geomorphology 21, 281-293.

Duckworth, H.W., Kirchman, D.L. 1983. Bacterial dynamics and distribution during a spring diatom bloom in the Hudson River plume, USA. Journal of Plankton Research 5, 333-355.

Dunne, T. 1979. Sediment yield and land use in tropical catchments. Journal of Hydrology 42, 218-300.

Dunne, T., Leopold, L.B. 1978. Water in Environmental Planning. W.H. Freeman and Co., San Francisco, CA., 818pp.

Erftermeijer, P.L.A., Lewis, R.R. 2006. Environmental impacts of dredging on seagrass: A review. Marine Pollution Bulletin 52, 1553-1572.

Erftermeijer, P.L.A., Riegl, B., Hoeksema, B.W., Todd, P.A. 2012. Environmental impacts of dredging and other sediment disturbances on corals: A review. Marine Pollution Bulletin 64, 1737-1765.

Fabricius, K.E. 2005. Effects of terrestrial runoff on the ecology of corals and coral reefs: review and synthesis. Marine Pollution Bulletin 50, 125-146.

Fabricius, K.E, Wolanski, E. 2000. Rapid smothering of coral reef organisms by muddy marine snow Estuarine, Coastal and Shelf Science 50, 115–120.

Fabricius, K., De'ath, G. 2001. Biodiversity on the Great Barrier Reef: Large-scale patterns and turbidity related local loss of soft coral taxa. In E. Wolanski (Ed) Oceanographic processes of coral reefs. CRC Press, Boca Raton, 127-143.

Fabricius, K.E., Wild, C., Wolanksi, E., Abele, D. 2003. Effects of transparent exopolymer particles and muddy terrigenous sediments on the survival of hard coral recruits. Estuarine, Coastal and Shelf Sciences 57, 613-621.

Fabricius, K., De'ath, G., McCook, L., Turak, E., Williams D. 2005. Changes in algal, coral and fish assemblages along water quality gradients on the inshore Great Barrier Reef. Marine Pollution Bulletin 51, 384-398.

Fabricius, K.E., Okaji, K., De'ath, G. 2010. Three lines of evidence to link outbreaks of the crown-of thorns seastar Acanthaster planci to the release of larval food limitation. Coral Reefs 29, 593-605.

Fabricius, K., Humphrey, C., De'ath, G., Schaffelke, B. 2011. Environmental drivers of changes in water clarity in the inshore Great Barrier Reef: Final Report. Australian Institute of Marine Science and Marine and Tropical Sciences Research Facility, Cairns. 32 pp.

Fabricius, K.E., De'ath, G., Humphrey, C., Zagorskis, I., Schaffelke, B. 2013. Inter-annual variation in turbidity in response to terrestrial runoff on near-shore coral reefs of the Great Barrier Reef. Estuarine, Coastal and Shelf Science 116, 57-65.

Fabricius, K.E., Logan, M., Weeks, S., Brodie, J. 2014. The effects of river run-off on water clarity across the central Great Barrier Reef. Marine Pollution Bulletin 84, 191-200.

Faithful, J.W., Griffiths, D.J. 2000. Turbid flow through a tropical reservoir (Lake Dalrymple, Queensland, Australia): responses to a summer storm event. Lakes and reservoirs: Research and management 5, 231-247.

Fielding, C.R., Alexander, J. 1996. Sedimentology of the Upper Burdekin River of North Queensland, Australia – an example of a tropical, variable discharge river. Terra Nova 8, 447-457.

Fleming, P.M., Loofs, M. 1991. Flood generation and transmission in the Burdekin and Haughton Rivers, North Queensland, CSIRO Technical Memorandum 91/15, Division of Water Resources, Canberra.

Flores, F., Hoogenboom, M.O., Smith, L.D., Cooper, T.F., Abrego, D., Negri, A. 2012. Chronic exposure of corals to fine sediments: lethal and sub-lethal impacts. PloS ONE 7, e37795.

Fox, J.M., Hill, P.S., Milligan, T.G., Boldrin, A. 2004. Flocculation and sedimentation on the Po River Delta. Marine Geology 203, 95-107.

Fu, B., Newham, L.T.H., Field, J.B., Vigiak, O. 2013. A weight-of-evidence approach to integrate suspended sediment source information. Journal of Environmental Management 128, 182-191.

Furnas, M. 2003. Catchments and corals: Terrestrial runoff to the Great Barrier Reef. Australian Institute of Marine Science, Townsville. 334 pp.

Furnas, M.J., Mitchell, A.W., Skuza, M., Brodie, J. 2005. In the other 90%: Phytoplankton responses to enhanced nutrient availability in the Great Barrier Reef lagoon. Marine Pollution Bulletin 51, 253-256.

Furnas, M., Alongi, D., McKinnon, D., Trott, L., Skuza, M. 2011. Regional-scale nitrogen and phosphorus budgets for the northern (14ºS) and central (17ºS) Great Barrier Reef shelf ecosystem. Continental Shelf Research 31, 1967-1990.

Gibbs, R.J. 1977. Clay mineral segregation in the marine environment. Journal of Sedimentary Petrology 47, 237-243.

Gibbs, R.J., Konwar, L. 1986. Coagulation and settling of Amazon River suspended sediment. Continental Shelf Research 6, 127-149.

Gingele, F., De Deckker, P. 2004. Fingerprinting Australia's rivers with clay mineralogy and the application for the marine record of climate change. Australian Journal of Earth Sciences 51, 339-348.

Gingele, F., De Deckker, P. 2005. Clay mineral, geochemical and Sr-Nd isotopic fingerprinting of sediments in the Murray–Darling fluvial system, southeast Australia. Australian Journal of Earth Sciences 52, 965-974.

Godiva, D., Evangelista., H., Kampel, M., Vinicius Licinio, M., Munita, C. 2010. Combined use of aerogammaspectrometry and geochemistry to access sediment sources in a shallow coral site at Armação dos Búzios, Brazil. Estuarine, Coastal and Shelf Science 87, 526-534.

Golbuu, Y., van Woesik, R., Richmond, R., Harrison, P., Fabricius, K. 2011. River discharge reduces reef coral diversity in Palau. Marine Pollution Bulletin 62, 824-831.

Gray, J.R., Glysson, G.D., Turcios, L.M., Schwarz, G.E. 2000. Comparability of suspended-sediment concentration and total suspended solids data. U.S. Geological Survey, Water-Resources Investigations Report 00-4191, Reston, Virginia, 14pp.

Great Barrier Reef Marine Park Authority. 2011. Impacts of tropical cyclone Yasi on the Great Barrier Reef: a report on the findings of a rapid ecological impact assessment, July 2011, GBRMPA, Townsville. pp. 26

Griffiths, D.J., Faithful, J.W. 1996. Effects of the sediment load of a tropical North-Australian river on water column characteristics in the receiving impoundment. Arch. Hydrobiol. Suppl. 113 Large Rivers 10 (1-4), 147-157.

Guyot, J.L., Jouanneau, J.M., Soares, L., Boaventura, G.R., Maillet, N., Lagane, C. 2007. Clay mineral composition of river sediments in the Amazon Basin. Catena 71, 340-356.

Haapkyla, J., Unsworth, R., Flavell, M., Bourne, D.G., Schaffelke, B., Willis, B.L. 2011. Seasonal rainfall and runoff promote coral disease on an inshore reef, PLoS ONE 6, e16893.

Ha Dang, T., Coynel, A., Orange, D., Blanc, G., Etcheber, H., Anh Le, L. 2010. Long-term monitoring (1960–2008) of the river-sediment transport in the Red River watershed (Vietnam): Temporal variability and dam-reservoir impact. Science of the Total Environment 408, 4654-4664.

Hill, P.S., Milligan, T.G., Geyer, W.R. 2000. Controls on effective settling velocity of suspended sediment in the Eel River flood plume. Continental Shelf Research 20, 2095-2111.

Hillier, S. 1995. Erosion, sedimentation and sedimentary origin of clays. In B. Velde (Ed) Origin and mineralogy of clays: Clays and the environment. Springer, Berlin Heidelberg, 162-219.

Hillier, S. 2003. Quantitative analysis of clay and other minerals in sandstones by X-ray powder diffraction (XRPD). Int. Assoc. Sedimentol. Spec. Publ. 34, 213-251.

Hosomi, M., Sudo, R. 1986. Simultaneous determination of total nitrogen and total phosphorus in freshwater samples using persulfate digestion. International Journal of Environmental Studies 27, 267-275.

Hughes, A.O., Olley, J.M., Croke, J.C., McKergow, L.A. 2009. Sediment source changes over the last 250 years in a dry-tropical catchment, central Queensland. Geomorphology 104(3-4), 262-75.

Hughes, T.P., Bellwood, D.R., Baird, A.H., Brodie, J., Bruno, J.F., Pandolfi, J. M. 2011. Shifting base-lines, declining coral cover, and the erosion of reef resilience: comment on Sweatman et al. 2011. Coral Reefs 30, 653-660.

Humphrey, C., Weber, M., Lott, C., Cooper, T., Fabricius, K. 2008. Effects of suspended sediments, dissolved inorganic nutrients and salinity on fertilisation and embryo development in the coral Acropora millepora (Ehrenberg, 1834). Coral Reefs 27, 837-850.

John, C.M., Adatte, T., Mutti, M. 2006. Regional trends in clay mineral fluxes to the Queensland margin and ties to middle Miocene global cooling. Palaeogeography, Palaeoclimatology, Palaeoecology 233, 204-224.

Jones, A.M., Berkelmans, R. 2014. Flood impacts in Keppel Bay, southern Great Barrier Reef in the aftermath of cyclonic rainfall. PloS ONE 9(1), e84739.

Jones, I., Verdel, C. 2015. Basalt distribution and volume estimates of Cenozoic volcanism in the Bowen Basin region of eastern Australia: Implications for a waning mantle plume, Australian Journal of Earth Sciences 62 (2), 255-263.

Jonkers, L., Prins, M.A., Brummer, G.A., Konert, M., Lougheed, B.C. 2009. Experimental insights into laser diffraction particle sizing of fine-grained sediment for use in palaeoceanography. Sedimentology 56, 2192-2206.

King, B., McAllister, F., Wolanski, E., Done, T., Spagnol, S. 2001. River plume dynamics in the central Great Barrier Reef. In E. Wolanski (Ed) Oceanographic processes of coral reefs. CRC Press, Boca Raton, 145-160.

Koiter, A.J., Owens, P.N., Petticrew, E.L., Lobb, D.A. 2013. The behavioural characteristics of sediment properties and their implications for sediment fingerprinting as an approach for identifying sediment sources in river basins, Earth-Science Reviews 125, 24-42.

Kroon, F., Kuhnert, K., Henderson, B., Wilkinson, S., Kinsey-Henderson, A., Brodie, J., Turner, R. 2012. River loads of suspended solids, nitrogen, phosphorus and herbicides delivered to the Great Barrier Reef lagoon. Marine Pollution Bulletin 65, 167-181.

Kroon, F., Schaffelke, B., Bartley, R. 2014. Informing policy to protect coastal coral reefs: Insight from a global review of reducing agricultural pollution to coastal ecosystems. Marine Pollution Bulletin 85, 167-181.

Kuhnert, P., Henderson, B., Lewis, S., Bainbridge, Z., Wilkinson, S., Brodie, J. 2012. Quantifying total suspended sediment export from the Burdekin River catchment using the loads regression estimator tool. Water Resources Research 48, W04533.

Laceby, J.P., Olley, J., Pietsch, T.J., Sheldon, F., Bunn, S.E. 2014. Identifying subsoil sediment sources with carbon and nitrogen stable isotope ratios. Hydrological Processes, DOI: 10.1002/hyp.10311.

Lambeck, A., Woolfe, K.J. 2000. Composition and textural variability along the 10 m isobath, Great Barrier Reef: evidence for pervasive northward sediment transport. Australian Journal of Earth Sciences 47, 327-335.

Lambrechts, J., Humphrey, C., McKinna, L., Gourge, O., Fabricius, K., Mehta, A., Lewis, S., Wolanski, E. 2010. The importance of wave-induced bed fluidisation in the fine sediment budget of Cleveland Bay, Great Barrier Reef. Estuarine, Coastal and Shelf Science 89, 154-162.

Laraque, A., Bernal, C., Bourrel, L., Darrozes, J., Christophoul, F., Armijos, E., Fraizy, P., Pombosa, R., Guyot, J.L. 2009. Sediment budget of the Napa River, Amazon basin, Ecuador and Peru. Hydrological Processes 23, 3509-3524.

Larcombe, P., Ridd, P.V., Prytz, A., Wilson, B. 1995. Factors controlling suspended sediment on inner-shelf coral reefs, Townsville, Australia. Coral Reefs 14, 163-171.

Leeder, M.R. 1982. Sedimentology; process and product. Chapman and Hall, London. 344pp.

Lewis, S., Brodie, J., Ledee, E., Alewijnse, M. 2006. The spatial extent of delivery of terrestrial materials from the Burdekin Region in the Great Barrier Reef lagoon. Technical Report 06'02 to North Queensland Dry Tropics, TropWATER, JCU, Townsville, 102pp.

Lewis, S.E., Bainbridge, Z.T., Brodie J.E. 2007. A review of load tools available for calculating pollutant exports to the Great Barrier Reef lagoon: A case study of varying catchment areas. In Oxley, L. and Kulasiri, D. (eds) MODSIM 2007. International Congress on Modelling and Simulation. Modelling and Simulation Society of Australia and New Zealand, December 2007, pp. 2396-2402. ISBN : 978-0-9758400-4-7. www.mssanz.org.au/MODSIM07/MODSIM07.htm

Lewis, S., Bainbridge, Z., Kuhnert, P., Sherman, B., Henderson, B., Dougall, C., Cooper, M., Brodie, J. 2013. Calculating sediment trapping efficiencies for reservoirs in tropical settings: A case study from the Burdekin Falls Dam, NE Australia. Water Resources Research 49, 1017-1029.

Lewis, S., Olley, J., Furuichi, T., Sharma, A., Burton, J. 2014. Complex sediment deposition history on a wide continental shelf: Implications for the calculation of accumulation rates on the Great Barrier Reef. Earth and Planetary Science Letters 393, 146-158.

Limmer, D.R., Köhler, C.M., Hillier, S., Moreton, S.G., Tabrez, A.R., Clift, P. 2012. Chemical weathering and provenance evolution of Holocene-Recent sediments from the Western Indus Shelf, Northern Arabian Sea inferred from physical and mineralogical properties. Marine Geology 326-328, 101-115.

Lohrenz, S.E., Fahnenstiel, G.L., Redalje, D.G., Lang, G.A., Dagg, M.J., Whitledge, T.E., Dortch, Q. 1999. Nutrients, irradiance, and mixing as factors regulating primary production in coastal waters impacted by the Mississippi River plume. Continental Shelf Research 19, 1113-1141.

Lotze, H.K., Lenihan, H.S., Bourque, B.J., Bradbury, R.H., Cooke, R.G., Kay, M.C., Kidwell, S.M., Kirby, M.X., Peterson, C.H., Jackson, J.B.C. 2006. Depletion degradation and recovery potential of estuaries and coastal seas. Science 312, 1806-1809.

Lough, J. 2001. Climate variability and change on the Great Barrier Reef. In E. Wolanski (Ed) Oceanographic processes of coral reefs. CRC Press, Boca Raton, 269-300.

Lough, J.M. 2007. Tropical river flow and rainfall reconstructions from coral luminescence: Great Barrier Reef, Australia. Paleoceanography 22, PA2218.

Lough, J.M. 2011. Great Barrier Reef coral luminescence reveals rainfall variability over northeastern Australia since the 17th century. Paleoceanography 26, PA2201.

Lough, J.M., Lewis, S.E., Cantin, N.E. In press. Freshwater impacts in the central Great Barrier Reef: 1648-2011. Coral Reefs, doi:10.1007/s00338-015-1297-8.

Mackenzie, N., Jacquier, D., Isbell, R., Brown, K. 2004. Australian soils and landscapes. CSIRO, Collingwood, Vic. 416pp.

Maher, B.A., Watkins, S.J., Brunskill, G., Alexander, J., Fielding, C.R. 2009. Sediment provenance in a tropical fluvial and marine context by magnetic 'fingerprinting' of transportable sand fractions. Sedimentology 56, 841-861.

Malone, E.J., Jensen, A.R., Gregory, C.M, Forbes, V.R. 1966. Geology of the southern half of the Bowen 1:250,000 sheet area, Queensland. Report No. 100. Bureau of mineral resources, geology and geophysics. Australian Government Publishing Service, Canberra.

Malvern Instruments Ltd. 2007. Mastersizer 2000 User Manual, England.

Mayer, L.M., Keil, R.G. Macko, S.A., Joye, S.B., Ruttenberg, K.C., Aller, R.C. 1998. Importance of suspended particulates in riverine delivery of bioavailable nitrogen to coastal zones. Global Biogeochemical Cycles 12, 573-579.

McCulloch, M., Fallon, S., Wyndham, T., Hendy, E., Lough, J., Barnes, D. 2003a. Coral record of increased sediment flux to the inner Great Barrier Reef since European settlement. Nature 421, 727-730.

McCulloch, M., Pailles, C., Moody, P., Martin, C.E. 2003b. Tracing the source of sediment and phosphorus into the Great Barrier Reef lagoon. Earth and Planetary Science Letters 210, 249-258.

McKenzie, L., Unsworth, R. 2011. Surving the flood; How long can seagrass "hold it's breath"? In McKenzie, L.J., Yoshida, R.L., Unsworth, R. (Eds) 2011. Seagrass-Watch News. Issue 43, April 2011. Seagrass-Watch HQ. 28pp.

McKergow, L.A., Prosser, I.P., Hughes, A.O., Brodie, J. 2005. Sources of sediment to the Great Barrier Reef World Heritage Area, Marine Pollution Bulletin 51, 200-211.

Milligan, T.G., Hill, P.S., Law, B.A. 2007. Flocculation and the loss of sediment from the Po River plume, Continental Shelf Research 27, 309-321.

Mitchell, A.W., Furnas, M.J. 1996. Terrestrial inputs of nutrients and suspended sediments to the GBR lagoon, In The Great Barrier Reef: Science, Use and Management – A National Conference, Proceedings, Vol. 1, November 1996, pp. 59–71. James Cook University, Townsville.

Moore, D.M., Reynolds, R.C.Jr. 1997. X-ray Diffraction and the Identification and Analysis of Clay Minerals (2nd edn). Oxford University Press, New York, 378pp.

Nagle, G.N., Fahey, T.J., Lassoie, J.P. 1999. Management of sedimentation in tropical watersheds. Environmental Management 23, 441-452.

Nyssen, J., Clymans, W., Poesen, J., Vandecasteele, I., De Baets, S., Haregeweyn, N., Naudts, J., Hadera, A., Moeyersons, J., Haile, M., Deckers, J. 2009. How soil conservation affects the catchment sediment budget- a comprehensive study in north Ethiopian highlands. Earth Surface Processes and Landforms 34, 1216-1233.

Olley, J., Brooks, A., Spencer, J., Pietsch, T., Borombovits, D. 2013. Subsoil erosion dominates the supply of fine sediment to rivers draining into Princess Charlotte Bay, Australia. Journal of Environmental Radioactivity 124, 121-129.

Orpin, A.R., Ridd, P.V. 2012. Exposure of inshore corals to suspended sediments due to wave-resuspension and river plumes in the central Great Barrier Reef: A reappraisal. Continental Shelf Research 47, 55-67.

Orpin, A.R., Ridd, P.V., Stewart, L.K. 1999. Assessment of the relative importance of major sediment-transport mechanisms in the central Great Barrier Reef lagoon. Australian Journal of Earth Sciences 46, 883-896.

Orpin, A.R., Brunskill, G.J., Zagorskis, I., Woolfe, K.J. 2004. Patterns of mixed siliciclastic-carbonate sedimentation adjacent to a large dry-tropics river on the central Great Barrier Reef shelf, Australia. Australian Journal of Earth Sciences 51, 665-683.

Packett, R., Dougall, C., Rohde, K., Noble, R. 2009. Agricultural lands are hot-spots for annual runoff polluting the southern Great Barrier Reef lagoon. Marine Pollution Bulletin 58, 976-986.

Panda, D.K., Kumar, A., Mohanty, S. 2011. Recent trends in sediment load of the tropical (Peninsular) river basins of India. Global and Planetary Change 75, 108-118.

Passow, U., Shipe, R.F., Murray, A., Pak, D.K., Brzezinski, M.A., Alldredge, A.L. 2001. The origin of transparent exopolymer particles (TEP) and their role in the sedimentation of particulate matter. Continental Shelf Research 21, 327-346.

Peel, M.C., Finlayson, B.L., McMahon, T.A. 2007. Updated world map of the Köppen-Geiger climate classification. Hydrology and Earth System Sciences 11, 1633-1644.

Perez, K. III., Rodgers, K.S., Jokiel, P.L., Lager, C.V., Lager, D.J. 2014. Effects of terrigenous sediment on settlement and survival of the reef coral *Pocillopora damicornis*. PeerJ 2, e387.

Perry, C.T., Smithers, S.G., Gulliver, P., Browne, N.K. 2012. Evidence of very rapid reef accretion and reef growth under high turbidity and terrigenous sedimentation. Geology 40, 719-722.

Petheram, C., McMahon, T.A., Peel, M.C. 2008. Flow characteristics of rivers in northern Australia: Implications for development. Journal of Hydrology 357, 93-111.

Petus, C., Collier, C., Devlin, M., Rasheed, M., McKenna, S. 2014. Using MODIS data for understanding changes in seagrass meadow health: A case study in the Great Barrier Reef (Australia). Marine Environmental Research 98, 68-85.

Philipp, E., Fabricius, F. 2003. Photophysiological stress in scleractinian corals in response to short-term sedimentation. Journal of Experimental Marine Biology and Ecology 287, 57-78.

Pollock, F.J., Lamb, J.B., Field, S.N., Heron, S.F., Schaffelke, B., Shedrawi, G., Bourne, D.G., Willis, B.L. 2014. Sediment and turbidity associated with offshore dredging increase coral disease prevalence on nearby reefs. PLOS ONE 9 (7), e102498.

Preen, A.R., Long, W.J.L., Coles, R.G., 1995. Flood and cyclone related loss, and partial recovery, of more than 1000 km^2 of seagrass in Hervey Bay, Queensland, Australia. Aquat. Bot. 52, 3–17.

Prosser, I., Young, B., Rustomji, P., Moran, C. Hughes, A. 2001. Constructing river basin sediment budgets for the national land and water resources audit. Tech. Report 15/01, CSIRO Land and Water, Canberra, 34pp.

Rabalais, N.N., Turner, R.E., Dortch, Q., Wiseman Jr., W.J., Sen Gupta, B.K. 1996. Nutrient changes in the Mississippi River and system responses on the adjacent continental shelf. Estuaries 19, 386-407.

Radke, L.C., Ford, P.W., Webster, I.T., Atkinson, I., Douglas, G., Oubelkheir, K., Li, J., Robson, B., Brooke, B. 2010. Biogeochemical zones within a macrotidal, dry-tropical fluvial-marine transition area: A dry-season perspective. Aquatic Geochemistry 16, 1-29.

Reef Rescue 2008. Australian Government's Caring for our Country Initiative – Reef Rescue. (Available at: www.nrm.gov.au/about/key-investments/reef-rescue.html, accessed 20 Sept. 2012).

Restrepo, J.D., Kjerfve, B. 2000. Magdalena river: interannual variability (1975–1995) and revised water discharge and sediment load estimates. Journal of Hydrology 235, 137-149.

Restrepo, J.D., Zapata, P., Diaz, J.M., Garzón-Ferreira, J., Garcia, C.B. 2006. Fluvial fluxes into the Caribbean Sea and their impact on coastal ecosystems: The Magdalena River, Colombia. Global and Planetary Change 50, 33-49.

Rijsdijk, A. 2005. Evaluating sediment sources and delivery in a tropical volcanic watershed. Sediment Budgets 2, Proceedings of symposium SI held during the 7th IAHS Scientific Assembly at Foz do Iguacu, Brazil, IAHS Publ. 292.

Risk, M.J. 2014. Assessing the effects of sediments and nutrients on coral reefs. Current Opinion in Environmental Sustainability 7, 108-117.

Robertson, A.I., Daniel, P.A., Dixon, P., Alongi, D.M. 1993. Pelagic biological processes along a salinity gradient in the Fly delta and adjacent river plume (Papua New Guinea). Continental Shelf Research 13, 205-224.

Rodriguez-Ramirez, A., Grove, C.A., Zinke, J., Pandolfi, J.M., Zhao, J-X. 2014. Coral luminescence identifies the Pacific decadal oscillation as a primary driver of river runoff variability impacting the southern Great Barrier Reef. PLoS ONE 9(1), e84305.

Roff, G., Clark, T.R., Reymond, C.E., Zhao, J., Feng, Y., McCook, L.J., Done, T.J., Pandolfi, J.M. 2013. Palaeoecological evidence of a historical collapse of corals at Pelorus Island, inshore Great Barrier Reef, following European settlement. Proc. R. Soc. B 280, 20122100.

Rogers, C.S. 1990. Responses of coral reefs and reef organisms to sedimentation. Marine Ecological Progress Series 62, 185-202.

Roth, C.H., Lawson, G., Cavanagh, D. 2002. Overview of key natural resource management issues in the Burdekin catchment, with particular reference to water quality and salinity. Report commissioned by Dept. Natural Resources and Mines on behalf of the Burdekin Dry Tropics Board. CSIRO Land and Water, Townsville. 99pp.

Rustomji, P., Bennett, N., Chiew, F. 2009. Flood variability east of Australia's Great Dividing Range. Journal of Hydrology 374, 196-208.

Rustomji, P., Shellberg, J., Brooks, A., Spencer, J., Caitcheon, G. 2010. A catchment sediment and nutrient budget for the Mitchell River, Queensland. A report to the Tropical Rivers and Coastal Knowledge (TRaCK) Research Program. CSIRO Water for a Healthy Country National Research Flagship. 119pp.

Schroeder, T., Devlin, M.J., Brando, V.E., Dekker, A.G., Brodie, J.E., Clementson, L.A., McKinna, L. 2012. Inter-annual variability of wet season freshwater plume extent into the Great Barrier Reef lagoon based on satellite coastal ocean colour observations. Marine Pollution Bulletin 65, 210-223.

Seitzinger, S.P., Mayorga, E., Bouwman, A.F., Kroeze, C., Beusen, A.H.W., Billen, G., Van Drecht, G., Dumont, E., Fekete, B.M., Garnier, J., Harrison, J.A. 2010. Global river nutrient export: A scenario analysis of past and future trends. Global Biogeochemical Cycles 24, GB0A08.

Sionneau, T., Bout-Roumazeilles, V., Biscaye, P.E., Van Vliet-Lanoe, B., Bory, A. 2008. Clay mineral distributions in and around the Mississippi River watershed and Northern Gulf of Mexico: sources and transport patterns. Quaternary Science Reviews 27, 1740-1751.

Slaymaker, O. 2003. The sediment budget as conceptual framework for management tool. Hydrobiologia 494, 71-82.

Smith, J., Douglas, G.B., Radke, L.C., Palmer, M., Brooke, B.P. 2008. Fitzroy River Basin, Queensland, Australia. III. Identification of sediment sources in the coastal zone. Environmental Chemistry 5, 231-242.

Sperazza, M., Moore, J.N., Hendrix, M.S. 2004. High-resolution particle size analysis of naturally occurring very fine-grained sediment through laser diffractometry. Journal of Sedimentary Research 74, 736-743.

Storlazzi, C.D., Field, M.E., Bothner, M.H., Presto, M.K., Draut, A.E. 2009. Sedimentation processes in a coral reef embayment; Hanalei Bay, Kauai. Marine Geology 264, 140-151.

Sweatman, H., Delean, S., Syms, C. 2011. Assessing loss of coral cover on Australia's Great Barrier Reef over two decades, with implications for longer-term trends. Coral Reefs 30, 521-531.

Sweatman, H., Syms, C. 2011. Assessing loss of coral cover on the Great Barrier Reef: A response to Hughes et al. (2011). Coral Reefs 30, 661-664.

Syvitski, J.P. 2003. Supply and flux of sediment along hydrological pathways: research for the 21st century. Global and Planetary Change 39, 1-11.

Takesue, R.K., Bothner, M.H., Reynolds, R.L. 2009. Sources of land-derived runoff to a coral reef-fringed embayment identified using geochemical tracers in nearshore sediment traps. Estuarine, Coastal and Shelf Science 85, 459-471.

Thompson, A., Costello, P., Davidson, J., Schaffelke, B., Uthicke, S., Liddy, M. 2013. Reef Rescue Marine Monitoring Program. Report of AIMS Activities–Inshore coral reef monitoring 2012. Report for Great Barrier Reef Marine Park Authority. Australian Institute of Marine Science, Townsville, 120 pp.

Thompson, A., Schroeder, T., Brando, V.E., Schaffelke, B. 2014. Coral community responses to declining water quality: Whitsunday Islands, Great Barrier Reef, Australia. Coral Reefs 33, 923–938.

Thorburn, P.J., Wilkinson, S.N., Silburn, D.M. 2013. Water quality in agricultural lands draining to the Great Barrier Reef: A review of causes, management and priorities. Agriculture, Ecosystems & Environment 180, 4-20.

Tooth, S. 2000. Process, form and change in dryland rivers: a review of recent research. Earth-Science Reviews 51, 67-107.

Turner, R.E., Rabalais, N.N., Nan, Z.Z. 1990. Phytoplankton biomass, production and growth limitations on the Huanghe (Yellow River) continental shelf. Continental Shelf Research 10, 545-571.

Verbist, B., Poesen, J., van Noordwijk, M., Widianto., Suprayogo, D., Agus, F., Deckers, J. 2010. Factors affecting soil loss at plot scale and sediment yield at catchment scale in a tropical volcanic agroforestry landscape. Catena 80, 34-46.

Viscarra Rossel, R. 2011. Fine-resolution multiscale mapping of clay minerals in Australian soils measured with near infrared spectra. Journal of Geophysical Research 116, F04023.

Walling, D.E. 2006. Human impact on land-ocean sediment transfer by the world's rivers. Geomorphology 79, 192-216.

Walling, D.E., Collins, A.L. 2008. The catchment sediment budget as a management tool. Environmental Science and Policy 11, 136-143.

Walling, D.E., Wilkinson, S.N., Horowitz, A.J. 2011. Catchment Erosion, Sediment Delivery, and Sediment Quality. In P. Wilderer (Ed) Treatise on Water Science (vol. 2). Academic Press, Oxford, 305-338.

Wasson, R, J., Caitcheon, G., Murray, A.S., McCulloch, M., Quade, J. 2002. Sourcing sediment using multiple tracers in the catchment of Lake Argyle, Northwestern Australia. Environmental Management 29, 634-646.

Waycott, M., Duarte, C., Carruthers, T., Orth, R., Dennison, W., Olyarnik, S., Calladine, A., Fourquean, J., Heck, K., Hughes, A., Kendrick, G., Kenworthy, W., Short, T., Williams, S. 2009. Accelerating loss of seagrasses across the globe threatens coastal ecosystems. PNAS 106 (30), 12377-12381.

Weber, M., Lott, C., Fabricius, K.E. 2006. Sedimentation stress in a scleractinian coral exposed to terrestrial and marine sediments with contrasting physical, organic and geochemical properties. Journal of Experimental Marine Biology and Ecology 336, 18-32.

Weber, M., de Beer, D., Lott, C., Polerecky, L., Kohls, K. Abed, R.M., Ferdelman, T.G., Fabricius, K.E. 2012. Mechanisms of damage to corals exposed to sedimentation. PNAS 109, 1558-1567.

Webster, I.T., Ford, P.W. 2010. Delivery, deposition and redistribution of fine sediments within macrotidal Fitzroy Estuary/Keppel Bay: Southern Great Barrier Reef, Australia. Continental Shelf Research 30, 793-805.

Wenger, A.S., McCormick, M.I. 2013. Determining trigger values of suspended sediment for behavioral changes in a coral reef fish. Marine Pollution Bulletin 70, 73-80.

Wenger, A.S., Johansen, J.L., Jones, G.P. 2012. Increasing suspended sediment reduces foraging, growth and condition of a planktivorous damselfish. Journal of Experimental Marine Biology and Ecology 428, 43-48.

Wilkinson, S.N., Hancock, G.J., Bartley, R., Hawdon, A.A., Keen, R.J. 2013. Using sediment tracing to assess processes and spatial patterns of erosion in grazed rangelands, Burdekin River basin, Australia. Agriculture, Ecosystems and Environment 180, 90-102.

Wilkinson, S.N., Dougall, C., Kinsey-Henderson, A.E., Searle, R.D., Ellis, R.J., Bartley, R. 2014. Development of a time-stepping sediment budget model for assessing land use impacts in large river basins. Science of the Total Environment 468-469, 1210-1224.

Whitehead, P.W., Stephenson, P.J. 1998. Lave rise ridges of the Toomba basalt flow, north Queensland, Australia. Journal of Geophysical Research 103(27), 371-382.

Wolanski, E., Jones, M. 1981. Physical properties of Great Barrier Reef lagoon waters near Townsville. I. Effects of Burdekin River floods. Marine and Freshwater Research 32, 505-19.

Wolanski, E., van Senden, D. 1983. Mixing of Burdekin River flood waters in the Great Barrier Reef. Marine and Freshwater Research 34, 49-63.

Wolanski, E., Fabricius, K., Spagnol, S., Brinkman, R. 2005. Fine sediment budget on an inner-shelf coral-fringed island, Great Barrier Reef of Australia. Estuarine, Coastal Shelf Science 65, 153-158.

Wolanski, E., Fabricius, K., Cooper, T., Humphrey, C. 2008. Wet season fine sediment dynamics on the inner shelf of the Great Barrier Reef. Estuarine, Coastal and Shelf Science 77, 755-762.

Appendix A:

Supplementary Figures and Tables

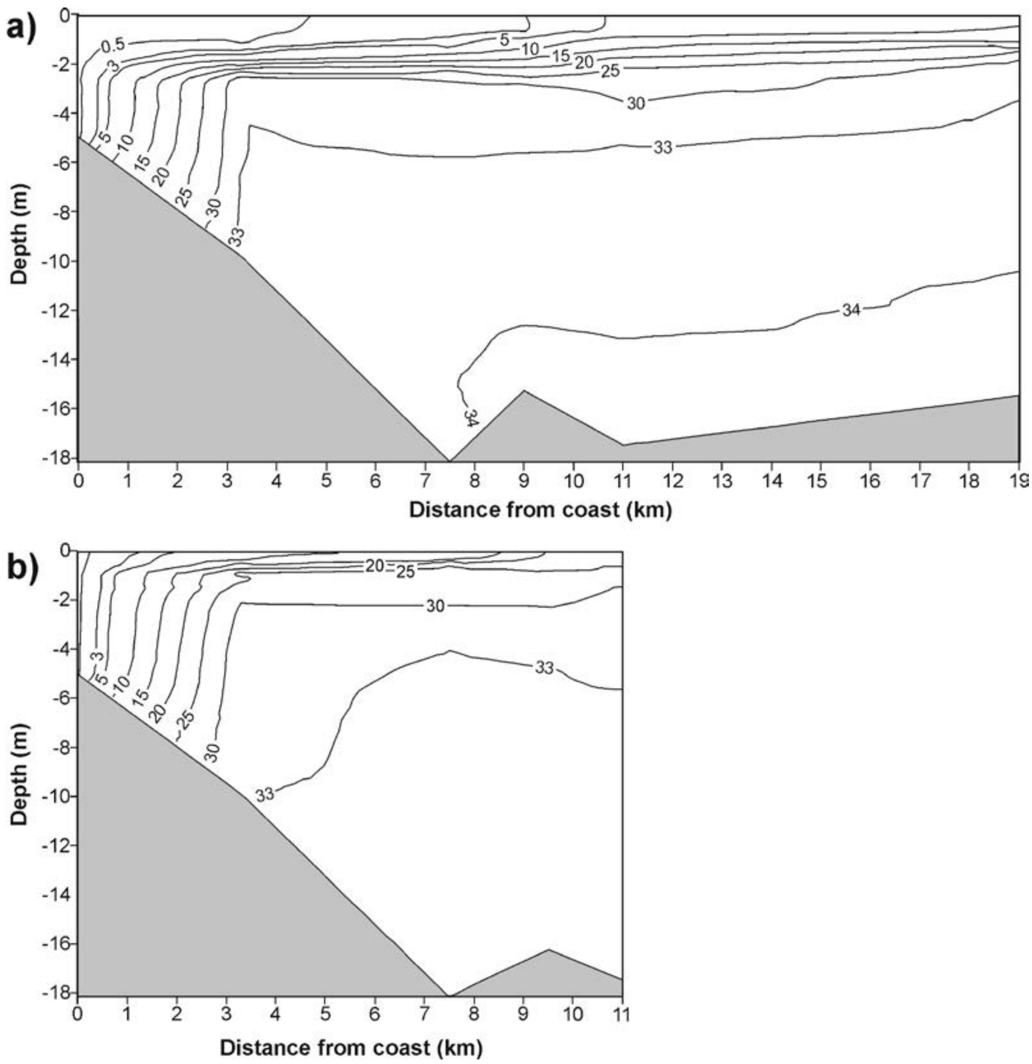

Figure A2.1 Salinity contour maps of the Burdekin River plume produced from Sea-Bird depth profiling conducted along Plume Transects (a) 1 (30/12/10) and (b) 3 (18/01/11).

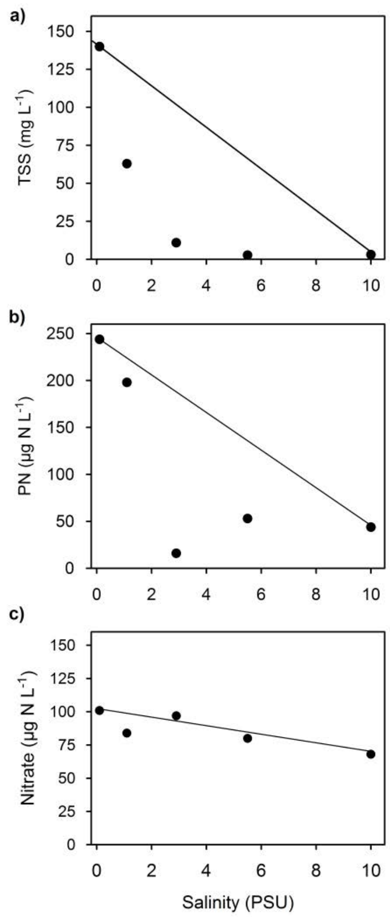

Figure A2.2 Relationship of (a) TSS, (b) particulate nitrogen and (c) nitrate concentrations with salinity for Plume Transect 1 (30/12/10) following peak discharge conditions. Straight lines have been drawn from the first to the last point to show the relationship for conservative mixing behaviour.

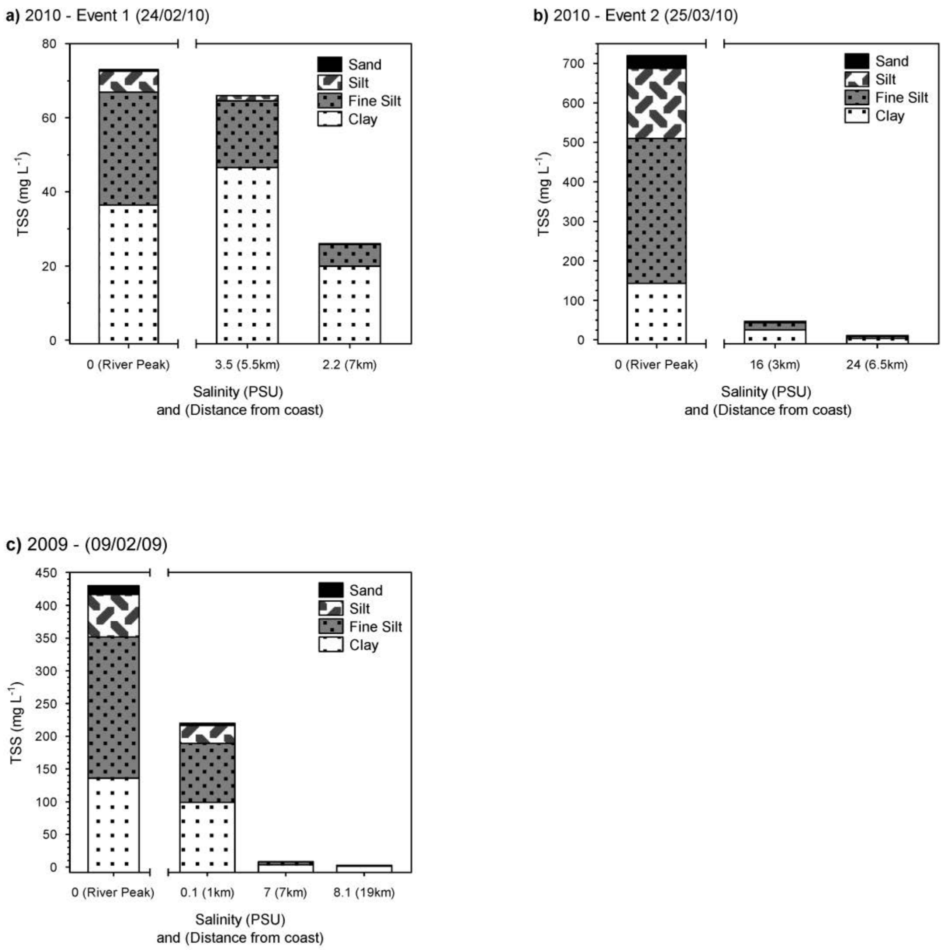

Figure A2.3 TSS concentrations and sediment particle size composition for the Burdekin River at Inkerman and adjacent plume samples along the salinity gradient collected during the peak of major discharge events that occurred in the 2008/2009 and 2009/2010 wet seasons. Data were collected (a) on the 24/02/10 (1 day after flood peak); (b) during a second 2010 flood peak (with a different catchment source) on the 23/03/10 (river sample collected day of peak) and 25/03/10 (plume transect data); and (c) on the 07/02/09 (river sample collected day of peak) and 09/02/09 (plume transect data) during the 4th largest discharge event on record at the Burdekin Rive Clare gauging station. Particle size classes represent clay, fine silt, coarse silt and sand size fractions.

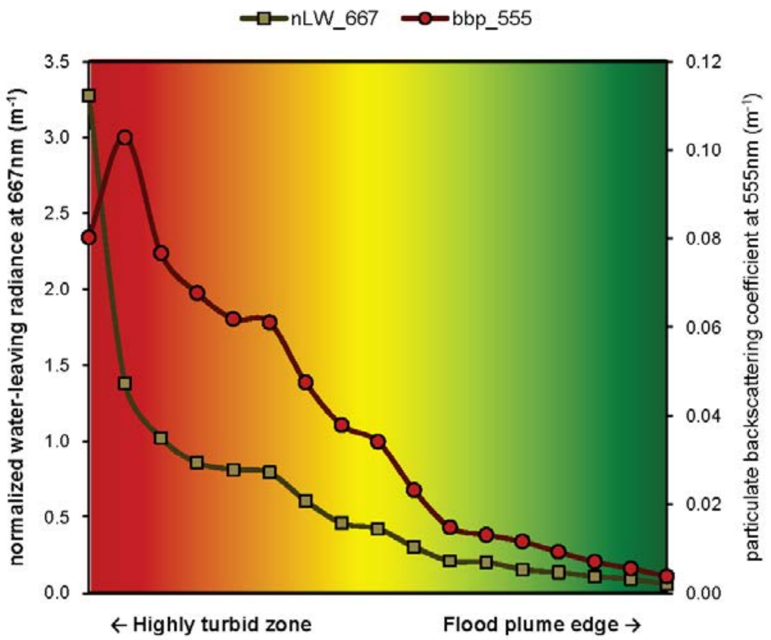

Figure A2.4 Variation in two MODIS-L2 variables within a river plume (4/01/11) along the colour gradient (from red to green) as depicted in the classified true-colour images presented in Fig. 2.3d. This exemplifies how the two proxies for TSS/turbidity (i.e., normalized water-leaving radiance at 667 nm (nLW_667) and particulate backscattering coefficient at 555 nm(bbp_555)) vary along the observable colour gradient, as further described by Devlin et al. (2012).

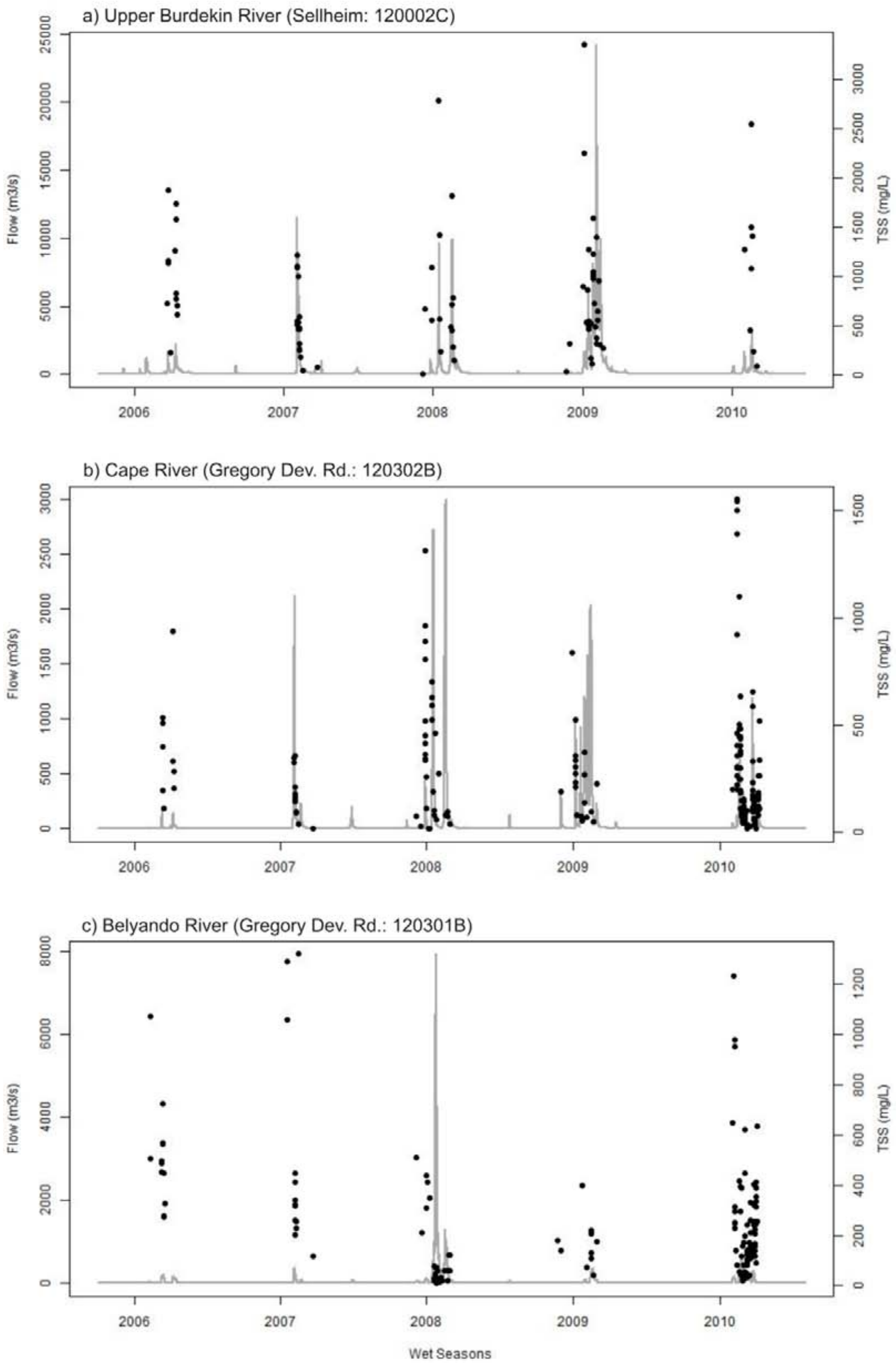

Figure A3.1a-c Time-series plots showing flow hydrographs (grey line) and TSS concentrations in mg L^{-1} (black circles) for each of the seven gauged sites over the five monitored wet seasons (2005–2010).

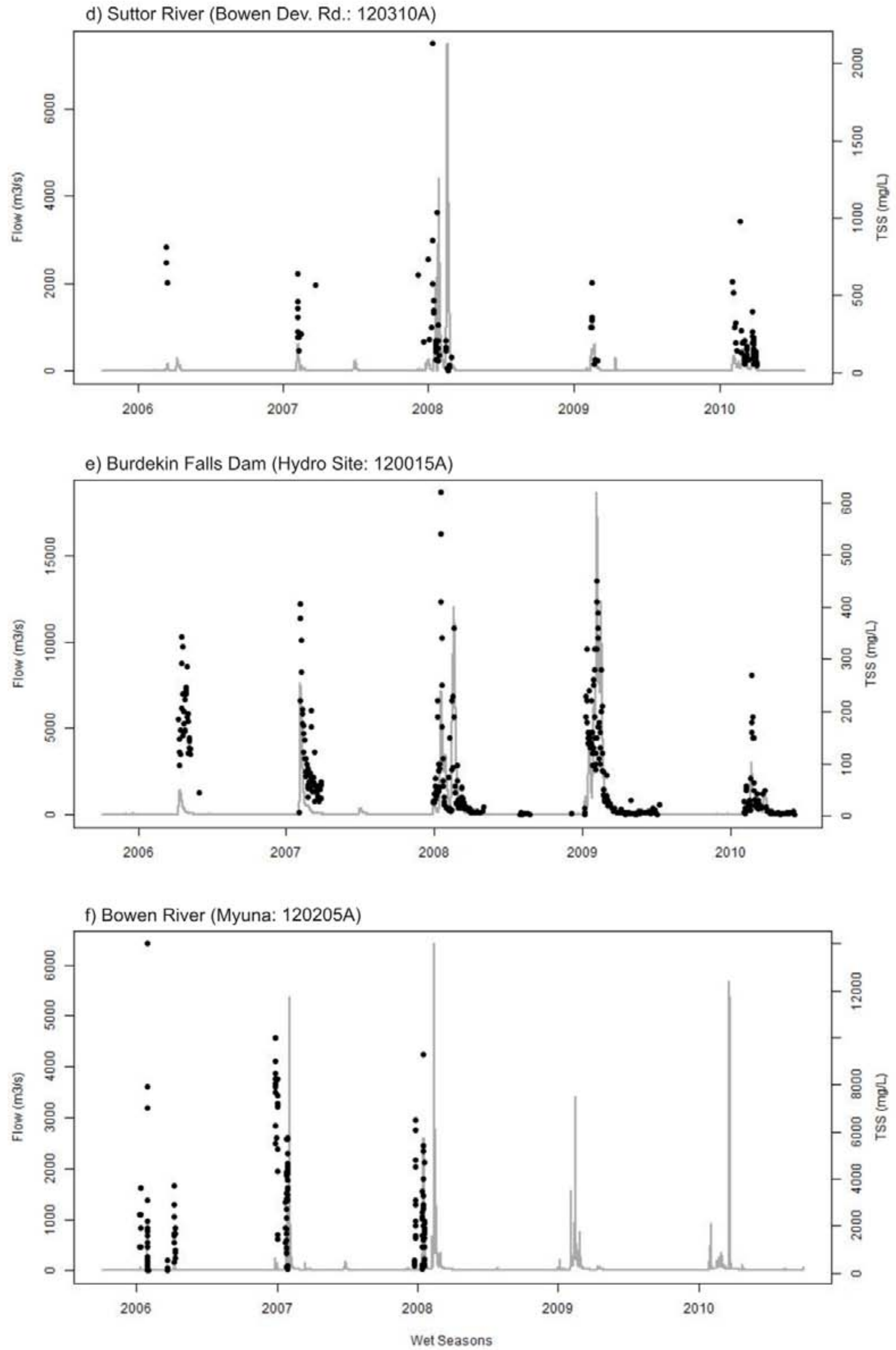

Figure A3.1d-f Time-series plots showing flow hydrographs (grey line) and TSS concentrations in mg L^{-1} (black circles) for each of the seven gauged sites over the five monitored wet seasons (2005–2010).

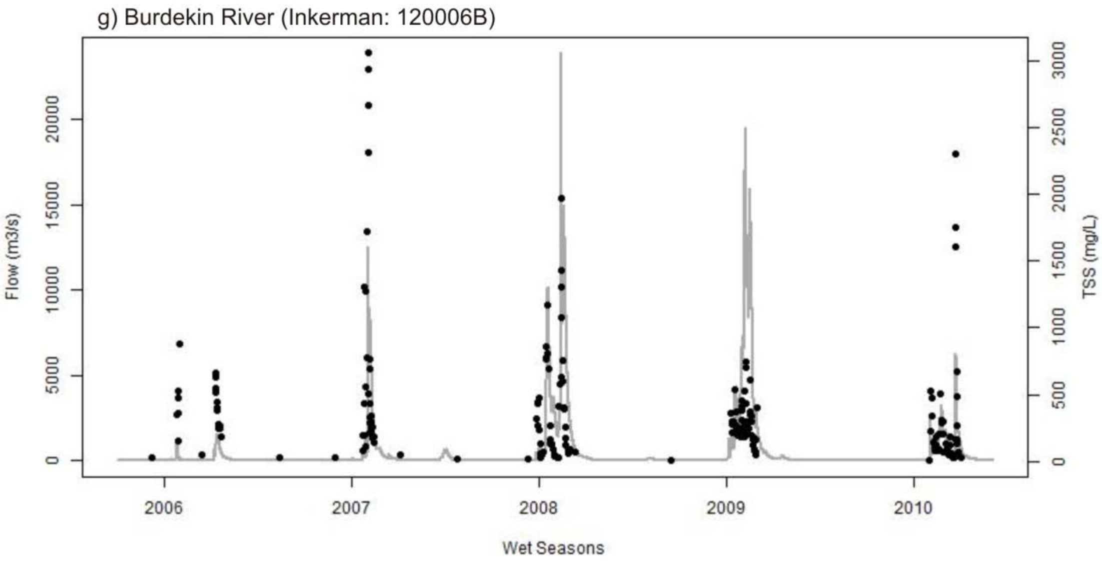

Figure A3.1g Time-series plots showing flow hydrographs (grey line) and TSS concentrations in mg L^{-1} (black circles) for each of the seven gauged sites over the five monitored wet seasons (2005–2010).

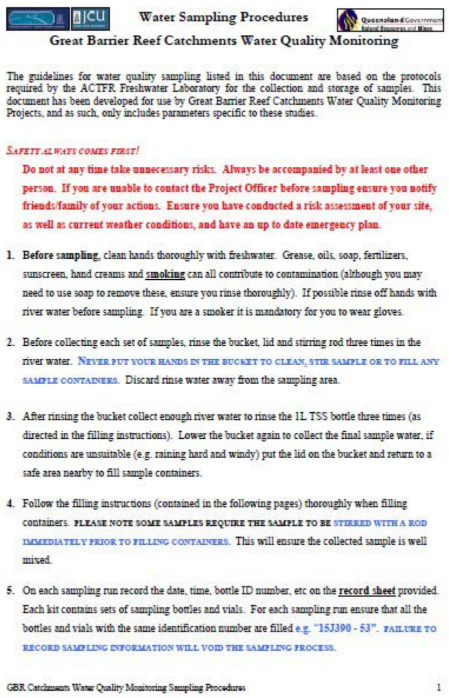

Water Sampling Procedures

Great Barrier Reef Catchments Water Quality Monitoring

The guidelines for water quality sampling listed in this document are based on the protocols required by the ACTFR Freshwater Laboratory for the collection and storage of samples. This document has been developed for use by Great Barrier Reef Catchments Water Quality Monitoring Projects, and as such, only includes parameters specific to these studies.

SAFETY ALWAYS COMES FIRST!

Do not at any time take unnecessary risks. Always be accompanied by at least one other person. If you are unable to contact the Project Officer before sampling ensure you notify friends/family of your actions. Ensure you have conducted a risk assessment of your site, as well as current weather conditions, and have an up to date emergency plan.

1. **Before sampling**, clean hands thoroughly with freshwater. Grease, oils, soap, fertilizers, sunscreen, hand creams and **smoking** can all contribute to contamination (although you may need to use soap to remove these, ensure you rinse thoroughly). If possible rinse off hands with river water before sampling. If you are a smoker it is mandatory for you to wear gloves.
2. Before collecting each set of samples, rinse the bucket, lid and stirring rod three times in the river water. NEVER PUT YOUR HANDS IN THE BUCKET TO CLEAN, STIR SAMPLE OR TO FILL ANY SAMPLE CONTAINERS. Discard rinse water away from the sampling area.
3. After rinsing the bucket collect enough river water to rinse the 1L TSS bottle three times (as directed in the filling instructions). Lower the bucket again to collect the final sample water, if conditions are unsuitable (e.g. raining hard and windy) put the lid on the bucket and return to a safe area nearby to fill sample containers.
4. Follow the filling instructions (contained in the following pages) thoroughly when filling containers. PLEASE NOTE SOME SAMPLES REQUIRE THE SAMPLE TO BE STIRRED WITH A ROD IMMEDIATELY PRIOR TO FILLING CONTAINERS. This will ensure the collected sample is well mixed.
5. On each sampling run record the date, time, bottle ID number, etc on the **record sheet** provided. Each kit contains sets of sampling bottles and vials. For each sampling run ensure that all the bottles and vials with the same identification number are filled e.g. "15J390 - 53". FAILURE TO RECORD SAMPLING INFORMATION WILL VOID THE SAMPLING PROCESS.

GBR Catchments Water Quality Monitoring Sampling Procedures 1

Figure A3.2a Volunteer water sampling procedures for GBR catchment events-based water quality monitoring developed by the candidate for the volunteer sampling component in conjunction with the Queensland Government community waterways program for other GBR catchments.

6. PLEASE ENSURE THE SAMPLES ARE STORED AS SOON AS POSSIBLE IN THE FRIDGE OR FREEZER (as specified in filling instructions), until collection by the Project Officer.

7. Note any significant change of conditions in the comments section of the record sheet (e.g. change from turbid to clear water, obvious differences in flow from the edge compared to the middle, rainfall – if available, etc). Draw a mud map of your site in the space provided on the back of the record sheet.

8. If possible, please take a few photos at each sampling run. Record the photo location (eg: upstream, downstream) on the record sheet next to the time of sampling.

9. **After sampling**, rinse bucket, lid and rod with tap water and allow to dry.
   Storing syringe
   - Pull syringe apart and rinse thoroughly in tap water. Be careful not to touch inside the vessel or the end of the plunger.
   - Place on tissue or paper towel to dry. Note it is still important to rinse the syringe with river water as instructed before sampling again.
   - When sampling a new event, start a new syringe.

10. Contact Project Officer after collecting samples or if you have any questions **at any time** during the event. Samples will be picked up as soon as possible.

✓ **Check off sheet**

- ❑ **Notify Project Officer and family/friends of actions**
- ❑ **Assess safety risks (e.g. current weather conditions, access to site, etc)**
- ❑ **Wash hands**
- ❑ **Rinse bucket, lid and rod**
- ❑ **Fill bottles and vials according to instructions**
- ❑ **Fill in record sheet**
- ❑ **Store samples in fridge/freezer according to instructions**
- ❑ **Rinse bucket and syringe, and store in safe (uncontaminated) location to dry**
- ❑ **Contact Project Officer for collection of samples**

GBR Catchments Water Quality Monitoring Sampling Procedures 2

1. One 1L Plastic bottle - Total Suspended Solids (TSS) and Conductivity (salts) — FRIDGE

- RINSE bottle out three (3) times with water to be sampled (shake with lid on).
- Discard rinse water away from sampling area.
- **Stir sample** (when not using the rod, place it on the lid of bucket to keep clean).
- Fill to overflowing and seal. Do not leave an air gap.
- **Place bottle in fridge** (preferably dark location) until collection, OR in an esky on ice until collected by project officer.
- DO NOT freeze bottle.

Sample can be stored safely in dark refrigerated conditions for up to 2 weeks.

Please note
- **To minimise contamination please keep fingers away from all tops and lids.**
- **Never place caps facing edge down when they are removed from the bottle/vial**

Do not dip container into sample water.

Pour water into container, avoid touching lips of bucket and container.

2. One 1L Brown glass bottle – Pesticides — FRIDGE

- **Stir sample**
- DO NOT RINSE bottles.
- Fill to the neck of the bottle leaving an air gap.
- **Place samples in fridge** (preferably dark location) until collection, OR in an esky on ice until collected by project officer.
- DO NOT freeze bottle.

* If you are running out of room in your fridge, preferably store pesticides before the TSS bottles

GBR Catchments Water Quality Monitoring Sampling Procedures 3

3. One 60mL Plastic vial – Total Nitrogen and Total Phosphorus (TNTP) — FREEZE

- **Stir sample**
- DO NOT RINSE vial.
- Fill vial to the black line with sample water
  - DO NOT OVERFILL vial, there must be an air gap to prevent vial splitting when frozen.
- Return vial to clip seal bag

Freeze the sample as soon as possible, but if not possible store in the dark, on ice as quickly as you can (e.g. in a refrigerator or in an esky on ice) until collected by the project officer.

4. One 20mL glass vial – Total Organic Carbon (TOC) — FRIDGE

- Carefully uncover the alfoil under lid.
- DO NOT touch the inside of the alfoil.
- DO NOT rinse the vessel.
- Fill to overflowing and re-place the alfoil seal back on the bottle with the same side facing down.
- Hands are contaminated with organic material, therefore be extremely careful when replacing alfoil cover and lid.

Place samples in fridge (preferably dark location) until collection, OR in an esky on ice until collected by project officer.

GBR Catchments Water Quality Monitoring Sampling Procedures 4

5. Six 10mL Plastic vials with yellow caps – Dissolved Nutrients — FREEZE

Dissolved Inorganic Nitrogen (DIN's – Nitrate & Nitrite)
Ammonia (NH_3)
Filterable Reactive Phosphorus (FRP) ~ PO_4 (Phosphate)
Total Dissolved Nitrogen/Total Dissolved Phosphorus (TDN/TDP)

- DO NOT RINSE vials.
- Samples must be FILTERED.
- Sample water does not need to be stirred. If extreme difficulty is experienced when filtering, allow the sample to settle for 15min.
- Firstly, rinse out syringe three (3) times with the water to be sampled.
- Discard rinse water away from sampling area.
- Fill the syringe with sample water.
- Attach orange filter to the tip of the syringe.
- Flush out filter with ~2mL of sample to prime the filter paper.
- DO NOT collect this rinse water in the vials.
- Now, using the primed syringe and filter collect the filtered sample in the plastic vials **to the line** (10mL).
- DO NOT OVERFILL vials, there must be an air gap to prevent vial splitting when frozen.
- Filters may be re-used for the same set of vials, but they must be detached from the syringe before re-filling. However, use a new filter for each new set of vials (i.e. next sample run). If waters are turbid it may require a few filters to provide enough sample water for each vial.
- Return vials to clip seal bag.

Freeze the samples as soon as possible, but if not possible store in the dark, on ice as quickly as you can (e.g. in a refrigerator or in an esky on ice) until collected by the project officer.

Do not touch the inlet/outlet of filter.

Attach filter to syringe from packet to avoid contamination through touching.

Do not touch top of vials.

Correct way to hold vial and syringe, avoiding touching lids, top of vials and filter. Place lid face up on a clear surface nearby if easier for filtering.

GBR Catchments Water Quality Monitoring Sampling Procedures 5

Figure A3.2b Volunteer water sampling procedures for GBR catchment events-based water quality monitoring developed by the candidate for the volunteer sampling component in conjunction with the Queensland Government community waterways program for other GBR catchments.

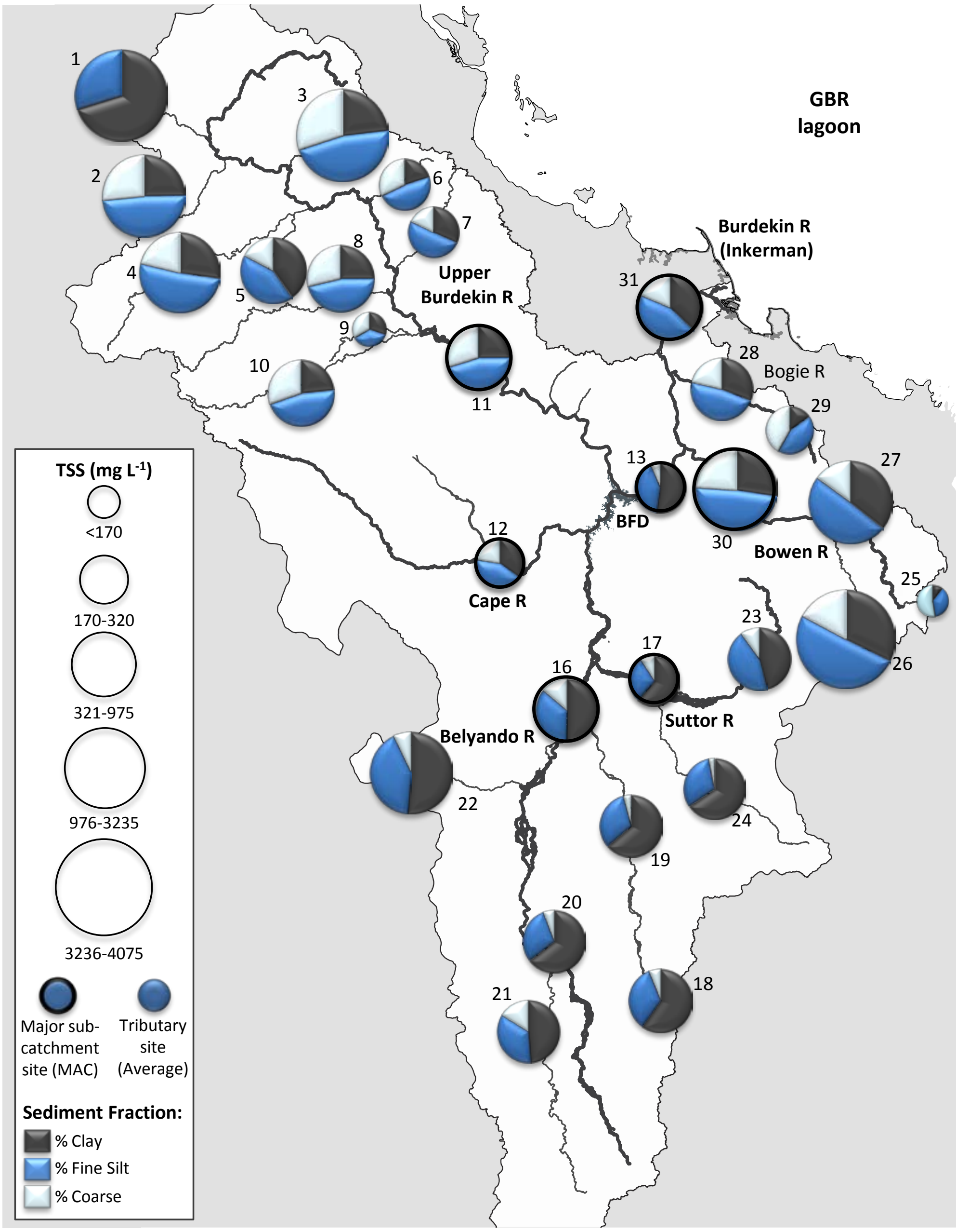

Figure A4.1 Proportion of clay, fine silt and coarse sediment contributed by each sub-catchment tributary site (see Table A3.1 for site names). Circle size represents mean TSS concentration (mg L^{-1}) over the study period. Major sub-catchment, reservoir and end-of-river sites are also included (represented by bold circle).

Table A3.1 Ungauged minor tributary sample site details and data collection summary. See Figure 1.1 for site locations.

Burdekin sub-catchment	Minor tributary sample site	Location		Upstream area (km^2)	# water years	Water years sampled	# TSS samples	Average TSS ($mg\ L^{-1}$)
		Lat	Long					
Upper Burdekin	(1) Dry River	-18.79	144.85	680	2	2003/04; 2006/07	6	3395
Upper Burdekin	(2) Grey Ck	-19.01	145.04	1,005	2	2006/07 - 2007/08	10	2465
Upper Burdekin	(3) Camel Ck	-18.84	145.47	260	2	2005/06 - 2006/07	8	4075
Upper Burdekin	(4) Clarke R	-19.22	145.43	6,425	3	2006/07 - 2008/09	37	1230
Upper Burdekin	(5) Maryvale Ck	-19.43	145.31	900	2	2006/07; 2008/09	7	910
Upper Burdekin	(6) Running R	-19.13	145.83	680	6	2005/06 - 2010/11	28	235
Upper Burdekin	(7) Star R	-19.44	145.97	1,690	6	2005/06 - 2010/11	36	210
Upper Burdekin	(8) Basalt R	-19.62	145.8	2,050	5	2004/05; 2006/07; 2008/09 - 2010/11	27	620
Upper Burdekin	(9) Fletcher Ck	-19.8	145.86	885	7	2004/05 - 2010/11	41	130
Upper Burdekin	(10) Lolworth Ck	-19.87	145.85	2,295	5	2004/05 - 2008/09	28	445
	(14) Kirk River	-20	146.75	210	6	2005/06 - 2010/11	32	170
	(15) Elphinstone Ck	-20.14	146.86	50	5	2005/06 - 2006/07; 2008/09 - 2010/11	16	1405
Belyando	(18) Upper Mistake Ck	-23.08	147.17	75	6	2005/06 - 2010/11	41	370
Belyando	(19) Mistake Ck	-21.81	146.88	8,770	2	2005/06 - 2006/07	10	555
Belyando	(20) Upper Belyando R	-22.89	146.57	11,260	4	2005/06 - 2007/08; 2009/10 - 2010/11	7	925
Belyando	(21) Native Companion Ck	-22.93	146.6	5,445	5	2005/06 - 2007/08; 2009/10 - 2010/11	16	450
Belyando	(22) Carmichael R	-22.09	146.26	2,280	1	2006/07	11	1100
Suttor	(23) Upper Suttor R	-21.6	147.6	2,100	6	2002/03 - 2004/05; 2006/07 - 2008/09	38	850
Suttor	(24) Logan Ck	-21.87	147.26	3,325	1	2006/07	5	350
Lower Burdekin	(25) Upper Broken R	-21.17	148.5	35	2	2006/07; 2010/11	5	115
Lower Burdekin	(26) Little Bowen R	-20.82	148.08	1,490	3	2006/07 - 2008/09	17	3270
Lower Burdekin	(27) Bowen R (Dartmoor)	-20.73	148.02	3,890	3	2006/07 - 2008/09	14	1055
Lower Burdekin	(28) Upper Bogie R	-20.29	147.91	255	3	2005/06 - 2007/08	9	305
Lower Burdekin	(29) Bogie R	-20.05	147.32	1,740	4	2005/06 - 2008/09	24	510

Table A3.2 Percent deviance explained by a simple rating curve relationship versus the LRE model for each of the seven gauged sites. Terms included in the final model are indicated by a ✓ in the table. Only those terms that contributed significantly to increasing the deviance explained were included in the final model. See Kuhnert et al. (2012) for graphical illustration of these terms fitted to the Burdekin River (Inkerman) site data.

Site	% Deviance Explained		Terms Included in Final LRE Model				
	Rating Curve (Linear flow term)	**LRE Model**	**Linear term**	**Quadratic term**	**Seasonal**	**Rising-Falling Limb**	**Discount terms**
Upper Burdekin (Sellheim)	30%	77%	✓	✓	✓		✓
Cape	12%	82%	✓		✓		✓
Belyando	22%	68%	✓	✓	✓		✓
Suttor	8%	79%	✓	✓	✓		✓
BFD	39%	76%	✓		✓	✓	✓
Bowen	3%	57%	✓	✓	✓	✓	✓
Burdekin R. (Inkerman)	23%	71%	✓	✓	✓	✓	✓

Appendix B:

Bartley et al. 2014 (Supporting publication)

Science of the Total Environment 468-469 (2014) 1138–1153

Contents lists available at ScienceDirect

Science of the Total Environment

journal homepage: www.elsevier.com/locate/scitotenv

Review

Relating sediment impacts on coral reefs to watershed sources, processes and management: A review

Rebecca Bartley [a,*], Zoe T. Bainbridge [b], Stephen E. Lewis [b], Frederieke J. Kroon [c], Scott N. Wilkinson [d], Jon E. Brodie [b], D. Mark Silburn [e]

[a] CSIRO Land and Water, PO Box 2583, Brisbane, Australia
[b] Catchment to Reef Research Group, TropWATER, James Cook University, Townsville, Queensland 4811, Australia
[c] CSIRO Ecosystem Sciences, PO Box 780, Atherton, Qld 4883, Australia
[d] CSIRO Land and Water, GPO Box 1666, Canberra, ACT 2601, Australia
[e] Department of Natural Resources and Mines, PO Box 318, Toowoomba 4350, Australia

HIGHLIGHTS

- This paper reviews the impact of sediment delivery to coral reefs.
- The sources, processes and management options of excess sediment are discussed.
- The synthesis is based primarily on *measured* data sets.
- The approaches and outcomes are relevant to coral reefs around the world.

ARTICLE INFO

Article history:
Received 18 March 2013
Received in revised form 6 August 2013
Accepted 9 September 2013
Available online xxxx

Editor: Christian EW Steinberg

Keywords:
Burdekin
Great Barrier Reef
Land management
Soil erosion
Water quality

ABSTRACT

Modification of terrestrial sediment fluxes can result in increased sedimentation and turbidity in receiving waters, with detrimental impacts on coral reef ecosystems. Preventing anthropogenic sediment reaching coral reefs requires a better understanding of the specific characteristics, sources and processes generating the anthropogenic sediment, so that effective watershed management strategies can be implemented. Here, we review and synthesise research on measured runoff, sediment erosion and sediment delivery from watersheds to near-shore marine areas, with a strong focus on the Burdekin watershed in the Great Barrier Reef region, Australia. We first investigate the characteristics of sediment that pose the greatest risk to coral reef ecosystems. Next we track this sediment back from the marine system into the watershed to determine the storage zones, source areas and processes responsible for sediment generation and run-off.

The review determined that only a small proportion of the sediment that has been eroded from the watershed makes it to the mid and outer reefs. The sediment transported >1 km offshore is generally the clay to fine silt (<4–16 μm) fraction, yet there is considerable potential for other terrestrially derived sediment fractions (<63 μm) to be stored in the near-shore zone and remobilised during wind and tide driven re-suspension. The specific source of the fine clay sediments is still under investigation; however, the Bowen, Upper Burdekin and Lower Burdekin sub-watersheds appear to be the dominant source of the clay and fine silt fractions. Sub-surface erosion is the dominant process responsible for the fine sediment exported from these watersheds in recent times, although further work on the particle size of this material is required. Maintaining average minimum ground cover >75% will likely be required to reduce runoff and prevent sub-soil erosion; however, it is not known whether ground cover management alone will reduce sediment supply to ecologically acceptable levels.

This publication has been removed due to copyright restrictions

http://dx.doi.org/10.1016/j.scitotenv.2013.09.030

Appendix C:

Brodie et al. 2012 (Supporting publication)

Marine Pollution Bulletin 65 (2012) 267–279

Contents lists available at SciVerse ScienceDirect

Marine Pollution Bulletin

journal homepage: www.elsevier.com/locate/marpolbul

An assessment of residence times of land-sourced contaminants in the Great Barrier Reef lagoon and the implications for management and reef recovery

Jon Brodie [a,*], Eric Wolanski [a,b], Stephen Lewis [a], Zoe Bainbridge [a]

[a] *Catchment to Reef Research Group, Australian Centre for Tropical Freshwater Research, James Cook University, Townsville, Queensland 4811, Australia*
[b] *Australian Institute of Marine Science, PMB No. 3, Townsville, Queensland 43810, Australia*

ARTICLE INFO

Keywords:
Watershed
River catchments
Sediment
Nutrient
Pesticides
Trapping
Flushing
Reef degradation
Reef recovery
Climate change

ABSTRACT

We argue that the residence times of key pollutants exported to the Great Barrier Reef (GBR) are greater in the GBR lagoon than those of the water itself, in contradiction to some previous assumptions. Adverse effects of the pollutant discharge will be greater and longer lasting than previously considered, in turn requiring stronger or more urgent action to remediate land practices. Residence times of fine sediments, nitrogen and phosphorus, pesticides and trace metals are suggested to be from years to decades in the GBR lagoon and highly likely to be greater than the residence time of water, estimated at around 15–365 days. The recovery of corals and seagrass in the central region of the GBR following current land-use remediation in the catchment depends on the residence time of these contaminants. Ecohydrological modeling suggests that this recovery may take decades even with adequate levels of improved land management practices.

Appendix D:

Lewis et al. 2013 (Supporting publication)

WATER RESOURCES RESEARCH, VOL. 49, 1017–1029, doi:10.1002/wrcr.20117, 2013

Calculating sediment trapping efficiencies for reservoirs in tropical settings: A case study from the Burdekin Falls Dam, NE Australia

Stephen E. Lewis,[1] Zoë T. Bainbridge,[1] Petra M. Kuhnert,[2] Bradford S. Sherman,[3] Brent Henderson,[4] Cameron Dougall,[5] Michelle Cooper,[6] and Jon E. Brodie[1]

Received 9 September 2012; revised 19 December 2012; accepted 21 January 2013; published 25 February 2013.

[1] The Brune and Churchill curves have long been used to predict sediment trapping efficiencies for reservoirs in the USA which typically experience winter and spring-dominant runoff. Their suitability for reservoirs receiving highly variable summer-dominant inflows has not previously been evaluated. This study compares sediment trapping efficiency (TE) data with the predictions of the two established curves for the Burdekin Falls Dam, a large reservoir in northern tropical Australia which receives highly variable summer-dominant runoff. The measured TE of the reservoir ranged between 50% and 85% and was considerably less than estimates using the Brune and Churchill curves over the 5 year study period. We modified the original equations so that daily trapping can be calculated and weighted based on daily flow volumes. This modification better accounts for shorter residence times experienced by such systems characterized by relatively high intraannual flow variability. The modification to the Churchill equation reasonably predicted sediment TEs for the Burdekin Dam for four of the five monitored years and over the whole monitoring period. We identified four key sediment particle classes: (1) <0.5 μm which exclusively passes over the dam spillway; (2) 0.5–5.0 μm which, on average, 50% is trapped in the reservoir; (3) 5.0–30 μm most (75%) of which is trapped; and (4) >30 μm which is almost totally (95%) trapped in the dam reservoir. We show that the modification to the Churchill equation has broader application to predict reservoir TE provided that daily flow data are available.

Citation: Lewis, S. E., Z. T. Bainbridge, P. M. Kuhnert, B. S. Sherman, B. Henderson, C. Dougall, M. Cooper, and J. E. Brodie (2013), Calculating sediment trapping efficiencies for reservoirs in tropical settings: A case study from the Burdekin Falls Dam, NE Australia, *Water Resour. Res.*, *49*, doi:10.1002/wrcr.20117.

1. Introduction

[2] The anthropogenic disturbance of the water cycle through reservoir construction, agriculture, deforestation, and urbanization has caused considerable changes in the fluxes of freshwater, sediment, and nutrients to the ocean [see *Vörösmarty and Sahagian*, 2000; *Syvitski et al*., 2005; *Horowitz et al*., 2008]. These changes have many geomorphological and ecological consequences for downstream environments. Increasing sediment and nutrient loads have been linked to, for example, decline in coral cover and seagrass abundance [e.g., *Fabricius*, 2005; *Restrepo et al*., 2006], while reductions in sediment and nutrient loads have caused coastal erosion and the collapse of inshore fisheries [reviewed in *Syvitski*, 2003; *Syvitski et al*., 2005]. Models have predicted that 3 – 5 Gt of sediment is trapped by reservoirs annually compared to a total global sediment flux of 20 Gt per year [*Syvitski*, 2003; *Vörösmarty et al*., 2003; *Syvitski et al*., 2005]. It is evident that large increases or reductions in sediment and associated nutrient loads disturb the dynamic balance of coastlines and delicate ecosystems.

[3] Accurate quantification of sediment trapping in reservoirs improves the estimates of river sediment export, allows the useful life of reservoirs to be determined, and provides insights into sediment transport and dynamics of watersheds. However, several of the empirical equations to estimate reservoir trapping efficiency (TE) [e.g., *Brown*, 1943; *Churchill*, 1948; *Brune*, 1953; *Chen*, 1975] have been developed in temperate environments for normally ponded reservoirs and their use in subtropical and tropical climatic regimes is questionable. In particular, differences in the timing (i.e., implications for the stratification of reservoir) and variability of

All Supporting Information may be found in the online version of this article.

[1]Catchment to Reef Research Group, TropWATER, James Cook University, Townsville, Queensland, Australia.
[2]CSIRO Mathematics, Informatics and Statistics, Glen Osmond, South Australia, Australia.
[3]CSIRO Land and Water, Canberra, ACT, Australia.
[4]CSIRO Mathematics, Informatics and Statistics, Canberra, ACT, Australia.
[5]Department of Natural Resources and Mines, Bundaberg, Queensland, Australia.
[6]Minerals and Natural Hazards Division, Geoscience Australia, Canberra, ACT, Australia.

Corresponding author: S. E. Lewis, Catchment to Reef Research Group, TropWATER, James Cook University, ATSIP Bldg. DB145, Townsville, Queensland 4811, Australia. (stephen.lewis@jcu.edu.au)

0043-1397/13/10.1002/wrcr.20117

inflows and fluctuating water levels throughout the year in these tropical systems considerably influence the residence time of such reservoirs which cannot be accounted by the empirical equations in their current form. Therefore, a new approach is required to provide relatively fast and accurate estimates of sediment TE for the large number of reservoirs situated in tropical settings.

[4] The Burdekin Falls Dam (BFD) is located in the Dry Tropics of north-east Australia and receives highly variable interannual and intraannual inflows which are concentrated in the wet season months (December to April). Estimates of the TE of the BFD vary greatly with the common empirical equations [e.g., *Brune*, 1953; *Heinemann*, 1981] suggesting that 80–90% of incoming sediment is trapped [*Prosser et al*., 2002; *McKergow et al*., 2005] while field studies suggest that negligible sediment (but not quantified) is retained in the reservoir [*Faithful and Griffiths*, 2000]. The BFD regulates 88% of the Burdekin River watershed which, in turn, is the largest contributor of suspended sediment to the Great Barrier Reef (GBR) [*Kroon et al*., 2012]. Thus, accurate quantification of the sediment TE of the BFD is important to prioritize remedial works to reduce sediment delivery from the Burdekin River. Moreover, the latest modeling framework for the GBR watershed (Source Catchments) has increased temporal resolution to a daily time step [*Carroll et al*., 2012] and so there is a need for a simple model to reliably predict daily reservoir TEs.

[5] The key objective of this research is to evaluate whether the *Brune* [1953], *Churchill* [1948], or *Chen* [1975] methods can reliably estimate sediment trapping for the BFD reservoir over five monitored water years. We quantify the proportion of sediment loads and particle size fractions delivered from the four upstream watersheds and examine the implications for management of "bulk sediment" versus "size-specific" fractions as a result of our findings. We explore potential modifications that can be made to the *Brune* and *Churchill* equations to improve reservoir trapping predictions for the BFD. Finally, we examine whether these modifications can be applied to other reservoirs where adequate data are available.

2. Empirical Trapping Efficiency Equations

[6] TE estimators calculate the percentage of the inflowing sediment mass that remains permanently in the reservoir. Several methods for calculating TE exist in the literature [*Borland*, 1971; *Heinemann*, 1984; *Chen*, 1975; *Verstraeten and Poesen*, 2000; *Espinosa-Villegas and Schnoor*, 2009]. Historically, the two most common approaches are (1) the relationship developed by *Brune* [1953] and (2) the sedimentation index curve of *Churchill* [1948]. The *Brune* [1953] curve, which equates "capacity to inflow ratio", requires little input data, is simple to apply, and has been widely adopted to estimate reservoir TE. In contrast, the *Churchill* [1948] curve incorporates both water retention period (hereafter referred to as residence time) and flow velocity to calculate a "sedimentation index" for the reservoir. The *Churchill* [1948] index produces two curves that describe TEs for "locally derived" sediment upstream of the reservoir and for "overflow sediments" that have passed through other upstream reservoirs. The data sets used to formulate both the *Brune* [1953] and *Churchill* [1948] curves are based on measured TEs from "normally ponded" reservoirs. These reservoirs are located in temperate climatic regimes that receive more regular inflows throughout the year (i.e., snowmelt influence) compared to tropical and subtropical rivers such as those of the GBR watershed which are characterized by highly variable seasonal flows. Importantly, these empirical equations specify the use of "average annual inflow" and do not account for watersheds with highly variable intraannual inflows. A seemingly more comprehensive technique for calculating reservoir TE was developed by *Chen* [1975]. This technique incorporates flow velocity and particle size data using *Camp*'s [1946] settling velocity equations to predict TE for each particle size class.

[7] In this study, we examine three commonly used methods for calculating TE statistics, the *Brune* [1953], *Churchill* [1948], and *Chen* [1975] methods (hereafter referred to as Brune, Churchill, and Chen, respectively), and apply them to the BFD. The Brune and Churchill curves were developed empirically using measured TEs of reservoirs whereas the Chen relations reflect essentially a theoretical analysis of particle settling. We investigate modifications to the Brune and Churchill equations so they may produce daily trapping estimates and assess their suitability for calculating TE for reservoirs with much shorter residence times due to high intraannual flow variability and stratified water columns which have not previously been accounted for.

[8] The Brune curve (TE_{BR}) as given by *Heinemann* [1981] is

$$TE_{BR} = 100 \times \left(\frac{\tau}{0.012 + 1.02}\right), \tag{1}$$

where $\tau = V/Q$ is the residence time (in years), V is the reservoir volume (m^3) at capacity and Q is the mean annual inflow ($m^3\ yr^{-1}$).

[9] The Churchill curve (TE_{CH}) is

$$TE_{CH} = 112 - 800 \times \left(\frac{9.61 \times 10^6 \tau}{u}\right)^{-0.2}, \tag{2}$$

where the constant, 9.61×10^6 represents a conversion from years to seconds and meters to feet to meet the requirements of the *Espinosa-Villegas and Schnoor* [2009] equation and u is the mean annual velocity of the inflow (in ms^{-1}) which is expressed as

$$u = \frac{3.17 \times 10^{-8} Q}{A}, \tag{3}$$

where the constant, 3.17×10^{-8} represents a conversion between inflow per year to inflow per second and A is the surface area of the reservoir (in m^2) which is calculated by V/L ($L =$ the length of the reservoir measured from the dam wall to the most upstream impounded water at dam capacity in m).

[10] Chen provides the upper and lower bounds for the TE of a basin. The highest efficiency occurs when the water column is completely still and the particles sink uniformly.

In this case, the reservoir is stratified where Chen's equation ($TE_{CN(stratified)}$) is

$$TE_{CN(stratified)} = wA/Q, \tag{4}$$

where w is the settling velocity of the different particle sizes [in m yr^{-1}: see Table 2 in Chen, 1975].

[11] The lowest TE occurs for a continuously mixing, i.e., actively turbulent, water column and is given by

$$TE_{CH(mixed)} = -\exp(-wA/Q). \tag{5}$$

[12] We note here that the lowest efficiency case is analogous to an inflow entering a well-mixed reservoir, a condition that is likely to occur in winter and early spring assuming ice-free conditions. The highest efficiency case (equation (4)) would be similar to an inflow entering a strongly stratified reservoir, i.e., late spring—early autumn, and assuming no actively mixing surface layer. Tropical and subtropical reservoirs, such as the BFD, often receive > 90% of their inflow over 1–2 months during the summer wet season when reservoir thermal stratification is the strongest. In addition, the seasonal inflow variability is much greater in the tropics compared to the North American streams upon which the Brune and Churchill relations are based. Finally, the North American inflows tend to occur in winter/spring when reservoir stratification is relatively weaker. As a consequence, the residence times for the North American streams are relatively greater than those in tropical environments (see discussion).

[13] Modifications to the Brune and Churchill equations were made so that daily TEs can be calculated to account for the reduction in residence times experienced by the BFD. The daily residence time, τ^*, is computed as

$$\tau^* = \frac{V}{Q_i}/365, \tag{6}$$

where Q_i is the inflow volume (m^3) on day i.

[14] The daily TEs, $TE_{BR,i}$, and $TE_{CH,i}$, are computed by substituting (6) for τ in equations (1) and (2). Because the majority of river sediment is transported during higher inflow periods, the daily TEs are then weighted based on daily flow volumes. The new set of equations for the Brune and Churchill methods, TE_{BR^*} and TE_{CH^*}, become

$$TE_{BR*} = \frac{\sum_{i=1}^{n} TE_{BR,i} Q_i}{\sum_{i=1}^{n} Q_i}, \tag{7}$$

$$TE_{CH*} = \frac{\sum_{i=1}^{n} TE_{CH,i} Q_i}{\sum_{i=1}^{n} Q_i}. \tag{8}$$

[15] We applied equations (7) and (8) for each water year (i.e., n = number of days from 1 October to 30 September) and also to those periods when the BFD was spilling to calculate sediment trapping in the BFD.

[16] We also performed the calculations assuming the measured discharge downstream of the dam was equivalent to the inflow rather than adding up the three upstream gauges and also accounting for the ungauged upstream area (8% of the total upstream area). Considering only periods when the dam was spilling, this assumption implicitly includes contributions from direct precipitation and evaporation. TEs computed using either estimate of inflow agreed to within 2%. We note that evaporation and the release of irrigation water would have significant effects on dam levels in the dry season. We estimate that annual evaporation amounts in the BFD are between 3.0×10^9 and 5.3×10^9 m^3 yr^{-1} based on our water budgets (although note uncertainties in flow gauge estimates) and average annual evaporation ($\sim$ 2400 mm yr^{-1}: *Bureau of Meteorology* [2012]; surface area of dam = 2.2×10^8 m^2). Thus, it generally represents < 10% of the total annual average inflows to the dam (i.e., within uncertainty estimates of inflow) or $\sim$ 25% of the dam capacity. We note that direct precipitation into the dam averages $\sim 1.5 \times 10^8$ m^3 yr^{-1} [650 mm yr^{-1}: *Bureau of Meteorology*, 2012].

3. Methods

3.1. Sample Collection

[17] Suspended sediment samples were collected using a combination of manual and automated sampling [*Lewis et al.*, 2009a, 2009b; supporting information] techniques over five consecutive wet seasons (2005/2006 to 2009/2010). Samples were collected from as close as practical to the stream flow gauging stations representing each major tributary upstream of the BFD (Burdekin, Cape, Belyando and Suttor Rivers) and the BFD spillway (Figure 1). A total of 868 samples were collected over the rising, peak, and falling stages of the hydrograph following significant rainfall events (Figure 2) and analyzed for total suspended solids (TSS).

[18] Previous sampling of the Burdekin River has shown that clay and silt particles (<63 μm) are well mixed throughout the water column, although the sand fraction can increase towards the river bed [see *Belperio*, 1979; *Amos et al.*, 2004]. Hence, our sampling method (i.e., mostly from the top 50 cm of the water column) adequately captures the clay and silt fractions but is likely to underestimate the coarser bed load component. We contend that this approach is suitable for the purpose of this study as very little of the sand fraction passes through the BFD [see *Faithful and Griffiths*, 2000; this study) and the particle size composition of sediments in grab samples collected from the reservoir floor (M. Cooper, unpublished data, 2005) is similar to that measured in the surface inflow waters (i.e., ≤6% sand: this study); these results suggest that the bed load fraction is largely deposited before it enters the reservoir. The TSS data collected from the autosamplers (i.e., samples from the lower to mid water column) in the 2009/2010 wet season also showed similar concentrations to those samples collected from the surface. Furthermore, the TE method of Churchill predicts the "percent of incoming silt passing through reservoir", and Chen has shown that both the Brune and Churchill methods are designed specifically to predict the trapping of silt sized particles.

3.2. Load Calculations

[19] Flow data from the Burdekin River at Sellheim (gauge no. 120002C), Cape River at Taemas (120302B),

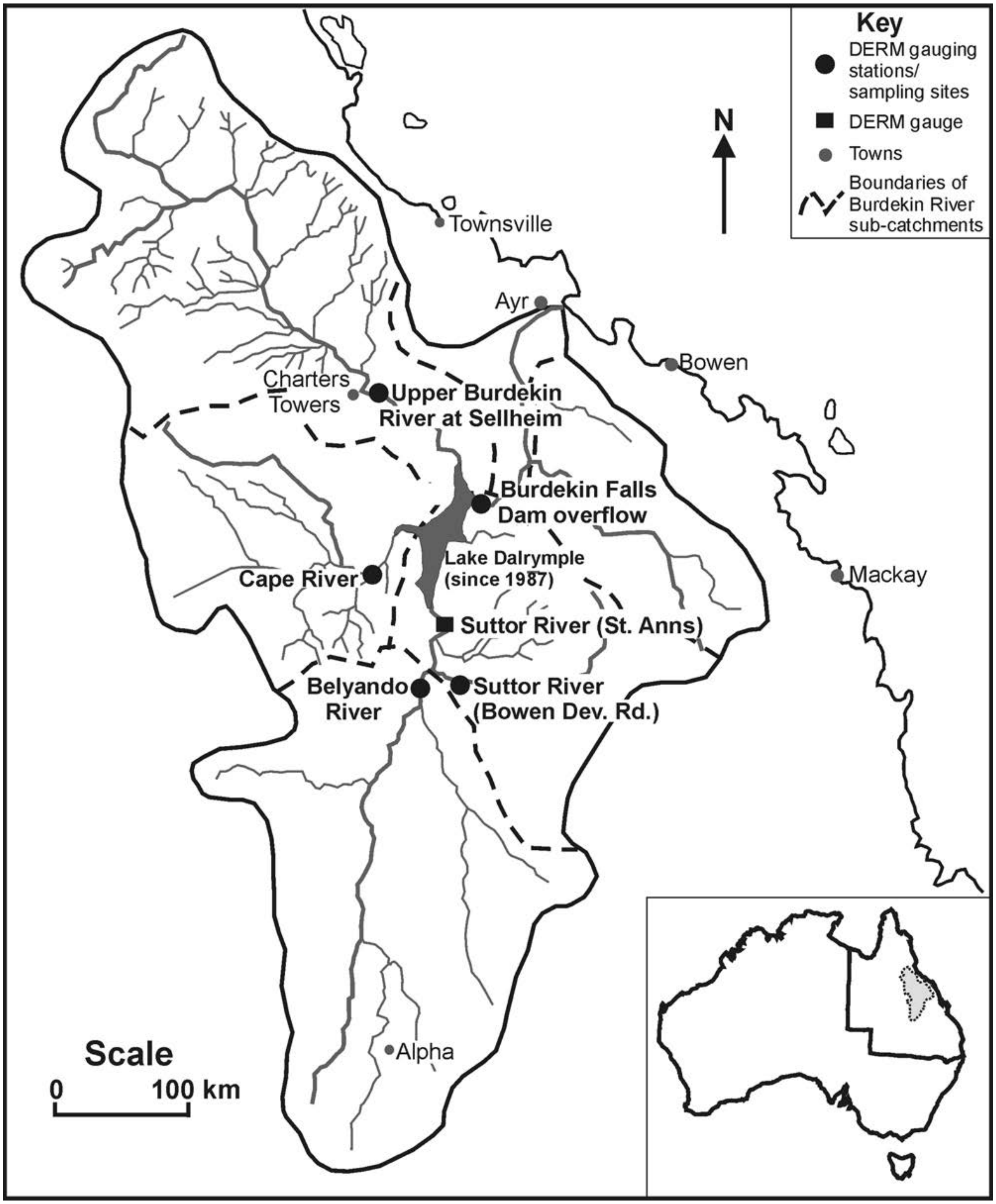

Figure 1. Map of the Burdekin River watershed, north Queensland, Australia showing sampling locations used in this study.

Belyando River at Gregory Developmental Road (120301B), Suttor River at St Anns (120303A), and the Burdekin River at Hydro Site (BFD overflow: 120015A) were used with the corresponding TSS data to calculate suspended sediment loads (Figure 2). The Suttor River at Bowen Developmental Road (120310A) gauge did not become operational until the 2006/2007 wet season and so we used the downstream Suttor River at St Anns gauge minus the Belyando River gauge

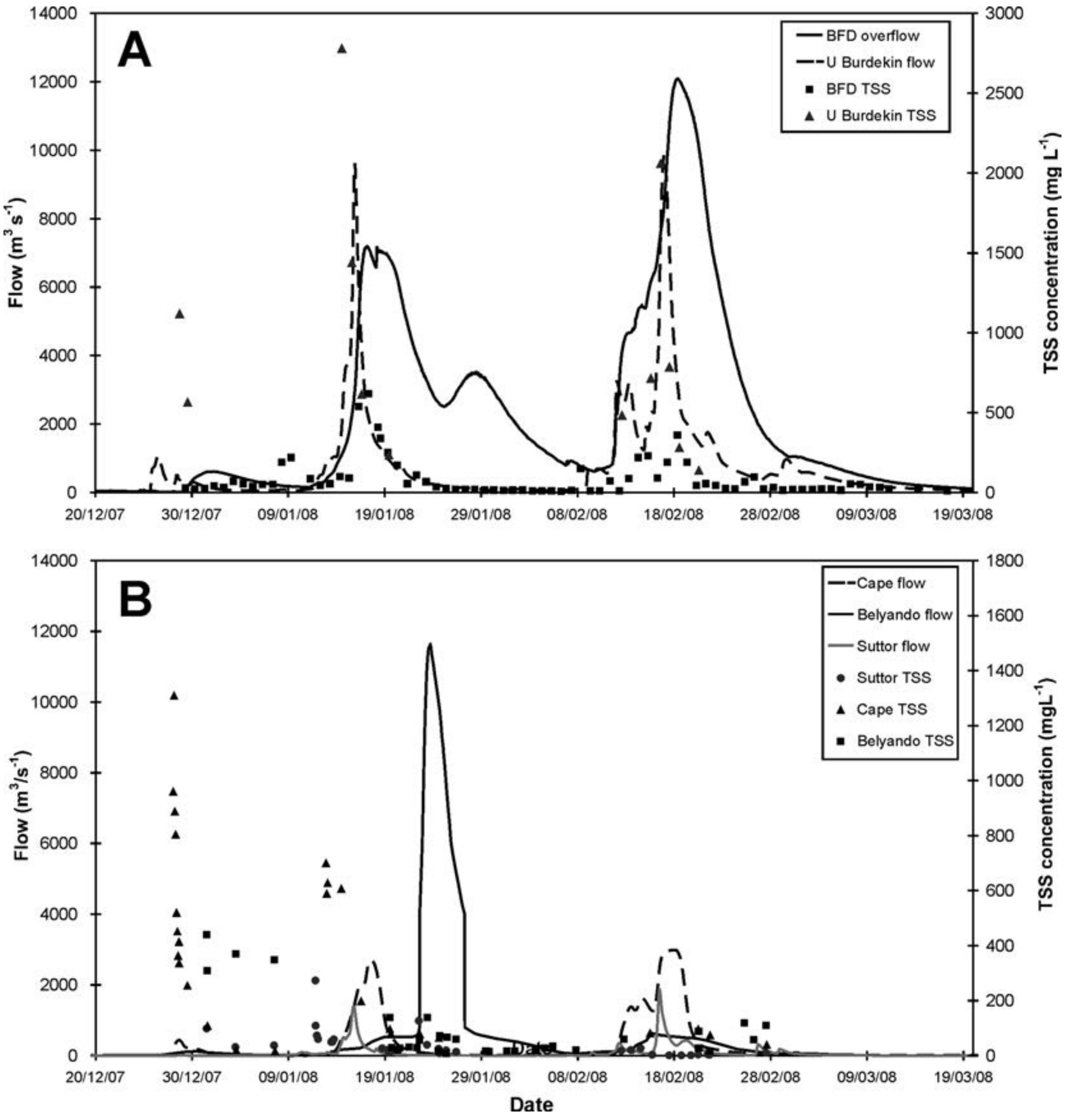

Figure 2. An example of typical flow hydrographs and total suspended sediment (TSS) concentrations for the four upstream rivers and BFD overflow for the 2007/2008 water year. (A) The upper Burdekin River consistently has the highest TSS concentrations and mostly produces the largest flows contributing to the BFD overflow. (B) The Cape, Belyando and Suttor Rivers, in comparison, generally have lower TSS concentrations (note change in scale) and have lower flows. Note the higher TSS concentrations on the rising limb of the flow and the relatively short durations (i.e., 5–10 days) of the highly variable inflows to the dam and over the dam spillway ($\sim$30 days).

flow data to estimate the total discharge (and thus suspended sediment load) for the Suttor River arm (Figure 1). This process assumes that the mean annual TSS concentration (MAC) for Rosetta Creek (a tributary of the Suttor River contributing to the measurement at the St Anns gauge) is identical to that measured at the Suttor River at Bowen Developmental Road.

[20] TSS loads were calculated using a regression (rating-curve) style "Loads Regression Estimator" (LRE) [*Kuhnert et al.*, 2012]. This estimator incorporates additional predictors that account for meaningful features in the flow and concentration relationship including the concept of a "first flush", sample distribution across the flow hydrograph and the exhaustion of sediment supply and therefore TSS concentrations over the flow period ("discounted flow"), all of which improve the prediction of concentration. A particular advantage of the LRE, compared to other methods, is the ability to quantify uncertainties in the load estimates that also incorporate the errors in flow rates [*Kuhnert et al.*, 2012]. These errors are input into the model as a coefficient of variation (CV) and represent the error due to spatial positioning of a gauge and measurement error of flow, both of which were assigned a CV of 10%. We note that this method is an important distinction between our previous investigations [*Lewis et al.*, 2009a, 2009b] which used the linear interpolation technique for load calculation and only provided a qualitative estimate of uncertainty. Moreover, the differences in the flow volumes reported in our previous work are likely related to the development of revised flow rating curves and improved flow

validation by the Queensland Department of Natural Resources and Mines [*State of Queensland*, 2012]. Output from the LRE model are load estimates in tonnes and a measure of uncertainty in the estimate that can be reported as a standard deviation, a confidence interval or a CV. We report the latter in the results section of this manuscript where the loads have been rounded to two significant figures (raw outputs are presented in supporting information Tables S2–S6).

[21] Sediment trapping in the BFD was calculated using the dam inflow and overflow sediment loads (note that overflow loads include release water for irrigation) and uncertainty in the trapping estimates were calculated as follows. Let R represent the ratio between the load (in tonnes) calculated at the BFD overflow (L_O) and the load calculated at the inflow to the Dam (L_I), such that $R = \frac{L_0}{L_I}$. Let T represent the proportion of the load that is trapped, such that $T = 1 - R$. Then the variance for the trapping estimate can be calculated as follows and 80% confidence intervals can be calculated in the usual way.

$$\begin{aligned} \mathrm{Var}\,(T) &= \mathrm{Var}\,(R) \\ &= \mathrm{Var}\left(\frac{L_O}{L_I}\right) \end{aligned} \tag{9}$$

$$\approx \frac{E^2 L_O}{E^2 L_I}\left[\frac{\mathrm{Var}(L_O)}{E^2 L_O} + \frac{\mathrm{Var}(L_\mathrm{I})}{E^2 L_I}\right]$$

assuming independence and appealing to a well-known statistical approximation for the variance of a ratio of two random variables [*Stuart and Ord*, 1987].

[22] Now $\mathrm{Var}(L_I) = \mathrm{Var}(\Sigma_s L_s)$

$$= \sum \mathrm{Var}(L_s) \tag{10}$$

where L_s represents the load at subcatchment s and assuming independence

$\mathrm{Var}(L_O)$ = variance of load at overflow site.

$E[L_O]$ = estimate of load at overflow site.

$E[L_I]$ = estimate of load at inflow site.

3.3. Particle Size Load Calculations

[23] We used a three-step process to calculate loads for each of the 83 particle bin sizes for the upstream rivers and BFD overflow to examine the trapping of specific particle sizes in the BFD and to quantify their watershed sources. First, we used linear interpolation to calculate daily particle size distribution on days where no sample was collected provided that data existed before and after that interpolated day. This interpolation was conducted on the particle size data from each river and for the BFD overflow. Second, we multiplied the daily suspended sediment load (calculated by the LRE) by the corresponding particle size distribution data. These daily particle size distribution load data were then summed for each river and BFD overflow for four individual monitored water years (2005/2006 to 2008/2009). Third, the particle size distribution load data were extrapolated to account for the period outside of the sample collection to match the total suspended sediment load calculated for each river and BFD overflow over the monitored water years. While the data provide important insights into the movement of different particle size fractions through the dam, the sparse collection of samples for the upstream rivers prohibits the calculation of a comprehensive mass balance.

4. Results

4.1. Flow Variability

[24] The 5 year monitoring program captured considerable variability in flow entering the BFD reservoir from the upstream watershed, ranging from small flows in 2005/06 (total inflow 3.4 × 10^9 m^3) to very large flows in 2007/2008 (19.2 × 10^9 m^3) and 2008/2009 (25.6 × 10^9 m^3) (Tables S2–S6, supporting information) compared to the mean annual inflow of 7.2 × 10^9 m^3 for the period 1987–2010. In particular, the flows in the Belyando and Suttor Rivers in 2007/2008 and in the Burdekin River in 2008/2009 were exceptionally large and likely represent 1 in 30 to 1 in 50 year events. Each of the contributing tributary watershed areas received widespread rainfall in at least three of the 5 years which caused appreciable flows and so our data set has complete coverage of available land-type and geological sources in the watershed that influence the characteristics of the suspended sediments that enter the BFD reservoir.

4.2. Suspended Sediment Concentrations

[25] TSS concentrations were highest on the rising/peak stages of the flow hydrographs in all watersheds (Figure 2). In the very large event flows of 2007/2008, TSS concentrations were considerably lower (mean annual concentration of 50–120 mg L^{-1}) in the Belyando and Suttor Rivers, than for other years (180–650 mg L^{-1}). This result suggests that sediment exhaustion/dilution or settling of sediments due to the overbank flows occurred during the 2007/2008 wet season. In comparison, the TSS concentrations in the upper Burdekin (mean annual concentration of 680–800 mg L^{-1}) and Cape Rivers (205–360 mg L^{-1}) were similar over all five wet seasons despite considerable variability in total discharge (see Tables S2–S6 in supporting information).

4.3. Sediment Budgets and Reservoir Trapping

[26] The sediment budgets constructed over the five sampled water years suggest that the BFD trapped 85% (80% CI = 79–91) of suspended sediment in the 2005/2006 water year, 56% (80% CI = 40–71) in 2006/07, 50% (80% CI = 36–64) in 2007/2008, 70% (80% CI=58–81) in 2008/2009 and 82% (80% CI = 77–86) in 2009/2010 (Table 1). TSS loads delivered to the BFD were predominantly sourced from the upper Burdekin River which contributed 70%–94% of the total sediment load delivered to the dam over the five sampled water years, with the other watersheds contributing ≤ 11% each (see Tables S2–S6 in supporting information).

4.4. Comparisons to Empirical Equations

[27] The measured data from the BFD do not agree with the standard Brune or Churchill curves used to predict reservoir trapping (Figure 3). These equations overestimate trapping in the BFD by as much as 26% while the Chen equations that incorporate particle size also overestimate trapping by as much as 28% (Table 2). The modifications

Table 1. Summary of Sediment Loads Received by the Burdekin Falls Dam and Sediment Loads Passing Over the Dam Spillway during the Five Monitored Water Years[a]

Year	2005/2006	CV	2006/2007	CV	2007/2008	CV	2008/2009	CV	2009/2010	CV
Dam overflow discharge (m^3)	2.1×10^9		6.5×10^9		18.0×10^9		25.0×10^9		5.5×10^9	
Upper Burdekin sediment load (tonnes)	2,100,000	14%	3,100,000	13%	4,700,000	10%	15,000,000	14%	1,700,000	12%
Cape River sediment load (tonnes)	34,000	15%	190,000	12%	500,000	11%	470,000	10%	160,000	6%
Belyando River sediment load (tonnes)	180,000	17%	130,000	26%	210,000	13%	110,000	11%	160,000	8%
Suttor River sediment load (tonnes)	96,000	19%	100,000	10%	710,000	13%	140,000	10%	220,000	7%
Other estimated sediment load (tonnes)[b]	10,000		360,000		150,000		300,000		200,000	
Sediment load inflow waters (tonnes)	2,500,000	12%	3,900,000	11%	6,200,000	8%	16,000,000	13%	2,500,000	9%
Sediment load overflow waters (tonnes)	370,000	28%	1,700,000	25%	3,100,000	21%	4,900,000	27%	450,000	16%
Sediment trapping (%)	85 (79–91)		56 (40–71)		50 (36–64)		70 (58–81)		82 (77–86)	

[a]Each load estimate in tonnes is accompanied by the CV as a measure of uncertainty. Sediment trapping estimates are presented as percentages accompanied with conservative 80% confidence intervals.

[b]Estimated loads for the ungauged catchment area above the dam.

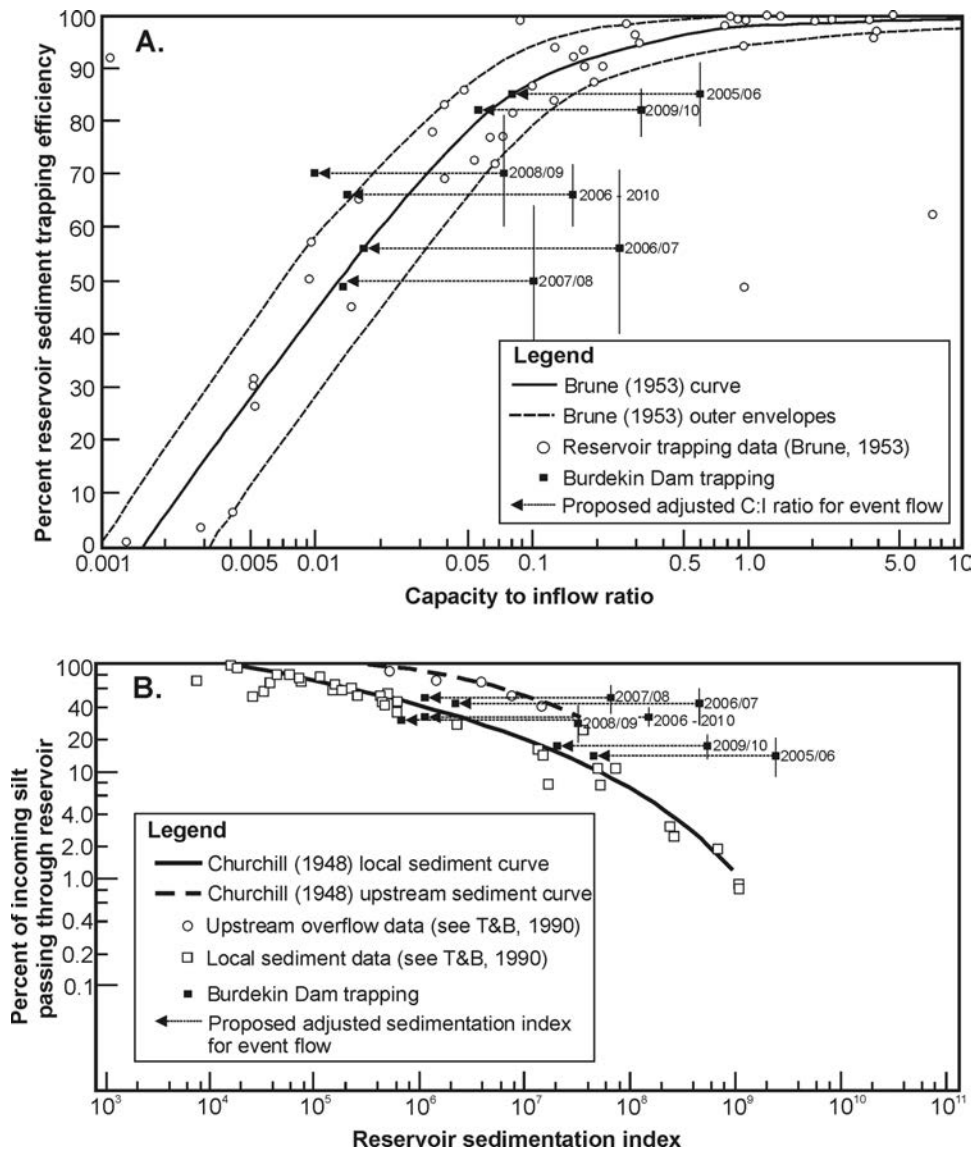

Figure 3. (A) The Brune (1953) and (B) Churchill (1948) curves used to predict the TEs of reservoirs with measured data (and associated error) from the Burdekin Falls Dam overlaid. Also shown are the results obtained when the equations were modified to account for the highly seasonal event flows from the Burdekin River (using the daily overflow calculations only in Table 2). T&B = Trimble and Bube (1990).

Table 2. Summary of TEs Estimated for the Burdekin Falls Dam[a]

Year	2005/2006	2006/2007	2007/2008	2008/2009	2009/2010	2006–2010
Measured sediment trapping (%)	**85 (79–91)**	**56 (40–71)**	**50 (36–64)**	**70 (58–81)**	**82 (77–86)**	**66 (60–72)**
Intraannual flow CV	**1.83**	**2.76**	**2.18**	**2.51**	**2.12**	**2.30**
Brune [1953]—std technique	97%	94%	88%	85%	95%	91%
Churchill [1948]—std technique	100%	97%	90%	87%	98%	94%
Chen [1975] mixed	97%	94%	89%	93%	N/A	N/A
Chen [1975] stratified	99%	96%	92%	97%	N/A	N/A
Brune—daily adjustment	**90%**	**62%**	**53%**	45%	**82%**	55%
Churchill—daily adjustment	95%	**71%**	**61%**	53%	**86%**	**63%**
Brune—daily event overflow only	**85%**	**56%**	**51%**	44%	**80%**	52%
Churchill—daily event overflow only	**89%**	**65%**	**60%**	52%	**84%**	**60%**

[a]The numbers in bold show the TE calculations that lie within the estimated 80% confidence intervals.

to the Brune and Churchill equations that calculate daily trapping and weight daily flow volumes over the water year greatly improve the trapping estimates for the BFD. Although the modified Brune equation agreed with measured trapping (within the 80% confidence intervals) for the individual 2005/2006, 2006/2007, 2007/2008, and 2009/2010 water years, it did not accurately predict trapping for the combined 5 year period. In contrast, the modified Churchill equation predicted TE to within 80% confidence intervals over the 5 year period and predicted annual trapping accurately for the 2006/2007, 2007/2008, and 2009/2010 water years. The predictions of the modified Churchill equation improve further when the period of the dam overflow is considered exclusively in which case it predicts the 2005/2006, 2006/2007, 2007/2008, and 2009/2010 water years within the confidence intervals as well as the TE over the 5 year period. While the same application of the modified Brune equation also predicted the same individual water years, it did not predict TE over the whole 5 year period (Table 2).

4.5. Particle Size Distribution

[28] The particle size data for the BFD overflow display a distinctive bimodal distribution. The finer distribution contains particles between 0.04 μm and 0.60 μm with a peak at 0.20 μm, while the coarser and more dominant fraction ranged between 1.0 and 30 μm with a peak centered at 4.5 μm (Figure 4A). Bimodal distributions were also characteristic of the four upstream rivers. Only the particles in the coarser distribution fraction were trapped in the BFD reservoir. The trapped sediments predominantly ranged in size between 1.0 and 200 μm with a peak at 12 μm (Figure 4A). The particle size fractions for the inflow sediments over the monitored years are composed of 27% clay (< 4 μm), 67% silt (4–63 μm), and 6% sand (> 63 μm). In comparison, the overflow fractions consist of 52% clay, 47% silt, and 1% sand. We note that the lack of samples collected from the upstream catchments for certain water years has resulted in the mass balance discrepancy apparent for the particles < 1 μm (Figure 4A).

[29] The particle size distribution load data suggest that four key fractions are important in transportation through the BFD (Figure 4B). The size fraction <0.5 μm was not trapped by the BFD and was predominantly delivered from the Suttor River (~50%) with the three other rivers contributing 15%–20% each of this fraction. On average, 50% of the 0.5–5.0 μm size fraction was trapped in the BFD reservoir which was largely delivered from the upper Burdekin River (87%). The 5.0–30 μm size fraction was mostly trapped (~75%) by the BFD and was predominantly sourced from the upper Burdekin River (91%). Finally, the size fraction >30 μm was almost totally trapped by the BFD (>95%) and this fraction was again mainly carried from the upper Burdekin River (95%).

5. Discussion

[30] The results of this study show that the vast majority (70–94%) of the suspended sediment load delivered to the BFD is derived from the upper Burdekin River arm. This finding supports the results of *Cooper et al.*'s [2006] trace element and isotopic tracing study which found that bottom sediments within Lake Dalrymple were sourced to this tributary. Therefore, any management intended to reduce bulk suspended sediment delivery (i.e., all size fractions) to the dam should focus remedial efforts on the upper Burdekin River watershed.

[31] Our data suggest that the two most commonly used methods to predict reservoir TEs, the Brune and Churchill equations [e.g., *Verstraeten and Poesen*, 2000], considerably overestimate trapping in the BFD. These curves have been developed for "normally ponded" reservoirs which experience relatively regular flows throughout the water year (see later). Furthermore, the Chen equations, which incorporate particle settling of different size fractions and consider both mixed and stratified systems, also considerably overestimate sediment trapping in the BFD (Table 2).

[32] There are several potential reasons, related to water transit time and sediment sinking velocity, that make the Brune, Churchill and Chen relationships not reliably predict sediment trapping in the BFD. These include (1) differences in dam stratification; (2) variability of the inflows; and (3) particle size, each of which is discussed below.

[33] The BFD receives most of its inflow during the summer period when the water column is temperature stratified [*Chudek et al.*, 1998; *Faithful and Griffiths*, 2000]. Under such conditions inflows with similar temperatures, lower ionic strength and higher TSS concentrations than the dam resident water, flow through either the surface layer or metalimnion [see *Faithful and Griffiths*, 2000] as an interflow. As such, the inflow waters experience a shorter travel time through the reservoir than would be the case were the

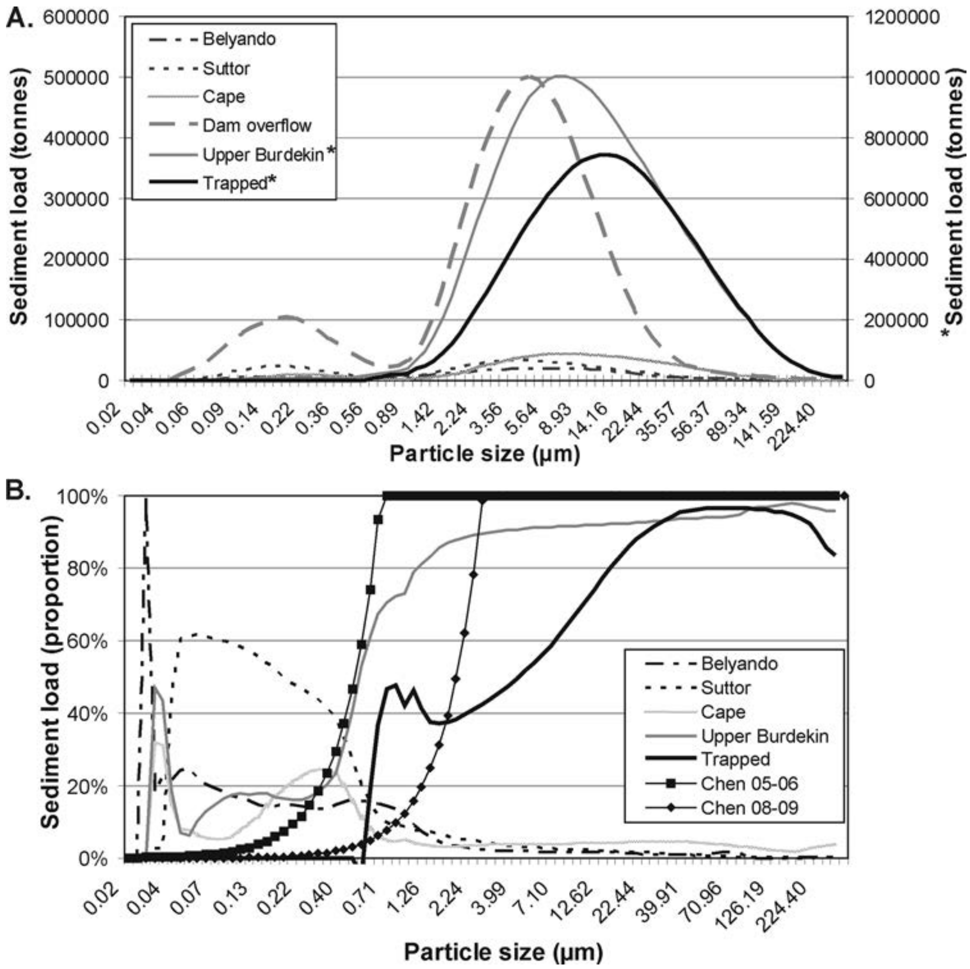

Figure 4. (A) Particle size distribution load data for the four inflow rivers, the BFD overflow and the size distribution of the sediment trapped in the reservoir over the 4 monitored years. Note that the upper Burdekin and trapped particle size distribution load have been plotted on the right *y* axis which has a different scale to the *y* axis on the left of the graph. (B) The proportion of particle size fractions contributed from each of the four inflow rivers and the proportion of different particle size fractions that have been trapped in the BFD reservoir are shown. Also shown is the predicted TE for particle size fractions using the *Chen* [1975] stratified equation.

water column fully mixed (i.e., in the case of cold, sediment-rich inflows that result in bottom density currents). The shorter travel time allows less sediment to sink to the bottom of the reservoir before the inflow passes through the storage. TSS measurements through the water column of the BFD reservoir during the large flows in the 2008/2009 water year were $\sim$ 100 mg L^{-1} higher in the bottom waters of the BFD (surface TSS = 250 $\pm$ 58 mg L^{-1}, $n = 9$; 15 m depth = 283 $\pm$ 6 mg L^{-1}, $n = 3$; 30 m depth = 350 $\pm$ 30 mg L^{-1}, $n = 3$); however, the concentrations in the surface waters still reflect the influence of the event flows and are much higher than during ambient no/low flow conditions ($<$ 10 mg L^{-1}). The relationships developed by Brune and Churchill are likely to be more accurate for systems where the timing of the inflow means it is much more likely to enter a well-mixed (or very weakly stratified) reservoir—possibly as an underflow (i.e., colder snow melt water) leading to greater residence times than are experienced in the BFD. In contrast, the depth (range from 15 to 40 m) and length (i.e., meandering) variation of the reservoir suggest changing residence times throughout the impounded water which would influence the actual residence time (and hence possibly explain departures from the predictions using Chen's method).

[34] The intraannual variability of inflows to the BFD is much higher than those from the empirical TE database (i.e., the data used to formulate the Brune and Churchill curves) which also result in much shorter residence times for the BFD. This implies that less trapping should occur than the empirical predictions and is consistent with our findings. The intraannual coefficients of variation for the reservoir stream inflows used to develop the Brune curve are considerably lower (typical range 0.06–0.95; mean 0.59: *United States Geological Survey*, 2012; note only data prior to the 1954 water year were used to reflect the data presented by Brune) than the rivers of the GBR watershed (range 0.65–1.5; mean 1.1: *State of Queensland*, 2010). In fact, the Burdekin River has one of the larger intraannual coefficients of variation (1.3) and also a relatively high interannual CV (1.1). Given the Brune, Churchill

and Chen equations specify the use of "annual" flow data, the TE of reservoirs that experience higher intraannual inflows are likely to be overestimated by these methods.

[35] Another possible mechanism why the Brune and Churchill methods overestimate TE could be that the incoming sediments to the BFD are relatively finer and sink more slowly than those upon which the empirical relationships were based. Unfortunately particle size data are unavailable for the USA reservoirs to draw direct comparisons with the Burdekin data set. However, *Chen*'s [1975] analysis showed that the Churchill curves for "local silt" and "upstream" sediments predict trapping for the very fine/fine silt fraction (4–16 μm) while the Brune curve covers both the very fine/fine silt and coarse/medium clay (1–16 μm) fractions. This analysis suggests that both the Brune and Churchill curves should predict trapping for the Burdekin data if particle size was the main influence on trapping (peak particle size of 4.5 μm for overflow sediments and 7.1 μm for the inflow sediments in normally distributed plots: Figure 4A). Indeed, the TE data for the BFD falls outside of Brune's envelope curves (Figure 3A) that reflect the trapping of finer and coarser sediments, respectively [see *Chen*, 1975; *Verstraeten and Poesen*, 2000].

[36] Since the measured dam TE data for the BFD plot well outside of the Brune curve envelopes (Figure 3A) and also well off the Churchill curve (Figure 3B), the lack of fit of our data to these empirical relationships is less influenced by particle size than flow variability and stratification. *Ward* [1980] showed that the Brune curve overestimated the TE for reservoirs on highly variable watersheds in Zimbabwe where the inflow sediments contained a coarser fraction (9%–19% sand) than the particle size distribution of the BFD inflow waters and of the bottom sediments (∼ 6% sand). Interestingly, Chen's equation for stratified reservoirs reliably predicts the change in particle size TE for the finer fractions (0.02–2.0 μm) when it is applied to the 2005/2006 and 2008/2009 flow data (i.e., the range of flows over the monitoring program) (Figure 4B); however, the equation does not accurately predict trapping for the coarser particles (2.0–30 μm).

[37] Our modifications to the Brune and Churchill equations account for the more variable residence times in the BFD by calculating the daily TEs and weighting the daily inflow volumes to calculate the annual (or seasonal) sediment trapping. While the TE data used to develop the Brune curve were based on "period of record" ranging from 0.75–72 years (mean = 17.2 years, median = 10.2 years), subsequent studies suggest that this relationship should only be used to predict "long-term" TEs [i.e., it is not suitable for single events, *Verstraeten and Poesen*, 2000]. We note, to our knowledge, no study has specified the length of record required for the optimal application of the Brune curve. In contrast, the Churchill curve was developed using quarterly (i.e., 3 monthly) TE data and *Borland* [1971] showed that this relationship could be applied to accurately predict trapping over both shorter (as short as 5 days) and longer (as long as 20 years) periods. Indeed, *Espinosa-Villegas and Schnoor* [2009] showed that the Churchill equation accurately predicted trapping over a 33 year period for the Coralville Reservoir, Iowa; we note that the particle size fraction ranges reported for clay, silt, and sand for this reservoir are comparable to the inflow sediments to the BFD.

[38] While our modifications to the Brune and Churchill equations better predicted the annual TEs of the BFD (within or just outside confidence intervals), only the modified Churchill equation accurately predicted trapping over the 5 year study period. Most previous studies [e.g., *Borland*, 1971; *Trimble and Bube*, 1990; *Verstraeten and Poesen*, 2000; *Espinosa-Villegas and Schnoor*, 2009] favor the Churchill curve as it incorporates the effective residence time (flow velocity plus residence time) compared to the Brune curve which is a function of residence time only. Hence, the modified Churchill equation is likely to have a wider application to predict trapping for a range of periods (from single events to decades) and account for a greater range of inflow variability. For the BFD, our modified Churchill equation provides accurate TE estimates when the period of dam overflow is considered exclusively. The only water year where the method is outside the uncertainty bounds coincides with the extreme 2008/2009 discharge from the upper Burdekin River. This method under-predicted trapping which likely reflects the relatively coarser material (and much larger sediment load) that was delivered from this event (i.e., sediment > 30 μm: Figure 5).

[39] We tested our modified Churchill and Brune equations on previous TE studies where daily flow data are available including the Coralville Reservoir [*Espinosa-Villegas and Schnoor*, 2009], the Corpus Christi Reservoir, the Imperial Dam [*Brune*, 1953] and Hales Bar [*Churchill*, 1948], USA (Figure 6; Tables S7 and S8 in the supporting information). The modified Churchill equation underestimates TEs for the Coralville Reservoir, Iowa where the trapping predicted over the whole 33 year period (70.2%) is lower than the measured (80.3%) and predicted (79.1%) trapping using the standard Churchill equation [*Espinosa-Villegas and Schnoor*, 2009]. However, the operation of the Coralville Reservoir (designed for flood protection) may strongly influence these trapping estimates and explain why the modified Churchill equation and other standard techniques (i.e., Dendy (69.3%), Brune (53.7%), Heinemann (63.5%), and Brown (64.9%)), have underestimated sediment trapping over this period [data analysis presented in *Espinosa-Villegas and Schnoor*, 2009]. Observations of the inflow and outflow data for the Coralville Reservoir show that, during certain flood events, the outflow peaks precede the inflows and hence suggest that waters were released from the reservoir prior to the event inflows reaching the impoundment. In these cases, the dam should trap more sediment than if it was operated as a "normally ponded" reservoir.

[40] For the other reservoirs examined, both the standard and modified Brune and Churchill equations could not accurately predict TEs for the Corpus Christi Reservoir or for Imperial Dam. Interestingly, the standard Churchill equation overpredicted sediment TEs for the Corpus Christi Reservoir over the two periods (1934–1942 and 1942–1948) while the modified Churchill equation under-predicted trapping over these same periods. Only the standard Brune equation accurately predicted trapping for one of the periods (1934–1942; Table S8 in supporting information). Unfortunately, annual TE data for the Corpus Christi Reservoir are not available which may have provided better

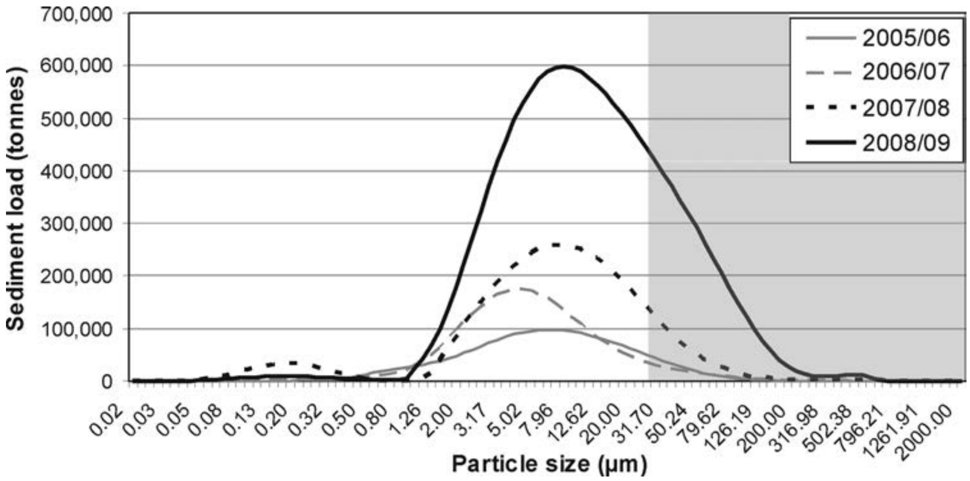

Figure 5. Particle size load data over the 2005/2006, 2006/2007, 2007/2008, and 2008/2009 water years. The shaded area shows the greater proportion of sediments that were above 30 µm during the extreme flows of the 2008/2009 water year which may explain why the Churchill equation underestimated TE for that year.

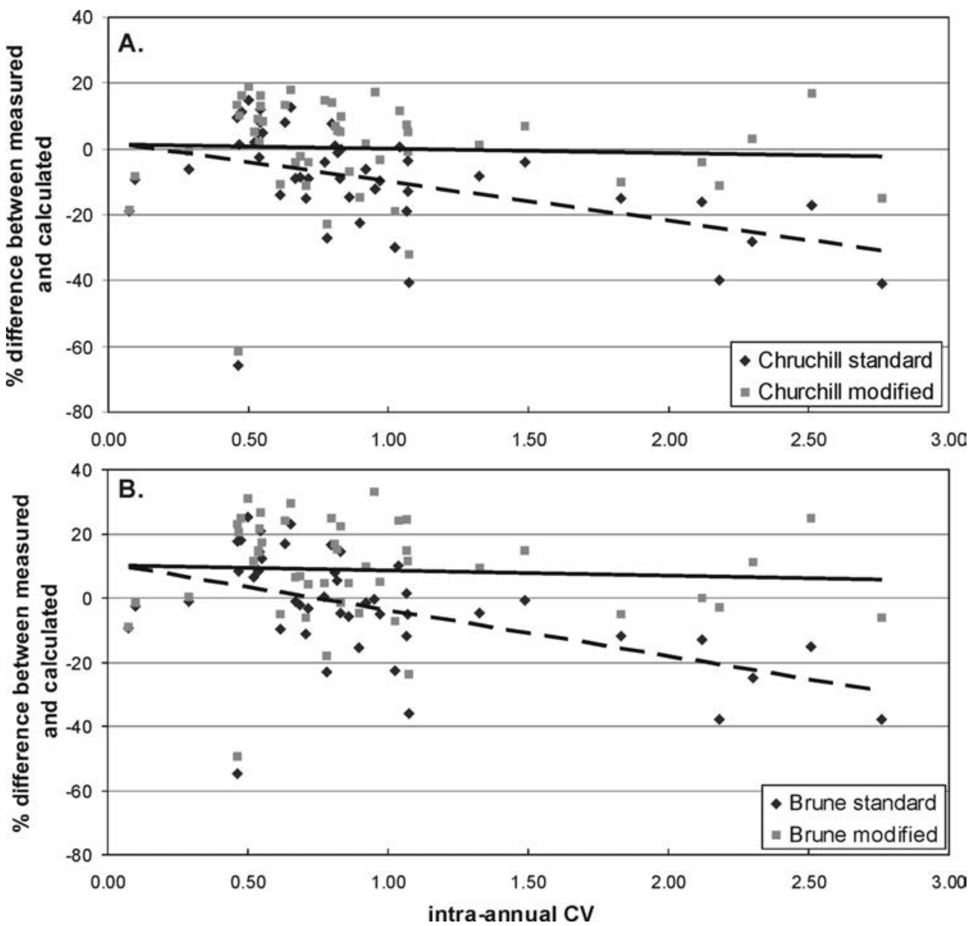

Figure 6. Plot of the differences in measured and calculated TEs for the standard and modified (A) Churchill and (B) Brune equations against the intraannual CV. The solid line is the line of best fit for the data using the modified Churchill and Brune equations and the dotted line is the line of best fit for the standard Churchill and Brune equations.

insights to examine the performance of these methods over individual years.

[41] Similarly, TE data for individual years are not available for the Imperial Dam Reservoir which limits our interpretation of these data. The Imperial Dam is situated on the Colorado River which is highly regulated with several upstream reservoirs and has a very low intraannual CV ($\leq$ 0.10). Indeed, this low CV explains the little difference (generally $< 1\%$) in the TEs predicted between the standard and modified techniques (Table S8 in supporting information). Both the standard and modified Brune equations accurately predicted trapping for the 1938–1942 period, although both overestimated trapping for 1943–1947. The standard and modified Churchill equations overestimated trapping for both periods. In this case, the Churchill curve for "fine silt discharged from an upstream reservoir" may be more appropriate to apply for this reservoir given the presence of several dams upstream of this site.

[42] For the Hales Bar Reservoir, the modified Churchill equation accurately predicted (values within 5% of the measured trapping) TEs for 12 of the 17 time periods examined compared to the standard technique which only predicted 6 of the 17 periods (Table S8 in supporting information). In comparison the standard and modified Brune equations accurately predicted trapping for 10 of 17 and 11 of 17 time periods, respectively. Given that the Hales Bar data were originally used to construct the Churchill curve for "local silt", we suggest that our modified Churchill equation generally improves trapping predictions compared to the standard technique and can be applied across a wider range of reservoirs. Indeed, the lines of best fit for all the TE data show that the modified Churchill and Brune methods provide greater predictability (i.e., the percentage difference between the measured and calculated trapping remains around 0%) across the range of intraannual coefficients of variation for the inflows (Figure 6). This result confirms that the modified equations better account for flow variability and show considerable promise to predict TEs of reservoirs across a wider range of locations. Our analysis shows that the modified Churchill equation cannot accurately predict TEs for all individual years or for dams that have certain operational protocols (e.g., flood mitigation), although it is likely to perform as well or better than the standard method. Indeed, the TE data for the BFD plot randomly along the Brune and Churchill curves when the modified equations are applied (Figure 3) reflecting the line of best fit in accordance with how the curves were originally developed.

[43] Physically based numerical modeling techniques can provide more accurate estimates of TE and using this approach it is possible to directly estimate the effects of sinking, particle aggregation, and diffusive transport on sediment dynamics [*Casamitjana and Schladow*, 1993]. Indeed, by the time a proposed reservoir enters the environmental impact assessment stage, it is likely that 2D or 3D hydrodynamic models will be employed to provide the best possible understanding of a dam's expected performance which consider various operational scenarios. However, the data requirements for reservoir hydrodynamic modeling may be excessive when the research objective requires coupling of such a model with large spatially distributed models of catchment erosion that simulate periods of decades. In comparison, the use of the modified Churchill equation can provide a rapid and relatively accurate assessment of reservoir sediment trapping which only relies on the availability of daily inflow data.

6. Conclusions

[44] A 5 year sediment TE study of the BFD, Australia shows that the classic Brune and Churchill empirical relationships overestimate TEs in this reservoir located in the tropics. This is most likely due to the reduction in effective residence time caused by highly variable intraannual inflows as well as the reservoir stratification characteristics (i.e., timing of inflows). When the Churchill equation was modified to account for this intraannual variability by weighting daily TEs with corresponding daily inflow volumes, the TE predictions were within confidence intervals for four of the five years as well as for the total sediment trapped over the 5 year monitoring period (when the period of overflow was considered exclusively). This simple modification shows promise to predict TEs of reservoirs that receive highly variable intraannual inflows as well as for the less variable streams of the USA but requires further testing at other locations. We caution that the particle size distribution of inflow sediments may affect this relationship particularly when they are skewed towards a finer or coarser fraction. The very fine suspended sediment fraction (<5 μm) largely passes over the Burdekin Falls Dam spillway and is predominantly sourced from the upper Burdekin and Suttor Rivers. The management of this fraction is important for the export of sediment to the Great Barrier Reef lagoon [e.g., *Bainbridge et al*., 2012].

[45] **Acknowledgments.** We are extremely grateful to Tony Bailey and Gary Caddies (SunWater) who collected the samples from the Burdekin Falls Dam (BFD) overflow over the 5 water years. Peter Burger (Department of Natural Resources and Mines, Queensland) developed the Churchill equations to calculate the daily reservoir trapping for the BFD. We thank the Queensland Department of Science, Information Technology, Innovation and the Arts GBR Loads Monitoring Program who partly funded the collection and analysis of total suspended solid samples from the major tributaries of the Burdekin. The Queensland Department of Natural Resources and Mines hydrographers (in particular Morgain Sinclair, Phil Kerr and Geoff Pocock) are acknowledged for supplying the flow data over the 5 water years. We thank Raphael Wüst (School of Earth and Environmental Sciences, James Cook University) for performing the particle size analysis. We acknowledge the efforts of the TropWATER laboratory staff for analysing the TSS samples. This research was supported by (1) the Australian Government's Marine and Tropical Sciences Research Facility, implemented in North Queensland by the Reef and Rainforest Research Centre Ltd., (2) North Queensland Dry Tropics and (3) the Australian Government's Caring for our Country Reef Rescue Research and Development Program grant to PMK. We are grateful to Peter Hairsine (CSIRO) who provided comments on an earlier draft of this manuscript. The comments of Greg Morris, James Syvitski and four anonymous reviewers greatly improved the manuscript.

References

Amos, K. J., J. Alexander, A. Horn, G. D. Pocock, and C. R. Fielding (2004), Supply limited sediment transport in a high-discharge event of the tropical Burdekin River, North Queensland, Australia, *Sedimentology*, *51*, 145–162.

Bainbridge, Z. T., E. Wolanski, J. G. Álvarez-Romero, S. E. Lewis, and J. E. Brodie (2012), Fine sediment and nutrient dynamics related to particle size and floc formation in a Burdekin River flood plume, Australia, *Mar. Pollut. Bull.*, *65*, 236–248.

Belperio, A. P. (1979), The combined use of was load and bed material load rating curves for the calculation of total load: An example from the Burdekin River, Australia, *Catena*, *6*, 317–329.

Borland, W. M. (1971), Reservoir sedimentation, in *River Mechanics*, Vol. *II*, edited by H. W. Shen, pp. 29.1–29.38, Colo. State Univ., Fort Collins, Colo.

Brown, C. B. (1943), Discussion of sedimentation in reservoirs, by B. J. Witzig, *Proc. Am. Soc. Civil Eng.*, *69*, 1493–1500.

Brune, G. M. (1953), Trap efficiency of reservoirs, *Trans. Am. Geophys. Union*, *34*, 407–418.

Bureau of Meteorology (2012) [Available at: www.bom.gov.au, accessed 22 Nov. 2012].

Camp, T. R. (1946), Sedimentation and the design of settling tanks, *Trans. Am. Soc. Civ. Eng.*, *111*, 895–936.

Carroll, C., et al. (2012), A paddock to reef monitoring and modelling framework for the Great Barrier Reef: Paddock and catchment component, *Mar. Pollut. Bull.*, *65*, 136–149.

Casamitjana, X., and G. Schladow (1993), Vertical-distribution of particles in stratified lake. *J. Environ. Eng.*, *119*, 443–462.

Chen, C-N. (1975), Design of sediment retention basins, paper presented at National Symposium on Urban Hydrology and Sediment Control, Univ. of Kentucky, 18–31 July 1975.

Chudek, E., M. Joo, A. Horn, and S. McLaren (1998), *Stratification behaviour of Queensland dams*, Res. Sci. Cent. Water Monit. Group, Queensland Dep. of Nat. Resour., Brisbane, Australia.

Churchill, M. A. (1948), Discussion of paper by L. C. Gottschalk "Analyses and use of reservoir sedimentation data," in *Federal Inter-agency Sedimentation Conference Proceedings*, pp. 139–140, U.S. Geol. Surv., Denver, Colo.

Cooper, M., G. Shields, J. Faithful, and J. Zhao (2006), Using Sr/Nd isotopic ratios to define sediment sources in the Burdekin Falls Dam, Queensland, Australia, *Geochim. Cosmochim. Acta*, *70*, A112.

Espinosa-Villegas, C. O., and J. L. Schnoor (2009), Comparison of long-term observed sediment trap efficiency with empirical equations for Coralville Reservoir, Iowa, *J. Environ. Eng.*, *135*, 518–525.

Fabricius, K. E. (2005), Effects of terrestrial runoff on the ecology of corals and coral reefs: Review and synthesis, *Mar. Pollut. Bull.*, *50*, 125–146.

Faithful, J. W., and D. J. Griffiths (2000), Turbid flow through a tropical reservoir (Lake Dalrymple, Queensland, Australia): Responses to a summer storm event, *Lakes Reservoirs Res. Manage.*, *5*, 231–247.

Heinemann, H. G. (1981), A new sediment trap efficiency curve for small reservoirs, *Water Resour. Bull.*, *17*, 825–830.

Heinemann, H. G. (1984), Reservoir trap efficiency, in *Erosion and Sediment Yield: Some Methods of Measurement and Modelling*, edited by R. F. Hadley and D. E. Walling, pp. 201–218, GeoBooks, Norwich.

Horowitz, A. J., K. A. Elrick, and J. J. Smith (2008), Monitoring urban impacts on suspended sediment, trace element, and nutrient fluxes within the City of Atlanta, Georgia, USA: Program design, methodological considerations, and initial results, *Hydrol. Process.*, *22*, 1473–1496.

Kroon, F. J., P. M. Kuhnert, B. L. Henderson, S. N. Wilkinson, A. Kinsey-Henderson, J. E. Brodie, and R. D. R. Turner (2012), River loads of suspended solids, nitrogen, phosphorus and herbicides delivered to the Great Barrier Reef lagoon, *Mar. Pollut. Bull.*, *65*, 167–181.

Kuhnert, P. M., B. L. Henderson, S. E. Lewis, Z. T. Bainbridge, S. N. Wilkinson, and J. E. Brodie (2012), Quantifying total suspended sediment export from the Burdekin River catchment using the loads regression estimator tool, *Water Resour. Res.*, *48*, W04533, doi:10.1029/2011WR011080.

Lewis, S. E., Z. T. Bainbridge, B. S. Sherman, J. E. Brodie, and M. Cooper (2009a), The trapping efficiency of the Burdekin Falls Dam: Estimates from a three-year monitoring program, Research Report 39 to the Marine and Tropical Sciences Research Facility, 31 p., Reef and Rainforest Res. Cent. Ltd., Cairns and Aust. Cent. for Trop. Freshwater Res. (ACTFR), Townsville..

Lewis, S. E., B. S. Sherman, Z. T. Bainbridge, J. E. Brodie, and M. Cooper (2009b), Modelling and monitoring the sediment trapping efficiency and sediment dynamics of the Burdekin Falls Dam, Queensland, Australia, in 18th World IMACS Congress and MODSIM09 International Congress on Modelling and Simulation, edited by R. S. Anderssen, R. D. Braddock, and L. T. H. Newham, pp. 4022–4028, Modell. and Simul. Soc. of Aust. and N. Z. and Int. Assoc. for Math. and Comput. in Simul. ISBN: 978-0-9758400-7-8 [Available at: http://www.mssanz.org.au/modsim09/I14/lewis.pdf].

McKergow, L. A., I. P. Prosser, A. O. Hughes, and J. Brodie (2005), Sources of sediment to the Great Barrier Reef World Heritage Area, *Mar. Pollut. Bull.*, *51*, 200–211.

Prosser, I. P., C. J. Moran, H. Lu, A. Scott, P. Rustomji, J. Stevenson, G. Priestly, C. H. Roth, and D. Post (2002), Regional patterns of erosion and sediment transport in the Burdekin River catchment, *CSIRO Land and Water Tech. Rep. 5/02*, CSIRO, Canberra, Australia.

Restrepo, J. D., P. Zapata, J. M. Diaz, J. Garzón-Ferreira, and C. B. Garcia (2006), Fluvial fluxes into the Caribbean Sea and their impact on coastal ecosystems: The Magdalena River, Colombia, *Global Planet. Change*, *50*, 33–49.

State of Queensland (2012), Department of Natural Resources and Mines 'Watershed', [Available at: http://www.derm.qld.gov.au/watershed/index.html, accessed 1 Nov. 2012].

Stuart, A., and J. K. Ord (1987), *Kendall's advanced theory of statistics*, Vol. 1, 5th ed., p. 325, Arnold, London.

Syvitski, J. P. M. (2003), Supply and flux of sediment along hydrological pathways: Research for the 21st century, *Global Planet. Change*, *39*, 1–11.

Syvitski, J. P., C. J. Vörösmarty, A. J. Kettner, and P. Green (2005), Impact of humans on the flux of terrestrial sediment to the global coastal ocean, *Science*, *308*, 376–380.

Trimble, S. W., and K. P. Bube (1990), Improved reservoir trap efficiency prediction. *Environ Prof.*, *12*, 255–272.

United States Geological Survey (2012), United States Geological Survey [Available at: http://waterdata.usgs.gov/nwis/inventory?search_criteria=state_cd&search_criteria=search_station_nm&search_criteria=site_tp_cd&search_criteria=alt_va&search_criteria=data_type&submitted_form=introduction, accessed 1 Aug. 2012].

Verstraeten, G., and J. Poesen (2000), Estimating trap efficiency of small reservoirs and ponds: Methods and implications for the assessment of sediment yield, *Prog. Phys. Geogr.*, *24*, 219–251.

Vörösmarty, C. J., and D. Sahagian (2000), Anthropogenic disturbance of the terrestrial water cycle, *BioScience*, *50*, 753–765.

Vörösmarty, C. J., M. Meybeck, B. Fekete, K. Sharma, P. Green, and J. P. M. Syvitski (2003), Anthropogenic sediment retention: Major global impact from registered river impoundments, *Global Planet. Change*, *39*, 169–190.

Ward, P. R. B. (1980), Sediment transport and a reservoir siltation formula for Zimbabwe-Rhodesia, *Die Siviele Ing. Suid-Afrika*, *22*, 9–15.

Appendix E:

Kuhnert et al. 2012 (Supporting publication)

WATER RESOURCES RESEARCH, VOL. 48, W04533, doi:10.1029/2011WR011080, 2012

Quantifying total suspended sediment export from the Burdekin River catchment using the loads regression estimator tool

Petra M. Kuhnert,[1] Brent L. Henderson,[2] Stephen E. Lewis,[3] Zoe T. Bainbridge,[3] Scott N. Wilkinson,[4] and Jon E. Brodie[3]

Received 24 June 2011; revised 14 March 2012; accepted 16 March 2012; published 28 April 2012.

[1] The loads regression estimator (LRE) was introduced by Wang et al. (2011) as an improved approach for quantifying the export of loads and the corresponding uncertainty from river systems, where data are limited. We extend this methodology and show how LRE can be used to analyze a 24 year record of total suspended sediment concentrations for the Burdekin River. For large catchments with highly variable discharge such as that of the Burdekin River, it is important to quantify loads and their uncertainties accurately to determine the current load and to monitor the effect of changes in catchment management. The extended methodology incorporates (1) multiple discounted flow terms to represent the effect of flow history on concentration, (2) a term that captures sediment trapping and spatial sources of flow in terms of the ratio of flow from above the Burdekin Falls Dam, and (3) catchment vegetation cover. Furthermore, we validated model structure and performance in relation to the application tested. We also considered errors in gauged flow rates of 10% that were consistent with the literature. The results for the Burdekin site indicate substantial variability in loads across years. The inclusion of vegetation cover as a predictor had a significant impact on total suspended sediment (TSS) concentration, with values up to 2.1% lower noted per increasing percentage of vegetation cover. TSS concentration was up to 38% lower in years with greater proportions of flow from above the dam. The extended LRE methodology resulted in improved model performance. The results suggest that management of vegetation cover in dry years can reduce TSS loads from the Burdekin catchment, and this is the focus of future work.

Citation: Kuhnert, P. M., B. L. Henderson, S. E. Lewis, Z. T. Bainbridge, S. N. Wilkinson, and J. E. Brodie (2012), Quantifying total suspended sediment export from the Burdekin River catchment using the loads regression estimator tool, *Water Resour. Res.*, *48*, W04533, doi:10.1029/2011WR011080.

1. Introduction

[2] Sediments and nutrients are high-priority river contaminants that can significantly affect freshwater and receiving estuarine and marine environments [*Brodie et al.*, 2012; *De'ath and Fabricius*, 2010; *Doney*, 2010; *Furnas*, 2003]. In the Great Barrier Reef (GBR) catchment area in northeastern Australia, a strong emphasis is placed on quantifying pollutant loads (suspended sediments, nutrients and pesticides) and their sources of uncertainty for the purpose of detecting trends in loads [*Reef Water Quality Protection Plan Secretariat*, 2009]. Estimates of loads with associated uncertainty from monitoring data are therefore required to determine current baseline exports, sources of pollution and a means to assess progress toward Australian and Queensland government "reef plan" targets. Although this could be met by improvements to measurement programs that focus on frequent sampling, in reality monitoring records will often contain gaps because of equipment failure or impaired site access. Even where sampling is reliable and representative, in variable climates it is desirable to utilize the available historical monitoring records of variable sampling frequency for assessing long-term loads. For monitoring current and future total suspended sediment (TSS) loads, turbidity meters can provide an alternative to statistical analysis of measured TSS concentrations, particularly in smaller channels where TSS concentrations can be highly variable during runoff events. However, the cost of deploying and maintaining these instruments means that standard TSS monitoring continues to be used at many sites. Furthermore, turbidity meters must be calibrated against measured TSS concentrations in water samples from the site. At large river cross sections variation with depth in the suspended concentration of sand can be an additional complication. For example, a transmissometer, described in the paper by *Mitchell and Furnas* [2001] was tested in the GBR catchment area. Because of the extreme depth range of the Burdekin River between low flow

[1]CSIRO Mathematics, Informatics and Statistics, Glen Osmond, South Australia, Australia.
[2]CSIRO Mathematics, Informatics and Statistics, Canberra, ACT, Australia.
[3]Centre for Tropical Water and Aquatic Ecosystem Research (TropWATER), Australian Tropical Sciences Innovation Precinct (ATSIP), James Cook University, Townsville, Queensland, Australia.
[4]CSIRO Land and Water, Canberra, ACT, Australia.

Published in 2012 by the American Geophysical Union

(where depth was minimal) and high flow (tens of meters), the probe was positioned near the bottom. However, a robust relationship between a transmissometer reading of turbidity and TSS in mg L^{-1} could not be developed. For several reasons therefore, a predictive load estimation tool incorporating explanatory variables and providing some diagnostic capability is useful for analyzing TSS concentrations and loads in large, complex and highly variable river systems.

[3] Estimating pollutant loads at river stations typically requires models that predict temporal patterns of pollutant concentration between sampling times [*Asselman*, 2000]. To date, methods used to calculate pollutant loads in the GBR consist of the popular ratio estimators and linear interpolation [*Cooper and Watts*, 2002; *Letcher et al.*, 2002; *Littlewood and Marsh*, 2005]. However, these estimators lack flexibility as they cannot identify the major contributors and sources of contaminants. They also do not provide estimates of uncertainty in concentration and flow rates and therefore do not incorporate those into standard error calculations, if indeed they are provided. Furthermore, they cannot quantify the loads in years where pollutant concentrations are poorly sampled or missing.

[4] Rating curves have been a widely used method for estimating pollutant loads and quantifying the respective uncertainty [*Cohn*, 1995; *Cohn et al.*, 1992; *Rustomji and Wilkinson*, 2008; *Thomas*, 1985, 1988; *Thomas and Lewis*, 1995; *Walling*, 1977; *Wang et al.*, 2011]. The latest of these approaches by *Wang et al.* [2011] provides estimates of loads from monitoring data and has recently been used to provide baseline estimates of loads for reporting [*Kroon et al.*, 2012] as well as provide a framework for sample size estimation to determine the number of years of monitoring data required to detect trends [*Darnell et al.*, 2012]. The method proposed by *Wang et al.* [2011], which we refer to as the Loads Regression Estimator, hereafter termed LRE, is based upon the traditional rating curve approach by *Cohn et al.* [1992] but extends the methodology to incorporate hydrological variables that attempt to mimic temporal characteristics of a river system using a flexible generalized additive modeling (GAM) framework. The method incorporates key measures of uncertainty: measurement error in the sampled flow and concentration; model uncertainty arising from a lack of understanding of the underlying hydrological processes; and sampling uncertainty arising from the way in which flow and concentration are sampled, i.e., more frequently during high-intensity discharge events. In addition to accommodating uncertainties in concentration, errors in flow rates can be directly incorporated into the uncertainty calculation of the loads estimate. Furthermore, this framework develops a historical representation of concentration and flow for the system, enabling the estimation of loads for years where no monitoring data were collected. Of course, the accuracy of the loads in these instances is subject to how well the model captures the system processes.

[5] In this paper we extend the LRE methodology proposed by *Wang et al.* [2011] to cater for highly variable river systems where monitoring data are limited. The LRE methodology and its extensions are illustrated using a long-term record of total suspended sediment sampled at the Inkerman Bridge site on the Burdekin River. As the Burdekin catchment represents one of the driest and largest catchments in the GBR catchment area, data captured at the Inkerman Bridge site are limited through the period 1986–2010. The primary purpose of the LRE applied to this site is to derive best estimates of past sediment yield to establish a baseline for assessing future changes.

2. Case Study: Inkerman Bridge, Burdekin River

2.1. Catchment Characteristics

[6] The Burdekin River drains the second largest basin (area ~130,000 km^2) draining to the GBR lagoon and it represents the largest in terms of mean gauged annual discharge and total annual sediment export to the GBR [*Furnas*, 2003] (Figure 1). Cattle grazing represents the dominant land use within the catchment (95%) with the remaining 5% composed of other uses, including cropping [*Furnas*, 2003]. The geology of the catchment is quite varied containing igneous, sedimentary and metamorphic rock provinces [*Bainbridge et al.*, 2008] and a wide variety of soil types. Precipitation within the catchment occurs primarily within a well-defined, summer wet season with higher falls near the coast and in the northern parts of the catchment [*Amos et al.*, 2004; *Furnas*, 2003]. The annual discharge of northern Australian rivers is highly variable in Australian and world terms [*Petheram et al.*, 2008]. The recorded annual discharge of the Burdekin River at Inkerman Bridge (water year: October 1 to September 30) ranges from 247,110 ML (1930/1931) to 54,066,311 ML (1973/1974) over the 90 year record to 2010. Development of the catchment by European settlers began in the mid-1800s with the introduction of sheep and cattle [*Lewis et al.*, 2007] and the commencement of alluvial mining. It is generally accepted these activities would have increased the annual average flux of sediment to the GBR lagoon [*Belperio*, 1979; *McKergow et al.*, 2005] and trace element analysis of coral cores has provided evidence in support of that proposition [*Lewis et al.*, 2007; *McCulloch et al.*, 2003].

[7] Several attempts have been made to estimate the current "annual average" suspended sediment export and the "natural" (pre-European settlement) load for the Burdekin River. The first estimate was reported by *Belperio* [1979], who used a regression-based sediment rating curve approach to calculate an annual average load of 3.45×10^6 t using monitoring data from the 1970s. Since then annual average suspended sediment load estimates (summarized by *Brodie et al.* [2009, Table 5]) have been derived using monitoring data (estimates range between 3.8 and 4.6 $\times 10^6$ t) and catchment models (2.4–9.0 $\times 10^6$ t yr^{-1}) with some models also predicting 'natural' loads (0.48–2.1 $\times$ 10^6 t). We note that no previous load calculations have included an estimate of the uncertainty apart from the recent work by *Kroon et al.* [2012] that used a base LRE model to obtain average annual estimates of loads.

2.2. TSS Sampling at Inkerman Bridge on the Burdekin River

[8] TSS data were collected from the Inkerman Bridge site on the Burdekin River between 1986 and 2010 (692 samples spanning 24 water years). This site is 20 river km upstream of the river mouth, with a catchment area of

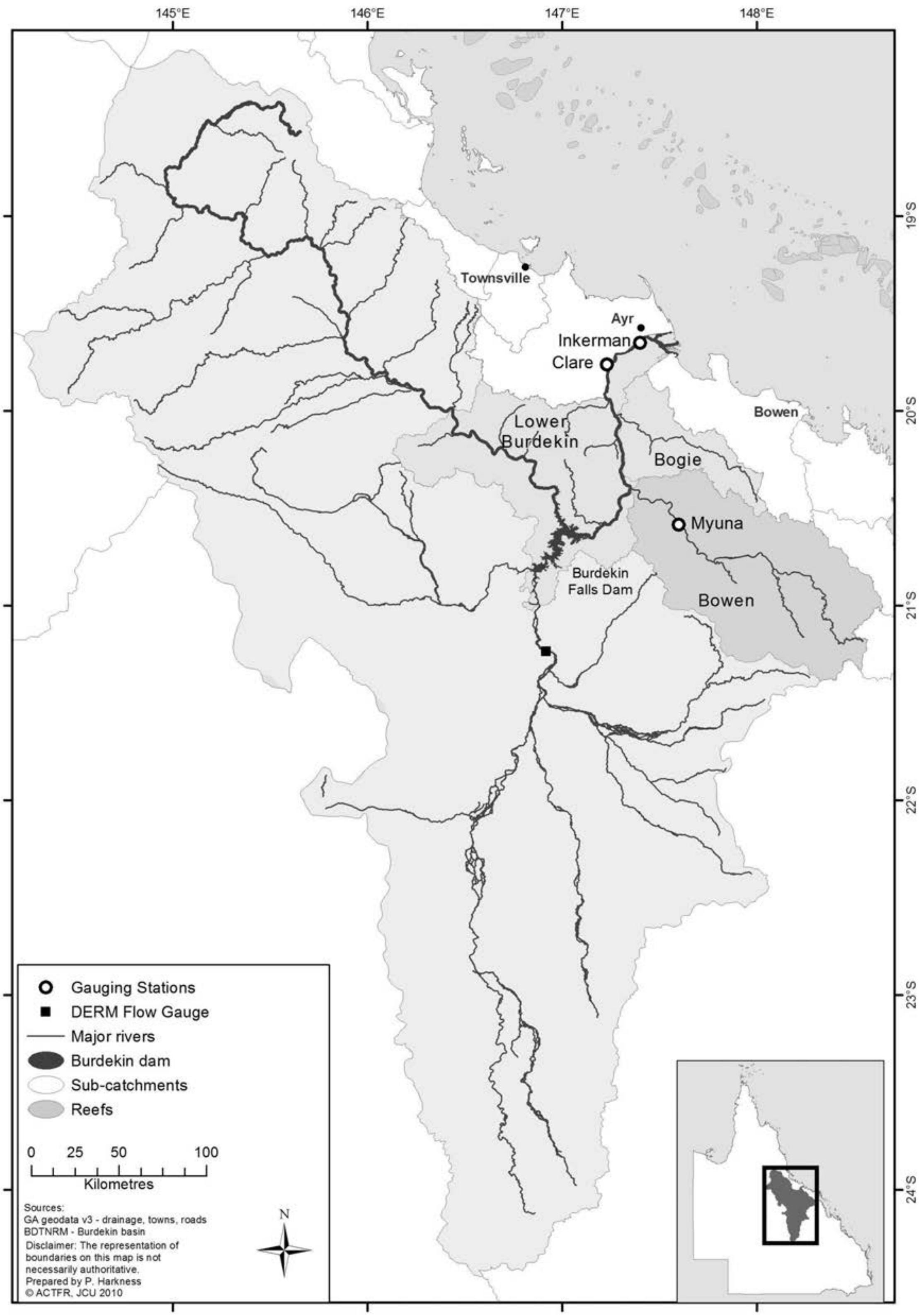

Figure 1. Map of the Burdekin catchment showing the Inkerman Bridge sampling site where total suspended sediment (TSS) samples were taken for this study. Flow samples were collected at the Inkerman gauge at Ayr.

~130,000 km^2. TSS samples were collected from the surface of the river (top 50 cm of water column). Samples were collected from the center of the channel flow over the rising, peak and falling stages of the flow hydrograph as well as during base flow conditions. Particle size analysis of the routine surface TSS samples as used in this study show that they are predominantly silt and clay size fractions, with a small amount of sand which is generally less than 10% of total mass [*Bainbridge et al.*, 2012]. Measurements of suspended sediment across the cross section and through the depth profile of the Burdekin River in the vicinity of Inkerman also found that sand composes less than 10% of the TSS concentration at the surface [*Belperio*, 1979, Figures 5 and 6; *Amos et al.*, 2004, Figure 8]. Further, these two latter studies show that the surface concentrations of silt and clay in the Burdekin River are representative of the entire cross section, and thus the load estimates in the present study are considered representative of the combined silt-clay size fractions. While the concentration of sand transported in suspension does increase with depth below the water surface [*Belperio*, 1979], sand load is not of interest for assessing TSS impacts beyond its point of deposition near the river mouth.

[9] The samples were cooled and transported to the laboratory for analysis. The samples have been collected through a number of programs and research providers over the 24 year period by the Australian Institute of Marine Science, the Queensland Department of Environment and Resource Management (DERM: both surface water data archive and GBR Loads Monitoring programs), University of Queensland and North Queensland Dry Tropics NRM. The sampling design for most of these programs was developed to calculate suspended sediment export from the Burdekin River and as such samples collected were biased toward high flows, when the vast majority of annual flow is discharged. However, the data archive in the DERM program targeted baseline flows. Figure 2 shows the TSS samples collected along with the temporal coverage of flow spanning 24 years of monitoring at the Inkerman Bridge site on the Burdekin catchment.

[10] While TSS analysis was performed at a number of laboratories, the same standard method was applied. Samples were filtered through preweighed filter membranes, oven-dried and reweighed to determine the dry TSS weight as described by *American Public Health Association* [2005]. TSS (in mg L^{-1}) was calculated by dividing the mass of the retained matter (in mg) by the volume of sample filtered (in L).

[11] Figure 3 shows the bias incurred from the sampling of concentration and flow for the Inkerman Bridge site on the Burdekin catchment. The relative bias in concentration was calculated by dividing the average flow recorded at concentration samples by the average flow recorded at regular time intervals. Note, if there are gaps in flow, the flow record will need to be infilled to a regular time series using a Hermite spline interpolation [*Fritsch and Carlson*, 1980] or equivalent. Similarly, the relative bias in flow was obtained by dividing the average observed flow by the average regularized flow. Since the flow was continuously measured the bias between predicted and observed flows was 1 (and thus no bias). Concentration however, is measured at irregular intervals with relative biases varying

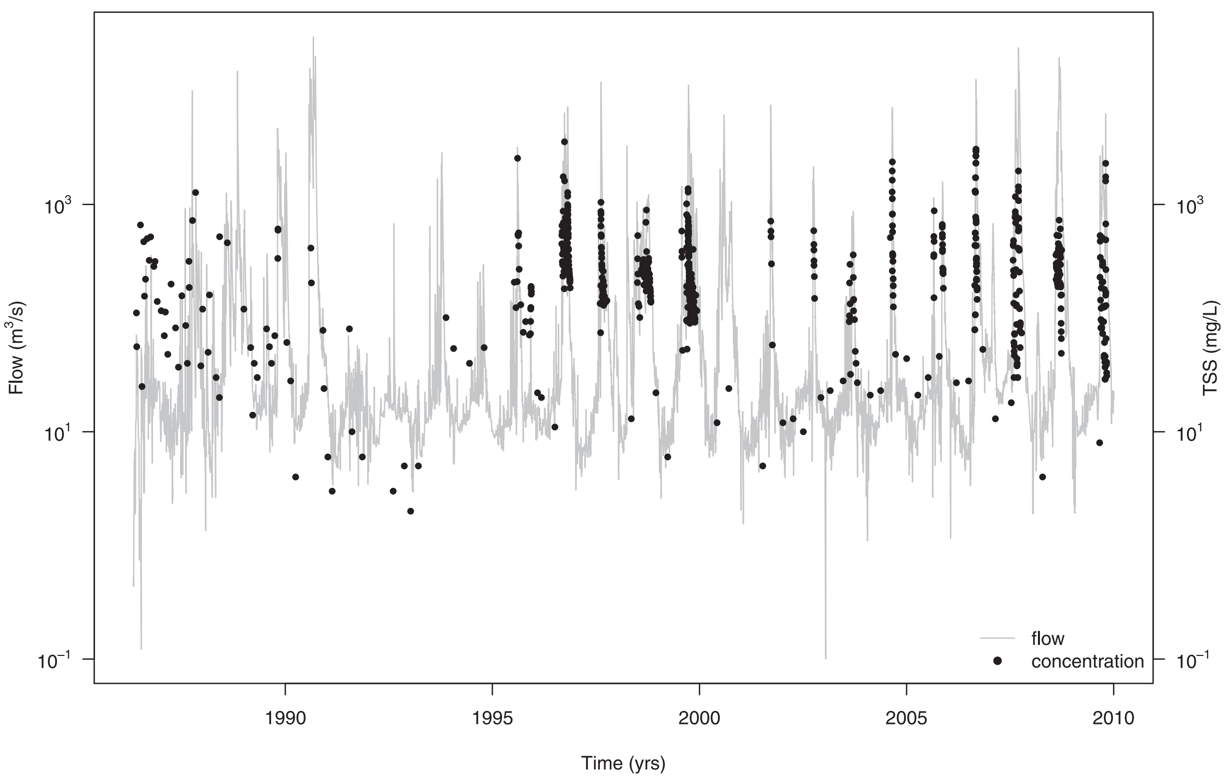

Figure 2. Observed flow (gray line) overlayed with TSS samples (points) showing the temporal coverage of data collected at Burdekin River at Inkerman Bridge between 1 October 1986 and 30 September 2010.

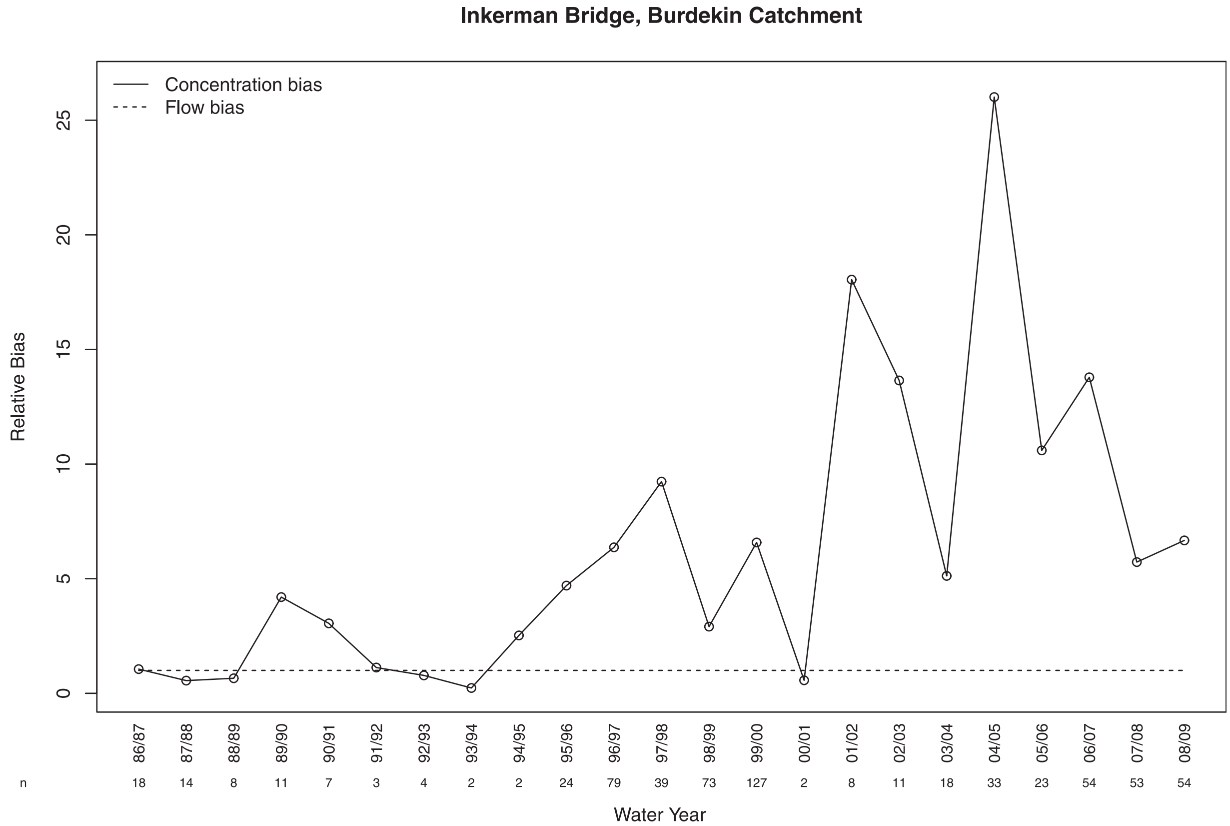

Figure 3. Summary of biases in flow (dashed line) and concentration (solid line) in TSS across water years for the Inkerman Bridge site in the Burdekin from 1973 to 2009. Sample sizes for each water year are shown beneath the x axis labels. Values above and below 1 indicate biases upward and downward, respectively.

between 0.01 and 26 across all water years, indicating substantial bias in concentration sampling, particularly during the later years where monitoring was restricted to high-flow discharge events only.

3. Quantifying Loads in the Burdekin River

[12] The LRE is built around a four-step process consisting of estimation steps for flow, estimation steps for concentration, estimation of the load including evaluation of model structure and calculation of the variance that incorporates errors in both concentration and flow [*Wang et al.*, 2011]. As flow at the Inkerman Bridge site is measured at regular intervals (hourly) from the Clare gauge (120006B) 15 river km upstream of Inkerman Bridge, no interpolation of the flow record is necessary and we concentrate on estimation steps for concentration and the corresponding load and variance estimates. Furthermore, we focus on the extensions of the LRE that are applicable for the case study presented.

3.1. A Predictive Model for Concentration

[13] The LRE methodology fits a GAM [*Wood*, 2006] to concentration (on the log scale) over the duration of the monitoring data. The model incorporates key hydrological processes of a river system (some of which are highlighted by *Morehead et al.* [2003]), through terms created from flow data with the aim of reducing the unexplained variance. The GAM introduces flexibility into the model by way of temporally smooth terms that are driven by the data.

[14] The GAM is composed of two components. The first includes terms that enter into the model linearly, while the second incorporates flexible (smooth) terms driven by the data. The model is considered semiparametric because of the inclusion of smooth terms in the model (second summation) and is represented mathematically as

$$\log(c_i) = \beta_0 + \sum_{k=1}^{p} \beta_k x_{ki} + \sum_{k=1}^{m} s_k(z_{ki}) + \varepsilon_i \qquad (1)$$

where x_{ki} and z_{ki} are covariates measured at the ith sample and $s_k(\cdot)$ represents a spline that fits a flexible function to the data. The basic suite of terms we consider in any base model include linear (x_{1i}) and quadratic terms (x_{2i}) for flow, to capture nonlinearity in the relationship between flow and concentration; a rising or falling limb term (x_{3i}), represented by a categorical variable that reflects concentration differences between the rising (+1), falling (−1) or stable (0) sections of hydrograph cover of an event; a cyclic term (z_{1i}) that captures seasonal effects throughout a water year; and a smooth discounting term (z_{2i}) that represents the effect of recent prior flow volume on concentration as an attempt to mimic exhaustion and hysteresis properties of the hydrological system. These base terms are all described by *Wang et al.* [2011]. Although arbitrary trend terms could be explored [*Wang et al.*, 2011] and these often explain considerable amounts of unexplained variation in the data, we suggest they be omitted from the analysis and include only terms that have a direct interpretation. That is, terms that could be interpreted easily by managers (e.g., changes to vegetation, land use and land structure) and therefore be used to determine necessary changes to the landscape that may reduce loads.

[15] In developing a predictive model for the Burdekin end of river site, we begin with the suite of base terms highlighted by *Wang et al.* [2011] and identify those terms important in describing the relationship between concentration and flow, which lead to the final predictive model. Although these terms have been described elsewhere [*Wang et al.* 2011], we provide a brief description of their meaning in the context of the case study presented here for ease of interpretation and highlight differences to the *Wang et al.* [2011] implementation where necessary.

3.1.1. Linear and Quadratic Terms for Flow

[16] The relationship between concentration and flow on the log scale is often linear or quadratic in terms of its shape and has been explored in the literature [*Belperio*, 1979; *Cohn*, 1995; *Cohn et al.*, 1992]. Figure 4 shows the relationship between TSS concentration and flow (log scale) for 692 samples taken at the Inkerman Bridge site on the Burdekin River. A loess smoother is overlayed to highlight linear and quadratic features of the relationship between concentration and flow, showing more than 2 orders of magnitude (log units) increase in concentration as the size of the flow increases. Inclusion of a quadratic term for flow in the model is therefore important.

3.1.2. Rising-Falling Limb

[17] The rising and falling limbs are periods of increase or decrease of flow over time during an event. The movement of concentration can behave differently during these flow stages and can be higher on either the rise or the fall, the nature and timing of the event and hydrological characteristics of the catchment [e.g., *Nistor and Church*, 2005; *Morehead et al.*, 2003]. Larger events have the capacity to move higher TSS concentrations, and can display more systematic concentration differences between rising and falling limbs (Figure 5). Therefore, we represent rising-falling limb behavior for events peaking above the 90th percentile flow in each water year, as shown in Figure 6a. On average, at the Burdekin site 67% of flow volume occurred above the 90th percentile in each water year. The 90th percentile, q^{90} is used as a trigger for the rising-falling limb term, x_{5i} which is a categorical variable as shown in equation (2) that indicates flow on the rise (+1), fall (−1) or flat (0), where the latter may also be an indication of base flow conditions. Figure 6b shows the resulting contribution of TSS concentration for the Inkerman Bridge site (estimate and 95% confidence intervals) from samples located on the rise or fall of an event in the Burdekin River and indicates a lack of significance as both bars cross the baseline at 1. Although this

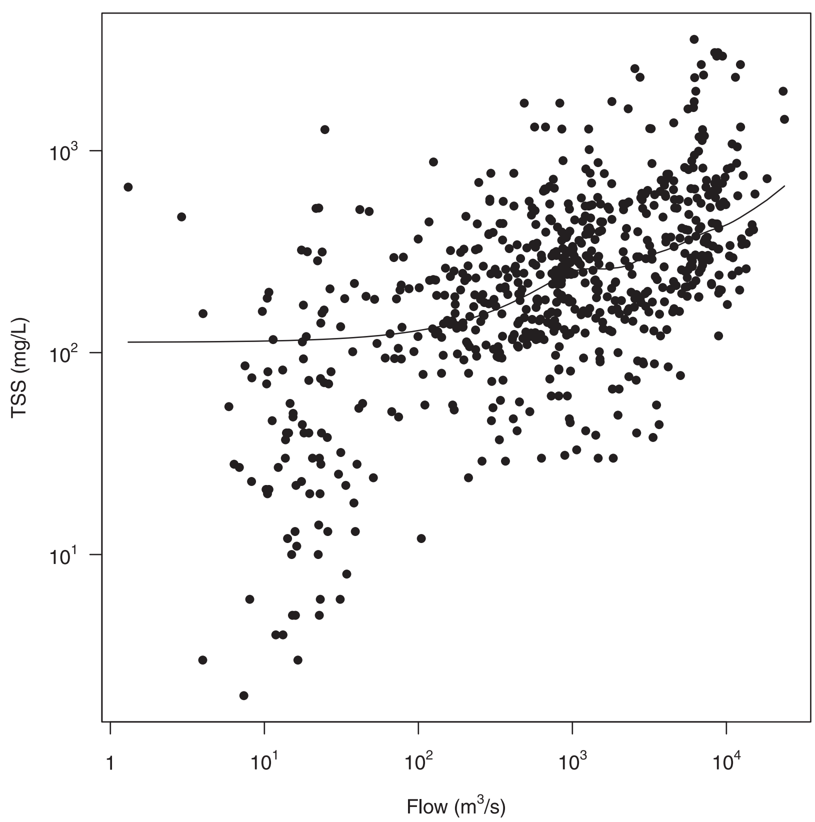

Figure 4. Relationship between TSS and flow for the Burdekin site at Inkerman Bridge with a loess smoother overlayed across the points.

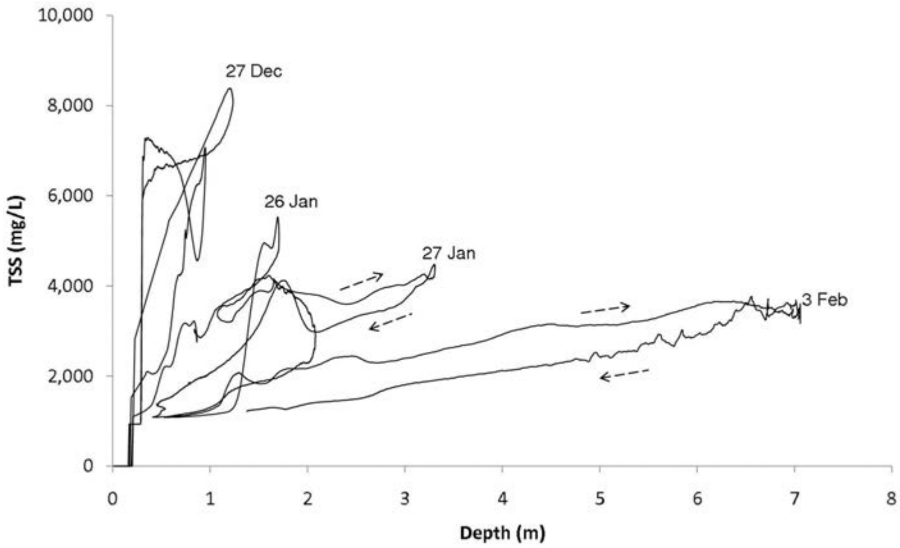

Figure 5. Total suspended solid concentration as estimated by a turbidity probe calibrated to measured concentrations, plotted against flow depth, for the Bowen River at Myuna, a tributary of the Burdekin River (location shown in Figure 1). The event peak concentrations declined through the wet season, suggesting decline or exhaustion of sediment availability. In events above the 2 m stage, concentration was consistently higher on the rising limb than on the falling limb.

term can be important in a baseline model for many river systems, for the Burdekin, it is shown to be insignificant.

$$x_{3i} = \begin{cases} 1 & \text{if } \hat{q}_i > \hat{q}_{i-1} \text{ and } q_i > q^{[90]} \\ -1 & \text{if } \hat{q}_i < \hat{q}_{i-1} \text{ and } q_i > q^{[90]} \\ 0 & \text{otherwise} \end{cases} \quad (2)$$

3.1.3. Cyclic Seasonal Terms

[18] Intra-annual variations in concentration can be important aspects of behavior in many climate zones, including tropical rivers like the Burdekin River. Here, tropical weather systems are prevalent during summer months, producing heavy rainfall that causes sediment erosion and transport through the watershed, resulting in the bulk of annual suspended sediment export to the GBR lagoon. We fit a seasonal term using a cyclic cubic regression spline to ensure that a smooth function of time fit across the year does not change discontinuously at the end of the year [*Wood*, 2006]. Note, this is a different representation to that used by *Wang et al.* [2011] that is more flexible, allowing the data to define the peaks and troughs through seasons. The cyclic spline was achieved by positioning 10 spline knots (locations in time where a change in concentration is likely to occur), equally spaced across the 12 months of the year to estimate the contribution of the seasonal term in the GAM as shown in Figure 7 using data from the Inkerman Bridge site. Peaks in TSS concentration are noted for November–December and April–May with declines noted between July–September. The decline from December to February occurs during the wet season when the majority of large events occur. This indicates dilution of concentration by volume of water, and/or exhaustion of the sediment supply from within the catchment. Concentrations in the Bowen River tributary of the Burdekin River also illustrate such a decline during the middle of the wet season (Figure 5). Inclusion of such a term in the final model for concentration is therefore advantageous.

3.1.4. Smooth Discounted Flow

[19] The discounted flow term z_{2i} represents a simple exponential weighting of flow history designed to allow the recent prior flow volume to influence concentration predictions. The term is expressed as

$$\begin{aligned} z_{2_i} &= s\{\log[\gamma_i(\delta)]\}, \\ \gamma_i(\delta) &= d\kappa_{i-1} + (1-\delta)\hat{q}_{i-1}, \end{aligned} \quad (3)$$

and $\kappa_i = \sum_{m=1}^{i} \hat{q}_m$ for discount factor δ, where κ_i represents the cumulative flow up to the ith day. As the discount variable δ approaches 1, the discounting term, γ becomes a cumulative summation of flow over the entire monitoring period. Conversely, as δ approaches 0, γ mimics the original flow time series. Choosing a value for δ between 0 and 1 therefore produces a discounting term that represents a mixture of the original flow series and a cumulative one, where δ represents the level of mixing or smoothing between the two (Figure 8). Including more than one discounting term in the model can therefore capture complex processes like hysteresis between events, where the movement of concentration at a particular point in time is related to past events and therefore exhibits a lag, for example, higher concentrations occurring following a dry period. The movement of concentration can also be affected by periods of exhaustion, where multiple large events reduce TSS availability into the system. Table 1 presents a range of discounting levels and shows that as the discount decreases, past events have little bearing on the current event. Figure 9 shows the contribution of four discounting

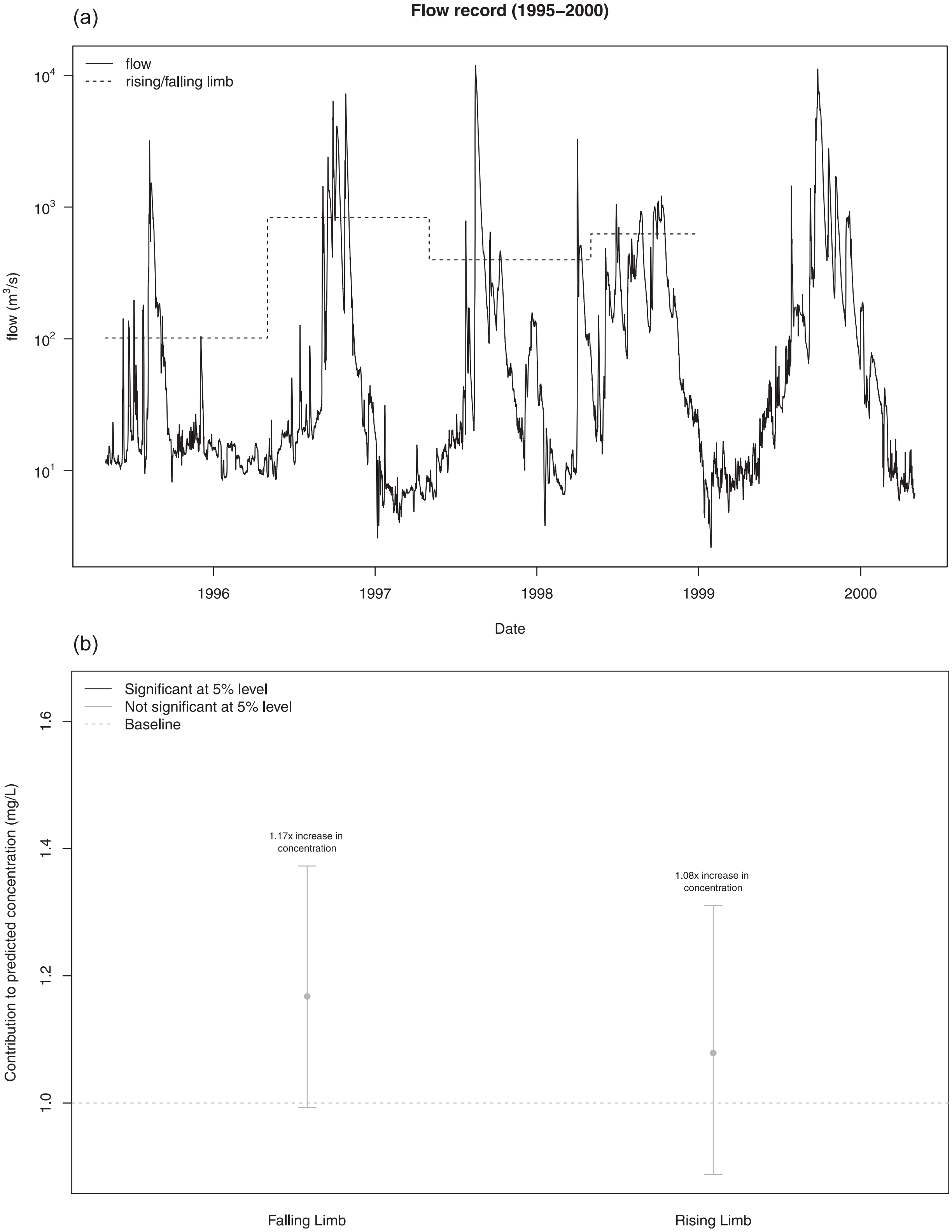

Figure 6. Construction of the rising-falling limb term and its contribution to sediment concentration in the loads regression estimator (LRE) model. (a) The rising-falling limb overlayed on top of a flow record (log scale) based on a 90th percentile cutoff determined for each water year between 1995 and 2000 to capture large events. (b) The estimated contribution (circles) of concentration from the fall or rise of an event with 95% confidence intervals. Baseline levels are indicated by a dashed gray line drawn at 1. Levels of increase or decrease are reported at the top of each bar.

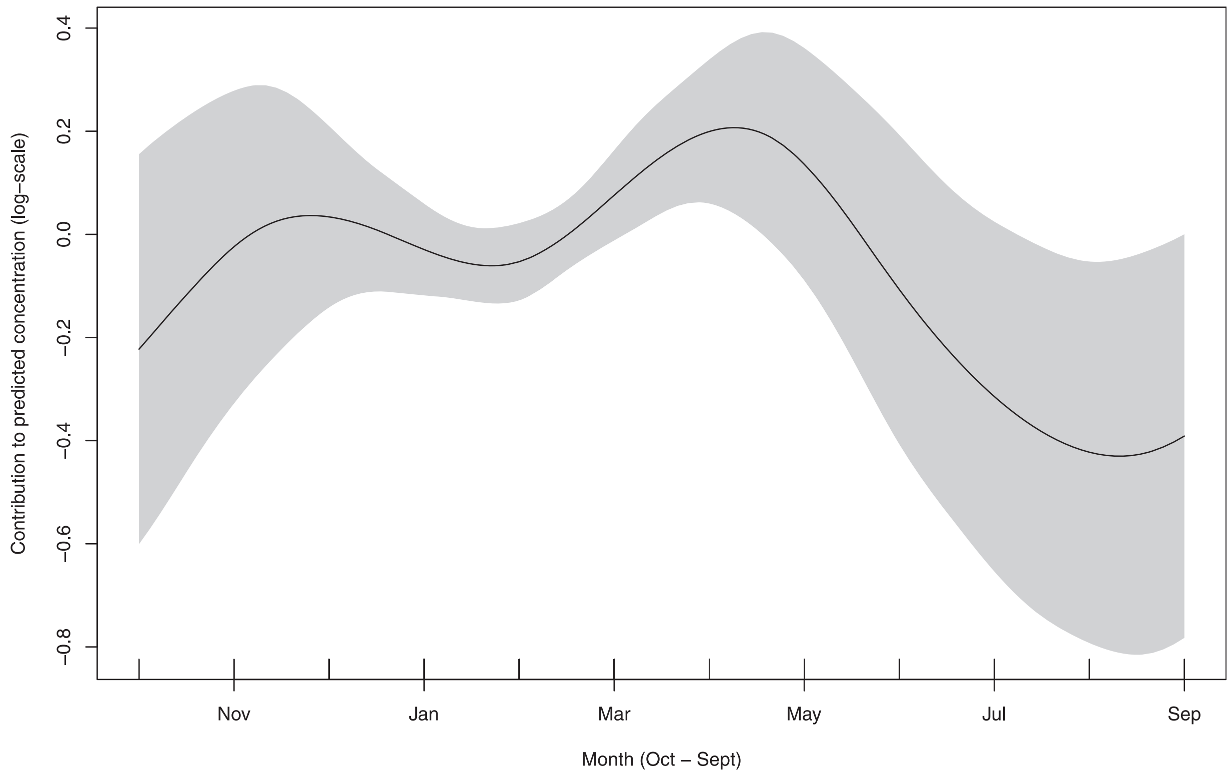

Figure 7. Seasonal term with 95% confidence intervals (shaded) showing the variation in TSS concentration (log scale) over a water year (October–September) at the Inkerman Bridge site in the Burdekin River.

terms fit in the one model for TSS concentration at the Inkerman Bridge site in the Burdekin River. In Figure 9a for example, TSS concentration increases linearly with increasing flow assuming a small flow discounting term. However, as $\delta \rightarrow 1$, flow accumulates producing a decrease in predicted TSS concentration at high flow (Figure 9d). The inclusion of more than one discounting term may therefore be appropriate and should be tested in the model. For the Burdekin model, all four terms were included.

3.1.5. Additional Covariates

[20] As is often the case, the base model may not be sufficient for every type of river system encountered, particularly if multiple years are being examined. Complex relationships may exist, particularly in variable river systems like the Burdekin where drought breaking years are not uncommon. In these instances, additional terms need to be investigated to explain the temporal variations in concentration. These variables may represent additional terms extracted from the hydrograph such as the rate of change (representing a surrogate for the rainfall intensity), or pollutant sources (e.g., total flow or proportion of flow arising from subcatchments), spatial structures (e.g., a dam) or terms that capture antecedent conditions and possible management intervention (e.g., ground cover and vegetation). Although the inclusion of such terms may only explain a small proportion of the variance in a model, their input can be valuable because of their ability to explain complex processes.

[21] To accommodate the complex features inherent in variable river systems like the Burdekin, we incorporated two additional covariates. The first of these investigated the ratio of flow from above and below the Burdekin Falls Dam, as the contributions from various subcatchments in the Burdekin can lead to considerably different suspended sediment loads because of different geology and soil types, stream and catchment characteristics (e.g., slope, bank heights, vegetation types, gully density, etc.), and the effect of the dam on trapping sediment from upstream. We obtained hourly flow data from the Burdekin River at Hydro site (gauge 120015A) which represents the flow contribution from the catchment area (115,000 km^2) above the Burdekin Falls Dam. We computed the ratio of this flow with the total flow occurring at the Burdekin River at Clare gauge, which represents the end-of-catchment site. This ratio is sometimes greater than 1 as some water is lost because of water offtake for irrigation in the lower Burdekin sugarcane industry during the relatively dry water years.

[22] The second covariate considered was dry-season vegetation cover for the catchment as it is well known that poor vegetation ground cover can lead to an increase in soil erosion [*McIvor et al.*, 1995; *Scanlan et al.*, 1996] and therefore an increase in TSS loads. Vegetation ground cover data (*Scarth et al.* [2006]), in the form of an annual (end of dry season) ground cover index (GCI) for 52 subcatchments of the Burdekin were obtained from the Department of Environment and Resource Management (Queensland Remote Sensing Centre). The GCI estimates the percentage of plant material (dead or alive) that is covering underlying soil or rock material, through a known statistical relationship between measurements of cover made by satellite sensors calibrated to

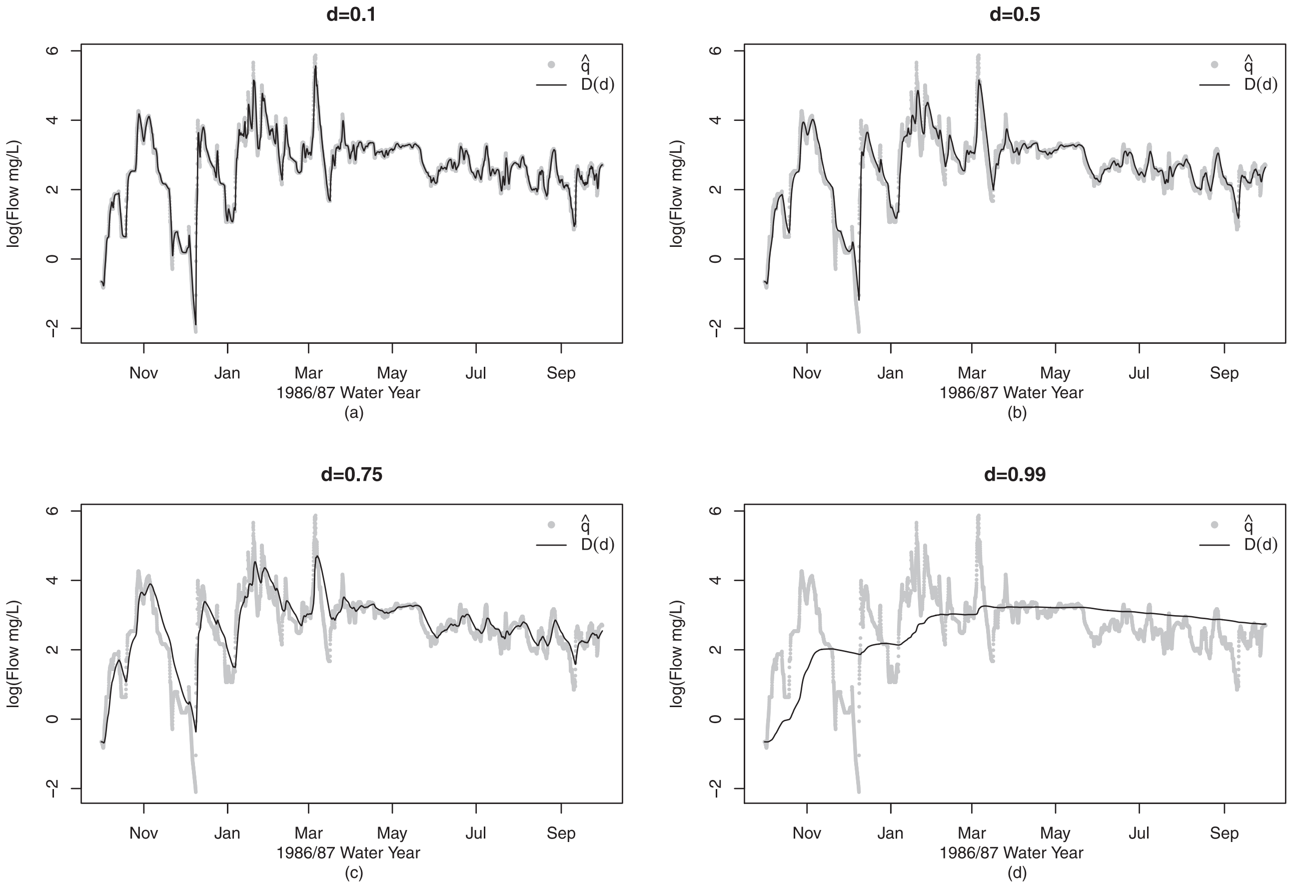

Figure 8. Illustration of different levels of discounting of flow, $\hat{q}$ for a sample water year (1986/1987) collected at Inkerman Bridge in the Burdekin River using discounts of (a) $\delta = 0.1$ (equivalent to the original flow), (b) $\delta = 0.5$ (minimal smoothing), (c) $\delta = 0.75$ (moderate smoothing), and (d) $\delta = 0.99$ (equivalent to the cumulative flow over the water year). The discounted term $\gamma(\delta)$ is overlayed as a black line.

field-based observations [*Schmidt et al.*, 2010]. We extracted the median GCI value across the Burdekin catchment for each year of the study period to be used as an input into the model.

3.2. A Model for Inkerman Bridge

[23] We fitted the base LRE model to data from the Inkerman Bridge site on the Burdekin River and investigated significant model terms using backward elimination. Additional discounting terms and covariates consisting of a vegetation term and the contribution of flow from above the dam were fit after the base model was identified and their significance was evaluated using the generalized cross-validation criterion (GCV) and p values for each term. Terms were eliminated that had the largest p value and therefore, decreased the GCV. The GCV is a criterion similar to ordinary cross validation but with better computational properties. It is used in this instance to evaluate the performance of spline-based terms in a GAM to identify the optimal set of knots and therefore the level of smoothness required to achieve a good fit without creating a model that is too complex.

Table 1. Summary of Discounting Values Used in the Exponential Weighting of Flow History That Can Be Chosen to Reflect How Much Weight of the Current Flow Is due to Flows That Occurred in the Past

Discount Percent	Days Until 50% of Weight of Current	Days Until 5% of Weight of Current
99%	69	>100
95%	14	59
90%	7	29
75%	3	11
50%	1	5

[24] Diagnostics were then examined to determine the fit of the model and whether there were any serious departures from normality. Among the standard diagnostics, we examined stationarity. That is, whether the residuals were autocorrelated and if present, we refitted the model with an AR1 term to capture the correlation between sampling times (i.e., how much of the concentration at time t is related to the concentration measured at $t - 1$) using generalized least squares [*Pinheiro and Bates*, 2000] and estimated the variance-covariance matrix accordingly. The LRE model was fit using the R programming language [*R Development Core Team*, 2005], making use of the mgcv [*Wood*, 2006] and nlme [*Venables and Ripley*, 1998] packages. Details regarding the code can be obtained from the first author.

[25] The values of each term in the final model, which explained approximately 71% of the variation in the data are shown in Table 2 and include linear and quadratic terms for flow, vegetation cover, the ratio of flow above the dam,

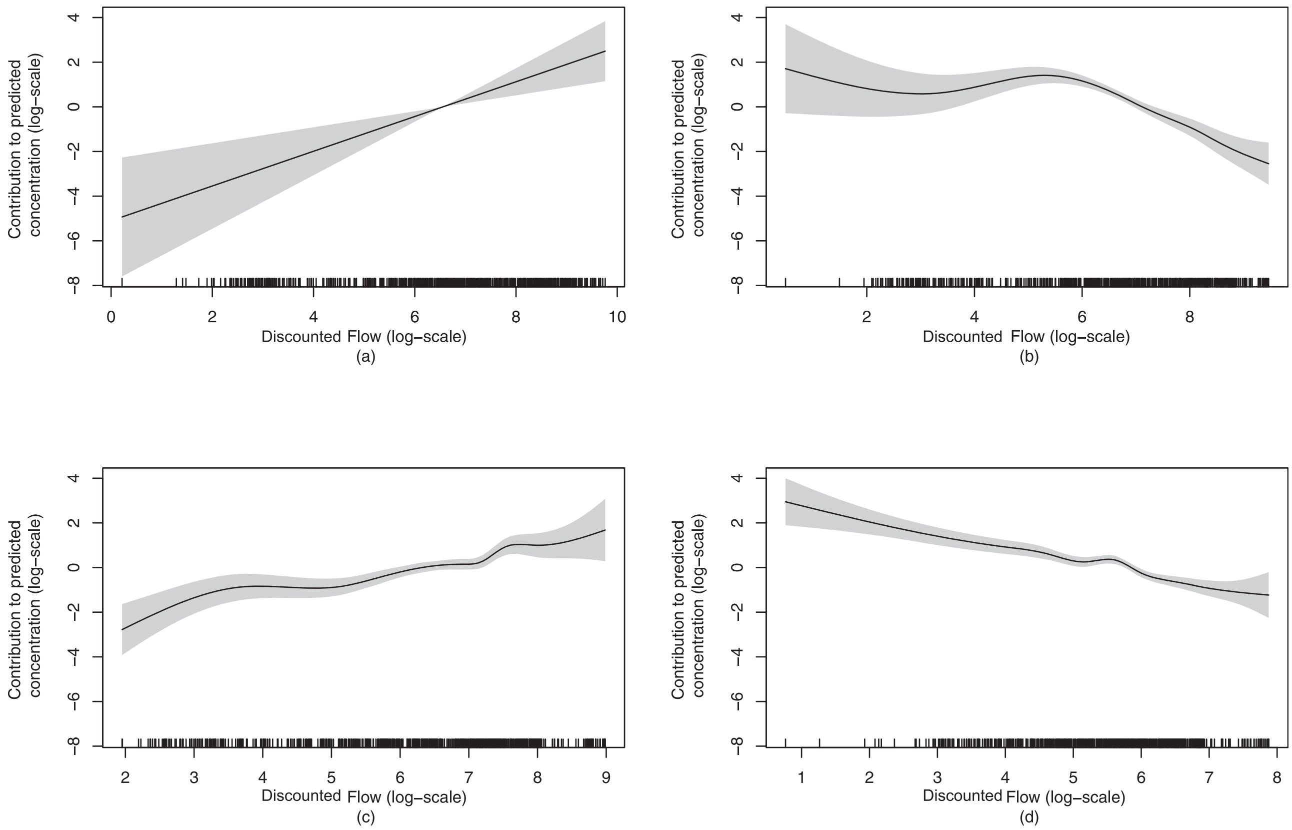

Figure 9. Smooth discounting terms fit to TSS concentrations (log-scale) at the Inkerman Bridge site in the Burdekin River computed for (a) $\delta = 0.1$, (b) $\delta = 0.75$, (c) $\delta = 0.95$, and (d) $\delta = 0.99$. Shaded regions in each figure indicated 95% confidence bounds on the estimates. A rug plot is shown at the base of each plot to indicate the distribution of data available.

a seasonal term and multiple discounting terms to capture hydrological features of the system. In this example, the correlation estimated from the autoregressive process is estimated to be 0.97, indicating quite strong correlation between concentration measurements taken from one time point to another. As the rising-falling limb term was not significant (p value >0.05) it was therefore not included in the final model. Table 3 shows a subset of models explored before identifying the optimal model. Model 1 fits all the terms in the model, while models 2–4 represent additional fits from a backward elimination that omits the term that contributes the least in terms of the percent variation explained and GCV value. These models are compared with the *Wang et al.* [2011] model (model 5) and a simple representation of concentration and flow (model 6). The results indicate the large contributions made by the inclusion of the hydrological terms outlined in *Wang et al.* [2011] (17.5%) and the inclusion of additional discounting terms (12.1%) introduced in this paper. The addition of vegetation cover and the contribution of flow from upstream sites provide an additional 4%.

Table 2. Parameter Estimates for the Fixed Effects, Smooth Terms, and Correlation Term Resulting From the Fitted Loads Regression Estimator (LRE) Model to the Inkerman Bridge Site in the Burdekin Catchment

Parameter	Estimate	Standard Error	p value
Intercept	12.280	1.195	<0.001
Log(flow)			
Linear	−1.464	0.249	<0.001
Quadratic	0.111	0.014	<0.001
Vegetation cover	−0.021	0.003	<0.001
Ratio of flow above dam	−0.977	0.186	<0.001
Smooth Terms	**Effective Degrees of Freedom**		**p value**
Seasonal			
s(month)	4.252		0.014
Discounting terms			
$s(d = 0.1)$	1.001		<0.001
$s(d = 0.75)$	6.073		<0.001
$s(d = 0.95)$	8.763		<0.001
$s(d = 0.99)$	8.035		<0.001
Correlation (AR1(ϕ))	0.9723		

[26] Of major interest in this model are the two additional covariates. The inclusion of vegetation cover indicated a significant decrease in TSS concentration as vegetation cover increases (i.e., 2.1% decrease per percentage increase in vegetation cover). Furthermore, for every unit increase in flow above the dam, we observe a significant decrease in TSS concentration (up to 38%). Although the inclusion of these terms explains only an additional 4% of the variation, they provide an explanation of the decrease in loads observed during the 1996/1997 and 1997/1998 water years, when consistent high volumes of flow entered the system but a much smaller load resulted in the latter of the two years. Similarly,

Table 3. Comparison of a Subset of Models Fit to the Inkerman Bridge Site, Burdekin River[a]

Model	Explanation	GCV	Percent Variation Explained	Percent Contribution
1. Intercept + flow terms + limb + seasonal + flow discount terms + vegetation cover + ratio of flow above dam	Base model (5) + additional discounting terms and covariates	0.409	71.3%	0.2%
2. Intercept + flow terms + seasonal + flow discount terms + vegetation cover + ratio of flow above dam	Model 1 − limb	0.409	71.1%	2.0%
3. Intercept + flow terms + seasonal + flow discount terms + ratio of flow above dam	Model 1 − limb − vegetation cover	0.445	69.1%	2.0%
4. Intercept + flow terms + seasonal + flow discount terms	Model 1 − limb − vegetation cover − ratio of flow above dam	0.472	67.1%	12.1%
5. Intercept + flow terms + limb + seasonal + flow discount term	Base model [*Wang et al.*, 2011]	0.607	55.0%	17.5%
6. Intercept + flow terms	Simple flow representation	0.808	37.5%	–

[a]Each model is accompanied by the generalized cross-validation (GCV) score, the percentage of variance explained by the model, and the percent contribution from the inclusion or exclusion of particular terms in each model. Model 2 is the final model used.

the load estimated in the 2008/2009 water year was 27% lower when compared to the load estimated in 2007/2008 despite the annual flows being within 6%.

[27] An interesting feature in Figure 10b is a possible cyclic pattern observed in the annual mean concentration, showing higher TSS loads in 1987/1988, 1996/1997, 2004/2005 and 2005/2006. Although we could not explicitly explain the higher loads during these periods with specific climatic terms in the model e.g., effects due to El Niño or La Niña cycles, it was hypothesized that major cyclones crossing the North Queensland coast, affecting areas around Innisfail (1986, 2006: Tropical Cyclones Winifred and Larry), Bowen (1988: Tropical Cyclone Charlie), Cairns/Townsville (1997: Tropical Cyclone Justin) (Bureau of Meteorology, Previous tropical cyclones, http://www.bom.gov.au/cyclone/history/index.shtml2011) and therefore impacting on the Burdekin catchment, could be the main contributor.

3.3. Estimating the Load and Quantifying the Variance

[28] The estimation of load in each water year involves multiplying the flow measured at regular time intervals by the concentration predicted at each regularized flow value and then summing over the water year. An expression of the load in any one water year is

$$\hat{L} = K \sum_{m=1}^{\mathrm{M}} \hat{c}_m \hat{q}_m \exp(\sigma_m) \quad (4)$$

where K is a unit conversion constant for producing a load in tons given concentration is measured in milligrams per liter (mg L^{-1}) for TSS and flow is measured in cubic meters per second, $\hat{q}_m$ and $\hat{c}_m$ represent predicted regularized flow and concentration at regular time, m, and $\exp(\sigma_m)$ represents the standard bias correction term for operating on the log scale. See *Wang et al.* [2011] for details.

[29] The expression shown in equation (5) incorporates errors in the flow rates that the user can provide in the form of a coefficient of variation, α_1 and α_2 [*Wang et al.* 2011].

$$\begin{aligned}\mathrm{var}(\hat{L}|\hat{C},\hat{Q}) &= \mathrm{trace}\{\mathrm{var}(\hat{\beta})X^T PP^T X\} \\ &+ \alpha_1^2 \sum_m \hat{l}_m^2 \{1 + \partial f/\partial \log \hat{q}_m\}^2 + \alpha_2^2 \{1 + \partial f/\partial \log \hat{q}_m\}^2\end{aligned} \quad (5)$$

For completeness, we outline the components of the variance expression. In equation (5), $P = (\hat{l}_1, \hat{l}_2, \ldots, \hat{l}_M)$, represents a vector of loads estimated for each regular time interval, m, $\hat{l}_m = K\hat{c}_m\hat{q}_m \exp(\sigma_m)$ and $f(\hat{Q}) = \beta X$, where M represents the maximum number of time intervals. The second term in equation (5) represents an error due to the spatial positioning of the gauge, while the third term represents a relative measurement error in the flow rate. A brief summary of the variance calculation is provided by *Wang et al.* [2011], however, the complete derivation of this expression is contained in the auxiliary material.[1] The calculation of the $(1-\alpha)$% confidence intervals can then be achieved in the usual way by taking $\exp\left(\hat{L} \pm v_{\alpha/2}\sqrt{\mathrm{var}(\hat{L})}\right)$ where α represents the significance value that you wish to attain and $v_{\alpha/2}$ represents the percentage point from a normal distribution for a given level of significance.

[30] The loads methodology produces a total load, in tons, for each water year. To facilitate the comparison of loads through time a method of standardizing the load to provide an annual flow-weighted mean concentration is required. We derive the flow-weighted concentration along with an expression of the variance.

[31] Let $\hat{L}_w$ represent the load in millions of tons calculated for a water year, w using the expression shown in equation (5) and let $\hat{F}_w$ represent the total volume of flow in mega liters occurring in a water year. We constructed an annual flow-weighted mean concentration, A_w by dividing the total load by the total volume of flow and multiplying by the necessary constant λ to obtain a result in mg L^{-1},

$$A_w = \lambda \hat{L}_w / \hat{F}_w \quad (6)$$

with corresponding variance

$$\mathrm{Var}(A_w) = \frac{\lambda^2}{\hat{F}_w^2}\mathrm{Var}(\hat{L}_w) \quad (7)$$

Confidence intervals can be computed accordingly

[32] The resulting estimates of loads are shown in Figure 10 and Table 4. Figure 10a shows the TSS load estimates (squares) and 80% confidence intervals for each water year, accompanied by the total volume of flow observed in that water year as a bar plot to the right. Annual flow weighted mean concentrations and associated 80% confidence intervals are shown in Figure 10b.

[1]Auxiliary materials are available in the HTML. doi:10.1029/2011WR011080.

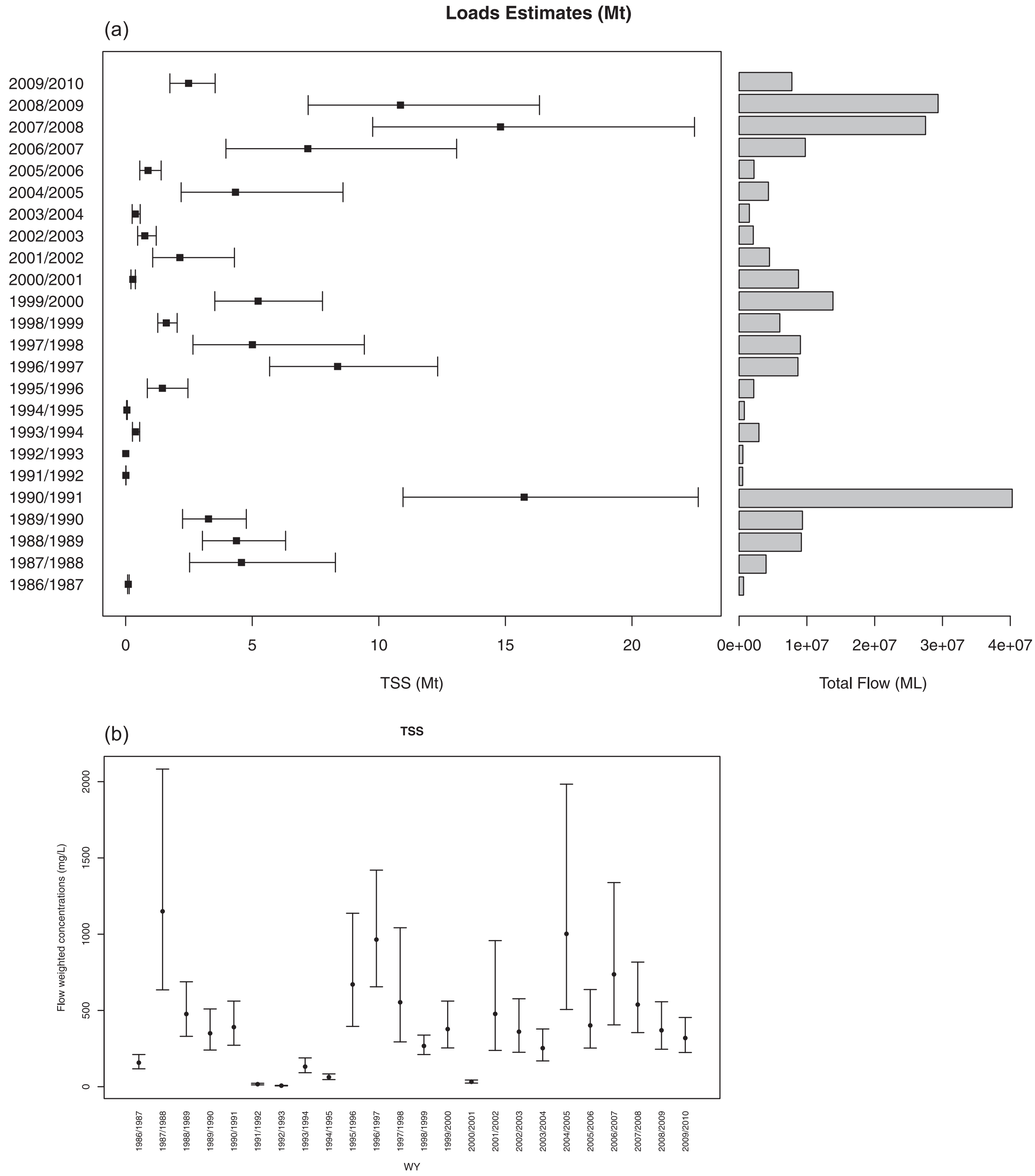

Figure 10. A summary of model estimates from fitting the LRE model to the Inkerman Bridge site in the Burdekin River showing (a) estimated TSS loads (Mt) and 80% confidence intervals produced for each water year with a corresponding bar plot showing the total volume of flow to the right and (b) the annual mean concentration (mg L^{-1}) and associated 80% confidence intervals.

[33] As a secondary analysis, we also recalculated the load estimates assuming errors in the flow rates; in particular, a 10%, 30% and 50% error related to the spatial positioning of the gauge and the measurement of flow. As expected, the results showed no change in the best estimate of load in each water year. However, the CV of load estimates in each year increased with increasing uncertainty in flow, as expected (Figure 11).

4. Validation of Model and Load Estimates

[34] We used k-fold cross validation [*Efron and Tibshirani*, 1993], where $k = 10$ to investigate the predictive performance of the model for the Burdekin data set. Cross validation is performed by dividing the data into k subsets of approximately equal size, fitting the LRE model k times, each time leaving out one of the subsets and predicting on

Table 4. Load Estimates Produced for Each Water Year From the Inkerman Bridge Site in the Burdekin River Using LRE[a]

Water Year w	Total Flow (ML)	$\hat{L}_w$ (Mt)	SE	CV (%)	n	$\hat{L}_w^{0.1}$	$\hat{L}_w^{0.9}$	$\hat{A}_w$ (mg L^{-1})	$\hat{A}_w^{0.1}$	$\hat{A}_w^{0.9}$
1986/1987	656,326	0.103	0.02	22.9	18	0.077	0.138	157	117	211
1987/1988	3,978,072	4.574	2.12	46.4	14	2.526	8.285	1150	635	2083
1988/1989	9,181,633	4.376	1.25	28.6	8	3.032	6.317	477	330	688
1989/1990	9,348,329	3.272	0.96	29.3	10	2.247	4.766	350	240	510
1990/1991	40,289,050	15.741	4.45	28.3	6	10.955	22.617	391	272	561
1991/1992	530,578	0.009	0.00	24.4	3	0.006	0.012	16	12	22
1992/1993	554,509	0.004	0.00	19.7	4	0.003	0.005	7	5	9
1993/1994	2,927,424	0.385	0.11	28.2	2	0.269	0.553	132	92	189
1994/1995	774,658	0.048	0.01	22.9	2	0.036	0.065	63	47	84
1995/1996	2,162,926	1.450	0.60	41.2	24	0.855	2.460	671	395	1137
1996/1997	8,679,227	8.371	2.53	30.2	79	5.686	12.324	965	655	1420
1997/1998	9,045,261	5.006	2.47	49.4	39	2.658	9.427	553	294	1042
1998/1999	6,007,503	1.605	0.30	18.4	73	1.268	2.033	267	211	338
1999/2000	13,849,068	5.232	1.62	30.9	122	3.521	7.775	378	254	561
2000/2001	8,765,625	0.283	0.07	23.8	2	0.209	0.384	32	24	44
2001/2002	4,485,247	2.141	1.16	54.3	8	1.067	4.296	477	238	958
2002/2003	2,092,792	0.755	0.28	36.6	10	0.472	1.207	361	226	577
2003/2004	1,516,142	0.384	0.12	31.4	18	0.256	0.574	253	169	378
2004/2005	4,328,213	4.338	2.31	53.3	23	2.192	8.585	1002	506	1983
2005/2006	2,199,683	0.884	0.32	36.0	23	0.557	1.401	402	253	637
2006/2007	9,768,650	7.195	3.35	46.6	52	3.960	13.073	737	405	1338
2007/2008	27,502,587	14.806	4.82	32.6	53	9.757	22.469	539	355	817
2008/2009	29,352,221	10.855	3.47	31.9	52	7.208	16.346	370	246	557
2009/2010	7,787,247	2.485	0.68	27.5	47	1.747	3.535	319	224	454

[a]Each load estimate is accompanied by the total flow (ML), the standard error (SE) of the load estimate, the coefficient of variation (CV) expressed as a percentage, the sample size (n) and lower and upper bounds ($\hat{L}_w^{0.1}$ and $\hat{L}_w^{0.9}$) corresponding to an 80% confidence interval. The average mean concentration ($\hat{A}_w$) and associated 80% confidence intervals are also presented in the last three columns and are reported to the nearest mg L^{-1} since laboratory measurements are only reported to this level of precision.

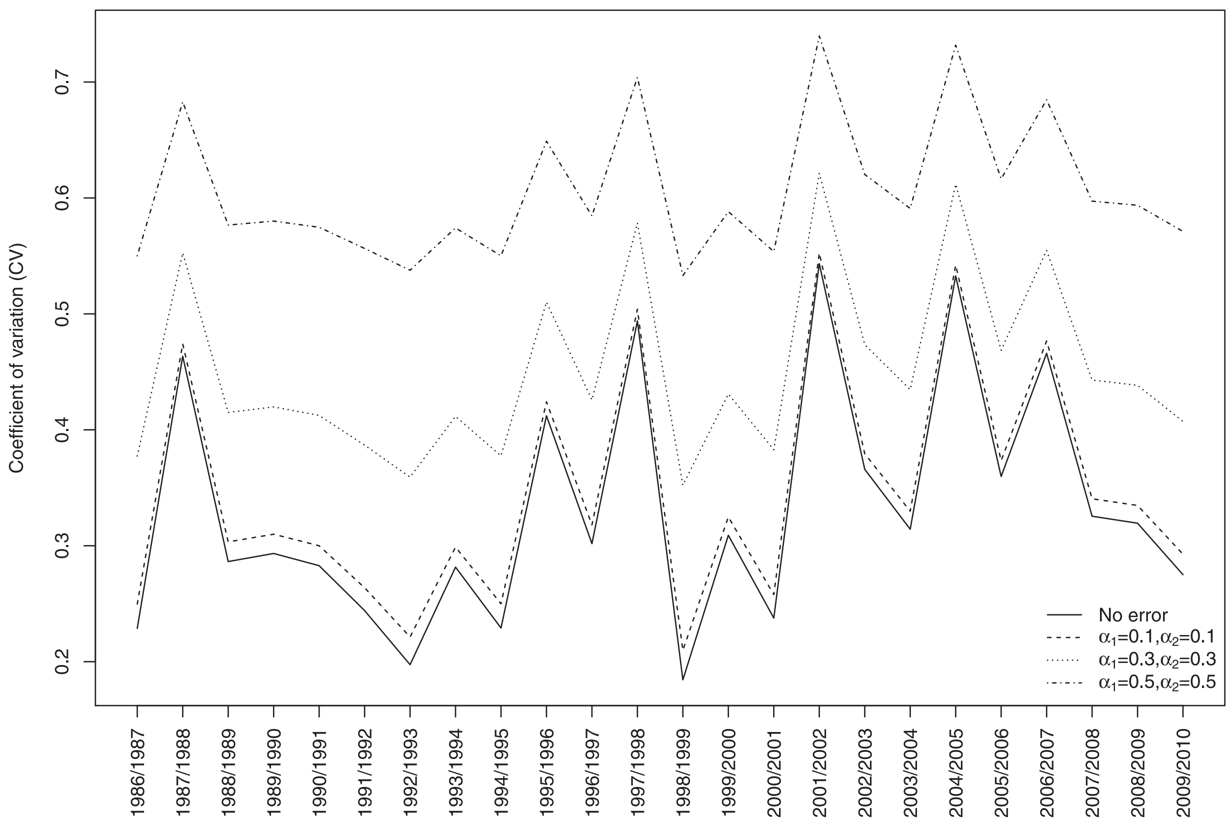

Figure 11. Coefficient of variation for the predicted loads at each water year shown for a model assuming no errors (solid line), 10% errors (dashed line), 30% errors (dotted line), and 50% errors (dot-dashed line) in the measurement and spatial location of flow gauges.

the omitted subset of data. The choice of k is typically tenfold so as to optimize the variance-bias tradeoff with values of either 10 or 20 optimally used [*Kohavi*, 1995]. For the Burdekin case study, this involves randomly selecting observations, stratified by water year to avoid unrealistic sampling scenarios where samples occur in 1 year. The LRE model was fit to the $k-1$ subsets of data with predictions formed on the k th subset. The approach has been shown to be superior to split-sample validation and is popular in machine learning and statistics applications for exploring the prediction error, a measure that determines how well a model predicts the response of a future observation. The prediction error is calculated as the expected squared difference between a future response and its prediction from the model [*Efron and Tibshirani*, 1993]. Therefore, if y_i represents the i th observed response and $\hat{y}_i^{-k(i)}$ represents the fitted value for the i th observation with the $k(i)$ th subset of data removed, then the cross-validated prediction error can be represented as $\mathrm{PE}^{\mathrm{CV}} = \frac{1}{n}\sum_{i=1}^{n}\left(y_i - \hat{y}_i^{-k(i)}\right)^2$. Errors close to 0 indicate robustness of the model to unseen observations.

[35] We implemented tenfold cross validation to the Burdekin example and produced a cross-validated prediction error in observed instantaneous concentrations of 0.464, indicating low prediction error and suggesting that the model is robust to new observations. Note, this is comparable to the GCV estimate produced for the model for the complete data set (GCV = 0.409) and reflects the close relationship between predicted and observed TSS concentrations as shown in Figure 12 (i.e., points are scattered along the diagonal).

5. Discussion and Conclusions

[36] The LRE model presents a methodology for modeling concentration to provide estimates of river pollutant loads with uncertainties with application to the Inkerman Bridge site on the Burdekin River. The method's ability to capture complex characteristics of this river system provides the ability to explain the sources of concentration changes over time and how this impacts on loads.

[37] Unlike standard methods for calculating loads, such as linear interpolation, ratio estimators and rating curves, the LRE methodology contains temporally dynamic terms which provides more credible estimates compared to steady state rating curve approaches. This is true for loads over short time periods, such as individual years, and variable

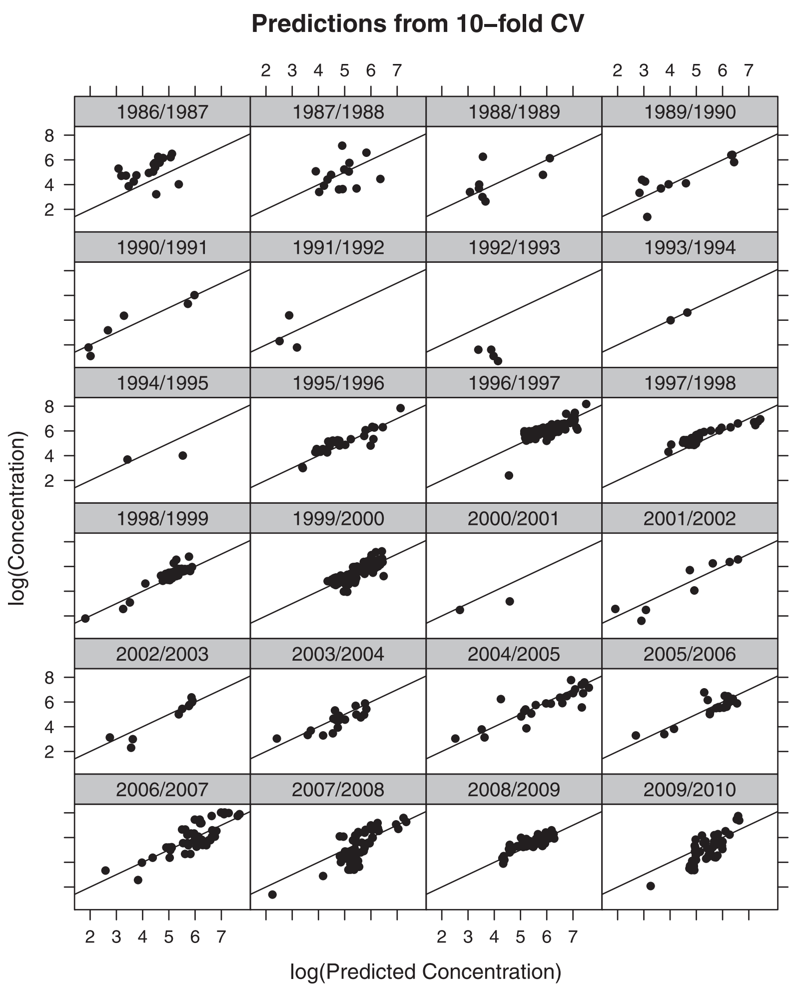

Figure 12. Results from performing tenfold cross validation showing the observed and predicted concentration in each water year.

climates where concentration is poorly predicted by flow alone. Multiple discounting terms help to represent hysteresis and exhaustion behavior evident in observed concentrations in many river systems as demonstrated by the Burdekin River. The inclusion of additional terms representing the spatial source of runoff and vegetation cover indicates that catchment conditions in 1 year influenced (reduced) the sediment load in the subsequent year. Further, the method can be applied to data independent of the sampling regime. We have also demonstrated methods for evaluating whether the terms included in the model describe the hydrological processes and adequately capture the variation and complex relationships exhibited by the system.

[38] The reliability of the model was examined through the GCV score, examination of residuals to test for stationarity and cross validation, the latter providing an estimate similar to GCV that indicates the model's ability to predict future observations accurately. The results from tenfold cross validation indicated that the model provided a reasonable fit to the data. Despite this, the load calculations in Figure 10 showed variability in loads spanning the 24 year period, with wide 80% confidence intervals for those water years exhibiting large discharges due to large rainfall events. These wide confidence intervals are the result of unexplained variation in the model. In fact, the large variations in loads and quantified uncertainties are a clear indication that the Burdekin River is a highly complex and variable river system, subjected to drought-breaking floods that lead to increases in sediment transport to the GBR lagoon [*McCulloch et al.*, 2003].

[39] Compared to the commonly used linear interpolation method, the load calculations presented by LRE are similar for the years calculated in Table 5, apart from one calculation in 2005/2006, where the linear interpolation estimate is at the lower bound the LRE 80% confidence interval. Table 5 provides some reassurance that the loads estimated by LRE are in line with standard methods but provides improved explanatory and predictive power in addition to providing confidence intervals to determine the variability in loads among years.

Table 5. Comparison of LRE and Linear Interpolation Loads Estimates for Years Spanning 1995–2000 and 2004–2010[a]

		TSS (10^6 t)		LRE 80% Confidence Intervals	
Year	Total Discharge (10^6 ML)	Linear Interpolation	LRE	Lower	Upper
1995/1996	2.16	1.5	1.45	0.86	2.46
1996/1997	8.66	6.8	8.37	5.69	12.32
1997/1998	8.97	3.5	5.01	2.66	9.43
1998/1999	5.98	1.4	1.61	1.27	2.03
1999/2000	13.32	4.0	5.23	3.52	7.78
2004/2005	4.27	2.7	4.34	2.19	8.59
2005/2006	2.00	0.5	0.88	0.56	1.40
2006/2007	8.50	6.1	7.20	3.96	13.07
2007/2008	26.50	12.3	14.81	9.76	22.47
2008/2009	29.20	9.0	10.86	7.21	16.35
2009/2010	7.79	1.9	2.49	1.75	3.54

[a]Only years where linear interpolation could be applied are listed. Total discharges for each water year are also listed. TSS, total suspended sediment.

[40] The LRE methodology is unbiased by gaps in flow and concentration monitoring data as it uses a regularized flow record to predict concentration for a given regression model and to calculate the loads accordingly. In the case of the Burdekin River, flow was recorded at regular hourly intervals, but this is not the case at all sites. The regularization method currently implemented in LRE deals with small gaps efficiently using a Hermite spline interpolation. However, one limitation of the method is the interpolation of large gaps in the flow record. In these instances, the spline interpolation does not work well. *Pagendam and Welsh* [2011] have developed an approach that provides a realization of the flow series that has the potential to infill large gaps in flow data more efficiently and accurately, provided that the covariates characterizing the mean has a strong relationship with flow. The method can also provide estimates of uncertainty in the flow record that could be used to inform the errors in flows and input into the LRE model. We are currently investigating this approach as a method for flow regularization in flow records that exhibit large gaps in flow.

[41] A second limitation of the approach is the ability of the model to predict concentration and to compute an accurate estimate of the load. We included two additional terms in the model to capture some of the complex features of the concentration-flow relationship for the Burdekin River. Other more complex covariates could have been considered. For instance, instead of just breaking flow up into "above dam" and "below dam" as we do here, we could have included a much more complex breakup into, say, six flow regions based on rainfall in each of the major subcatchments: Bowen, Belyando, Suttor, upper Burdekin, Cape, and the lower Burdekin. However, the creation of these terms becomes challenging as the detailed location of major rainfall gauges is not always known and this information has marked effects on load. Of course the model is only as good as the data and covariates that are used to develop it. If the data are not representative of the system, then the calculated loads will not adequately reflect the movement of pollutants at the site. Even if we have the best data and covariates included in the model, sampling bias may still be an issue. In these instances, provided that we have covered enough of the hydrological conditions to ensure the prediction errors are minimized, the model can still be confidently used to predict concentrations and estimate loads. To facilitate this, diagnostic checks that examine the predictive performance of the model need to be performed to ensure the final model is representative of the system being studied. It is important to acknowledge that the methodology presented here is not intended to replace monitoring programs but complement them by using historical data to establish baselines against which to assess future change. Of course where significant future changes are likely, these will need to be monitored independently as they will not be represented by the model and any predictions from the model are likely to be underestimated. Furthermore, the uncertainty associated with baseline estimates may make it virtually impossible to comment scientifically on changes incurred by the implementation of management strategies. Although not an ideal outcome, this highlights the complexity of quantifying sediment fluxes.

[42] The application of the method to other water quality data sets [*Kroon et al.*, 2012] for broader management

purposes shows promise as a tool for quantifying pollutant loads with associated uncertainties. Recent examples of LRE implementation have included that of *Kroon et al.* [2012], where pollutant baseline loads were estimated for all GBR end-of-catchment sites having adequate monitoring data. Estimates of a catchment-wide sediment budget for the Burdekin is another example, where LRE methodology was used to provide estimates of loads with uncertainties for each water year from 2005–2010 for five river stations within the Burdekin catchment. These estimates were then combined and the uncertainties propagated to give sediment trapping estimates for the Burdekin Falls Dam during each year monitored by S. E. Lewis et al. (manuscript in preparation), to identify years where trapping was highest, and compare results with standard reservoir trapping algorithms developed for more temperate climates.

[43] Load estimates with attached confidence intervals from LRE are complementary to, and potentially useful for constraining, deterministic and spatially resolved models of pollutant delivery through river networks such as the SedNet conceptual process model of pollutant sources and transport [*Wilkinson et al.*, 2009], and land use concentration-based models of pollutant generation [*Argent et al.*, 2009]. A natural extension to the problem of loads estimation is the integration or assimilation of monitoring data with spatially resolved pollutant transport models [*Berliner*, 2003; *Wikle and Berliner*, 2007]. Through this integration, the prediction of a system's state is averaged with a new measurement about that state, thus incorporating errors in not only the state of the system but the measurement about it, in a similar way to how meteorological observations are used to improve the predictions of process-based weather models [*Kalnay*, 2003]. This is currently an area of future research, which we are exploring using the Burdekin catchment as a case study.

[44] **Acknowledgments.** We thank Paul Rustomji and the two anonymous reviewers for reviewing this work and providing useful feedback that has been incorporated into this paper. We also acknowledge the contributions from Erin Peterson to the model structure and hydrological terms used in the model. We thank the Queensland Department of Environment and Resource Management (DERM) and Alan Mitchell and Miles Furnas (AIMS) who supplied suspended sediment concentration data for load calculations. The DERM hydrographers (in particular, Morgain Sinclair, Phil Kerr, and Geoff Pocock) are acknowledged for supplying the flow data, and the DERM Queensland Remote Sensing Centre and Terry Beutel (DEEDI) are acknowledged for supplying the Burdekin GCI data. We would also like to acknowledge the support of the DERM Paddock to Reef Monitoring group for testing an earlier version of the methodology, and in particular, we thank Ryan Turner, Jason Dunlop, Rae Huggins, and Marianna Joo for their input. This research was financially supported by the Australian government's Marine and Tropical Sciences Research Facility, implemented in north Queensland by the Reef and Rainforest Research Centre Ltd. Finally, we acknowledge the funding support from the CSIRO Julius Award for the first author.

References

American Public Health Association (2005), *Standard methods for the examination of water and wastewaters*, 21st ed., pp. 2–56, edited by A. E. Eaton et al., Am. Public Health Assoc., Washington, D. C.

Amos, K., J. Alexander, A. Horn, G. Pocock, and C. Fielding (2004), Supply limited sediment transport in a high discharge event of the tropical Burdekin River, north Queensland, Australia, *Sedimentology*, *51*, 145–162.

Argent, R. M., J. M. Perraud, J. M. Rahman, R. B. Grayson, and G. M. Podger (2009), A new approach to water quality modelling and environmental decision support systems, *Environ. Modell. Software*, *24*, 809–818.

Asselman, N. E. M. (2000), Fitting and interpretation of sediment rating curves, *J. Hydrol.*, *234*, 228–248.

Bainbridge, Z., S. Lewis, A. Davis, and J. Brodie (2008), Event-based community water quality monitoring in the Burdekin dry tropics region: 2007/08 wet season update, *ACTFR Rep. 08/19*, Aust. Cent. for Tropical Freshwater Res., James Cook Univ., Townsville, Queensl., Australia. [Available at http://www-public.jcu.edu.au/tropwater/reports/2007/index.htm.]

Bainbridge, Z., E. Wolanski, J. G. Álvarez-Romero, S. E. Lewis, and J. E. Brodie (2012), Fine sediment and nutrient dynamics related to particle size and floc formation in a Burdekin River flood plume, Australia., *Mar. Pollut. Bull.*, doi:10.1016/j.marpolbul.2012.01.043, in press.

Belperio, A. (1979), The combined use of wash load and bed material load rating curves for the calculation of total load: An example from the Burdekin River, Australia, *Catena*, *6*, 317–329.

Berliner, L. M. (2003), Physical-statistical modeling in geophysics, *J. Geophys. Res.*, *108*(D24), 8776, doi:10.1029/2002JD002865.

Brodie, J. E., J. Waterhouse, S. E. Lewis, A. T. Bainbridge, and J. Johnson (2009), Current loads of priority pollutants discharged from Great Barrier Reef Catchments to the Great Barrier Reef, *Rep. 09/02*, Aust. Cent. for Tropical Freshwater Res., James Cook Univ., Townsville, Queensl., Australia. [Available at http://www-public.jcu.edu.au/public/groups/everyone/documents/technical_report/jcuprd_057072.pdf.]

Brodie, J. E., F. J. Kroon, B. Schaffelke, E. C. Wolanski, S. E. Lewis, M. J. Devlin, I. C. Bohnet, Z. T. Bainbridge, J. Waterhouse, and A. M. Davis (2012), Terrestrial pollutant runoff to the Great Barrier Reef: An update of issues, priorities and management responses, *Mar. Pollut. Bull.*, doi:10.1016/j.marpolbul.2011.12.012, in press.

Cohn, T. A. (1995), Recent advances in statistical methods for the estimation of sediment and nutrient transport in rivers, U.S. Natl. Rep. Int. Union Geod. Geophys. 1991–1994, *Rev. Geophys.*, *33*, 1117–1124.

Cohn, T. A., D. L. Caulder, E. J. Gilroy, L. D. Zynjuk, and R. M. Summers (1992), The validity of a simple statistical model for estimating fluvial constituent loads: An empirical study involving nutrient loads entering Chesapeake Bay, *Water Resour. Res.*, *28*, 2353–2363.

Cooper, D. M., and C. D. Watts (2002), A comparison of river load estimation techniques: Application to dissolved organic carbon, *Environmetrics*, *13*, 733–750.

Darnell, R., B. Henderson, F. Kroon, and P. Kuhnert (2012), Determining the number of years of monitoring pollutant loads necessary to detect trends, *Mar. Pollut. Bull.*, doi:10.1016/j.marpolbul.2012.04.002, in press.

De'ath, G., and K. E. Fabricius (2010), Water quality as a regional driver of coral 1666 biodiversity and macroalgae on the Great Barrier Reef, *Ecol. Appl.*, *20*, 840–850.

Doney, S. C. (2010), The growing human footprint on coastal and open-ocean biogeochemistry, *Science*, *328*, 1512–1516.

Efron, B., and R. J. Tibshirani (1993), *An Introduction to the Bootstrap*, Chapman and Hall, New York.

Fritsch, F. N., and R. E. Carlson (1980), Monotone piecewise cubic interpolation, *SIAM J. Numer. Anal.*, *17*, 238–246.

Furnas, M. (2003), Catchment and corals: Terrestrial runoff to the Great Barrier Reef, report, Aust. Inst. of Mar. Sci., Townsville, Queensl., Australia.

Kalnay, E. (2003), *Atmospheric Modeling, Data Assimilation and Predictability*, Cambridge Univ. Press, New York.

Kohavi, R. (1995), A study of cross-validation and bootstrap for accuracy estimation and model selection, in *Proceedings of the Fourteenth International Joint Conference on Artificial Intelligence*, vol. 2, pp. 1137–1143, AAAI Press, Quebec, Quebec, Canada.

Kroon, F. J., P. M. Kuhnert, B. L. Henderson, S. N. Wilkinson, A. Kinsey-Henderson, B. Abbott, J. E. Brodie, and R. D. R. Turner (2012), River loads of suspended solids, nitrogen, phosphorus and herbicides delivered to the Great Barrier Reef lagoon, *Mar. Pollut. Bull.*, doi:10.1016/j.marpolbul.2011.10.018, in press.

Letcher, R. A., A. J. Jakeman, M. Calfas, S. Linforth, B. Baginska, and I. Lawrence (2002), A comparison of catchment water quality models and direct estimation techniques, *Environ. Modell. Software*, *17*, 77–85.

Lewis, S. E., G. Shields, B. Kamber, and J. Lough (2007), A multi-trace element coral record of land-use changes in the Burdekin River catchment, NE, Australia, *Palaeogeogr. Palaeoclimatol. Palaeoecol.*, *246*, 471–487.

Littlewood, I. G., and T. J. Marsh (2005), Annual freshwater river mass loads from Great Britain, 1975–1994: Estimation algorithm, database and monitoring network issues, *J. Hydrol.*, *304*, 221–237.

McCulloch, M., S. Fallon, T. Wyndham, E. Hendy, J. Lough, and D. Barnes (2003), Coral record of increased sediment flux to the inner Great Barrier Reef since European settlement, *Nature*, *421*, 727–730.

McIvor, J. G., J. Williams, and C. J. Gardener (1995), Pasture management influences runoff and soil movement in the semi-arid tropics, *Aust. J. Exp. Agric.*, *35*, 55–65.

McKergow, L. A., I. P. Prosser, A. O. Hughes, and J. E. Brodie (2005), Sources of sediment to the Great Barrier Reef World Heritage area, *Mar. Pollut. Bull.*, *51*, 200–211.

Mitchell, A. W., and M. J. Furnas (2001), River logger—A new tool to monitor riverine suspended particle fluxes, *Water Sci. Technol.*, *43*(9), 115–120.

Morehead, M. D., J. P. Syvitski, E. W. H. Hutton, and S. D. Peckham (2003), Modeling the temporal variability in the flux of sediment from ungauged river basins, *Global Planet. Change*, *39*, 95–110.

Nistor, C. J., and M. Church (2005), Suspended sediment transport regime in a debris-flow gully on Vancouver Island, British Columbia, *Hydrol. Processes*, *19*, 861–885.

Pagendam, D. E., and A. H. Welsh (2011), Statistical estimation of total discharge volumes, paper presented at MODSIM2011, 19th International Congress on Modelling and Simulation, Modell. and Simul. Soc. of Aust. and N. Z., Brisbane, Queensl., Australia.

Petheram, C., T. A. McMahon, and M. C. Peel (2008), Flow characteristics of rivers in northern Australia: Implications for development, *J. Hydrol.*, *357*, 93–111.

Pinheiro, J. C., and D. M. Bates (2000), *Mixed-Effects Models in S and S-Plus*, Springer, New York.

R Development Core Team (2005), *R: A Language and Environment for Statistical Computing, Reference Index Version 2.12.1*, R Found. for Stat. Comput., Vienna.

Reef Water Quality Protection Plan Secretariat (2009), Reef water quality protection plan 2009: For the Great Barrier Reef world heritage area and adjacent catchments, report, Queensl. Dep. of Premier and Cabinet, Brisbane, Queensl., Australia.

Rustomji, P., and S. Wilkinson (2008), Applying bootstrap resampling to quantify uncertainty in fluvial suspended sediment loads estimated using rating curves, *Water Resour. Res.*, *44*, W09435, doi:10.1029/2007WR006088.

Scanlan, J. C., A. J. Pressland, and D. J. Myles (1996), Runoff and soil movement on mid-slopes in north-east Queensland grazed woodlands, *Rangeland J.*, *18*, 33–46.

Scarth, P., M. Byrne, T. Danaher, B. Henry, R. Hasset, J. Carter, and P. Timmers (2006), State of the paddock: Monitoring condition and trend in groundcover across Queensland, paper presented at 13th Australasian Remote Sensing Conference, BAE Syst., Canberra, ACT, Australia.

Schmidt, M., D. Tindall, K. Speller, P. Scarth, and C. Dougall (2010), *Ground cover management practices in cropping and improved pasture grazing systems: Ground cover monitoring using remote sensing, final report*, Dep. of Environ. and Resour. Manage., Queensland, Australia.

Thomas, R. B. (1985), Estimating total suspended sediment yield with probability sampling, *Water Resour. Res.*, *21*, 1381–1388.

Thomas, R. B. (1988), Monitoring baseline suspended sediment in forested basins: The effects of sampling of suspended sediment rating curves, *Hydrol. Sci. J.*, *33*, 499–514.

Thomas, R. B., and J. Lewis (1995), An evaluation of flow-stratified sampling for estimating suspended sediment loads, *J. Hydrol.*, *170*, 27–45.

Venables, W. N., and B. D. Ripley (1998), *Modern Applied Statistics With S-Plus*, 2nd ed., Springer, New York.

Walling, D. E. (1977), Assessing the accuracy of suspended sediment rating curves for a small basin, *Water Resour. Res.*, *13*, 531–538.

Wang, Y.-G., P. M. Kuhnert, and B. Henderson (2011), Load estimation with uncertainties from opportunistic sampling data—A semiparametric approach, *J. Hydrol.*, *396*, 148–157.

Wikle, C. K., and L. M. Berliner (2007), A Bayesian tutorial for data assimilation, *Physica D*, *230*, 1–16.

Wilkinson, S., I. P. Prosser, P. Rustomji, and A. Read (2009), Modelling and testing spatially distributed sediment budgets to relate erosion processes to sediment yields, *Environ. Modell. Software*, *24*, 489–501.

Wood, S. N. (2006), *Generalized Additive Models: An Introduction With R*, Chapman and Hall, Boca Raton, Fla.

Z. T. Bainbridge, J. E. Brodie, and S. E. Lewis, Centre for Tropical Water & Aquatic Ecosystem Research (TropWATER), Australian Tropical Sciences Innovation Precinct (ATSIP), Bldg. DB145, James Cook University, Townsville, QLD 4811, Australia.

B. L. Henderson, CSIRO Mathematics, Informatics and Statistics, GPO Box 664, Canberra, ACT 2601, Australia.

P. M. Kuhnert, CSIRO Mathematics, Informatics and Statistics, Private Bag 2, Glen Osmond, SA 5064, Australia. (petra.kuhnert@csiro.au)

S. N. Wilkinson, CSIRO Land and Water, GPO Box 1666, Canberra, ACT 2601, Australia.